U.S. DEPARTMENT OF COMMERCE
National Technical Information Service
PB-299 195

Evaluation of Granular Bed Filters for High-temperature/High-pressure Particulate Control

Air Pollution Technology, Inc, San Diego, CA

Prepared for

Industrial Environmental Research Lab, Research Triangle Park, NC

Jan 79

BIBLIOGRAPHIC INFORMATION

PB-299 195

Evaluation of Granular Bed Filters for
High-temperature/High-pressure Particulate Control.

Jan 79
Shui-Chow Yung, Ronald
and
PERFORMER: Air Pollution Technology, Inc., San Diego, CA.
Contract EPA-68-02-2183

SPONSOR: Industrial Environmental Research Lab., Research
Triangle Park, NC.
EPA/600/779/020
Research rept.

The status and potential of granular bed filter (GBF) technology for fine particulate control has been critically reviewed and evaluated with emphasis on high temperature and pressure (HTP) applications. Available theoretical models and experimental data have been evaluated and found to be inadequate for predicting the performance of industrial GBF systems. Additional experimental data were obtained with a bench scale GBF. These data were used as the basis for a clean bed performance model based on inertial impaction as the primary collection mechanism. Predictions were in good agreement with data from industrial GBF systems. The performance and economics of fixed, continuously moving, and intermittently moving GBF systems have been evaluated for HTP applications. This study shows that GBF systems have potential for HTP applications but further development and design improvements will be necessary before these systems can be considered adequate HTP particulate control technologies. Recommendations are made for improving the efficiency and reliability of GBF system, ...

KEYWORDS: *Air pollution control equipment, *Filters,
*Fines, *Granular bed filters.

Available from the National Technical Information Service,
Springfield, Va. 22161

PRICE CODE: PC A11/MF A01

PB 299195

United States
Environmental Protection
Agency

Industrial Environmental Research
Laboratory
Research Triangle Park NC 27711

EPA-600/7-79-020
January 1979

EPA

Evaluation of Granular Bed Filters for High-temperature/ High-pressure Particulate Control

Interagency Energy/Environment R&D Program Report

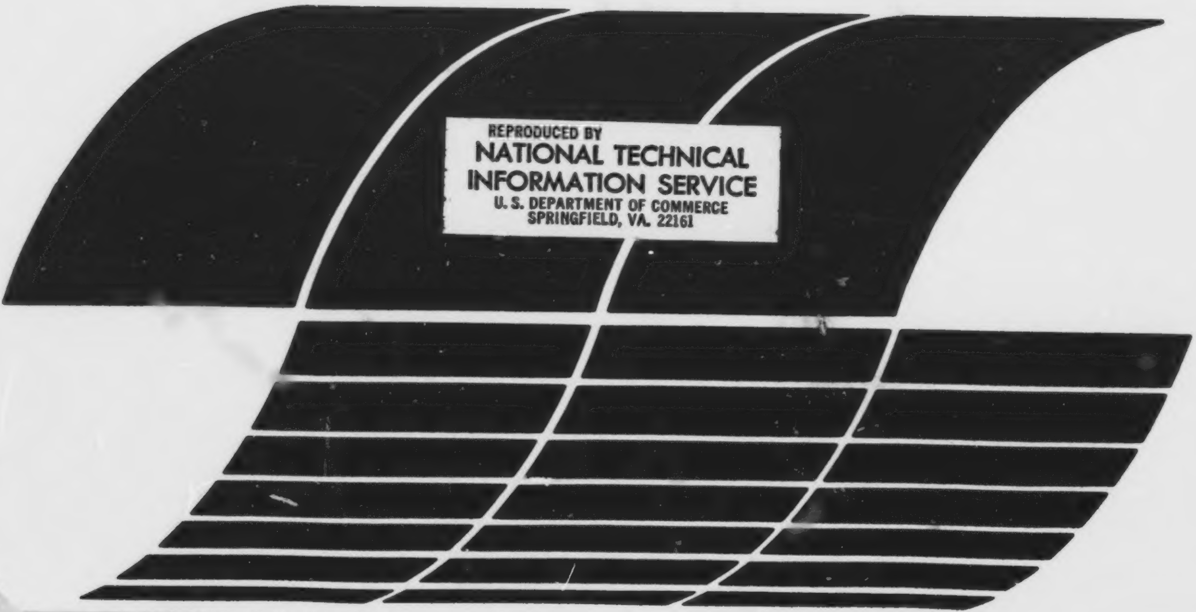

REPRODUCED BY
NATIONAL TECHNICAL
INFORMATION SERVICE
U. S. DEPARTMENT OF COMMERCE
SPRINGFIELD, VA. 22161

RESEARCH REPORTING SERIES

Research reports of the Office of Research and Development, U.S. Environmental Protection Agency, have been grouped into nine series. These nine broad categories were established to facilitate further development and application of environmental technology. Elimination of traditional grouping was consciously planned to foster technology transfer and a maximum interface in related fields. The nine series are:

1. Environmental Health Effects Research
2. Environmental Protection Technology
3. Ecological Research
4. Environmental Monitoring
5. Socioeconomic Environmental Studies
6. Scientific and Technical Assessment Reports (STAR)
7. Interagency Energy-Environment Research and Development
8. "Special" Reports
9. Miscellaneous Reports

This report has been assigned to the INTERAGENCY ENERGY-ENVIRONMENT RESEARCH AND DEVELOPMENT series. Reports in this series result from the effort funded under the 17-agency Federal Energy/Environment Research and Development Program. These studies relate to EPA's mission to protect the public health and welfare from adverse effects of pollutants associated with energy systems. The goal of the Program is to assure the rapid development of domestic energy supplies in an environmentally-compatible manner by providing the necessary environmental data and control technology. Investigations include analyses of the transport of energy-related pollutants and their health and ecological effects; assessments of, and development of, control technologies for energy systems; and integrated assessments of a wide range of energy-related environmental issues.

EPA REVIEW NOTICE

This report has been reviewed by the participating Federal Agencies, and approved for publication. Approval does not signify that the contents necessarily reflect the views and policies of the Government, nor does mention of trade names or commercial products constitute endorsement or recommendation for use.

This document is available to the public through the National Technical Information Service, Springfield, Virginia 22161.

EPA-600/7-79-020

January 1979

Evaluation of Granular Bed Filters for High-temperature/ High-pressure Particulate Control

by

Shui-Chow Yung, Ronald Patterson,
Richard Parker, and Seymour Calvert

Air Pollution Technology, Inc.
4901 Morena Boulevard, Suite 402
San Diego, California 92117

Contract No. 68-02-2183
Program Element No. 1NE624

EPA Project Officer: Dennis C. Drehmel

Industrial Environmental Research Laboratory
Office of Energy, Minerals, and Industry
Research Triangle Park, NC 27711

Prepared for

U.S. ENVIRONMENTAL PROTECTION AGENCY
Office of Research and Development
Washington, DC 20460

ABSTRACT

The status and potential of granular bed filter (GBF) technology for fine particulate control has been critically reviewed and evaluated with emphasis on high temperature and pressure (HTP) applications.

Available theroretical models and experimental data have been evaluated and found to be inadequate for predicting the performance of industrial GBF systems. Additional experimental data were obtained with a bench scale GBF. These data were used as the basis for a clean bed performance model based on inertial impaction as the primary collection mechanism. Predictions were in good agreement with data from industrial GBF systems.

The performance and economics of fixed, continuously moving, and intermittently moving GBF systems have been evaluated for HTP applications. At the present stage of development, GBF performance is neither efficient enough nor sufficiently reliable to satisfy HTP particulate control requirements. Therefore, cost estimates are highly speculative and serve mainly to indicate areas where further development work might substantially reduce capital and operating costs.

This study shows that GBF systems have potential for HTP applications but further development and design improvements will be necessary before these systems can be considered adequate HTP particulate control technologies. Recommendations are made for improving the efficiency and reliability of GBF systems.

CONTENTS

Page

Abstract. iii

Figures vi

Tables. xii

Abbreviations and Symbols xiv

Acknowledgement xviii

Sections

1. Summary and Conclusions 1
   - Current Technology Evaluation. 1
   - Engineering Design Equations 13
   - Potential for HTP Applications 16
   - Conclusions. 17
2. Introduction. 20
3. Literature Review 22
   - Patents. 22
   - GBF Studies. 27
   - Theory 63
4. Comparison Between Model Prediction and Data. 105
   - Data Reported by McCain. 105
   - Data Reported by Hood. 110
   - Data Reported by Knettig and Beeckmans 111
   - Data by Paretsky, et al. 116
   - Data by Gebhart, et al 116
   - Conclusions. 118
5. Experiment. 119
   - Apparatus. 119
   - Data Analysis. 122
   - Pressure Drop Data 131

CONTENTS (continued)

Page
6. Design Model. 135
    Mathematical Modeling. 135
    Comparing Model Predictions with Performance Data. . . .141
7. Present Technology Evaluation 145
    Granular Bed Filter Systems. 145
    Industrial Users and Performances. 161
    Evaluation 175
8. Potential for HTP Applications. 185
    Cleanup Requirements .185
    Predicted GBF Performance. 188
    Gaseous Pollutants 192
    Preliminary Cost Estimate. 193
    Permissible Costs. 200
    Summary and Conclusions. 203
9. Recommendations fur Future Research and Development . . .205
    Efficiency Improvement 205
    Bed Cleaning Methods .208
    Other Research Recommendations 209
    Recommended Research Program 209

References. 212

FIGURES

Number Page

1 Filtration of aerosols through bed packed with lead shot (Thomas and Yoder data). 30

2 Time vs. efficiency - 0.033 m deep granular bed filtering fly ash (Taub's data) 33

3 Penetration of 1.1 μm aerosol as a function of superficial gas velocity: 10-14 mesh sand (Paretsky, et al. data). 36

4 Penetration of 1.1 μm aerosol as a function of superficial gas velocity: 20-30 mesh sand (Paretsky, et al. data). 36

5 Experimental results obtained by Gebhart, et al.: Penetration vs. particle diameter for different flow velocities and granule size 37

6 Experimenta results obtained by Gebhart, et al: Penetration vs. particle diameter for different flow velocities and granule size 37

7 Experimental results obtained by Gebhart, et al.: Penetration vs. particle diameter for different flow velocities and granule size 38

8 Experimental results obtained by Gebhart, et al: Penetration vs. particle diameter for different flow velocities and granule size 38

9 Gravity effect in granular beds measured with an upward and downward directed aerosol stream (Gebhart, et al. data). 40

10 Gravity effect in granular beds measured with an upward and downward directed aerosol stream (Gebhart, et al. data). 40

11 Capture efficiency (transfer units) vs. bed height for the grid supported fixed bed (Knettig and Beeckmans' data) 41

FIGURES (continued)

Number		Page
12	Capture efficiency (transfer units) vs. bed height for the screen supported fixed bed (Knettig and Beeckmans' data).	41
13	Effect of mean gravel diameter and particulate load on granular bed collection efficiency (Miyamoto and Bohn's data).	43
14	Effect of gravel layer thickness and particulate load on granular bed collection efficiency (Miyamoto and Bohn's data).	43
15	Effect of superficial gas velocity and particulate load on granular bed collection efficiency (Miyamoto and Bohn's data).	43
16	Penetration tests on 420 to 710 micrometers plastic beads by monodispersed polystyrene latex aerosol (downflow) (Figueroa and Licht's data).	46
17	Effect of bed height and bed granule (bead) size on the downflow penetration of 0.5 micrometers polystyrene latex aerosol particles on plastic beads (Figueroa and Licht's data)	46
18	Comparison of downflow penetration of polystyrene latex aerosol particle on 420 to 710 micrometers plastic beads and -25+40 mesh sand granules (Figueroa and Licht's data)	47
19	Effect of bed granule (bead) size and flow direction on the penetration of 0.5 micrometer polystyrene latex aerosol particles on plastic beads.	47
20	Schematic of granular bed filter (Westinghouse setup)	49
21	Schematic of test equipment (Westinghouse).	50
22	Electrified packed bed.	61
23	Performance characteristics of electrostatically augmented packed bed (Research-Cottrell data)	62
24	Dendrite initiation, growth and idealization of the dendrite configuration.	75
25	Particle deposition on single collector	79
26	Typical isotherms for Langmuir and BET adsorption patterns.	82

FIGURES (continued)

Number		Page
27	Schematic representation of fly ash emission mechanisms	93
28	Fraction of total fly ash emitted by various mechanisms as a function of deposit thickness	95
29	A comprehensive plot of pressure drop in fixed beds	97
30	Effect of mean granule diameter on pressure drop (Miyamoto and Bohn's data)	99
31	Effect of bed depth on pressure drop (Miyamoto and Bohn's data)	99
32	Effect of superficial gas velocity on pressure drop (Miyamoto and Bohn's data)	99
33	Comparison of McCain's gravel bed particle collection data with design equation predictions	106
34	Comparison of Hood's data with predictions by available design equations	112
35	Experimental and predicted performance of CPC GBF (A.P.T. data)	112
36	Experimental and predicted performance of CPC GBF (A.P.T. data)	113
37	Experimental and predicted performance of CPC GBF (A.P.T. data)	113
38	Comparison of Paretsky, et al. data with predictions by available design equation	117
39	Comparison of Gebhart, et al. data and predictions by Paretsky, et al. equation. Collection is in the diffusion regime	117
40	Schematic diagram of the experimental apparatus	120
41	Particle size distribution for iron shot	121
42	Experimental particle penetration of a clean granular bed filter	123
43	Experimental particle penetration of a clean granular bed filter	123

FIGURES (continued)

Number Page

44 Experimental particle penetration of a clean granular bed filter. 124

45 Experimental particle penetration of a clean granular bed filter. 124

46 Experimental particle penetration of a clean granular bed filter. 125

47 Experimental particle penetration of a clean granular bed filter. 125

48 Experimental particle penetration of a clean granular bed filter. 126

49 Experimental particle penetration of a clean granular bed filter. 126

50 Experimental particle penetration of a clean granular bed filter. 127

51 Experimental particle penetration of a clean granular bed filter. 127

52 Experimental particle penetration of a clean granular bed filter. 128

53 Experimental particle penetration of a clean granular bed filter. 128

54 Experimental and predicted pressure drops across a clean granular bed filter. 132

55 Experimental and predicted pressure drops across a clean granular bed filter. 132

56 Experimental and predicted pressure drops across a clean granular bed filter. 133

57 Experimental and predicted pressure drops across a clean granular bed filter. 133

58 Experimental and predicted pressure drops across a clean granular bed filter. 134

59 Diagram of granular bed showing impaction concept. . 136

60 K_p vs. η for round jet model for particle collection in a GBF 139

FIGURES (continued)

Number Page

61 K_p vs. η for round jet. 140

62 Efficiency vs. inertial impaction parameter for comparison 140

63 Comparison of McCain's gravel bed particle collection data with design equation predictions 142

64 Comparison of Hood's data with predictions by available design equations 142

65 Experimental and predicted performance of CPC GBF (A.P.T. data) 143

66 Experimental and predicted performance of CPC GBF (A.P.T. data) 143

67 Experimental and predicted performance of CPC GBF (A.P.T. data) 144

68 Dorfan impingo filter 147

69 Consolidation Coal Company filter 148

70 Combustion Power Company "dry scrubber" 151

71 The integral cyclone model of the "dry scrubber". . . 152

72 Possible design for Squires panel bed filter. 153

73 Lurgi MB filter 155

74 Rexnord gravel bed filter 157

75 Ducon granular bed filter 159

76 Filter element. 160

77 Collection cycle. 162

78 Cleaning cycle. 162

79 Experimental grade efficiency curve of a Rexnord gravel bed filter (McCain, 1976). 165

80 Experimental penetration curves for CPC dry scrubber (Hood, 1976). 168

FIGURES (continued)

Number | | Page

81 Continuous moving bed GBF. 169

82 Experimental grade penetration (CPC data for nominal configuration) 172

83 Experimental grade penetration (CPC data for thick bed configurations). 172

84 Experimental grade penetration (CPC data for thick bed configuration) 173

85 Experimental grade penetration (CPC data for short bed configuration) 173

86 Experimental grade penetration (CPC data for small granule configuration) 174

87 Fractional penetration curve for Ducon granular bed. . 176

88 Fractional penetration for Ducon GBF (from Bertrand, et al., 1977). 176

89 Predicted GBF performance. 189

90 Particle size distributions from Exxon miniplant fluidized bed coal combustors. 191

91 Fixed bed GBF. 195

92 Summary G.E. comparison cycles (cost of electricity at an assumed capacity factor of 65%). 202

TABLES

Number Page

1 Summary of experimental investigations of GBFs. . . . 2

2 GBF evaluation summary. 9

3 Available equations for the prediction of particle collection in a granular bed. 14

4 Results of Hanford sand filter tests. 28

5 Summary of Zahradnik, et al. data 32

6 Slopes and intercepts of fitted lines 34

7 Experimentally determined properties of the granular materials (Figueroa, 1974). 45

8 Westinghouse GBF data, series #2. 51

9 Westinghouse GBF data, series #3. 52

10 Westinghouse GBF data, series #5. 53

11 Westinghouse GBF data, series #6. 54

12 Westinghouse GBF data, series #7. 55

13 Data obtained from Strauss and Thring granular bed filter study. 57

14 Available equations for the prediction of particle collection in a granular bed. 107

15 Comparison of Knettig and Beeckmans' data and predictions 115

16 Pressure drop and collection efficiency for 1.09 μm diameter particles at a superficial gas velocity of 50 cm/s 129

17 Pressure drop for 50% collection of 1.1 μm diameter particles 130

18 Measured and calculated void fraction of the granular bed 131

TABLES (continued)

Number Page

19 Typical operating characteristics of Consolidation Coal Company granular bed filters. 149

20 Summary of Rexnord gravel bed users. 164

21 Design specifications of the system as tested. 166

22 Test parameters for CPC moving bed filter (from Wade, et al., 1978). 171

23 CPC moving bed filter overall penetration correlation. 171

24 Granular bed filter performance (from Bertrand, et al. 1977). 177

25 Conditions for high temperature and pressure particulate collection 186

26 Summary of ECAS phase II performance and cost results. 201

ABBREVIATIONS AND SYMBOLS

a = effective mass transfer area, cm^2/cm^3

a = a constant, $cm^2/dyne$

A_p = fraction of the projected area of a single collector particle which is available for capturing the aerosol by settling, fraction

b = stoichiometry constant, dimensionless

B = a constant expressive of the energy of interaction with the surface, ℓ/mol

c = concentration of adsorbate in gas phase, g/cm^3

c_e = equilibrium concentration of sorbate in bulk gas phase, g/cm^3

c_s = saturation concentration of the adsorbate, g/cm^3

C = empirical constant defined by equation (5), dimensionless

C_{pi} = inlet particle concentration, g/cm^3

C' = Cunningham slip correction factor, dimensionless

d_c = granule diameter, cm

d_j = jet diameter, cm

d_o = initial capillary diameter, cm

d_p = particle diameter, cm or μm

D_e = effective diffusion coefficient of gaseous reactant in the residue layer, cm^2/s

D_G = gas phase diffusivity, cm^2/s

D_p = particle diffusivity, cm^2/s

D_{pe} = effective particle diffusion coefficient in granule layer, cm^2/s

D_{pore} = pore diffusivity, cm^2/s

f = fraction factor, dimensionless

f' = ratio of collector diameter to initial capillary diameter, dimensionless

F = compression stress, $dyne/cm^2$

g = gravitational acceleration, cm/s^2

j = ratio of channel width to packing diameter, dimensionless

ABBREVIATIONS AND SYMBOLS (cont.)

k = Boltzmann's constant = 1.38×10^{-16} erg/°K

k = chemical reaction rate constant, ℓ/mol-s

k_G = mass transfer coefficient, cm/s

k_{pore} = pore diffusion coefficient, cm^2/s

K = equilibrium constant, ℓ/mol

K = proportionality factor, dimensionless

K_d = D'Arcy permeability, cm^2

K_p = inertial parameter, dimensionless

m_k = expected particle number in the k'th layer of a dendrite, number

M = molar weight, g/mol

M_m = granule recirculation rate, kg/kg of gas

N = number of impaction stages, dimensionless

Pt = overall penetration, fraction or percent

Pt_d = penetration for particles with diameter "d_p", fraction or percent

q = amount of sorbate adsorbed per unit weight of sorbent, g/cm^3

q_e = amount of sorbate adsorbed per unit weight of adsorbent in equilibrium with concentration "C", g/cm^3

Q° = number of moles of adsorbate adsorbed per unit weight of adsorbent in forming a complete monolayer on the surface

$\bar{r}$ = average pore radius, cm

r_c = radius of unreacted core, cm

r_c = collector radius, cm

r_H = hydraulic radius, cm

R = original radius of the reacting particle, cm

R = universal gas constant, J/g mol-s

t = time, seconds

T = absolute temperature, °K

u_G = superficial gas velocity, cm/s

u_{Gb} = actual gas velocity in bed, cm/s

u_{Gi} = interstitial gas velocity, cm/s

u_j = gas velocity in the jet, cm/s

u_t = terminal settling velocity of the particle, cm/s

w = particulate load, g/cm^2

ABBREVIATIONS AND SYMBOLS (cont.)

x_B = fraction of reactant "B" converted into product, fraction
X = dust deposit thickness, cm
y_A = mole fraction of reactant "A" in gas phase, fraction
y_{crit} = critical trajectory of the aerosol, cm
Z = bed depth, cm

Greek

α = rate of particles approaching a clean fiber per unit length, cm^2/s
ΔP = pressure drop, $dyne/cm^2$
ρ_G = gas density, g/cm^3
ρ_p = particle density, g/cm^3
ρ_s = density of solid, g/cm^3
η = overall single granule collection efficiency or single stage collection efficiency, fraction
η_D = single granule collection efficiency by diffusion mechanism, fraction
η_{DI} = single granule collection efficiency by direct interception mechanism, fraction
η_{GS} = single granule collection efficiency by gravity settling, fraction
μ_G = gas viscosity, poise
ε = bed porosity, fraction
ε_i = initial void fraction, fraction
ϕ = relative force field, dimensionless
λ = tortuosity factor, dimensionless
Θ = angular cylindrical coordinate, measured counterclockwise from the downstream stagnation point, radian
θ = pressure drop function defined in equation (93)
$\Theta_{k,k}^{(r)}$ = rate of increase of "m_k" by deposition on particles already occupying the k'th layer due to the radial flow component, cm^{-1}
$\Theta_{k-1,k}^{(r)}$ = rate of increase of "m_k" by deposition on particles occupying the (k-1)'st layer due to radial flow component, s^{-1}
$\Theta_{k,k}^{(\theta)}$ = rate of increase of "m_k" by deposition on particles already occupying the k'th layer, due to the angular flow component, s^{-1}

ABBREVIATIONS AND SYMBOLS (cont.)

${}^{(\Theta)}_{k-1,k}$ = rate of increase of "m_k" by deposition on particles occupying the (k-1)'st layer due to the angular flow component, s^{-1}

τ = time for complete reaction, s

ξ = internal void fraction of the solid, fraction

Dimensionless Numbers

N_{Nu} = Nusselt number, dimensionless

N_{Pe} = Peclet number, dimensionless

N_{Re} = Reynolds number, dimensionless

N_{Sc} = Schmidt number, dimensionless

N_{Sh} = Sherwood number, dimensionless

ACKNOWLEDGEMENT

A.P.T., Inc. wishes to express its appreciation for excellent technical coordination and for very helpful assistance in support of our technical effort to Dr. Dennis C. Drehmel of the U.S. Environmental Protection Agency.

SECTION 1

SUMMARY AND CONCLUSIONS

A number of advanced energy conversion processes under development require high temperature and/or high pressure removal of particulate matter to protect critical system components. These processes must also meet existing and anticipated particulate emission standards. Granular bed filter (GBF) systems have been proposed as suitable devices for removing fine particles from high temperature and high pressure (HTP) gas streams. However, theoretical and experimental performance data for GBFs are sparsely scattered throughout the literature. A thorough survey and evaluation of current GBF technology has been performed. The results are presented in this report.

The objectives of this program have been to:

1. Assess current GBF technology for control of airborne particulate pollutants,
2. Evaluate existing GBF systems,
3. Develop engineering models and design equations to predict filter performance,
4. Survey present usage problems, and
5. Evaluate the potential of GBFs for high temperature and pressure applications.

CURRENT TECHNOLOGY EVALUATION

Performance Characteristics

The literature was searched to assess the current state of GBF technology. Table 1 summarizes the experimental investigations reported in the literature. Most of the studies were laboratory scale experiments. The results of these studies show that the collection efficiency of a GBF is a function of particle diameter, face velocity, bed depth, granule diameter,

TABLE 1. SUMMARY OF EXPERIMENTAL INVESTIGATIONS OF GBFs.

Investigator	Granular Bed Configuration	Test Conditions	Parameter Studied	Bed Performance	Comments
I. Laboratory Studies					
A. Thomas and Yoder (1956)	(a) Bed type: Fixed bed (b) Bed material: Sand (c) Average sand grain diameters: 0.161 cm, 0.071 cm, 0.036 cm (d) Bed height: 3.6 and 7.6 cm	Aerosol: DOP Aerosol particle size: 0.1 - 1.0 μm Face velocity: 0.11 - 2.2 cm/s	Sand particle size, particle shape, face velocity	(a) Penetration varied with sand particle size - decreasing diameter of sand. (b) Rough and irregular sand showed higher collection efficiency than smooth sand. (c) Penetration varied with sand particle size, face velocity and aerosol particle size. Efficiencies ranged from 40 to 99.8%.	Experimental result demonstrated the existance of an aerosol size of maximum penetration of about 0.3 μm. Particle size of maximum penetration decreased with increasing face velocity.
B. McFee and Sedlet (1968)	(a) Bed type: Fixed bed (b) Bed material: Sand (c) Sand grain diameter: 0.036 to 0.071 cm (d) Bed height: 15.2 to 76.2 cm	Aerosol: Pu-U-Mo Alloy fume Aerosol particle size: Geometric mean = 0.07 μm, standard deviation = 2.7. (Discrete sizes ranged from 0.02 to 4 μm) Face velocity: 0.5-68 cm/s Aerosol grain loading: approximately 0.11 g/m^3	Bed height, face velocity	(a) Penetration through 15.2 cm of sand varied from 0.08 to 0.57% over range of face velocities from 0.5 to 67.5 cm/s. Maximum penetration of 0.57% occurred in range of 20 to 40 cm/s. (b) Penetration through 76.2 cm of sand varied from 0.004% at 14.2 cm/s to 0.019% at 25 cm/s. (c) Penetration decreased with increase in bed depth up to depth of 30.5 to 45.7 cm, but relatively small improvement occurred for beds of greater depth.	Experimental results indicate the percentage of penetration varies with aerosol particle size, face velocity, bed depth and degree of packing of bed. Experimental observations confirm and extend finding of Thomas and Yoder.

Continued

TABLE 1. (CONTINUED)

Investigator	Granular Bed Configuration	Test Conditions	Parameter Studied	Bed Performance	Comments
				(d) Maximum penetration occurs at lower face velocity with increasing bed depth. (e) Pressure drop through sand varied with bed depth and face velocity and ranged from 1.4 to 259 cm W.C.	
C. Ducon Company (Avco, Inc.) (1969)	Bed type: Fixed bed with reverse gas flow cleaning.	Aerosol: a) Iron oxide from oxygen-lanced electric arc furnace b) Iron oxide from oxygen-lanced open hearth furance c) Nickel ore d) Fly ash e) Talc dust f) Plastic dust Face velocity: 26 cm/s	Aerosol type, inlet grain loading (4.6 to 11.4 g/m^3)	(a) Collection efficiency ranged from 98 to 99.9%. (b) Pressure drop: 10.1 to 15.2 cm W.C.	Collection efficiency was found to be higher for the finer sized iron oxide aerosols than for coarse fly ash. Indicates that physical characteristics of aerosol are an important factor in performance of filter-possibly with regard to agglomeration behavior.
D. Kovach and Hannan (1970)	(a) Bed type: Fixed bed (b) Bed material: Carbon (c) Granule diameter: 0.4 to 0.16 cm (d) Bed height: 38 cm	Aerosol: DOP, fly ash Aerosol particle size: fly ash - 5 to 100 μm Face velocity: 5 to 102 cm/s	Aerosol type, face velocity, granule size	(a) Penetration varied with bed granule size-decreasing with decreasing granule size (b) Penetration varied with face velocity	Penetration of fly ash aerosol was less than that for DOP aerosol. However, particle size of fly ash varied over a wide range, and effect may be due to both changes in particle size and aerosol type.

continued

TABLE 1. (CONTINUED)

Investigator	Granular Bed Configuration	Test Conditions	Parameters Studied	Bed Performance	Comments
E. Zahradnik, et al. (1970)	(a) Bed type: Shaft filter (bed of slowly falling granules through which gas stream passes horizontally) (b) Bed material: Alkalized alumina (1/16 in. beads) (c) Bed width: 30.5 cm	Aerosol: Fly ash Aerosol particle size: 11% 13.7 μm Gas velocity: Up to 28 cm/s Fly ash loading: 4.6 to 6.9 g/m^3	Gas mass velocity	(a) Collection efficiency: 99% at flow rate of 0.88 m^3/min and gas temperature of 400 F. (b) Pressure drop: 5.1 cm W.C.	Primary intent of study was to investigate simultaneous removal of fly ash and SO$_2$ by shaft-filter system.
F. Squires (1970)	(a) Bed type: Fixed bed with intermittent movement of solids (b) Bed material: Sand (c) Bed width: 3.5 cm (d) Sand particle diameter: approximately 0.05 cm	Aerosol: Fly ash Face velocity: 6 cm/s Fly ash loading: 4.6 to 9.2 g/m^3	Puffback cleaning	(a) Collection efficiency: > 99% (b) Pressure drop: 1.3 cm W.C.	High collection efficiency may be due in part to preagglomeration of fly ash before entering filter
G. Paretsky (1972)	(a) Bed type: Fixed bed (b) Bed material: Sand (c) Sand particle diameter: 10 to 14 and 20 to 30 mesh (approximately 0.15 cm and 0.07 cm) (d) Bed height: 3.7 to 19.2 cm	Aerosol: Polystyrene Aerosol particle size: 1.1 μm Face velocity: 0.3 to 80 cm/s	Face velocity, bed height, granule size	(a) Penetration at a given face velocity decreased as the granule size decreased	Results in agreement with those reported by other investigators.
H. Gebhart, et al. (1973)	(a) Bed type: Fixed (b) Bed material: glass beads (c) Bead diameter: 0.4, 0.16, 0.05, and 0.0185 cm (d) Bed height: 10.2, 20.5, and 41 cm	Aerosol: Polystyrene latex Aerosol diameter: 0.1 to 2 μm Face velocity: 0.29 to 6.6 cm/s	Granule diameter, aerosol diameter, face velocity, bed height, and direction of gas flow	(a) Downward gas flow gives lower penetration than upward gas flow. (b) Diffusional collection and gravity settling decrease with increasing gas velocity (c) Smaller granules give higher efficiency (d) Deeper bed gives higher efficiency (e) There exists a maximum penetration which is shifted to larger particles with decreasing bead diameter	Gas velocity is too low to be of any practical interest.

continued

TABLE 1. (CONTINUED)

Investigator	Granular Bed Configuration	Test Conditions	Parameters Studied	Bed Performance	Comments
I. Knettig and Beeckmans (1974)	(a) Bed type: Fixed and fluidized (b) Bed material: Glass beads (c) Bead diameter: 0.043 cm (d) Bed height: 1-12 cm (e) Bed support: Screen or grid	Aerosol: Uranine and methylene blue Aerosol diameter: 0.8, 1.6 and 2.9 μm Face velocity: 8.2 and 11.2 cm/s	Aerosol diameter, support and face velocity	(a) Linear relationship between collection efficiency and bed height (b) Collection efficiency per unit volume of bed increased with both aerosol diameter and superficial gas velocity.	
J. Miyamoto and Bohn (1975)	(a) Bed type: Fixed (b) Bed material: Gravel	Aerosol: Ammonium chloride Aerosol diameter: 0.1-3 μm	Particulate load, on collection efficiency	(a) Collection efficiency increased with increasing particulate load. (b) Thicker bed has higher initial collection efficiency but little effect when there is filter cake. (c) Smaller granules have higher collection efficiency and have sharper increase in collection efficiency with particulate load. (d) Higher face velocity decreases the rate of increase in efficiency with particulate load.	Results show the trend of cake filtration.

continued

TABLE 1. (CONTINUED)

Investigator	Granular Bed Configuration	Test Conditions	Parameters Studied	Bed Performance	Comments
K. Figueroa (1975)	(a) Bed type: Fixed and fluidized (b) Bed material: Plastic beads, sand (c) Granule diameter, plastic beads, 339 and 495 µm diameter, sand - 702 µm	1 and 2 µm diameter methylene blue, 0.5, 1.1 and 2.0 diameter polystyrene latex	Granule size, bed height, face velocity, flow direction, aerosol size	(a) Due to electrostatic charges plastic beads exhibited higher collection efficiency. (b) Highest collection efficiencies were obtained on the largest aerosol diameter, with the deepest bed of the finer granules.	Studied low gas velocity region.
L. Westinghouse (Ciliberti, 1977)	(a) Bed type: Fixed bed with reverse gas flow cleaning (b) Bed material: Sand (c) Sand particle size: -15 +30 mesh	10 µm limestone dust	Face velocity and bed depth	(a) Filter performance improves as dust accumulates in the bed.	Experiment not well controlled.
M. Schmidt, et al. (1978)	(a) Bed type: Fixed bed (b) Bed material: Polystyrene beads, quartz gravel (c) Granule diameter: polyethylene beads- 33 mm quartz gravel - 5 mm	Aerosol: DBP and room aerosol Face velocity: 15.2, 45.8, and 101 cm/s	Face velocity granule size, and aerosol size	(a) At constant face velocity, the grade efficiency curve exhibits a minimum at a particular particle diameter.	

granule shape, aerosol type and packing density or bed porosity. Other general results are listed below.

1. At a constant face velocity, the grade penetration curve exhibits a maximum penetration at a particular aerosol diameter. The particle diameter corresponding to maximum penetration decreases with increasing face velocity and with increasing bed depth.

2. Particle penetration decreases as the granule diameter is decreased, as packing density is increased, and as bed depth is increased.

3. Collection efficiency of a GBF composed of rough, irregular granules is higher than that of beds composed of smooth granules.

4. Aerosols which tend to agglomerate are more readily collected.

5. Surface and internal filter cakes tend to improve the collection efficiency of the GBF.

6. There is a maximum particle loading that can be retained in the bed. Above this maximum loading, the collection efficiency of the GBF declines.

7. The collection efficiency of the GBF can be increased by the use of augmenting forces. The filtration efficiency of the GBF can be enhanced by imposing an electric field or a magnetic field on the filtration medium. A.P.T. is performing laboratory experiments with charged and uncharged GBFs collecting charged and uncharged particles. Preliminary results revealed that the collection efficiency of the GBF improved significantly without any increase in pressure drop when the bed and/or particles were charged.

Present GBF Systems

A granular bed filter is any filtration system utilizing a non-fluidized bed of discrete granules or particles as the filtration medium. A variety of types of GBFs are identified in the literature.

GBFs may be classified according to the bed structure or according to the cleaning method. With respect to the bed structure, GBFs may be classified as fixed bed, continuously moving bed, or intermittently moving bed filters. The advantages and disadvantages of each bed structure are summarized in Table 2. The following is a more detailed discussion.

Moving Bed Filters -

The continuously moving bed filter is usually arranged in a cross-flow configuration. The bed is a vertical layer of granular material held in place by louvered walls. The gas passes horizontally through the granular layer while the granules and collected dust move continuously downward and are removed from the bottom. The dust is separated from the granules by mechanical vibration. The cleaned granules are then returned to the overhead hopper and the panel by a granule recirculation system.

The Combustion Power Company's dry scrubber is an example of a continuously moving bed filter. The performance of this device has been reported by Wade, et al. (1978). They conducted extensive cold flow tests to investigate the effects of bed depth, granule diameter and other parameters on the collection efficiency.

In general the CPC moving bed filter was found to be capable of particulate removal efficiencies in excess of 98% for particles in the 1 to 10 μmA diameter range. Submicron particles were collected at an efficiency in excess of 90% in cases with high velocities, high inlet particle loadings, and low granule rates. Beds with larger thickness to granule diameter ratios were most effective in the capture and retention of particles in the 2 to 5 μmA diameter range. Also, intermittent granule movement was shown to improve efficiency by a few percent.

High temperature tests of the moving bed filter are planned. No high temperature data are available at this time.

The major advantage of the moving bed filter design is that the bed granules are removed and cleaned out of the primary gas stream. This enables efficient cleaning and relatively steady collection efficiency. Also it is not necessary to isolate filter units during cleaning so that the total filter area open to gas flow is available for filtration at any time.

TABLE 2. GBF EVALUATION SUMMARY

GBF Type	FIXED BED	MOVING BED	INTERMITTENT BED
Advantages	1. No granule recirculation. 2. Lower operating cost.	1. External separation of granule and dust.	1. External separation of granule and dust.
Disadvantages	1. Plugging of retaining grids 2. Particle seepage through bed during cleaning cycle. 3. Fluidization redisperse fine dust during cleaning. 4. Ineffective bed cleaning causes particle buildup in bed. 5. HTP valving required for reverse air cleaning.	1. Erosion of retaining grids and transport system. 2. Particle reentrainment in moving bed. 3. Granule recirculation may cause high operating cost. 4. Difficult to form a filter cake in moving bed. 5. Needs a granule recirculation and granule/dust separation system. No suitable mechanical device identified. Transport by pneumatic means needs large quantity of compressed air and energy to heat the transport air to bed temperature.	1. Low gas capacity can cause high capital cost. 2. Erosion of retaining grids and transport systems. 3. Granule recirculation may cause high operating cost. 4. Surface cake must be found to avoid bed plugging problem. 5. HTP three-way valving required for cleaning air. 6. It requires large quantities of cleaning air and energy to heat the cleaning air to bed temperature.

The moving bed design also has some limiting operating characteristics. Particle reentrainment caused by the relative motion of the granules limits the granule flow rate and affects the overall collection efficiency. Erosion of the retaining grids, louvers, and transport system components may be a problem, especially in high temperature and pressure systems. The collected dust particles cannot form a filter cake so that the operating efficiency will be essentially that of a clean bed.

No suitable HTP mechanical granule recirculation system and granule/dust separation system were identified in the literature. CPC used a pneumatic method. Granule transport and granule/dust separation by the pneumatic method add significantly to the operating cost because large quantities of compressed air are required. In order to maintain the high gas temperature at the gas turbine inlet, it is necessary to heat the transport air to bed temperature to minimize the heat energy loss from the recirculating granules. This can be an important factor in the operating cost.

It may be possible to resolve most of these problems through further development and testing. Performance data at high temperatures and high pressures will be important in identifying the most serious operational problems.

Intermittently Moving Bed -

In the late 1950s, Squires modified the continuously moving bed design to obtain a fixed bed device with an intermittent movement of granular solids. The bed is stationary during filtration. The accumulated filter cake and the surface layer of granules are ejected from the panel by a sharp backwash pulse and fall to the bottom of the filter vessel. The expelled granules are immediately replaced by downward movement of fresh granules from the overhead hoppers.

The principal advantage of this type of bed structure is the capability for external granule/dust separation with minimum disturbance to the rooting cake. A rooting cake is the foundation for the formation of a surface cake. After cleaning, the surface cake is formed readily without disturbing the rooting cake and filtration efficiencies can be much higher.

The intermittently moving bed also has the advantage that granule cleaning is off-line and potentially more effective.

The major disadvantage is that the gas capacity is lower than for other granular bed filter designs and this results in high capital costs for a given installation. The face velocity is about one third the velocity used in the fixed bed and continuously moving bed GBFs. Thus, more filtration area is required.

Bed plugging also can be a problem if the surface cake is not formed properly. Erosion of the retaining grids, louvers, and other components may be a problem.

For HTP applications, Squire's design has another disadvantage. It requires large quantities of compressed air for cleaning. Compressed air requirements could be as much as 1% of the gas treated. The cleaning air is mixed with the gas being treated. In order to maintain the HTP conditions at gas turbine inlets, it is necessary to preheat the cleaning air. Cost to heat the cleaning air can be an important factor in the operating cost.

Fixed Bed Filters -

Fixed bed filters operate in two modes; the filtration mode and the cleaning mode. During filtration the bed is stationary. The gas passes through the bed and collected particles are deposited within the bed and on the bed surface. During cleaning the bed is isolated from the main flow and agitated mechanically or pneumatically by a reverse flow of gas.

There are two fixed bed devices currently being developed; the Rexnord gravel bed filter and the Ducon granular bed filter. The Rexnord filter uses a rake-shaped stirring device to agitate the bed during cleaning. This loosens the filter cake which is then removed by a reverse flow of clean air.

The Ducon granular bed filter cleans the bed by a reverse flow of gas which fluidizes the bed and elutriates the collected particles.

The Rexnord filters have been used successfully to control emissions from clinker coolers in the cement industry. They operate in the range of 100 to 200°C and near atmospheric pressure. No Rexnord filters have been tested at high temperature and pressure.

The Ducon filter was tested on the effluent from a fluid bed catalytic cracking unit regenerator at an oil refinery. The gas was at 370°C to 480°C and 1 to 1.5 atm. A collection efficiency of 85 to 98% was obtained on dust with a mass median diameter of 35 μm and a geometric standard deviation of about 4.

Various high temperature and pressure designs of the Ducon filter were tested at the Exxon miniplant (Hoke, et al., 1978). A number of operating problems were encountered during these tests.

The lowest demonstrated particulate outlet concentration was 68.6 mg/Nm³ (0.03 gr/SCF) which was considered to be too large to protect a gas turbine and borderline for meeting current emissions regulations. The use of smaller filter granules could be expected to improve efficiency. However, at times the filtration efficiency was very poor and the outlet particulate concentrations were as high as 700 to 1,200 mg/Nm³ (0.3 to 0.5 gr/SCF). It was also observed that the efficiency decreased with time in the longer runs, dropping from 90% initially to about 50% later in the run. Loss of filter medium during blow back was another recurring problem. Further attempts were made to use 50 mesh retaining screens but they failed because of plugging. Additional tests made with 10 mesh screens also resulted in significant screen plugging.

A significant buildup of particles in the filter beds was also observed amounting to about 30% of the weight of the filter medium. A possible steady long term increase in filter pressure drop may result because of this. However, no significant increase in filter pressure drop was noted during any of the shakedown runs.

It was also observed that the particles were not only building up in the beds but were uniformly mixed with the filter medium. It is possible that the buildup and mixing of particles in the bed could be responsible for the increase in the particle concentration in the outlet gas with time.

Another potential problem with the current design was its vulnerability to upsets. When upsets occurred, such as bed plugging or loss of filter medium, the operating problems caused by such upsets required shutdown of the system. Another problem which may be unique to the miniplant was the interaction of the granular bed filter with the rest of the FBC system during the blow back cycle. An increase in system pressure was noted during blow back resulting in problems with the coal feed system which is controlled by the differential pressure between the coal feed vessel and combustor. This required modifications to the coal feed control system to minimize the effects.

The Exxon's granular bed filter test program was suspended in November, 1977. In all runs in which more than one outlet concentration was measured, it was observed that the outlet concentration increased with time. They were not able to demonstrate that the current EPA emission standard (0.1 lb/10^6 Btu or 0.05 gr/SCF) could be met for more than a few hours of operation. In no runs was the anticipated new standard (0.0 3 lb/10^6 Btu or approximately 0.0 5 gr/SCF) satisfied.

ENGINEERING DESIGN EQUATIONS

The literature search provided information concerning theoretical and empirical design and performance equations for GBFs. Table 3 is a summary of the available equations. Most of the theoretical work considers the flow through a packed granular bed to be similar to the flow around single granules. This assumption appears to be inadequate for describing the efficiency and pressure drop of actual granular bed filters. These equations do not adequately predict the collection efficiency of a GBF at face velocities normally encountered in practice.

In this study, a performance model was developed which predicts collection efficiency for granular bed filters. The model is based on the assumption that the GBF is equivalent to a large number of impaction stages connected in series.

TABLE 3. AVAILABLE EQUATIONS FOR THE PREDICTION OF PARTICLE COLLECTION IN A GRANULAR BED

Investigator	Equation	Notes
Jackson and Calvert (1968)	$Pt_d = \exp\left[-C_1 \frac{Z}{d_c} K_p\right]$	Impaction only.
Paretsky et al. (1971)	$Pt_d = \exp\left[-\frac{3}{2}\frac{1-\varepsilon}{\varepsilon}\frac{Z}{d_c}\eta\right]$	
Miyamoto and Bohn (1974)	$Pt_d = \exp\left[-\frac{6(1-\varepsilon)Z}{d_c}\frac{N_{Nu}}{N_{Pe}}\right]$	Collection by diffusion only.
Gebhart et al. (1973)	$Pt_d = \exp\left[-6.39\frac{D_p{}^{2/3} Z}{u_{Gi}{}^{2/3} R_c{}^{5/3}}\right]$	Collection by diffusion only
Böhm and Jordan (1976)	$Pt_d = \exp\left[-\left(\frac{2\,k\,T\,\varepsilon\,f}{3\pi\,d_p\,u_G} + \frac{d_p^2\,g\,\rho_p\,\varepsilon\,d_c}{36\,u_G} + \frac{\pi\,d_p^2\,\rho_p\,u_G}{18\varepsilon}\right)\frac{4\,f\,Z}{\mu_G\,d_c{}^2}\right]$	Collection by diffusion. Gravity settling and impaction.

Continued

TABLE 3. (continued)

Investigator	Equation	Notes
Goren (1977)	$Pt_d = \exp\left[-\frac{3}{2}(1-\varepsilon)\frac{Z}{d_c}\left(1250\ K_p^{2.25} + \left(\frac{u_t}{u_G}\right)^{0.75} + 200\ N_{Pe}^{-2/3}\right)\right]$	Collection by impaction, gravity settling, and diffusion
Westinghouse (Ciliberti, 1977)	$Pt_d = \exp\left[-5.8\frac{K_p Z}{d_c} - 3.75\left(\frac{d_p}{d_c}\right)^2\frac{Z}{d_c} - 3.572\frac{D_p^{2/3}\ Z}{u_G^{2/3}\ d_c^{5/3}}\right]$	Collection by impaction, interception, and diffusion
Schmidt, et al. (1978)	$Pt_d = \exp\left[\frac{-7.5\ Z\ (1-\varepsilon)}{d_c}\left(\frac{8}{N_{Pe}} + 2.038\ N_{Re}^{1/8}\ N_{Pe}^{-5/8} + 1.45\left[\frac{d_p}{d_c}\right]^2 + 3.97\ K_p + \frac{u_t}{u_G}\right)\right]$	Semi-empirical equation, collection by diffusion, interception, impaction, and gravity settling.

The model is based on the collection of particles in a clean granular bed. The collection efficiency should be higher than predicted if there is a significant filter cake on the bed surface and within the bed. The presence of a surface cake, however, has not been observed by investigators working with large-scale filters. The clean bed model predicts a conservative estimate of the efficiency attainable by granular filtration and is a satisfactory model for filters which operate primarily without the presence of a filter cake.

This model has been used to predict the performance of industrial GBF systems. The particle collection efficiency predicted with this model compares favorably with available field data.

POTENTIAL FOR HTP APPLICATIONS

The feasibility of advanced energy processes, such as pressurized fluidized bed coal combustion, depends on the availability of a very efficient HTP particulate cleanup device. The particulate control equipment should be capable of operating at a gas temperature up tc 950°C and a gas pressure up to 20 atm.

The suitability of GBFs for controlling particulate emissions from advanced energy processes is not limited by the gas temperature and pressure. By properly selecting adequate granules and structural materials, the granular bed filters could be capable of operating at any temperatures and pressures encountered in advanced energy processes. The Ducon GBF, Combustion Power Company's moving bed filter, and the CCNY panel bed filter, all can be designed to operate at HTP.

The use of GBFs for HTP applications is limited by the particulate removal efficiencies and operating difficulties. Required efficiencies depend on the future emissions standards and on the tolerance of gas turbines for fine particles. Turbine requirements are not well established at this time.

At this time granular bed filters have not been demonstrated to be efficient enough to perform as the final cleanup stage in high temperature and pressure gas cleanup systems.

There are several methods that may be used to increase the collection efficiency. One method is to use a deep bed of fine granules. This is not a good approach as the pressure drop would be very high. Other methods such as electrostatic augmentation and cake filtration should be more effective.

Quantitative data on the costs of HTP granular bed filters are difficult to find. However, we have completed cost comparisons for various types of GBFs. The cost estimates are based on the cleanup requirement for a combined cycle steam turbine-gas turbine power plant.

The estimated capital costs of moving beds and intermittently moving beds are about 141% and 247% higher than those of fixed beds,respectively. With regard to operating cost (not including depreciation), moving beds are about 7.4 times higher than fixed beds and intermittently moving beds are 4 times higher than fixed beds.

The Energy Conversion Alternatives Study (ECAS) reported estimates that the difference in the overall cost of electricity between a pressurized fluidized bed boiler without cleanup and a conventional steam power plant with stack gas cleaning is about 14 mills/kWhe. Thus, a gas cleanup cost on the order of a few mills/kWhe should allow sufficient economic advantages to warrant continued development of the PFB boiler process.

Based on the preliminary cost analysis, all three of the GBF systems appear to be economically competitive. However, at the present stage of development, GBF performance is neither efficient enough nor sufficiently reliable to satisfy HTP particulate control requirements. Therefore, relative cost estimates must be considered highly speculative and serve mainly to indicate areas where further development work might substantially reduce costs.

CONCLUSIONS

The principal objectives of this study were achieved and the following conclusions may be drawn.

Present Technology

1. GBFs of present design are used successfully to control emissions from clinker coolers in the cement industry and on hog-fuel boilers in the forest products industry. The particles emitted from these sources are relatively large and present GBFs are capable of cleaning the gas sufficiently to meet the emission standards.

2. GBF collection efficiency may be increased by using smaller granules and deeper beds. It may also be increased significantly by imposing an electrostatic field on the bed and by building a good filter cake on the bed surface.

3. Further research work is required to increase the reliability of the bed cleaning methods and granular solids transport systems.

Design Equations

1. None of the design equations reported in the literature are adequate to predict the collection efficiency of a GBF at face velocities normally encountered in the field. A performance model is presented which predicts collection efficiency for GBFs. The particle collection predicted by this model compares favorably wtih available field data.

2. The pressure drop across a clean bed may be predicted by Ergun's equation for a packed bed.

HTP Potential

1. Granular bed filters may be designed to operate in high temperature and high pressure environments. The available GBF designs show potential for cleaning the gas to meet the current New Source Performance Standard if fine granules (<500 μm in diameter) are used as bed material.

2. Limited research work has been conducted to demonstrate the feasibility of simultaneous removal of particulates and gaseous pollutants with GBFs. It has been shown that packed beds of dolomite are capable of removing sulfur dioxide and particles simultaneously. Celatom MP-91 diatomaceous earth, Burgess No. 10 pigment and activated bauxite appear to be possible candidates

as packed bed sorbents for removing alkali metal vapor from hot combustion gases.

3. The capital and operating costs of HTP GBF systems appear to be within the acceptable range. A combined-cycle power plant with GBFs for HTP particulate cleanup is economically competitive when compared to a conventional power plant.

4. Although granular bed filters appear to have the potential for controlling particulate at high temperature and pressure in an economically acceptable manner, they are far from a proven, state-of-the-art technology.

There are many operational problems and uncertainties which need to be resolved before HTP granular bed filters can be considered sufficiently reliable for commercial application. These problems include the need to:

a. Prevent particle seepage through the bed (during cleaning or filtration.
b. Reduce temperature losses (especially during cleaning).
c. Improve the efficiency and reduce the cost of granule regeneration and recirculation.
d. Prevent attrition of granules causing particle reentrainment.
e. Prevent sintering of granules.
f. Prevent plugging of retaining grids.
g. Reduce pressure drop across the bed.
h. Improve primary and overall fine particle collection efficiency.

SECTION 2

INTRODUCTION

High temperature and pressure gas streams are encountered in the development of advanced energy processes such as coal gasification and pressurized fluidized bed combustion. To increase the thermal efficiency of these processes it has been proposed that a combined gas turbine and steam turbine cycle be used for the generation of power. However, the presence of particulate matter in the gas at the gas turbine can damage the turbine blades and render them inoperative. Thus it is necessary to remove the particulate matter to a level which will meet the turbine requirement for gas cleanliness with minimal loss of gas temperature and pressure.

There are a number of particulate removal systems under development that are capable of operating at high gas temperature and pressure. The granular bed filter is one of these systems.

Names like "granular bed filters," "gravel bed filters," "panel bed filters," "sand filters," "moving bed filters," and "loose surface filters" are used by various researchers to describe the type of air filtration equipment which consists of a bed of graded sand or gravel. In this report the general term "granular bed filters" is used and it is defined as any filtration system comprised of a stationary or slowly moving bed of separate, relatively close packed granules or particles as the filtration medium. In order to prevent the collected particulate matter from plugging the interstices between the granules and causing excessive pressure drops, the device should embody some means for either periodic or continuous removal of the collected particles from the collecting surfaces. This description then excludes fluidized or dispersed beds where granular particles are kept in motion by the gas being treated. It does include fixed bed or closely packed moving bed systems.

This report reviews and evaluates the status and potential of GBF technology for air pollution control with emphasis on high temperature and high pressure applications. The principles of operation, design performance of granular bed filters for removing fine particles from gas streams, and the effects of physical parameters such as granule diameter, bed depth and the design of bed containment structures are discussed. Filtration mechanisms are described, as are several alternative procedures for regenerating the granular bed filters.

Current practices in the application of granular bed filters for air pollution control and existing granular bed filter systems are critically reviewed and evaluated. Usage problems are identified.

The potential of granular bed filters for control of particulate emissions from advanced energy processes such as fluidized combustion and combined cycle power plants is evaluated. For each potential application, the energy costs of high temperature and high pressure particulate cleanup are compared with conventional power plants.

SECTION 3

LITERATURE REVIEW

PATENTS

Granular bed devices and processes for the removal of particles from gas streams have been reported as far back as the late 1800's. The following is a brief description of principal patents issued since then.

Solvay (1889) patented a filter to remove dusts and vapors from gases. It consisted of a cylindrical granular bed of sand (or alternatively a fibrous bed of asbestos) arranged in layers of increasing fineness upward from a foundation bed of coarse gravel or pebbles. A steam jacket was added to the vessel if a condensible vapor was to be removed. An internal rake or scraper on a central vertical shaft provided cleaning during operation. This pioneering patent contained many of the ideas later incorporated into the design of large coke beds for the removal of sulfuric acid mists and large sand beds for the removal of radioactive particles.

The early decades of the twentieth century produced a series of diverse patents involving granular filters. Fiechter (1919) patented a device in which the gaseous medium to be cleaned is introduced at the top of a rotating disc of perforated metal (or a screen mesh) covered with a layer of sand or other granular filter material. The gas is purified as it is passed downward through the sand layer and is drawn off at the bottom by a suction fan. Removal and purification of filter media may be done continuously or intermittently using a revolving screw conveyor, mounted over the disc, and a vertically adjustable scraper bar to spread the cleaned filter medium to the desired layer thickness. The method of cleaning the spent sand or filter medium is not specified.

Another patent by Fiechter (1922) involved the use of a moving sieve on an endless belt, carrying a horizontal layer of sand through which a gaseous medium can be filtered downward under suction or pressure. A pair of inner guide walls prevent sand from slipping off the belt, which is slightly lower at one end, allowing spent sand to trickle into a cleaning device and be returned via an elevator to the hopper above the opposite or higher end of the belt.

Klarding (1921) patented a filter device for constantly purifying hot blast-furnace and generator gases, containing large quantities of dust, without reduction in the temperature of the gases. Granular filtering material flows continuously from an upper hopper, downward through a main filter chamber, through a lower funnel onto a vibrating sieve for dust removal and then onto a conveyor that returns the clean filter material to the upper feed hopper. Dusty gases are introduced at the side above the main filter bed, flow downward through the bed, and exit at the opposite side. Part of the cleaned gas is directed against the dust-laden filter material as it is shaken on the sieve to aid in removing the dust, which falls through the sieve.

Nordström (1922, 1924) devised an improved means of separating dust, smoke, and the like from gases in a cement-burning process, a process for manufacturing chloride of lime, and the copper smelting process. The gases are passed through a granular filtering material in a filter tower. A separate current of atmospheric air moves dust from the filtering material as it falls through a step-like bottom chamber; cleaned filter material is conveyed back to the top of the filter; the removed dusty matter may be returned to the original process or used for another purpose. The filter tower, located between a furnace and a chimney, consists of two concentric perforated walls with the filter material contained between them. Gases from the furnace enter the inner chamber and pass outward through the filter wall to an outer chamber connected to the chimney and are discharged to the atmosphere in a purified state.

Thomson and Nisbet (1924) invented a filter for cleaning dust-laden gases from a blast furnace by allowing the gases to be drawn horizontally through a vertical downward moving screen of suitable ballast material. Ballast is continuously fed into a V-shaped hopper at top, slips downward over metal slots arranged in louver fashion, and is conveyed by a worm extractor down a chute to a sloping metal screen at the bottom. The screen can be agitated to facilitate separation of dust from ballast, which is then conveyed to the top hopper by an elevator mechanism. Suggested ballast material includes granulated or coarsely powdered quartz, flint, or metallic fragments.

Lynch (1930) patented a filter designed to handle large volumes of air or gas at high temperatures. It consists of a thick bed of granular filter material falling downward into piles in separate chambers. Gas flows through the bed at a slow rate, not exceeding 3 m/s (10 ft/sec), and discharges in a direction approximately opposite to the direction of filter material flow after passing downward and then upward through each chamber. Filter material is continuously cleaned, being carried by conveyor to a rattler or other device for dust removal, and then is hoisted back to the feed chutes by an elevator with bucket conveyor.

Lynch (1936) described a granular filter consisting of a bed of gravel 1.2 to 2.5 cm (0.5 to 1 inch) in diameter that is continuously withdrawn from the bottom of the filter, passed over a screen for dust removal, and returned to the top of the bed. Superficial gas velocity was approximately 91 cm/s (3 ft/s) for beds 30 to 122 cm (1 to 4 ft) deep and pressure drop was about 2.5 cm (1 inch) W.C. Units of steel, high chromium steel, and brick have been used to filter gases having temperatures up to 454°C (850°F), 816°C (1,500°F), and 1,093°C (2,000°F), respectively.

Fournier (1936) designed an apparatus for filtering gases by means of a filtering material such as sand falling over horizontal slats that may be vibrated on a combined system of slots and sieves. The gas passes transversely through the layer of filtering material and between the slots of each series. Hammer vibrators are suggested as a means of increasing the filter surface by facilitating the flow of filter material and partially cleaning it. An endless chain of buckets or rakes continuously feeds clean sand into the upper hoppers and transports soiled sand flows by gravity down a sinuous channel against an upflow of cleaning gas that removes the dust to a cyclone dust separator.

Berry and Fournier (1939) presented a more limited version of the above as a German patent. Dust, soot, etc. are removed from gases and vapors by passing the gas transversely through a granular filter of material falling in piles with natural angles of repose over a series of horizontal slats. The angle of the slats may be varied, and filter material may be removed at the bottom of the apparatus, cleaned, and replaced at the top.

Carney (1944) devised an apparatus for separating carbon-black dust entrained in a stream of gas or air by passing the gas upward through a bed of carbon-black granules contained in a rotating cylinder. A spiral conduit, connected at the bottom of the cylinder and wrapped around it, rotates with the cylinder and lifts the granules to the top of the cylinder while the carbon dust is agglomerated to the granules

Mercier and Ehlinger (1950) developed a filter using sand or other granular material to remove dust from hot gases issuing from a boiler firebox or from a boiler heated by gases under pressure. The filter is designed to handle gases of any temperature or pressure. In principle, a sand of suitable size and quality is arranged to provide small volumes, small depth of mass, and considerable surface area so that gases may pass through the filter without excessive pressure loss. Fine sand is held by walls formed by cone frustrums vertically aligned and concentrically disposed approximately opposite one another with conical surfaces tapering in opposite directions. For coarse sand (> 4 mm), vertical layers are held between two grids or between two perforated cylindrical metal sheets. The filter unit is radially divided into cells and is rotated.

Gases to be cleaned enter at the top of a container designed to withstand a high pressure (such as 150 kg/cm^2), zigzag through the sand filter, and exit at the bottom during one-half revolution of the filter. During the other half-revolution, sand and dust are emptied down pipe to a rotating screen. Dust falls through the screen while the sand passes into a screw conveyor or similar device to be raised to the top of the unit for recycling. Continuous cleaning and reuse of the sand permits uninterrupted operation without loss of the heat the sand has acquired through contact with the hot gases.

Veron (1951) designed a sand filter for removing entrained dust from gases produced by the combustion of pulverized coal at high temperature and pressure and destined to feed a turbine. The filter is contained in a cylindrical body having a domed cap and conical bottom - a form suitable for high gas pressures. An inner lining able to withstand high temperature forms a cooling jacket, through which compressed air is circulated. Gas enters at the bottom of the filter and passes upward through stepped tiers of sand in multiple trays through a network of interconnecting channels and pipes. Clean gas then flows through a separate system of inner chambers between the trays, exiting at the bottom of the filter on the opposite side of the filter.

When the sand becomes heavily dust laden, as indicated by an increase in pressure drop, slide valves are opened individually, tier by tier, releasing the sand for cleaning by any suitable method, and then the sand is returned to the top of the filter. Sand was chosen as a readily available filter medium that can stand high temperatures without damage or diminished filtering power.

Various designs of granular bed filters for removal of aerosols from industrial air and gas streams continued to appear in the 1950's and 1960's. Among those are Dorfan Impingo Filter (U.S. Patent 2,604,187) Squires (U.S. Patent 3,296,775), Berz and Berz (U.S. Patent 3,090,187), Kalen (U.S. Patent 3,798,882) and Zenz (U.S. Patent 3,410,055; 3,880,508). All these designs were tested at least in pilot scale and some were introduced commercially. These designs will be discussed in a later section.

GBF STUDIES

Low Temperature Filtration

Among the earliest of granular bed filter tests were those carried out in 1948-1949 at the General Electric Company, Hanford Works. The granular bed filters were used to remove radioactive particles from air ventilation systems.

The results of the tests were reported by Lapple (1948). The test chambers consisted of vertical cylinders, 25 to 30 cm (10 to 12 inches) in diameter and 91 to 153 cm (3 to 5 ft) long. The filter sand was supported on a 8 mesh screen welded to the sides of the tank upon which was placed successively finer grades of sand. Gas from the main ventilation system was passed through the bed in an upflow manner for the tests.

Total concentration of suspended particles at the inlet was on the order of 2.46 mg/m^3 (0.001 gr/ft^3) of which less than 0.025 mg/m^3 was radioactive. Particle diameter was 0.5 to 2.0 μm. Effects of bed depth, granule diameter, types of sand, and gas velocity on collection efficiency were studied. Collection efficiencies were based on the decrease of measured radioactivity of the gas passing through the bed rather than on a decrease of total particle concentration.

Table 4 shows a summary of the test results. At low gas velocities (<5 cm/s), laboratory tests indicated that collection efficiency increased with increased bed depth and finer sand grain size. Irregular grained sands gave better collection efficiencies; increasing gas velocity lowered collection efficiency. The following approximation was derived:

TABLE 4. RESULTS OF HANFORD SAND FILTER TESTS

Effect of Depth of Sand

Depth of Sand (cm)	Collection Efficiency, %
30.5	91.6
61	99.5
91.5	99.8
122	99.9

Effect of Sand Size

Sand Type	d_c (cm)	u_G (cm/s)	Collection Efficiency,%
Hanford-16+20 mesh	0.1	1.93	96.3
Hanford-20+40 mesh	0.056	1.93	99.98
Hanford-16+20 mesh	0.1	5.1	89.5
Hanford-20+40 mesh	0.056	5.1	99.88
Ottawa-20+30 mesh	0.071	2.6	96.2
Ottawa-30+40 mesh	0.048	2.6	98.6
Ottawa-20+30 mesh	0.071	5.1	92.9
Ottawa-30+40 mesh	0.048	5.1	98.2

Effect of Type of Sand

Type of Sand	Collection Efficiency, %
Hanford -20+40 mesh	99.93
A.G.S. Flint-30+40 mesh	99.84
Monterey Type G	99.61
Ean Claire Type G	99.38

Effect of Gas Velocity

u_G (cm/s)	Collection Efficiency, %
0.91	99.97
3.1	99.83
5.1	98.9
9.3	92.7
20.3	97

$$\overline{Pt} = \exp\left[\frac{-K\ Z^{0.5}}{u_G^{0.33}\ d_c^{1.33}}\right] \qquad (1)$$

where $\overline{Pt}$ = overall particle penetration on an activity basis, fraction
K = proportionality factor, dimensionless
Z = bed depth, cm
u_G = superficial gas velocity, cm/s
d_c = granule diameter, cm

On the basis of these preliminary tests, large scale sand filters were designed and set up at Hanford with a capacity of 14.2 m^3/s (30,000 CFM) each. The design face velocity was 3 cm/s (6 ft/min), and the granular layer consisted of a 61 cm (2 ft) depth of -20+40 mesh Hanford sand. Seven layers of coarser sand were also used in the bed to aid in flow distribution. Overall pressure drops were in the range of 10.2 to 17.8 cm W.C. (4 to 7" W.C.), and the average collection efficiency was about 99.7%. The potential lifetime of these sand beds was estimated at about 5 years based on estimated accumulation of particles.

Thomas and Yoder (1956 a, b) investigated the filtration of aerosols through a column of lead shot. Their data are shown in Figure 1. The experiments were conducted at low flow rates and with large diameter granules so that the effects of interception and inertia must have been negligible; the efficiency was very low. Collection was primarily by diffusion and and sedimentation, the former prevailing in the ascending branches of the curves and the later in descending. Hence, collection efficiency decreased rapidly with an increase in flow rate. Sedimentation caused the collection efficiency to differ for upwards and downwards flow as shown in Figure 1. Similar curves were obtained with columns of sand in which collection efficiency diminished appreciably with increasing flow rate and grain size; grains of irregular shape gave higher efficiency than round ones.

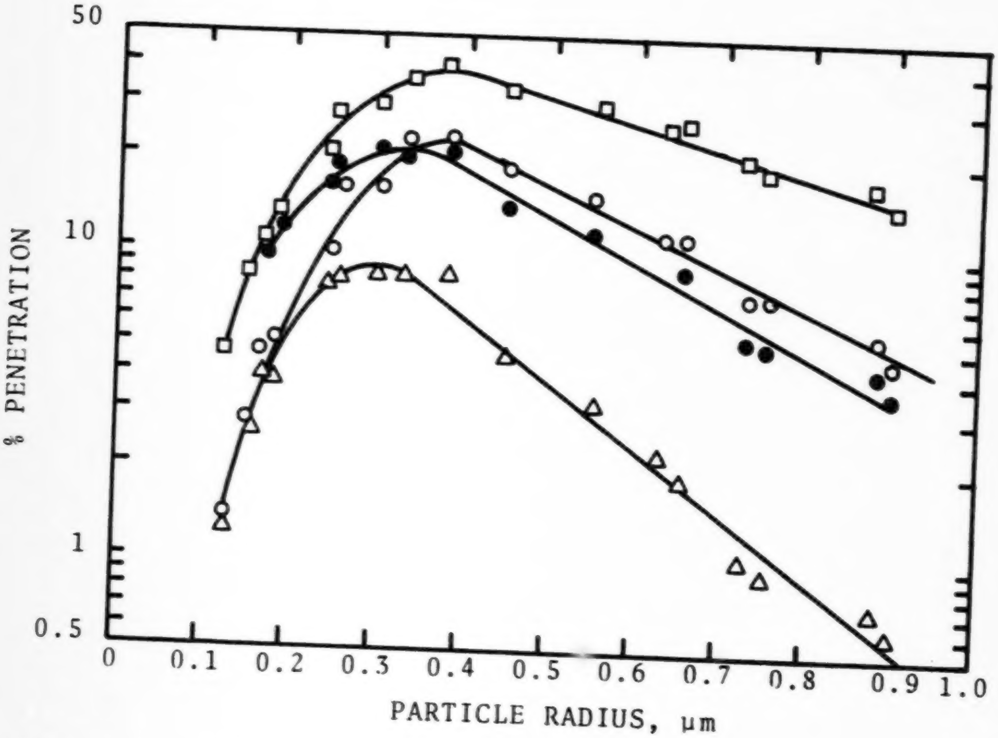

Figure 1. Filtration of aerosols through bed packed with lead shot (Thomas and Yoder data).

□ Flow up column 1.49 cm/s
● Flow down column 1.49 cm/s
○ Flow up column 0.745 cm/s
△ Flow down column 0.745 cm/s
Column height 89 cm
Column area 11.17 cm
Lead shot 0.15 cm dia.

Zahradnik et al. (1970) carried out a study on the simultaneous removal of fly ash and sulfur dioxide using a granular bed. The granular bed was a square cross-section shaft, total length 224 cm (8 ft); the top 214 cm (7 ft) served as the storage area, the remaining 30 cm (1 ft) was the actual filtering section. The cross-sectional area was 930 cm^2 (1 ft^2). The filtering medium was a slowly moving bed of 0.16 to 0.32 cm (1/16 to 1/8 in) diameter alkalized alumina particles with the solids rate controlled by a vibratory feeder at the bottom. The gas, fly ash, and sulfur dioxide flowed horizontally across the filter.

Data on the simultaneous removal runs are shown in Table 5. The SO_2 removal efficiency was 100% as determined by standard iodometric titration of inlet and outlet gas samples. The filtration efficiency was determined by passing the gas through a Cuno filter which collected all particles larger than 1 μm in diameter. For the size distribution of fly ash listed in Table 6, the overall filtration efficiency was about 99%.

Taub (1970) studied the transient behavior of granular bed filters while collecting dispersed fly ash. His results show high efficiencies are possible with clean filters, but performance deteriorates as the dust content of the filter increases.

When a clean bed is put into operation, particles are collected in the interstices of the filter near the surface. As the dust deposit builds up, the saturation zone or dust may work its way through from the dirty to the clean side of the filter. This results from the drag force exerted on the particle deposits by the gas flow. As the deposit extends through the bed, the bed is saturated with dust and reentrainment occurs causing the collection efficiency to decrease. The result of Taub's work (Figure 2) shows this trend. The collection efficiency remains initially constant with time. As the saturation zone extends through the bed, the collection efficiency declines. The work of Taub shows that a 3.3 cm deep bed of 1,500 μm particles has a capacity of approximately 3,000 g/m^2 (0.61 lb/ft^2) before the collection efficiency begins to fall.

TABLE 5. SUMMARY OF ZAHRADNIK ET AL.'S DATA

Experimental Parameter	Run #6	Run #7
Gas flow rate, Nm^3/min	0.83	0.84
Nominal space velocity, hr^{-1}	3,500	3,500
Sorbent rate, kg/hr	4.76	3.89
Temperature, °C	204	204
Inlet SO_2 mole fraction	0.006	0.006
Outlet sorbent loading, g/100 g	19	10
Fly ash loading, g/m^3	6.45	7.09
Filtration efficiency, %	99.3	98.7
SO_2 removal, %	100	100
Pressure drop, cm W.C.	5.1	5.1
Sorbent diameter, cm	0.16	0.16

Size Distribution of Fly Ash

Particle diameter, μm	% less than
104.8	100
82.2	75.5
71.6	50.0
60.8	40.0
54	23.6
39.6	17.0
32	13.9
27.4	11.0

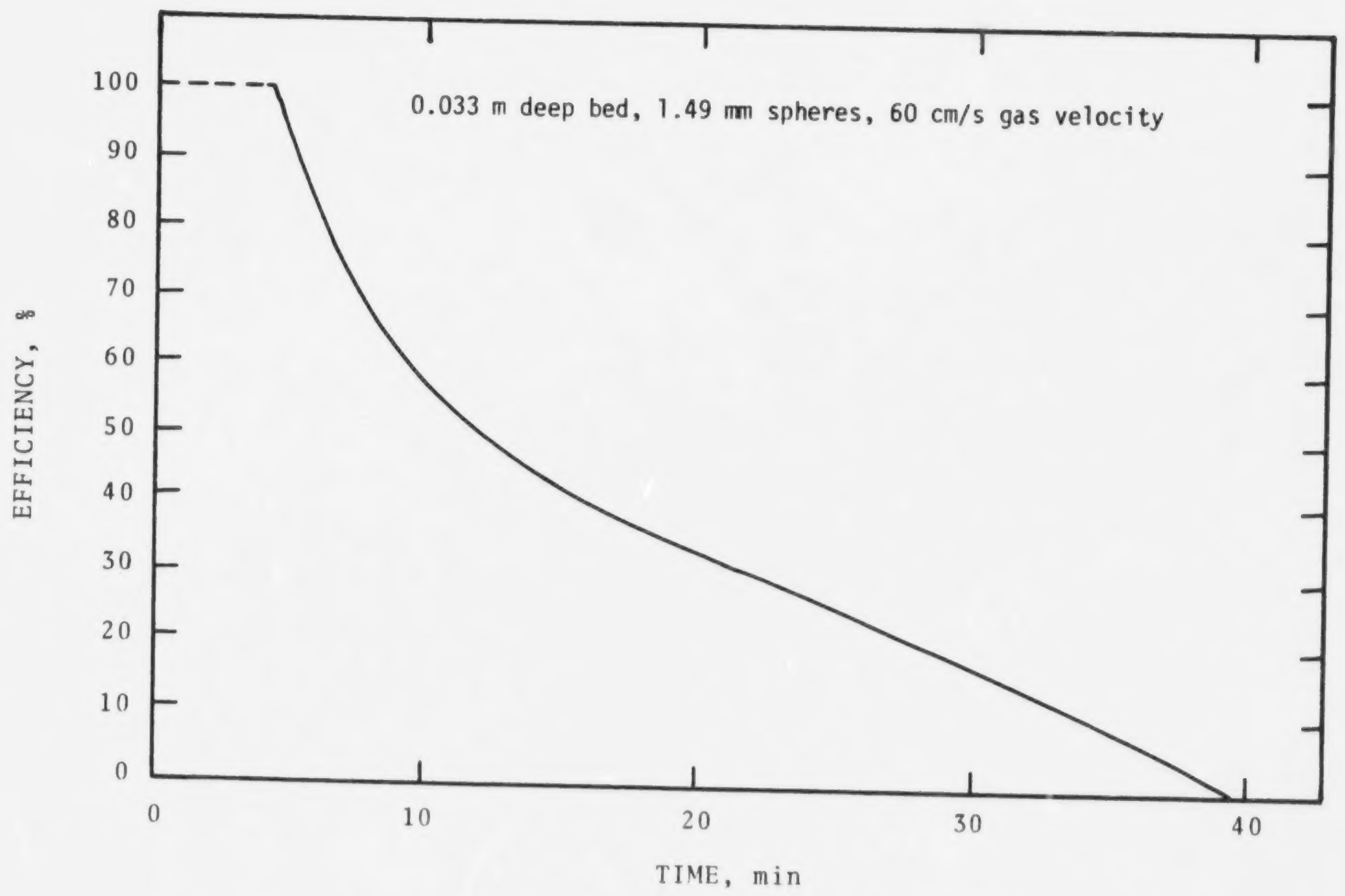

Figure 2. Time vs efficiency - 0.033 m deep granular bed filtering fly ash, (Taub's data).

TABLE 6. SLOPES AND INTERCEPTS OF FITTED LINES

Support	Superficial Velocity (cm/sec)	Particle Diameter (μm)	Slope (Transfer unit/cm)	Intercept (Transfer units) (Percent)
Screen Support	8.2	0.8	0.050	0.017 (1.7)
		1.6	0.076	0.12 (11.0)
		2.9	0.27	0.66 (48.0)
	11.2	0.8	0.054	0.017 (1.7)
		1.6	0.080	0.16 (15.0)
		2.9	0.306	0.56 (43.0)
Grid Support	8.2	0.8	0.042	0.46 (37.0)
		1.6	0.058	0.81 (55.0)
		2.9	0.336	1.04 (65.0)
	11.2	0.8	0.044	0.46 (37.0)
		1.6	0.074	0.81 (55.0)
		2.9	0.362	1.04 (65.0)

Paretsky, et al. (1971) studied the filtration of dilute aerosols by beds of sand. They studied a bed of -10+14 mesh angular sand at superficial velocities between 0.3 and 80 cm/s in a 5.1 cm diameter bed at bed heights of 3.7, 8.2, and 19.2 cm. Flow directions studied were vertically upward, vertically downward, and horizontal. Figure 3 gives data obtained at a bed height of 19.2 cm.

At superficial velocities less than about 20 cm/s, upward flow exhibited higher penetration than downward flow, the difference in penetration being greater at lower velocity. Horizontal gas flow through the sand bed resulted in penetrations between those for upward and downward flows.

Figure 4 gives data obtained at 8.2 cm height for finer sand (-20+30 mesh). The relationship between upward and downward flow data is approximately the same for the coarse sand.

Gebhart, et al. (1973) published an extensive experimental study on the collection of aerosol particles in packed beds consisting of uniform glass spheres. Monodisperse aerosols were produced by atomizing a diluted suspension of polystyrene particles and drying the spray with clean air. Aerosol particles had diameters in the 0.1 to 2 μm range. Concentration measurements in front and behind the packed bed were carried out with a Laser Aerosol Spectrometer.

The bed filter consisted of a glass cylinder with an inside diameter of 8 cm. The cylinder can be filled with glass beads to a maximum height of 41 cm. The inlet and outlet of the filter were funnel shaped to give uniform flow distribution over the filter. Bead sizes investigated were 0.4, 0.16, 0.05 and 0.0185 cm in diameter. The bed was a horizontal bed and gas flow was in a downward direction.

The particle penetrations are plotted against particle diameter for four different bead sizes in Figures 5-8. The parameter in each of the diagrams is the mean air velocity inside the filter; i.e., interstitial velocity. Interstitial gas velocity is related to superficial gas velocity by:

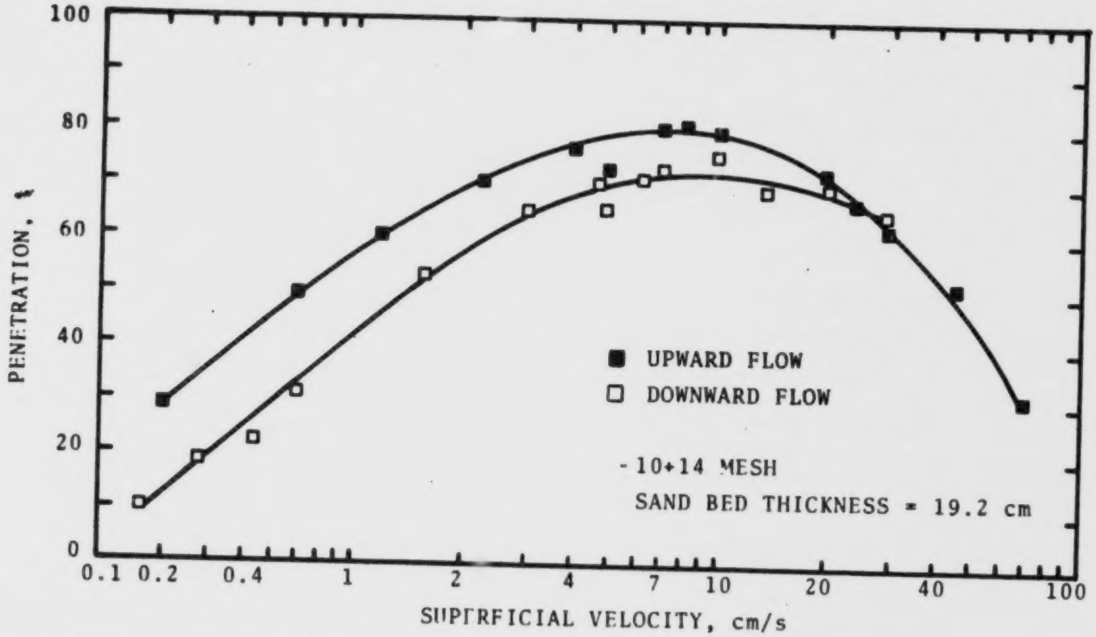

Figure 3. Penetration of 1.1 μm aerosol as a function of superficial gas velocity: 10-14 mesh sand (Paretsky et al. data).

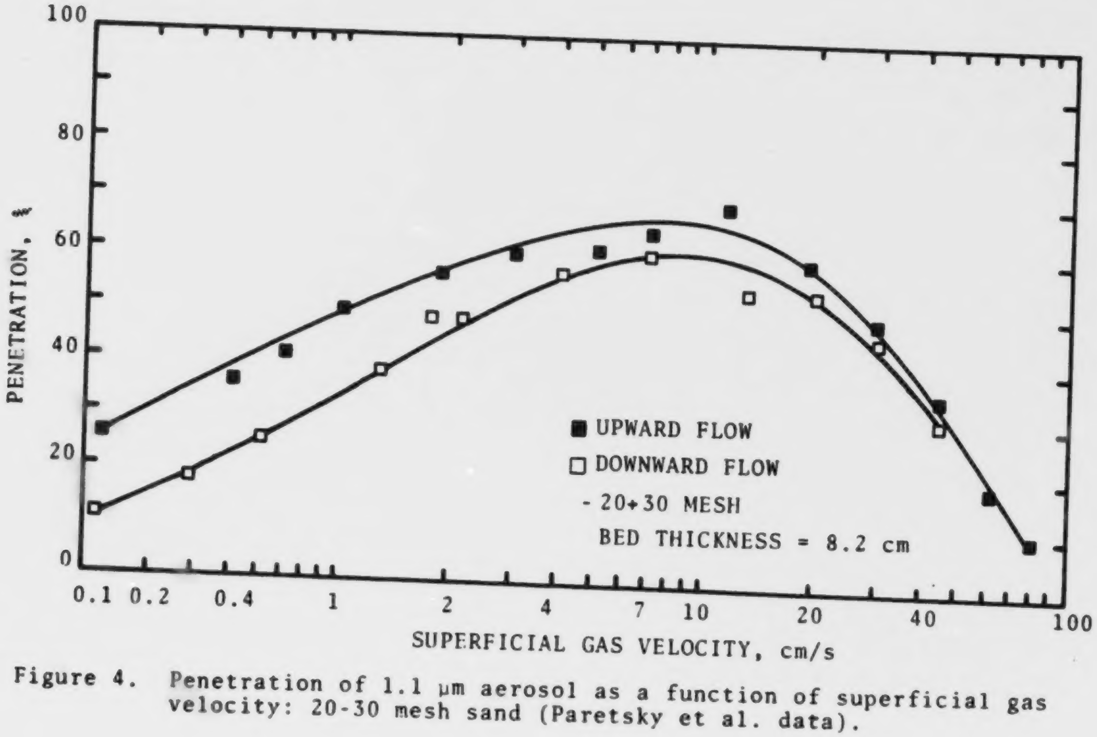

Figure 4. Penetration of 1.1 μm aerosol as a function of superficial gas velocity: 20-30 mesh sand (Paretsky et al. data).

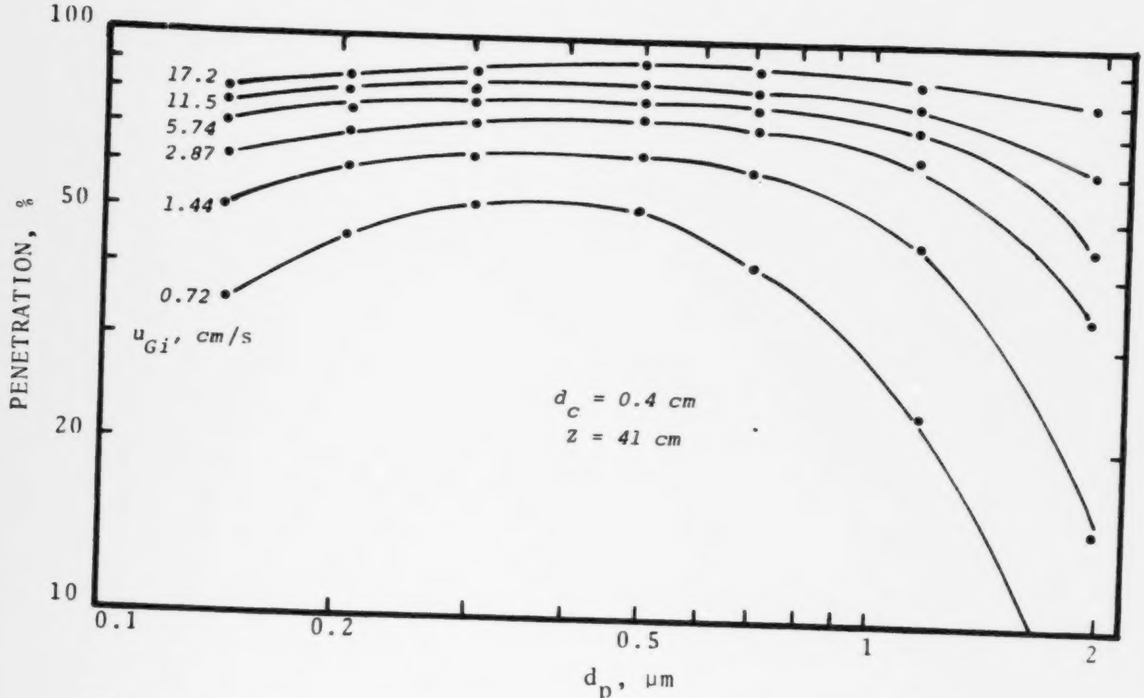

Figure 5. Experimental results obtained by Gebhart et al: Penetration versus particle diameter for different flow velocities and granule size.

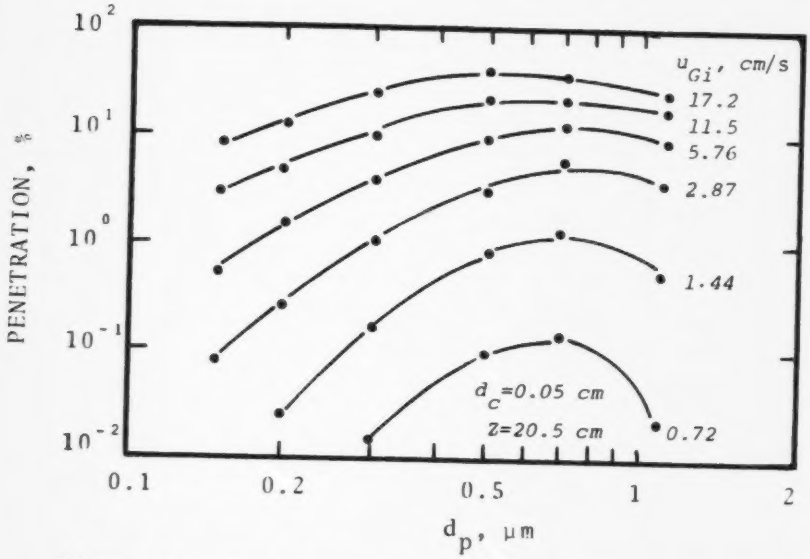

Figure 6. Experimental results obtained by Gebhart et al: Penetration versus particle diameter for different flow velocities and granule size.

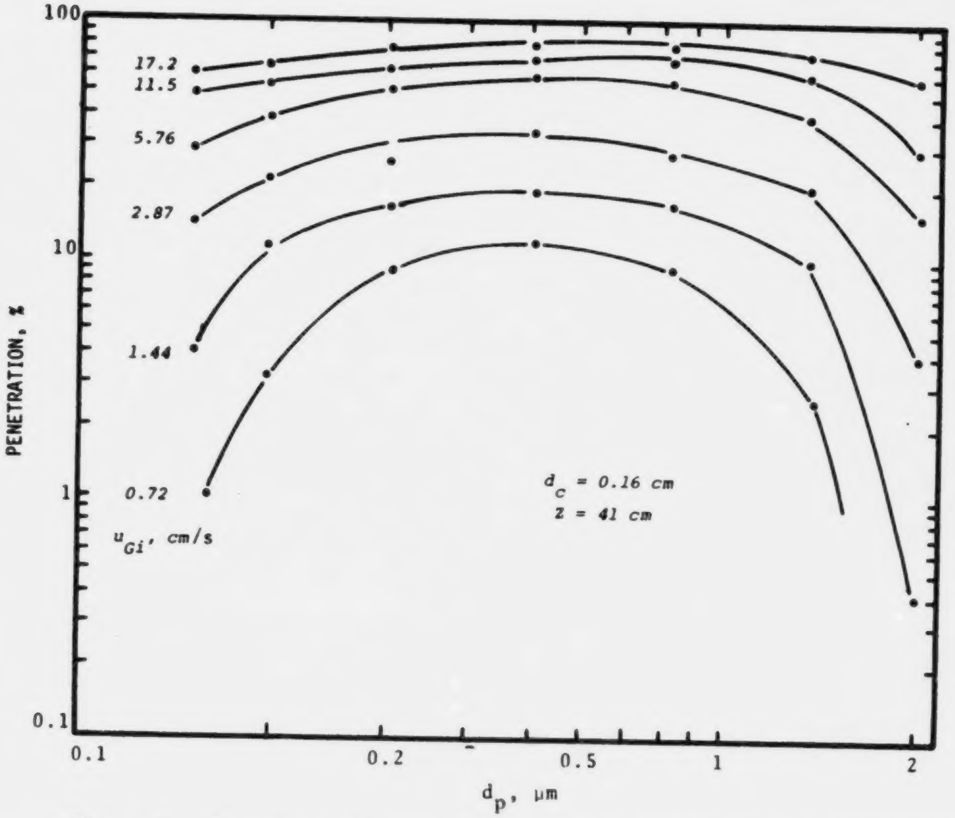

Figure 7. Experimental results obtained by Gebhart et al: Penetration versus particle diameter for different flow velocities and granule size.

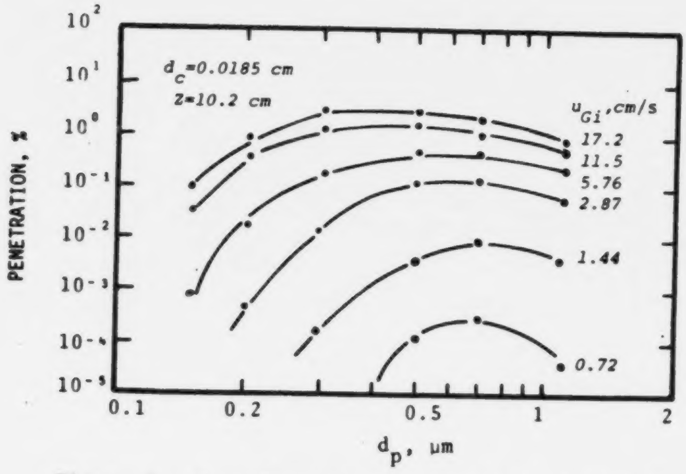

Figure 8. Experimental results obtained by Gebhart et al: Penetration versus particle diameter for different flow velocities and granule size.

$$u_{Gi} = \frac{u_G}{\varepsilon} \qquad (2)$$

The porosity of the bed, ε, was found to be 0.385 for all bead sizes used.

The diffusion and the sedimentation branches of the penetration curves are clearly distinguishable. In between there exists a penetration maximum. The position of this maximum is shifted to larger particles with decreasing bead diameter. The exact position of maximum penetration is a characteristic feature of the size and shape of the bed material.

There is a difference in measured penetrations for downward and upward flow, as shown in Figures 9 and 10. This is an indication that gravity is important. Downward flow gives lower penetration because the vectors of the flow velocity and settling velocity are complimentary. For aerosols with diameter less than 0.3 μm, the gravity effect is negligible.

Knettig and Beeckmans (1974) studied the capture of monodisperse aerosol particles in the size range 0.8-2.9 μm in a screen-supported and in a grid-supported fixed bed of 425 μm glass beads. Monodispersed aerosol particles (1:2 weight ratio of uranine and methylene blue) were obtained from a spinning disk aerosol generator. The charges on the aerosol particles were neutralized by a radioactive source in the aerosol generator. The aerosol particles were sampled isokinetically upstream and downstream of the test bed, and were analyzed quantitatively by fluorometry. All experiments were performed at ambient temperature and pressure. The bed was a horizontal bed with a diameter of 12.7 cm. The gas flow was in an upward direction.

Figures 11 and 12 are experimental results. Figure 11 shows collection efficiency, expressed in transfer units (number of transfer units, NTU = -lnPt), plotted against bed height, for the bed supported on a screen, at a superficial velocity of 8.2 cm/s. The screen was a 100-mesh screen (open area 30.3%). Figure 12 shows a similar plot for a perforated aluminum plate, 1.6 mm thick. The plate had 144 holes spaced at 10 mm from center to

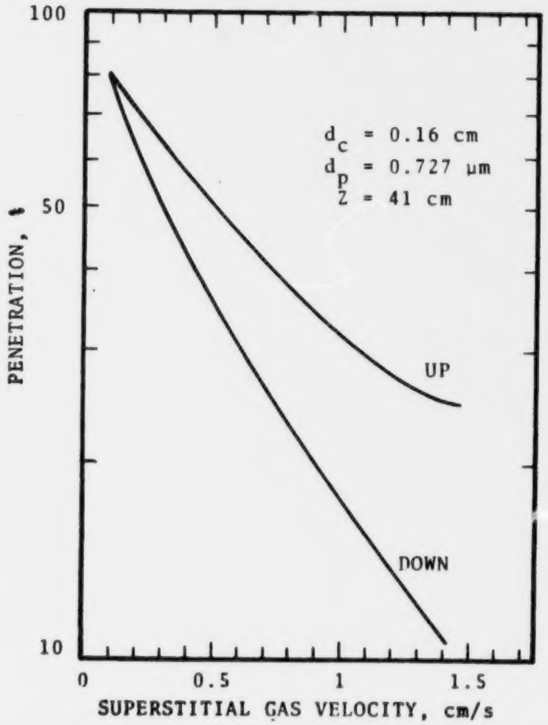

Figure 9. Gravity effect in granular beds measured with an upward and downward directed aerosol stream (Gebhart et al. data).

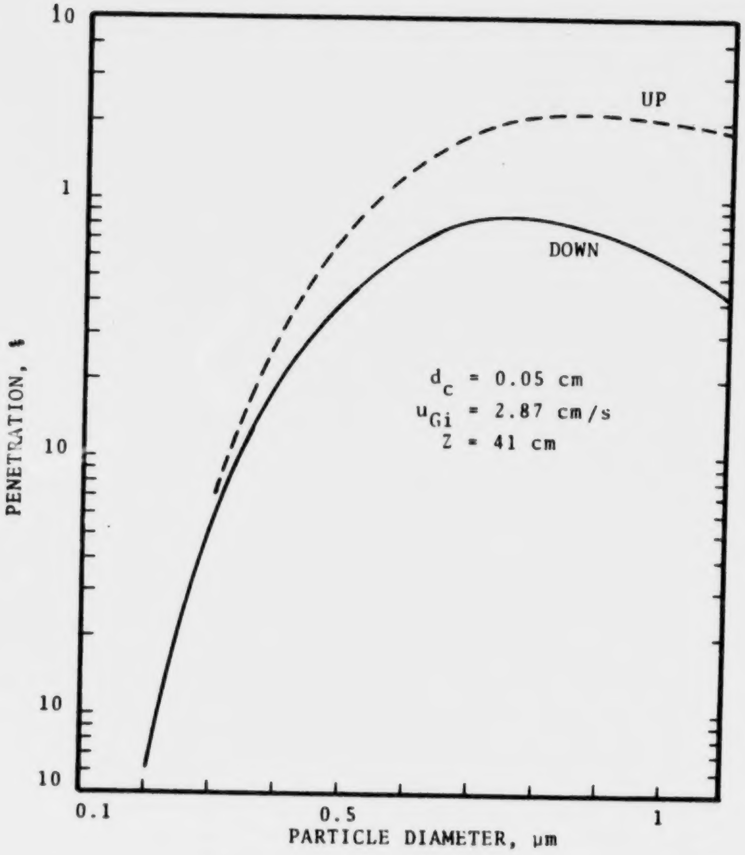

Figure 10. Gravity effect in granular beds measured with an upward and downward directed aerosol stream (Gebhart et al. data).

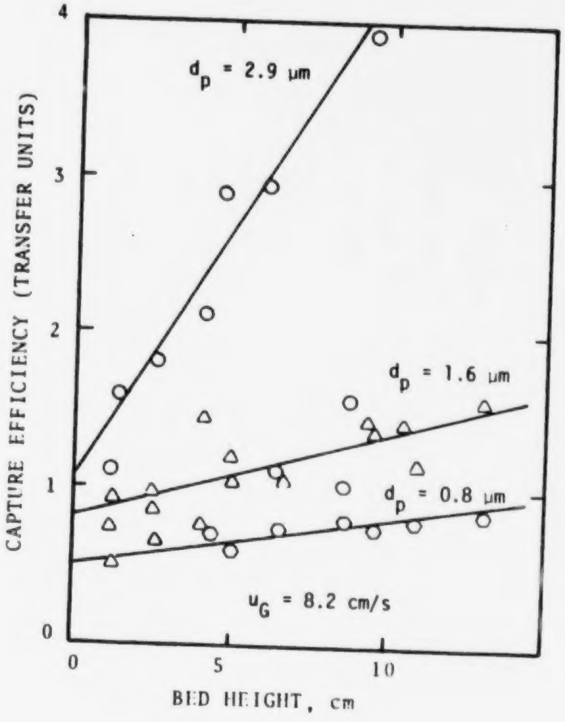

Figure 11 . Capture efficiency (transfer units) versus bed height for the grid supported fixed bed (Knettig and Beeckmans data).

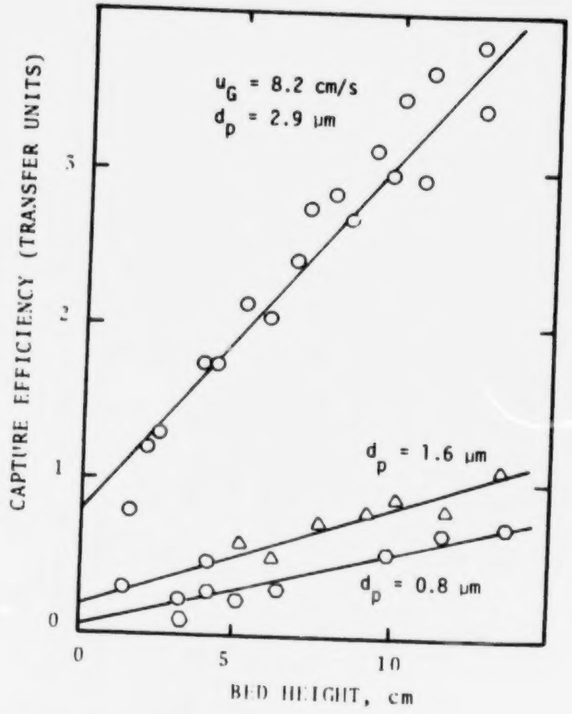

Figure 12 . Capture efficiency (transfer units) versus bed height for the screen supported fixed bed (Knettig & Beeckman).

center. The diameter of the holes was 0.794 mm, resulting in an open area of 0.569%.

All of the curves gave a linear relationship between collection efficiency, expressed in transfer units, and bed height. Straight lines were fitted to the data by least squares. Table 6 shows the results for other superficial gas velocities. A linear relationship implies that collection efficiency per unit volume of bed is independent of bed height. Impaction appears to have been the primary collection mechanism in the body of the bed because collection efficiency per unit volume of bed increased with both superficial gas velocity and aerosol particle size.

Substantial aerosol capture occurred at the bed supports, especially the grid support. This is because each grid hole acted as a jet and caused the aerosol particles to be collected on the glass beads by inertial impaction. However, the slopes of the least square fitted lines for screen-supported and grid-supported beds are the same.

Miyamoto and Bohn (1975) studied the effect of particle loading on collection efficiency of granular bed filters. They used water-washed river gravel for granules and ammonium chloride fume for particles. The particle diameter was 0.1 to 3 μm.

The relationship between granular bed collection efficiency and particle loading on the filter is presented for different gravel diameter (Figure 13), bed depth (Figure 14) and superficial gas velocity (Figure 15). Particle loading is defined as the weight of particles collected per unit bed area. From Figures 13 through 15 the following observations may be made:

1. The collection efficiency increased with increasing particle loading. The collected particles decrease bed porosity and thereby increase filtering efficiency.

2. Smaller granule diameters result in higher collection efficiency and a sharper increase of collection efficiency with particle loading.

3. Thicker gravel layers had higher initial collection efficiencies but little influence on collection efficiency at

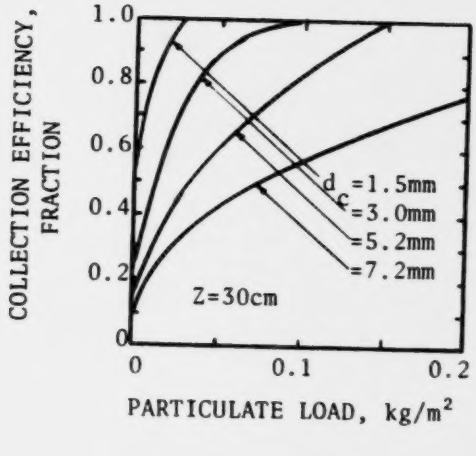

Figure 13.
Effect of mean gravel diameter and particulate load on granular bed collection efficiency (Miyamoto and Bohn's data).

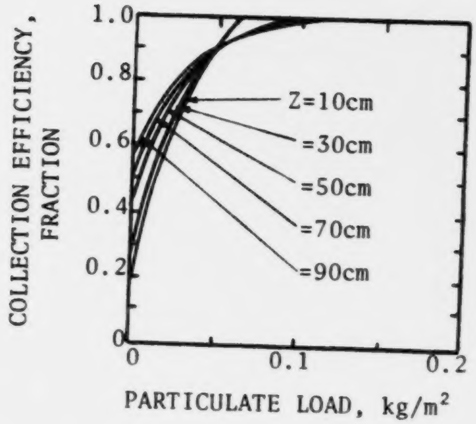

Figure 14.
Effect of gravel layer thickness and particulate load on granular bed collection efficiency (Miyamoto and Bohn's data).

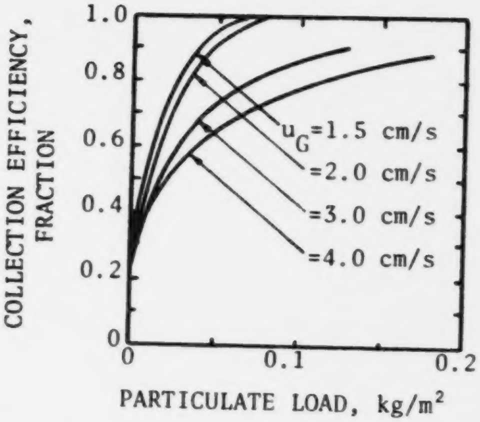

Figure 15.
Effect of superficial gas velocity and particulate load on granular bed collection efficiency (Miyamoto and Bohn's data).

higher particle loading because the collection is preferentially near the surface where collected particles tend to form a cake.

4. Higher superficial gas velocities markedly decreased the rate of increase in efficiency with particle loading, probably because filter cake is less stable at higher velocities.

Figueroa (1974) and Figueroa and Licht (1976) conducted an experimental program to determine the aerosol filtration efficiency of a bed of granular solids. The bed was a 10.2 cm (4 inch) I.D. column packed with plastic beads and sand to various depths. The bed support was made of 325 mesh stainless steel screen.

Two different size fractions of plastic beads (polyacrylonitrile) and one grade of sand were used as granular bed solids. The properties of the granular materials are listed in Table 7.

Two test aerosols were used: monodispersed methylene blue (MB) particles 1 μm and 2 μm in diameter and monodispersed polystyrene latex microspheres 0.50, 1.10, and 2.02 μm in diameter. Aerosol number concentrations before and after the bed were measured with an optical counter.

Bed penetration was measured as a function of aerosol particle diameter, granule diameter, bed depth, direction of flow, and superficial gas velocity. Figures 16 through 19 summarize their data. For the low gas velocity range (20 cm/s), they observed, for a fixed bed, that particle collection efficiency always increases with decreasing granule diameter and increasing bed depth. Downward flow gives higher collection efficiency than upward flow. The collection efficiency of a granular material with inherent electrostatic charging properties (e.g., plastic beads) is higher than for a granular material without those properties (e.g., sand).

Westinghouse Research Laboratories (Ciliberti, 1977) carried out an experimental program to investigate efficiency and operability of granular bed filters. The experimental bed was designed with a 233 cm (0.25 ft) cross section. The bed was cleaned by fluidization. A distributor consisting of several independent drilled tubes was used to control the fluidizing gas flow. The

TABLE 7. EXPERIMENTALLY DETERMINED PROPERTIES OF THE GRANULAR MATERIALS (Figueroa, 1974)

			POLYACRYLONITRILE		SAND
PROPERTY	SYMBOL	UNITS	-25 + 40 mesh	-40 + 60 mesh	-25 + 40 mesh
Number Median Diameter	d_{cN}	micrometers	495	305	680
Sauter Diameter	d_{32}	micrometers	514	339	702
Geometric Standard Deviation	σ_g	micrometers	1.13	1.23	1.12
Solid Granule Density	ρ_s	g/cm³	1.10	1.12	3.10
Bulk Density	--	g/cm³	0.67	0.66	1.85
Porosity or Voidage Fraction	ε	--	0.39	0.38	0.41

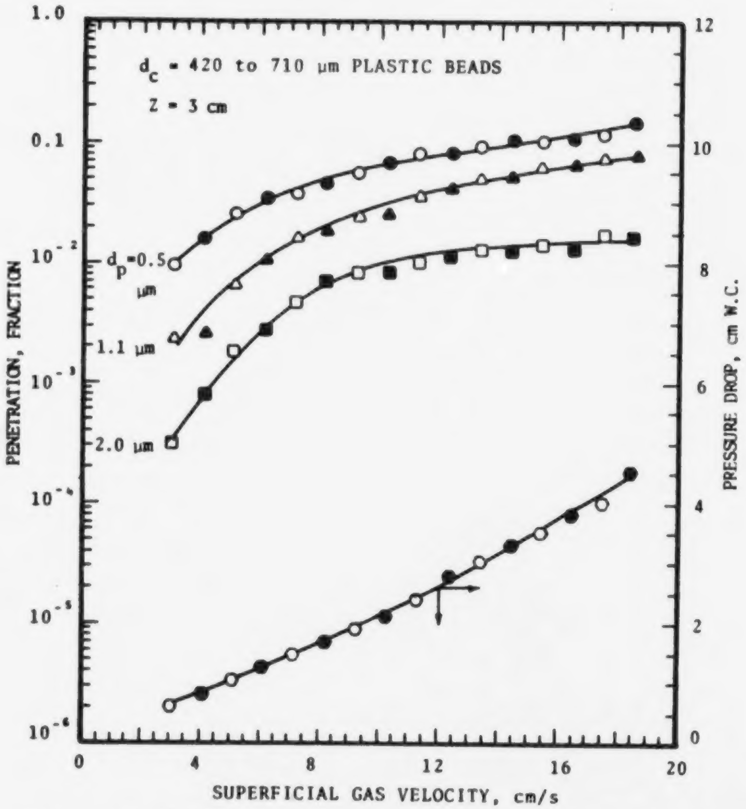

Figure 16. Penetration tests on 420 to 710 micrometers plastic beads by monodispersed polystyrene latex aerosol (downflow) (Figueroa and Licht's data).

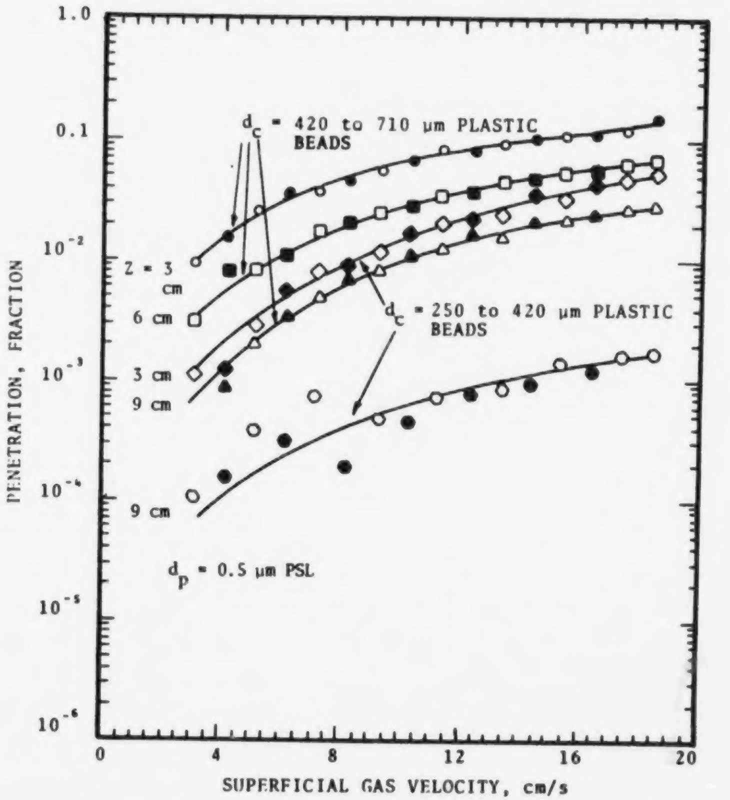

Figure 17. Effect of bed height and bed granule (bead) size on the downflow penetration of 0.5 micrometers polystyrene latex aerosol particles on plastic beads (Figueroa and Licht's data).

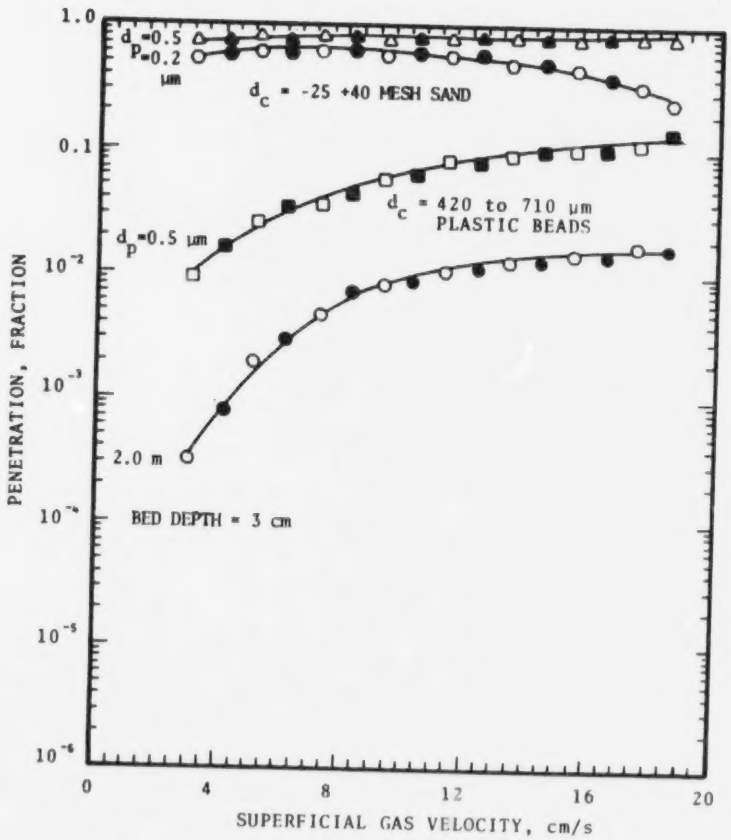

Figure 18. Comparison of downflow penetration of polystyrene latex aerosol particle on 420 to 710 micrometers plastic beads and -25 +40 mesh sand granules (Figueroa and Licht's data).

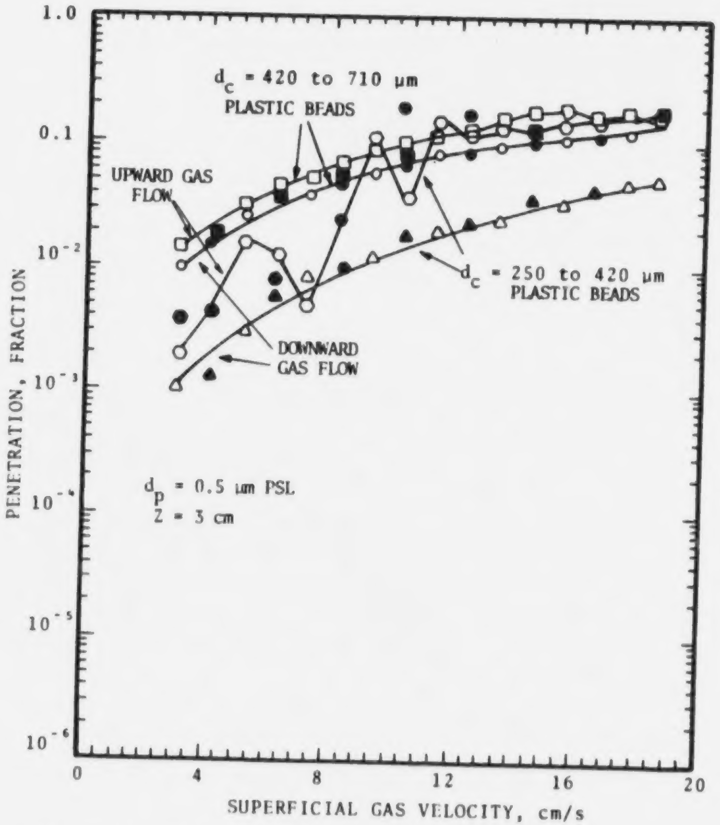

Figure 19. Effect of bed granule (bead) size and flow direction on the penetration of 0.5 micrometer polystyrene latex aerosol particles on plastic beads. Bed weight = 150 grams, bed height = 3 cm (Figueroa and Licht's data).

arrangement of the bed is illustrated in Figure 20.

Bed depth ranged from 7.6 cm to 15.2 cm (3 to 6 in.) based on requirements to minimize pressure drop while maintaining a bed that can be successfully fluidized for cleanup. Granule size was in the range of 15 to 30 mesh to achieve efficient dust collection with small bed depth and reasonable pressure drop. Superficial gas velocity ranged from 9 to 30 cm/s. The test dust was finely ground (<10 μm) limestone dispersed in a high velocity air jet. The layout of the experimental equipment is shown in Figure 21.

Test results are summarized in Tables 8 through 12. Particle size and mass data were taken with cascade impactors. Collection efficiency for submicron particles was high. The grade efficiency curves were flat and showed high collection efficiency for all particle sizes. This was consistent with the observed formation of a filter cake.

To investigate dust accumulation in the bed, Westinghouse made a series of five runs. The initial clean bed material was sampled, then after five consecutive runs bed samples were taken at four levels through the bed.

The clean bed contained 0.5 wt % fine dust. After five runs the dust content of the bed was 1.3 wt %. At the end of the filtration cycle, the dust level at the bed surface was 10 wt %. However, at levels 2.5 cm below the surface and greater the dust level was uniform at 1.3 wt %.

A second test over ten cycles showed dust accumulation of 1.0 to 1.8 wt % in the bed.

Another filter, 0.65 m^2 (7 ft^2), was tested at temperature of 1,100°F at atmospheric pressure. Because of operating problems tests were discontinued.

Combustion Power Company has conducted extensive cold flow tests on a moving bed granular bed filter. These results will be discussed later.

High Temperature Filtration

Dennis et al. (1960), in designing an incinerator for disposal of low-level radioactive wastes from hospitals or biological

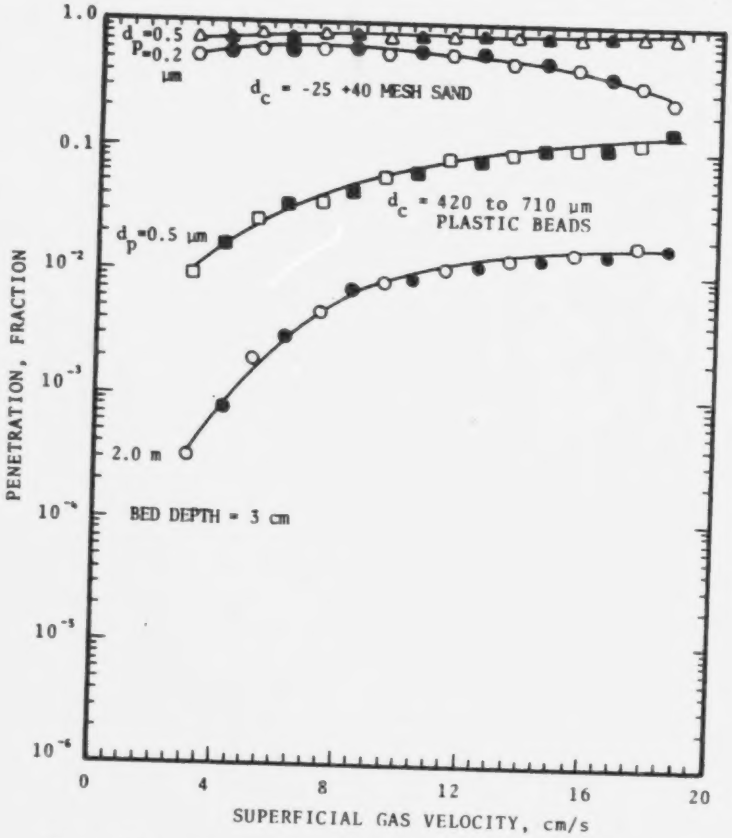

Figure 18. Comparison of downflow penetration of polystyrene latex aerosol particle on 420 to 710 micrometers plastic beads and -25 +40 mesh sand granules (Figueroa and Licht's data).

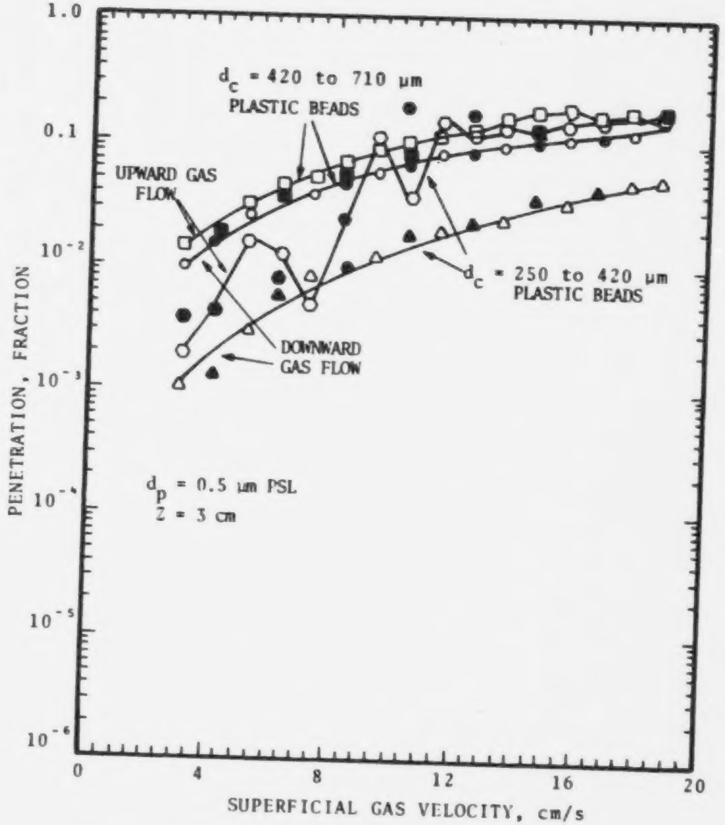

Figure 19. Effect of bed granule (bead) size and flow direction on the penetration of 0.5 micrometer polystyrene latex aerosol particles on plastic beads. Bed weight = 150 grams, bed height = 3 cm (Figueroa and Licht's data).

arrangement of the bed is illustrated in Figure 20.

Bed depth ranged from 7.6 cm to 15.2 cm (3 to 6 in.) based on requirements to minimize pressure drop while maintaining a bed that can be successfully fluidized for cleanup. Granule size was in the range of 15 to 30 mesh to achieve efficient dust collection with small bed depth and reasonable pressure drop. Superficial gas velocity ranged from 9 to 30 cm/s. The test dust was finely ground (<10 μm) limestone dispersed in a high velocity air jet. The layout of the experimental equipment is shown in Figure 21.

Test results are summarized in Tables 8 through 12. Particle size and mass data were taken with cascade impactors. Collection efficiency for submicron particles was high. The grade efficiency curves were flat and showed high collection efficiency for all particle sizes. This was consistent with the observed formation of a filter cake.

To investigate dust accumulation in the bed, Westinghouse made a series of five runs. The initial clean bed material was sampled, then after five consecutive runs bed samples were taken at four levels through the bed.

The clean bed contained 0.5 wt % fine dust. After five runs the dust content of the bed was 1.3 wt %. At the end of the filtration cycle, the dust level at the bed surface was 10 wt %. However, at levels 2.5 cm below the surface and greater the dust level was uniform at 1.3 wt %.

A second test over ten cycles showed dust accumulation of 1.0 to 1.8 wt % in the bed.

Another filter, 0.65 m^2 (7 ft^2), was tested at temperature of 1,100°F at atmospheric pressure. Because of operating problems tests were discontinued.

Combustion Power Company has conducted extensive cold flow tests on a moving bed granular bed filter. These results will be discussed later.

High Temperature Filtration

Dennis et al. (1960), in designing an incinerator for disposal of low-level radioactive wastes from hospitals or biological

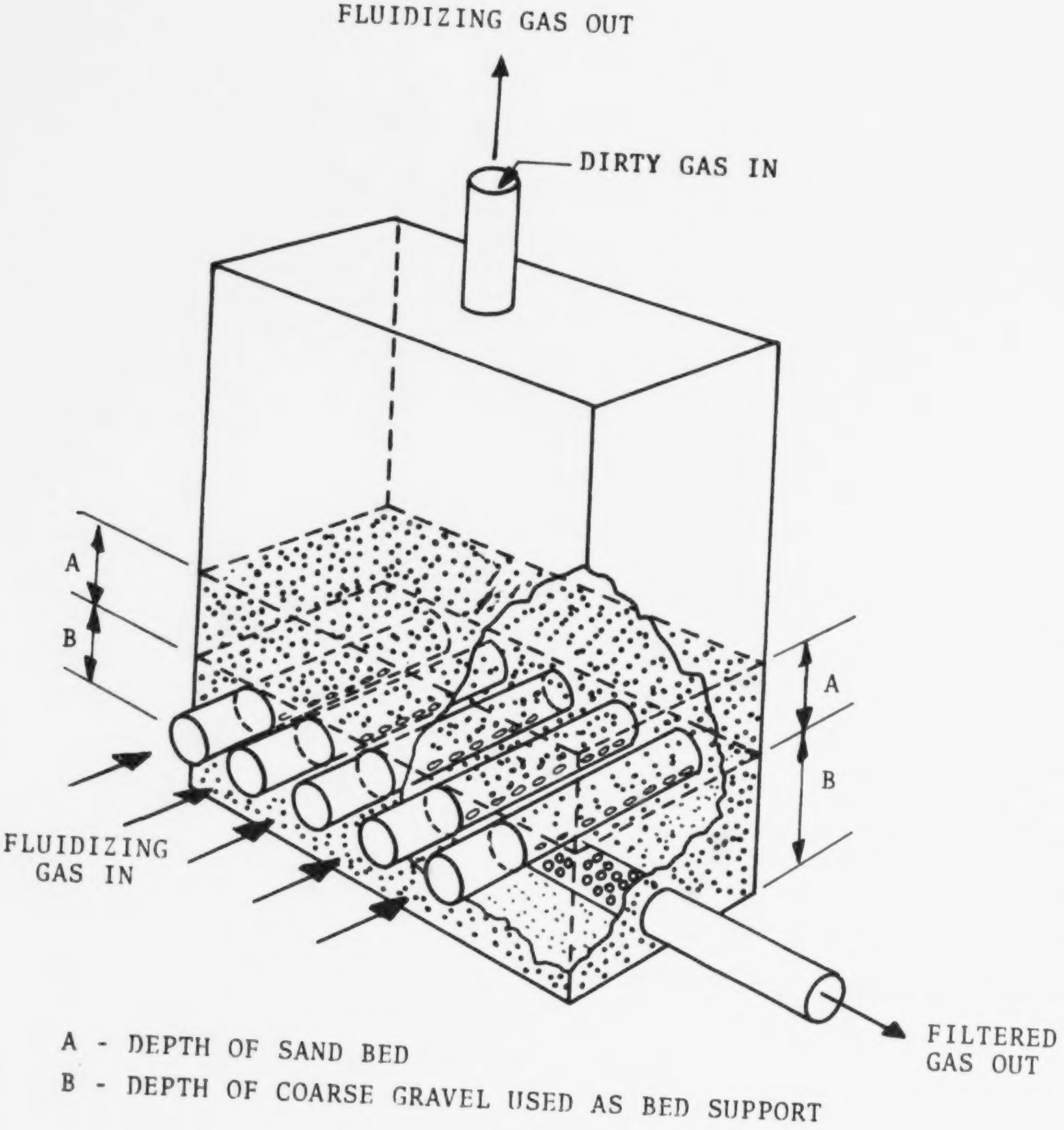
FLUIDIZING GAS OUT
DIRTY GAS IN
A
B
A
B
FLUIDIZING GAS IN
FILTERED GAS OUT
A - DEPTH OF SAND BED
B - DEPTH OF COARSE GRAVEL USED AS BED SUPPORT

Figure 20. Schematic of granular bed filter (Westinghouse setup).

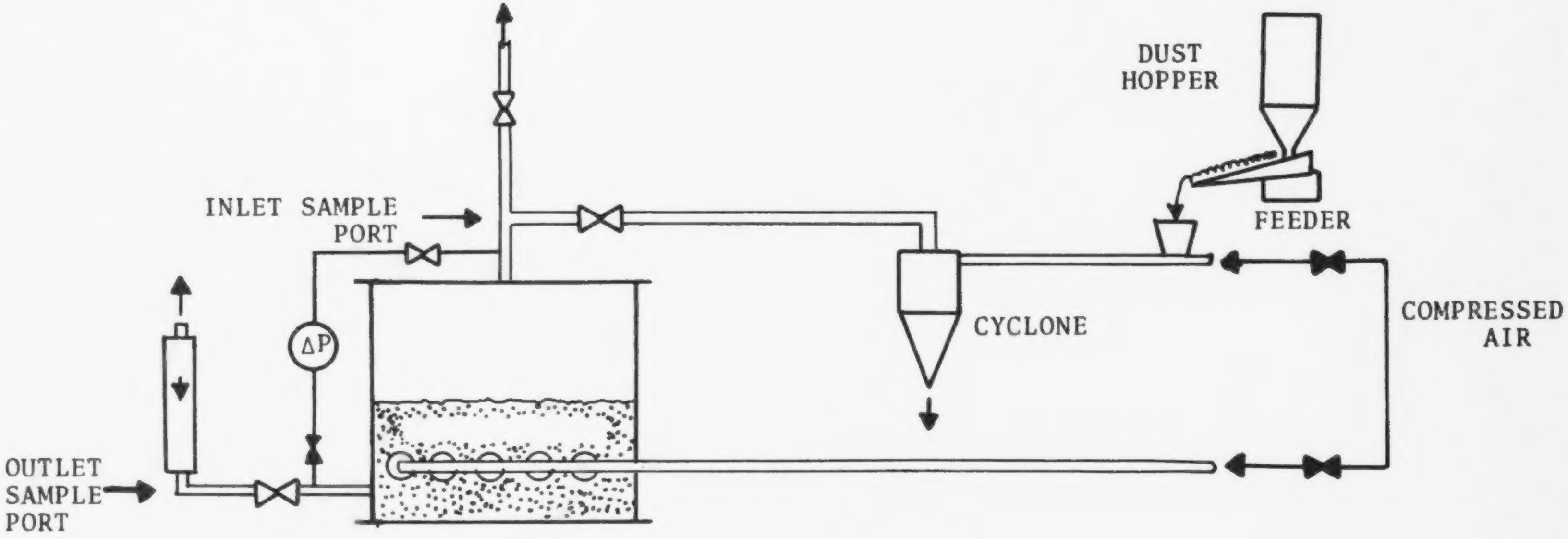
DUST
HOPPER
FEEDER
INLET SAMPLE
PORT
ΔP
CYCLONE
COMPRESSED
AIR
OUTLET
SAMPLE
PORT

Figure 21. Schematic of test equipment (Westinghouse).

TABLE 8. WESTINGHOUSE GBF DATA

Series #2 Gas Velocity: 17.8 cm/s (± 10%)
Bed Material-20+30 mesh Ottawa sand
Bed Depth: 7.6 cm (3 in.)

Particle Size (μm)	Inlet Dust (Typical) mg/m³	Outlet Dust (Typical) mg/m³	Collection Efficiency, %
0-0.3	30.6	0.93	96.9
0.3-0.45	71.8	1.81	97.5
0.45-0.75	120.6	2.6	97.8
0.75-1.5	132.4	1.5	98.9
1.5-2.3	59.0	0.3	99.4
2.3-3.3	10.5	0.25	97.6
3.3-5.0	12.3	0.25	98.0
5.0-8.0	10.5	0.05	99.5
8.0+	10.0	0.1	99.0
8.0+	14.1	0.1	99.2

Run No.	Inlet Loading g/m³	Overall Efficiency, %
2.7	0.28	98.8
2.8	0.47	98.3
2.9	2.5	97.9
2.10	1.5	97.5

TABLE 9 . WESTINGHOUSE GBF DATA

Series #3

Gas Velocity: 10.2 cm/s (± 10%)
Bed Material-20+30 mesh Ottawa sand
Bed Depth: 7.6 cm

Particle Size (μm)	Inlet Dust (Typical) mg/m³	Outlet Dust (Typical) mg/m³	Collection Efficiency, %
0-0.3	12.9	1.1	91.5
0.3-0.45	43.5	2.7	93.8
0.45-0.75	102.0	3.6	96.5
0.75-1.5	194.0	2.5	98.7
1.5-2.3	203.0	0.5	99.8
2.3-3.3	105.0	0.1	99.9
3.3-5.0	108.0	0.05	99.95
5.0-8.0	59.0	--	100.0
8.0 +	111.0	--	100.0
8.0 +	230.0	--	100.0

Run No.	Inlet Loading g/m³	Overall Efficiency, %	
3.11	0.6	97.2	(95.5)
3.12	1.16	99.0	(98.8)
3.13	0.72	99.2	(98.5)
3.14	0.72	97.7	(96.2)
3.15	0.78	99.4	(99.4)*

*Increased gas rate to 17.8 cm/s

TABLE 10. WESTINGHOUSE GBF DATA

Series #5

Gas Velocity: 25.4 cm/s (± 10%)
Bed Material-20+30 mesh Ottawa sand
Bed Depth: 7.6 cm

Particle Size (μm)	Inlet Dust mg/m³	Outlet Dust mg/m³	Collection Efficiency, %
0-0.3	52	--	100.0
0.3-0.45	66	0.1	99.8
0.45-0.75	100	0.14	99.8
0.75-1.5	138	0.2	99.8
1.5-2.3	79	--	100.0
2.3-3.3	37	--	100.0
3.3-5.0	41	--	100.0
5.0-8.0	34	--	100.0
8.0+	73	--	100.0
8.0+	221	--	100.0

Run No.	Inlet Loading mg/m³	Overall Efficiency, %
5-22	1.0	99.96
5-23	0.8	99.95

TABLE 11. WESTINGHOUSE GBF DATA

Series #6 Gas Velocity: 25.4 cm/s (± 10%)
Bed Material-16+20 mesh Ottawa sand
Bed Depth: 10.2 cm

Particle Size (μm)	Inlet Dust mg/m³	Outlet Dust mg/m³	Collection Efficiency, %
0-0.3	32	0.39	98.8
0.3-0.45	20	0.08	99.6
0.45-0.75	33	0.12	99.6
0.75-1.5	53	0.08	99.8
1.5-2.3	47	0.04	99.9
2.3-3.3	32	0.04	99.9
3.3-5.0	53	0.04	99.9
5.0-8.0	46	--	100.0
8.0	108	--	100.0
8.0	513	--	100.0

Run No.	Inlet Loading mg/m³	Overall Efficiency, %	
6-24	5.8	99.96	(99.92)
6-25	0.94	99.92	(99.8)
6-26	1.17	99.90	(99.7)

TABLE 12. WESTINGHOUSE GBF DATA

Series #7

Gas Velocity: 17.8 cm/s (± 10%)
Bed Material-16+20 mesh sand
Bed Depth: 10.2 cm

Particle Size (µm)	Inlet Dust Run 7-27 (mg/m³)	Inlet Dust Run 7-28 (mg/m³)
0-0.3	9.4	11.7
0.3-0.45	25.9	42.4
0.45-0.75	51.8	73.0
0.75-1.5	56.5	88.3
1.5-2.3	16.5	41.2
2.3-3.3	--	7.1
3.3-5.0	--	2.4
5.0-8.0	--	1.2
8.0+	1.2	--
8.0+	2.4	--
TOTAL	163.5	266.0

Overall Efficiency

7-27	99.55%
7-28	99.58%

laboratories, used a 20 cm (8 in.) layer of 0.64 cm (0.25 in.) gravel to screen out coarse particles before the gas passed through a 5.1 cm (2 in.) bed of slag wool. This filter unit, with a 2,600 cm^2 (2.8 ft^2) filter area, was housed in half of a 55-gal drum located approximately 244 cm (8 ft) downstream from the incinerator. Gases exiting from the incinerator at 870 to 982°C (1,600 to 1,800°F) were passed at negative pressure through a water-cooled condenser so that filtration gas temperatures were 93 to 427°C (200 to 800°F) with a pressure drop of about 2.5 cm W.C. (1 in. W.C.). In one series of tests in which 408 kg (900 lb) of sawdust was burned, the pressure drop increased from 1.3 cm W.C. to 1.8 cm W.C. (0.5 to 0.7 in. W.C.) with a 90-98% filter collection efficiency on a weight basis.

Strauss and Thring (1960) carried out studies on filtration of submicron fumes from open hearth furnace gases using a granular bed. The bed was 5.1 cm (2 inches) in diameter and consisted of 0.79 (5/16 in.) crushed high temperature insulating bricks. Experiments were run with variety of bed thicknesses and gas flow rates. Collection efficiency tests were carried out on cold and preheated beds.

Table 13 shows data obtained from Strauss and Thring's granular bed filter study.

Collection efficiencies of 59.3 to 96.3% were obtained with a bed depth of 25 to 26.7 cm (1 to 10.5 in.), average gas velocities of 36.3 to 102.2 cm/s (1.2 to 3.4 ft/s), and maximum pressure drops of 0.97 to 12.4 cm W.C. (0.38 to 4.9 in W.C.) at gas temperatures from 230 to 520°C.

Further theoretical studies by Thring and Strauss (1963) considered the effect of high temperature on particle collection mechanisms. The controlling mechanism in these tests might be inertial impaction, but they emphasized the importance of the effect of inlet dust concentration on efficiency. It was maintained that dust particle agglomeration in the bed occurring in the tortuous paths between the collecting granules plays a highly significant role in collection. Increased mass flow

TABLE 13. DATA OBTAINED FROM STRAUSS AND THRING GRANULAR BED FILTER STUDY

Test No.	Furnace Operation	Test Time (min)	Gas Mass Flowrate kg/m² -hr	u_G cm/s	T_G °C	Inlet Fume Concentration g/Nm³	Fe_2O_3 in Fume Wt %	Z (cm)	Collection Efficiency Wt %	Collection Efficiency of Fe_2O_3, Wt %	Pressure Drop cm W.C.
3	R*	13	1,103	43.6	230	1.63	--	26.7	90.5	--	5.6
4	R	15	996	36.6	230	4.14	--	26.7	96.3	--	5.6
5	C	19	1,098	44.8	275	0.123	--	26.7	87.3	--	6.6
8	C	4.88	839	36.3	290	6.26	--	26.7	87.6	--	8.9
9	R	13.13	708	29.3	270	3.83	--	26.7	94.7	--	10.2
10	O	6.95	683	24.1	237	6.24	78	22.9	85.0	87.3	11.9
12	R	15.1	1,044	50.9	345	0.93	64	22.9	90.2	96.0	5.6
14	A	14.4	1,035	47.0	303	0.54	20	22.9	84.0	97.1	6.1
15	T	12.7	996	46.4	317	0.60	23	22.9	87.5	98.1	6.4
32	M	24.9	615	28.1	305	0.127	36	22.9	84.6	85.7	12.4
36	M	20.4	786	38.4	352	0.163	44.2	22.9	74.3	74.1	9.1
37	R	10.3	976	45.8	300	1.24	55.2	22.9	94.2	--	9.9
41	R	20.6	1,650	102.2	520	1.73	--	7.6	85.3	--	5.3
45	R	13.0	1,005	39.3	225	0.595	--	7.6	65.5	--	1.8
49	F	10.4	1,547	89.7	460	0.232	--	7.6	82.7	--	6.0
56	R	15.1	1,249	63.7	370	0.573	--	2.5	59.3	--	0.97
71	R	22.2	1,532	76.6	360	1.18	--	2.5	87.0	--	2.2
80	R	15.9	1,728	70.2	455	4.94	--	2.5	88.2	--	1.3

* These letters refer to the phase of the steelmaking cycle in progress at the time of the test.

O = Oxygen lancing M = Melting

R = Refining C = Charging

rate of gas and increased temperature also increased collection, but to a lesser extent. When the temperature of the gases differs greatly from that of bed, thermal precipitation plays a role, but other mechanisms are more important.

Goldman (1964) reported that gravel bed filters have been used for several years in Germany as large-pore filters that are wear resistant in high temperature applications (to 350°C). The theory of the collection process is given briefly. Prior to adoption of these filters, tests were made with various dusts, including coke dust in the off-gases from a coke-drying operation, phosphate dust, dust in the fumes from a carbide furnace, and dust in the waste gases from a mixture of phosphorescents. Gases contained 0.5 to 3 g/Nm^3 of dust; the outlet gases contained 10 to 95 mg/Nm^3.

Dust removal was in the range of 93 to 97%, with pressure drops of 11 to 20 cm W.C. and flow rates of 4,000 to 7,000 m^3/hr. When the pressure drop became too high, the gravel was washed and the clean gravel returned to the bed for reuse.

The U.S. Bureau of Mines, Morgantown Coal Research Center tested a GBF of Squires' design at high temperature (540°C, 1,000°F) (Wu, 1977). The bed is a vertical layer of sand held in place by louvered walls. The filtering surface of the bed was 7.6 cm (3 inches) wide and 30.5 cm (12 inches) tall. Several grades of sand were used as bed material.

The test dust was derived directly from a boiler furnace. Pulverized coal with 70% passing through a 200 mesh sieve was burned. The coal was fed by a screw feeder driven by a variable speed motor into a combustor with a capacity of 2.3 kg/hr (5 lb/hr). The temperature inside the combustor was about 1,093°-to 1,315°C (2,000 to 2,400°F). Natural gas was also burned during the coal combustion in order to insure complete combustion because of a coal feed rate problem.

At a face velocity of 10 cm/s (20 ft/min), the overall collection efficiency was 98%. No particle size distribution data were given.

The City College of New York tested the same design of the GBF at room temperature. Redispersed coal fly ash was used as the test dust. The overall collection efficiency was 99.99%. The particle size distributions might not be the same for the two tests, we cannot be sure whether the lower efficiency was a result of operating at high temperature.

One observation regarding the difference in the filter cake was recorded. In the Bureau of Mines' high temperature tests, no filter cake over the sand surface was observed. At near room temperature, a good surface filter cake was observed. Squires (Wu, 1977) attributed this difference in filter cake to the decrease of adhesive and autohesive forces of fly ash at high temperatures. Adhesion is defined as the interaction of particles with a solid surface and autohesion is defined as the interaction of particles among themselves.

A high temperature and pressure design of the Ducon granular bed filter was tested at the miniplant of Exxon Research and Engineering Company (Hoke, et al., 1978). Exxon's experience with this filter will be discussed in a later section.

GBF With Flux Forces

Anderson and Silverman (1957, 1958) reported on a study conducted at the Harvard University Air Cleaning Laboratory to investigate electrostatic filtration in fixed and fluidized granular beds. They observed that triboelectrification or friction charging of fibrous and granular filter media can improve collection efficiency with no increase in flow resistance. Similar results have recently been reported by Figueroa and Licht (1976).

Fuchs and Kirsch (1965) conducted tests to determine the effect of vapor condensation on the collection efficiency of granular beds. Monodispersed aerosols of selenium in nitrogen (particle diameter of 0.2 and 0.4 μm) were passed through a column of silica gel, both directly and upon addition of some ether vapor. It was found that with the addition of ether vapor, the collection efficiency of the granular bed increased. Condensation of the vapor and deposition of the particles occur simultaneously in the bed. The vapor molecules diffusing towards the granules sweep the particles along with them.

A study of the collection of submicron aerosol particles in an electrified granular bed was carried out by Research-Cottrell, Inc., Bound Brook, New Jersey. One such device is described in U.S. Patent No. 2,990,912, July 4, 1961. Collection of particles occurred in a bed of 3 to 6 mm diameter glass beads held between two screens maintained at different electrical potentials (Figure 22). The aerosol particles were electrically charged upstream from the bed. Data taken on collection of a 0.5 to 0.7 μm diameter methylene blue particles are shown in Figure 23. It is noted that a 99.5% efficiency was obtained in a bed under 5.1 cm (2 in.) in thickness with a pressure drop of 0.5 cm W.C. (0.2 in W.C.) and a a face velocity of 61 cm/s (2 ft/s).

Sharapov (1975) tested a high gradient magnetic filter with a bed of 8 mm steel balls for the removal of dust from open-hearth furnace. The capacity of the filter was 60 m^3/min. At the optimum voltage of 80 to 120 kV/m, the collection efficiency was 80 to 90%, and the energy consumption was 0.05 kWh/1,000 m^3 of gas. Without the magnetic field the collection efficiency was 25 to 30%.

Gaseous Pollutants

Only limited work has been done in this area. Zahradnik et al. (1970) and Squires and Graft (1971) have demonstrated the feasibility of simultaneous removal of fly ash and SO_2 from gas streams using a granular bed filter packed with alkalized alumina and half calcined dolomite. Swift et al. (1977) are studying the removal of alkali metal (sodium and potassium) compounds from the combustion gases at high temperature with a packed bed. NaCl is passed through beds packed with alundum, Celatom MP-91 diatomaceous earth, Burgess No. 10 pigment (kaoline clay), attapulgus clay (magnesium aluminum silicate), and activated bauxite. The temperatures of the vapor and bed are maintained at about 870°C. The gas velocity passing through the bed is 7.5 cm/s (3 in./s). Preliminary test results revealed that Celatom MP-91 diatomaceous

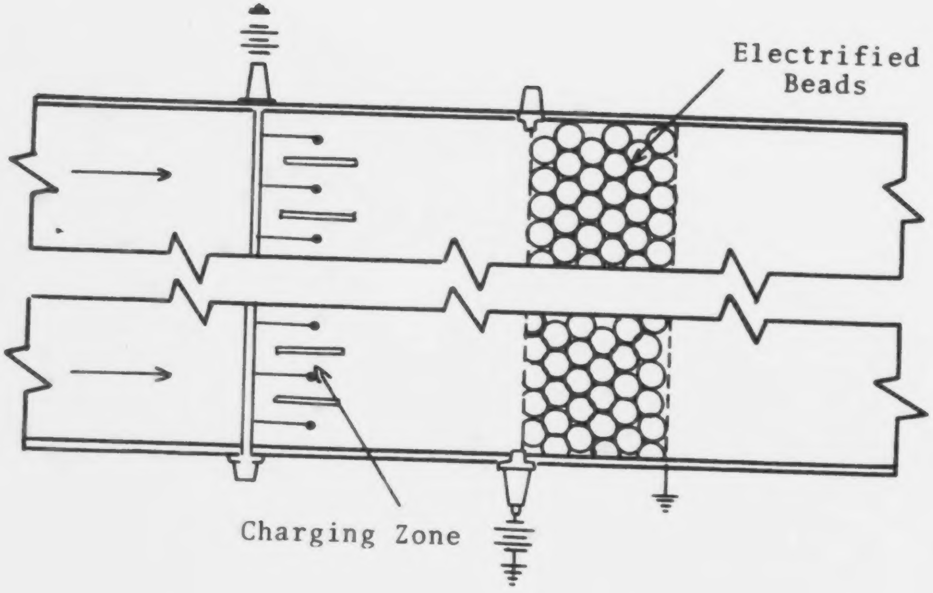
Electrified Beads
Charging Zone

Figure 22. Electrified packed bed.

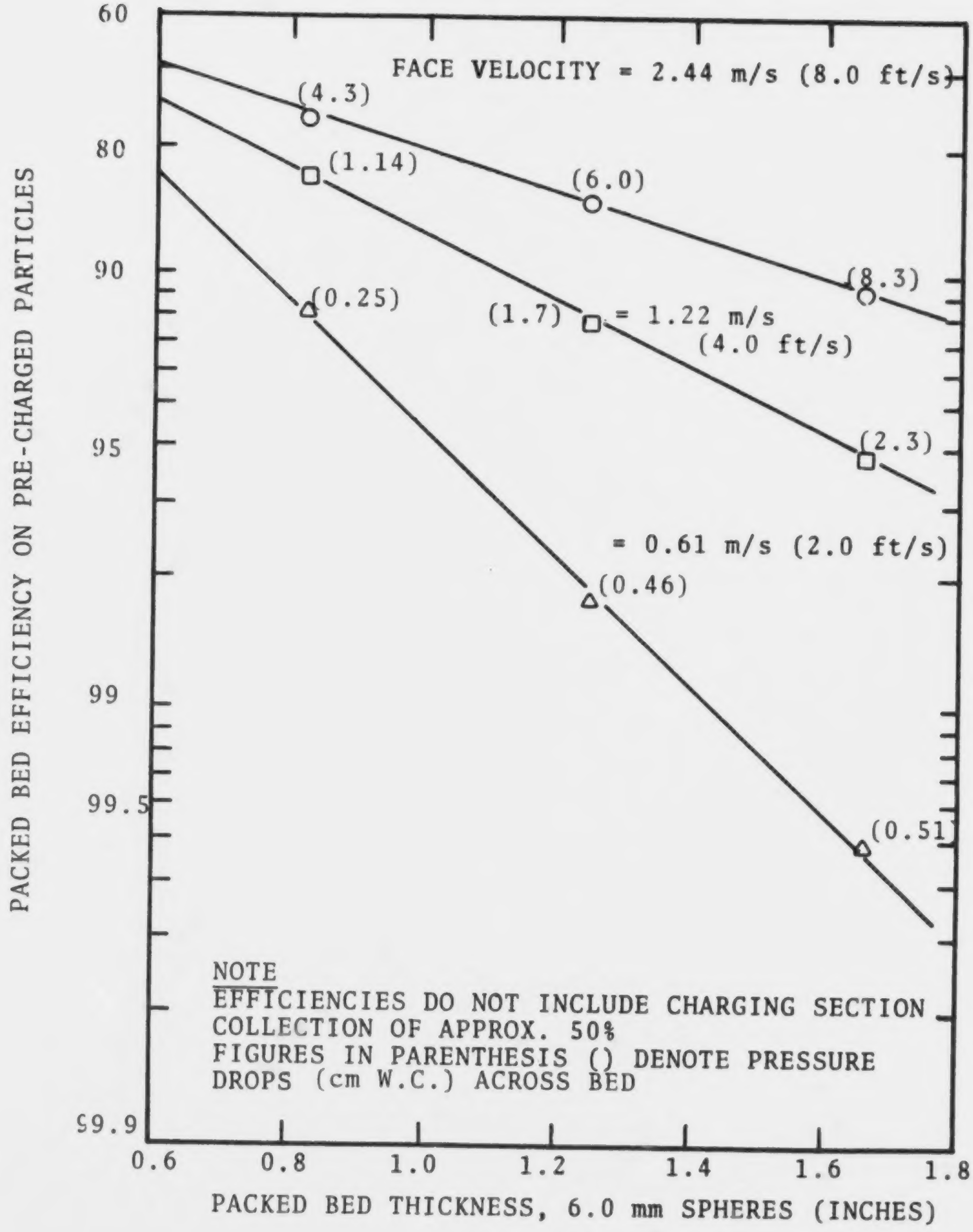

Figure 23. Performance characteristics of electrostatically augmented packed bed (Research-Cottrell data).

earth, Burgess No. 10 pigment, and activated bauxite are promising candidates as hot packed bed sorbents to remove alkali vapor from hot coal combustion gases. Among the three, activated bauxite, which is thermally treated high-alumina-content natural bauxite ore, is the most active for removing NaCl vapor under the test conditions.

THEORY

Particulate Collection

The primary mechanisms for particulate collection in a bed of granular solids are:

1. Inertial impaction
2. Flow-line interception
3. Diffusional collection
4. Gravity settling

Inertial Impaction -

The inertial impaction mechanism is based on the inertial force of the particle. The inertial force tends to move particles across the gas flow lines toward the collecting surface in regions where the flow is diverging upstream of a fixed boundary surface. Inertial forces increase with particle velocity and mass.

Diffusion -

Diffusion of the aerosol particle is based on the theory of Brownian motion. The diffusion mechanism becomes increasingly effective with decreasing particle diameter.

Gravity Settling -

The gravitational force can be significant for collection of particles as small as 0.4 μm in diameter. This effect has been demonstrated experimentally by the decrease in penetration observed for downward flow compared with upward flow in sand beds (Thomas and Yoder, 1956b). A gravitational force in the direction of the bulk flow will tend to increase collection due to settling across flow lines.

Interception -

Interception is the mechanism whereby particles are collected on surfaces while following the gas streamlines. Collection by this mechanism usually is negligible for a clean granular bed. However, during a filtration cycle, particles will deposit in the interstices of the bed to form an internal cake and on the surface to form a surface cake. As the cake builds up the bed porosity and flow channels decrease and interception becomes an important collection mechanism. When the flow channels are too small to allow particles to pass, collection is ensured, being referred to as complete interception or sieving.

In finely packed beds operated at low gas velocities, gravity settling and diffusional deposition will predominate. The collection efficiency will be expected to decrease as the gas velocity increases. Coarsely packed beds operating at higher velocities (but still below fluidizing velocities) provide separation mainly by inertial deposition and interception. The collection efficiency will increase with velocity provided that the gas velocity is not so high as to reentrain collected material.

The operation of granular bed filters is similar to fabric filters even though granular bed filters have larger pore sizes and deeper beds. Payatakes (1977) classified the filtration cycle into four successive stages.

1. When the filter is new, particles deposit directly on the granule surfaces. This is referred to as clean bed filtration. The collection efficiency for this stage of filtration depends primarily upon the granule size and the depth of the bed.

2. Particles deposit not only directly on granules but also and preferentially on deposited particles, thereby forming particle dendrites.

3. The dendrites grow to the extent that they intermesh with their neighbors forming a particulate coating around each granule which is non-uniform in thickness.

4. If the granules of the bed are sufficiently small, particle coatings of neighboring granules will bridge the gap to form an internal cake. Lee (1975) called the internal cake a rooting cake

and it is the foundation which supports the formation of a surface cake. Once a surface cake is formed, filtration efficiency no longer depends upon the depth of the granular bed but rather on the thickness and structure of the surface cake. The cake filtration results in a much higher efficiency than the original granular bed, and particle collection by sieving becomes a more important collection mechanism.

Mathematical Models -

Currently there are several mathematical models available for the prediction of particle collection in a granular bed. All models are for the prediction of particle collection by clean beds; i.e., stage 1 filtration. Stage 1 filtration is very brief compared to the total filtration cycle.

Model by Jackson and Calvert - Jackson and Calvert (1966) and Calvert (1968) have developed a theoretical relationship between particle collection efficiency and packed bed operating parameters. They assumed that the gas (and particle) flow through the bed may be modeled by the flow through a series of semicircular channels and that particles are collected by centrifugal force on the outside channel walls as gas and particles pass through the channels. Their equation for predicting the particle penetration for a packed bed is:

$$Pt_d = \exp\left[-\, C_1 \frac{Z}{d_c} K_p\right] \tag{3}$$

where Pt_d = penetration for particles with diameter "d_p", fraction

C_1 = empirical constant, dimensionless

Z = depth of the bed, cm

d_c = granule diameter, cm

K_p = inertial parameter, dimensionless

$$= \frac{d_p^{\,2}\, C'\, \rho_p\, u_G}{9\, \mu_G\, d_c}$$

d_p = particle diameter, cm
C' = Cunningham slip factor, dimensionless
ρ_p = particle density, g/cm³
u_G = superficial gas velocity, cm/s
μ_G = gas viscosity, g/cm-s

The empirical constant, "C_1", is a function of bed porosity, channel width and granule diameter. It can be calculated by the following formula:

$$C_1 = \frac{\pi}{2(j+j^2)\varepsilon} \tag{4}$$

where j = ratio of channel width to packing diameter, dimensionless
ε = bed porosity, dimensionless

For a packed bed with a granule diameter of 1.27 cm (0.5 in), the empirical constant was found to be 21.4.

Model by Paretsky et al. - Paretsky et al. (1971) proposed the following equation (based on Happel's "free surface model") for particle penetration through a granular bed:

$$Pt_d = \exp\left[-\frac{3}{2}\,\frac{1-\varepsilon}{\varepsilon}\,\frac{Z}{d_c}\,\eta\right] \tag{5}$$

where Pt_d = penetration of particles with diameter "d_p", fraction
ε = bed porosity, fraction
Z = bed depth, cm
d_c = granule diameter, cm
η = overall single granule collection efficiency, fraction

Single granule collection efficiency includes the collection by: (1) Brownian diffusion, (2) direct interception, (3) inertial impaction, and (4) gravity settling. The theoretical equations using the "free surface" model for each of these four collection mechanisms are:

$$\text{Brownian Diffusion:}\quad \eta_D = \frac{4(N_{Sh})_{avg}}{N_{Pe}} \tag{6}$$

$$= 5.04\ f(\varepsilon)^{-1/3}\ N_{Pe}^{\ 2/3}$$

where η_D = single granule collection efficiency, fraction

ε = bed porosity, fraction

N_{Sh} = Sherwood number, dimensionless

N_{Pe} = Peclet number, dimensionless

$$f(\varepsilon) = \frac{2 - 3(1-\varepsilon)^{1/3} + 3(1-\varepsilon)^{5/3} - 2(1-\varepsilon)^2}{1 - (1-\varepsilon)^{5/3}} \tag{7}$$

$$\text{Direct Interception:}\quad \eta_{DI} = \frac{3}{f(\varepsilon)}\left(\frac{d_p}{d_c}\right)^2 \tag{8}$$

where η_{DI} = single granule collection efficiency by direct interception, fraction

d_p = particle diameter, cm

d_c = collector diameter, cm

$$\text{Inertial Impaction:}\quad \eta_I = \left(\frac{2y_{crit}}{d_c}\right)^2 = f(K_p) \tag{9}$$

where η_I = single granule collection efficiency by impaction, fraction

y_{crit} = critical trajectory of the aerosol, cm

$$\text{Gravity Settling:} \quad \eta_{GS} = \frac{u_t}{u_G} A_p \qquad (10)$$

where η_{GS} = single granule collection efficiency by gravity settling, fraction

u_t = terminal settling velocity of the particle, cm/s

u_G = superficial gas velocity, cm/s

A_p = fraction of the projected area of a single collector particle which is available by capturing the aerosol by settling, fraction

"A_p" can be taken as the minimum projected area available for flow between particles. For a triangular packing it is 0.0377 and for a square packing it is 0.0871.

Model by Miyamoto and Bohn - Miyamoto and Bohn (1974) derived the following equation for the particle collection in a clean bed (diffusion only) based on the expression of a single sphere collection efficiency by Friedlander (1957).

$$Pt_d = \exp\left[- \frac{6(1-\varepsilon)Z}{d_c} \frac{N_{Nu}}{N_{Pe}}\right] \qquad (11)$$

where Pt_d = penetration for particles with diameter "d_p", fraction

ε = bed porosity, fraction

Z = bed depth, cm

d_c = single granule diameter, cm

N_{Nu} = Nusselt number, dimensionless

$= \dfrac{d_c\, k_G}{D_{pe}}$

N_{Pe} = Peclet number, dimensionless

$$= \frac{d_c\ u_{Gb}}{D_{pe}}$$

k = mass transfer coefficient, cm/s

D_{pe} = effective particle diffusion coefficient in granule layer, cm^2/s

u_{Gb} = actual gas velocity in bed, cm/s

The effective particle diffusion coefficient in granule layer is related to particle diffusivity by:

$$D_{pe} = D_p\ \varepsilon\ \phi\ \lambda^2$$

where D_p = particle diffusivity, cm^2/s

ϕ = relative force field, dimensionless

λ = tortuosity factor, dimensionless

Interstitial gas velocity can be calculated from superficial gas velocity by:

$$u_{Gb} = \frac{\lambda\ u_G}{\varepsilon} \tag{12}$$

Model by Gebhart, et al. - Gebhart et al. (1973) performed an experimental study on the filtration of aerosol particles in the 0.1-2 μm size range by a packed bed of glass beads. Based on their data, they proposed an empirical equation for aerosol penetration through packed beds of spheres under conditions at which Brownian diffusion dominates:

$$Pt_d = \exp\left[-6.39\ \frac{D_p^{2/3}\ Z}{u_{Gi}^{2/3}\ (0.5d_c)^{5/3}}\right] \tag{13}$$

where Pt_d = particle penetration for particles with diameter "d_p", fraction

D_p = particle diffusivity, cm^2/s

ε = bed porosity, fraction
u_{Gi} = interstial gas velocity = u_G/ε, cm/s
d_c = collector diameter, cm
Z = bed depth, cm

Balasubramanian and Meisen (1975) showed that this equation may be derived independently from Wilson and Geankoplis' (1966) correlation for mass transfer coefficients. Wilson and Geankoplis' correlation is:

$$k_G = 1.09\ (u_G/\varepsilon)\ N_{Pe}^{-2/3} \qquad (14)$$

where k_G = mass transfer coefficient, cm/s
N_{Pe} = Peclet number, dimensionless
$= \dfrac{d_c\ u_G}{D_p}$

Equation (16) is valid for $0.35 < \varepsilon < 0.75$, $0.0016 < N_{Re} < 55$, and $950 < N_{Sc} < 70{,}600$. The equation derived by Balasubramanian and Meisen is:

$$Pt_d = \exp\left[-2.06\ \frac{(1-\varepsilon)\ D_p^{\ 2/3}}{\varepsilon\ u_G^{\ 2/3}\ (0.5 d_c)}\ Z\right] \qquad (15)$$

This equation is more general than the equation by Gebhart et al. After substituting $\varepsilon = 0.385$ (bed porosity used by Gebhart et al.) equation (17) reduces to equation (15).

Model by Böhm and Jordan - Böhm and Jordan (1976), using capillary flow for describing the behavior of sand bed filters, derived an expression for particle penetration.

$$Pt_d = \exp\left[-\left(\frac{2k\ T\ \varepsilon f}{3\pi\ d_p\ u_G} + \frac{d_p^{\ 2}\ g\ \rho_p\ \varepsilon\ d_c}{36\ u_G} + \frac{\pi\ d_p^{\ 2}\ \rho_p\ u_G}{18\varepsilon}\right)\frac{4\ f'Z}{\mu_G\ d_c^{\ 2}}\right] \qquad (16)$$

where Pt_d = particle penetration for particles with diameter "d_p", fraction
k = Boltzmann's constant
= 1.38×10^{-16} erg/°K
T = absolute temperature, °K
d_p = particle diameter, cm
ε = bed porosity, fraction
u_G = superficial gas velocity, cm/s
g = gravitational acceleration, cm/s^2
d_c = collector diameter, cm
ρ_p = particle density, g/cm^3
μ_G = gas viscosity, g/cm-s
Z = bed depth, cm
f' = d_c/d_o, dimensionless
d_o = initial capillary diameter, cm

The first part of the exponent stands for diffusional deposition, the second for gravity settling and the third for inertial impaction. Interaction terms between the three collection mechanisms are neglected.

Model by Goren - Goren (1977) derived a semi-empirical equation for granular bed collection efficiency. The model is based on collection by individual granules:

$$Pt_d = \exp\left[-\frac{3}{2}(1-\varepsilon)\frac{Z}{d_c}\eta\right] \qquad (17)$$

where: Pt_d = particle penetration for particles with diameter "d_p", fraction
ε = bed porosity, fraction
Z = bed depth, cm
d_c = granular diameter, cm
η = overall single granule collection efficiency, fraction

Goren ran a small scale experiment with 2 mm diameter granules as bed material. He then derived an expression for "η" from data and equation (17). Collection by diffusion, settling, and impaction were considered. The expressions are:

$$\eta_D = 200\ N_{Pe}^{-2/3} = 200 \left(\frac{d_c\ \mu_G}{D_p} \right)^{-2/3} \tag{18}$$

$$\eta_{GS} = \left(\frac{u_t}{u_G} \right)^{0.75} = \left(\frac{d_p^{\ 2}\ \rho_p\ C'\ g}{18\ \mu_G\ \mu_G} \right)^{0.75} \tag{19}$$

$$\eta_I = 1250\ K_p^{\ 2.25} = 1250 \left(\frac{d_p^{\ 2}\ \rho_p\ C'\ u_G}{18\ \mu_G\ d_c} \right)^{2.25} \tag{20}$$

where η_D, η_{GS}, η_I = single granule collection efficiency due to diffusion, gravity settling, and impaction, respectively, fraction

N_{Pe} = Peclet number, dimensionless

d_c = granule diameter, cm

u_G = gas velocity, cm/s

D_p = particle diffusivity, cm²/s

u_t = terminal settling velocity, cm/s

d_p = particle diameter, cm

g = gravitational acceleration, cm/s²

μ_G = gas viscosity, g/cm-s

C' = Cunningham slip factor, dimensionless

ρ_p = particle density, g/cm

K_p = inertial parameter, dimensionless

Model by Westinghouse - Westinghouse Research Laboratories (Ciliberti, 1977) also developed a mathematical model. They took into account three collection mechanisms: impaction, interception, and diffusion. Their equation is:

$$Pt_d = \exp\left[-5.8\,\frac{K_p\ Z}{d_c}\ -3.75\left(\frac{d_p}{d_c}\right)^2\frac{Z}{d_c}\ -\ 3.752\,\frac{D_p^{2/3}\ Z}{u_G^{2/3}\ d_c^{5/3}}\right] \qquad (21)$$

where Pt_d = penetration for particle diameter "d_p", fraction
K_p = inertial parameter, dimensionless
d_c = collector diameter, cm
A = bed depth, cm
D_p = particle diffusivity, cm²/s
u_G = superficial gas velocity, cm/s

Model by Schmidt, et al. - Schmidt, et al. (1978), used the semi-empirical theories of Johnstone and Roberts (1949) for diffusion, Friedlander (1957) for interception, Jackson and Calvert (1966) for inertial impaction, and Ranz (1951) for gravity settling, and proposed the following equation for granular bed collection efficiency.

$$Pt_d = \exp\left[-7.5\ (1-\varepsilon)\ \frac{Z}{d_c}\ (\eta_D + \eta_{DI} + \eta_I + \eta_{GS})\right] \qquad (22)$$

where Pt_d = particle penetration for particle diameter d_p, fraction
d_c = collector diameter, cm
Z = bed depth, cm
ε = bed porosity, dimensionless
η_D , η_{CI}, η_I , η_{GS} = single granule collection efficiency due to diffusion, direct interception, impaction, and gravity settling, respectively, fraction

Single granule collection efficiencies for various collection mechanisms were obtained from:

$$\eta_D = \frac{8}{N_{Pe}} + \frac{2.038\ N_{Re}^{1/8}}{N_{Pe}^{-5/8}} \qquad (23)$$

$$\eta_{DI} = 1.45 \left(\frac{d_p}{d_c}\right)^2 \tag{24}$$

$$\eta_I = 3.97 \, K_p \tag{25}$$

$$\eta_{GS} = \frac{u_t}{u_G} \tag{26}$$

where d_c = granule diameter, μm
d_p = particle diameter, μm
K_p = impaction parameter, dimensionless
u_t = terminal settling velocity of particles, cm/s
u_G = gas velocity, cm/s
N_{Pe} = Peclet number, dimensionless
N_{Re} = Reynolds number, dimensionless

Stage 2 Filtration - Stage 2 filtration has been observed experimentally by several researchers. Billings and Wilder (1970) summarized the studies of many investigators concerned with the cake formation process during the initial stage of filtration. They concluded that aerosol deposition occurs primarily on previously deposited particles.

Based on this observed dendrite-like growth, Payatakes and Tien (1976) proposed a model describing the dendrite growth over the entire filtration period. This model was expanded and revised by Payatakes (1977).

To express the growth process and to describe the dendrite configuration, Payatakes (1977) divided the space adjacent to the collector surface into layers of thickness "d_p" by planes which are all parallel to a plane tangential to the collector surface. He numbered them in ascending order; i.e., the first layer is immediately adjacent to the collector surface (Figure 24).

The dendrite configuration is idealized with the convention that if a particle of the dendrite structure has at least half of its volume in the k'th layer it is assumed to lie entirely

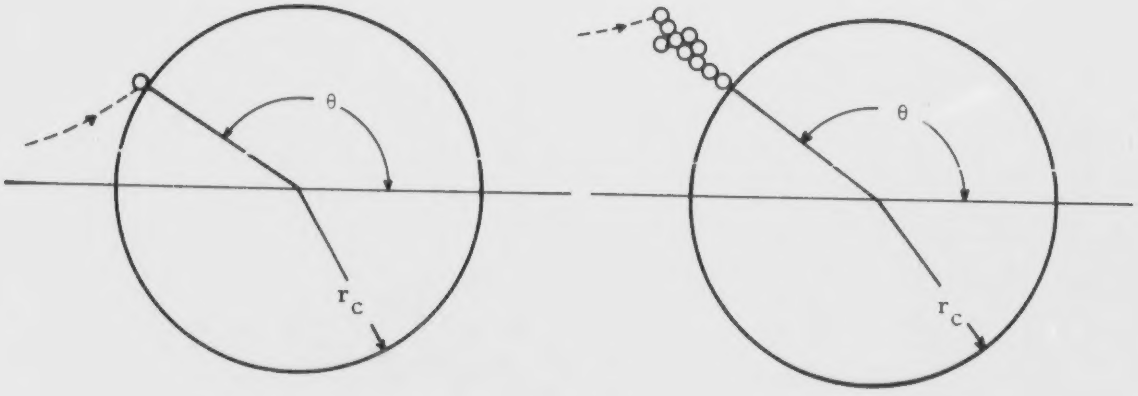

(a) at t = 0 (b) t = >0

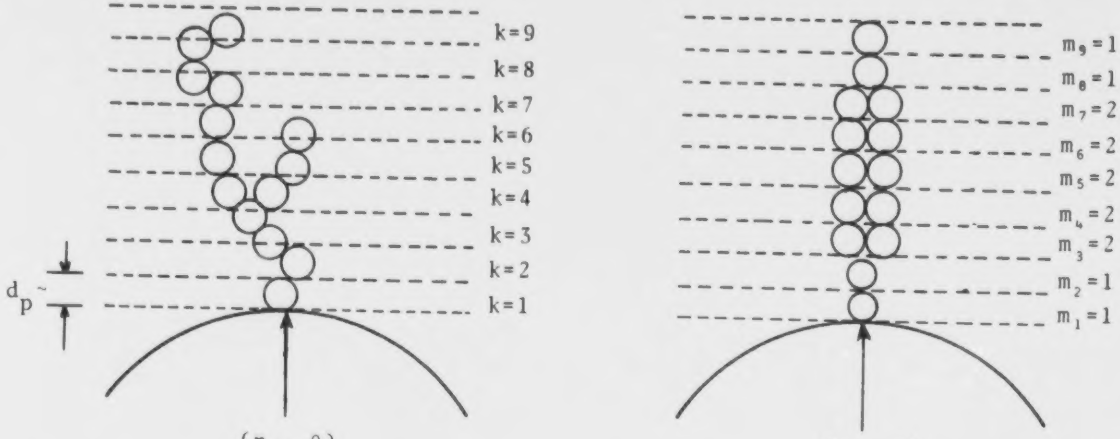
d_p
k=9
k=8
k=7
k=6
k=5
k=4
k=3
k=2
k=1
(r_c, θ)
$m_9=1$
$m_8=1$
$m_7=2$
$m_6=2$
$m_5=2$
$m_4=2$
$m_3=2$
$m_2=1$
$m_1=1$
(r_c, θ)

(c) Actual dendrite (d) Idealized dendrite

Figure 24. Dendrite initiation, growth and idealization of the dendrite configuration.

in the k'th layer. He also assumed that dendrite particles are of uniform size.

By considering both the radial and angular contributions to deposition, Payatakes (1977) set,

$$\frac{d\ m_k}{dt} = \Theta_{k-1,k}^{(\theta)} + \Theta_{k,k}^{(\theta)} + \Theta_{k-1,k}^{(r)} + \Theta_{k,k}^{(r)} \qquad (27)$$

where m_k = expected particle number in the k'th layer of a dendrite, number

$\Theta_{k-1,k}^{(\theta)}$ = rate of increase of m_k by deposition on particles occupying the (k-1)'st layer due to the angular flow component, number/s

$\Theta_{k,k}^{(\theta)}$ = rate of increase of m_k by deposition on particles already occupying the k'th layer, due to the angular flow component, number/s

$\Theta_{k-1,k}^{(r)}$ = rate of increase of m_k by deposition on particles occupying the (k-1)'st layer due to radial flow component, number/s

$\Theta_{k,k}^{(r)}$ = rate of increase of m_k by deposition on particles already occupying the k'th layer due to the radial flow component, number/s

In the formulation, terms involving addition of particles to the k'th layer by deposition onto particles occupying the (k+1)'st layer are neglected. The solution to equation (27) is,

$$m_k = \sum_{i=1}^{k} C_{ki}\ (\theta) \exp\ [\alpha\ b_i\ (\theta)\ t], \text{ for } k = 1, 2, 3, \ldots \qquad (28)$$

where m_k = expected particle number in the kth layer of a dendrite

t = time measured from the instant of deposition of the first particle of the dendrite, seconds

α = rate of particles approaching a clean fiber per unit length = $d_c\ u_{Gi}\ n$

θ = angular cylindrical coordinate, measured counter-clockwise from the down stream stagnation point
d_c = collector diameter, cm
u_{Gi} = interstitial gas velocity, cm/s
n = particle number concentration, number/cm

"C_{ki} (Θ)" and "b_i (Θ)" are functions defined by the following equations:

$$C_{11} = 1 \tag{29}$$

$$C_{21} = \frac{a_2}{(b_1 - b_2)} \tag{30}$$

$$C_{22} = \frac{a_2}{b_2 - b_1} \tag{31}$$

$$C_{k1} = \prod_{2 \le j \le k} \frac{a_j}{b_1 - b_j} \tag{32}$$

$$C_{ki} = \frac{a_i}{(b_i - b_1)} \prod_{\substack{2 \le j \le k \\ j \neq i}} \frac{a_j}{(b_i - b_j)}, \text{ for } k = 3,4\ldots, \; i = 2,3\ldots \tag{33}$$

$$b_1 = \phi^{(\theta)}_{1,1} + \phi^{(r)}_{1,1} \tag{34}$$

$$b_k = \phi^{(\theta)}_{k,k} + \phi^{(r)}_{k,k} - \frac{1}{\rho}\left[\phi^{(\theta)}_{k-1,k} + \phi^{(r)}_{k-1,k}\right] \tag{35}$$

$$k = 2,3\ldots$$

where ρ = maximum number of particles in the (k+1)'st layer which can be attached directly to the same particle of the k'th layer

$\phi_{i,j}^{(s)}$ = function defined so that "$\alpha\ \phi_{i,j}^{(s)}$" is the rate of increase of "m_i" by deposition on a particle in the i'th layer due to the flow component in the "s" direction ($s = r$ = radial direction, $s = \theta$ = angular direction).

$a_k = \phi_{k-1,k}^{(\theta)} + \phi_{k-1,k}^{(r)}$

Equation (28) coupled with the assumed flow field (e.g.; Happel's free surface model, Kuwabara flow field, etc.) can be used to predict the increases in filtration efficiency and pressure drop for the filter. Payatakes (1976 a,b) presented some sample calculations by applying the model to pure interception.

Payatakes and Tien's model described the rate of dendrite growth. It did not explain the reason for dendrite formation. Wang et al. (1977) and Tien et al. (1977) proposed a concept, the shadow effect, for dendrite growth.

They hypothesized that once a particle is deposited, it creates a shadow area around itself on the collector surface, within which no subsequent particle deposition may take place. This is represented by arc B'BB" for the deposited particle "A" shown in Figure 25.

The creation of shadow areas by deposited particles has two consequences. Since there will be no deposition with any shadow area, it means that particle collection takes place at a discrete position along a collection surface, the deposited dust cannot be in the form of a smooth coating.

The second consequence arises from the fact that with the creation of shadow area, subsequent approaching particles which would have deposited within the shadow area had there been no deposition, now attach themselves to the deposited particle. This results in the formation and growth of chain-like particle dendrites.

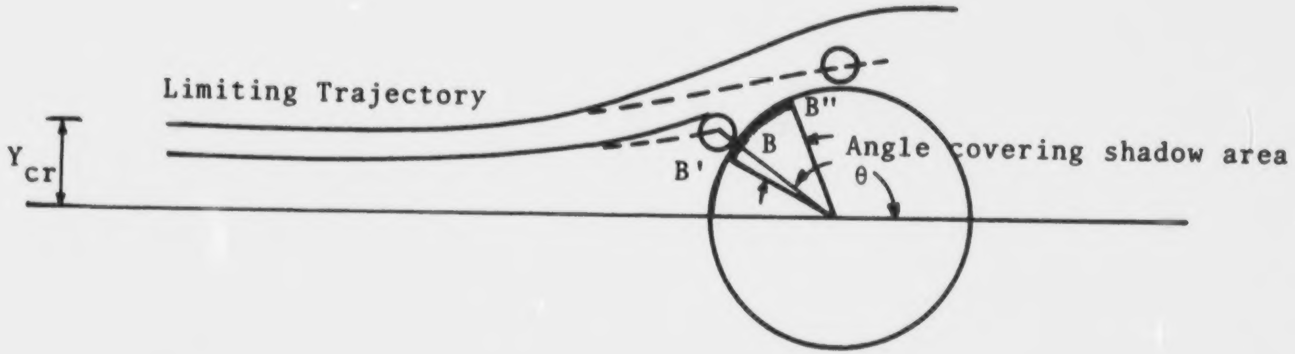
Limiting Trajectory
Y_{cr}
B'
B
B"
Angle covering shadow area
θ

Figure 25. Particle deposition on single collector.

The magnitude of the shadow area is a function of many variables including the location of its deposition, particle diameter, and the inertial parameter. They performed a simulation by using this concept and the trajectories of random particles to verify this concept.

Gaseous Pollutants

It is feasible to use various bed materials to remove metal vapors and other gaseous pollutants. The mechanisms expected to be important in removing gaseous pollutants with a granular bed include:

1. Adsorption
2. Absorption
3. Chemical reaction
4. Condensation without nucleation

Adsorption -

The Chemical Engineers' Handbook gives a detailed treatment of this subject. The following is a brief discussion. Adsorption involves the interphase accumulation or concentration of substances at a surface or interface. The process can occur at an interface between any two phases, such as gas-solid, gas-liquid, liquid-solid, or liquid-liquid interfaces. The material being concentrated or adsorbed is the adsorbate, the the adsorbing phase is termed the adsorbent.

There are three principal types of adsorption: electrical attraction of the solute to the adsorbent, van der Waals attraction and chemical adsorption. Adsorption of the first type falls within the realm of ion-exchange and is often referred to as exchange adsorption. Van der Waals attraction is generally termed "physical" adsorption, a term which has come to represent cases in which the adsorbed molecule is not affixed to a specific site at the surface but is free to undergo translational movement within the interface. Adsorption of this type is sometimes referred to also as "ideal" adsorption. If the adsorbate undergoes chemical interaction with the adsorbent, the phenomenon is referred to as "chemical" adsorption, "activated" adsorption, or "chemisorption." Chemically adsorbed molecules are considered not to be free to move on the surface or within the interface.

Performance of a solid sorbent depends upon four factors.

1. Stoichiometric capacity of the solid. This is the ultimate capacity of the sorbent for the sorbate, which may or may not be fully utilized under actual process conditions.

2. The phase equilibrium, which influences the efficiency with which that capacity is reached, and in many cases controls the actual capacity of the surbent.

3. The rate behavior including the mechanism and resistance controlling the mass transfer rate.

4. The process arrangement and its effect on the material balance.

Equilibrium Behavior - When the concentration of the sorbate remaining in the gas phase is in a dynamic equilibrium with that at the surface of the solid, there is a definite distribution of the sorbate between the gas and solid phases. One form used to depict this distribution is to express the quantity "q_e" as a function of "c" at a fixed temperature. The quantity "q_e" is the amount of sorbate adsorbed per unit weight of sorbent and "c" is the concentration of sorbate remaining in gas phase at equilibrium. An expression of this type is termed an adsorption isotherm. The adsorption isotherm is a functional expression for the variation of adsorption with adsorbate concentration in the gas at constant temperature. Usually the amount of adsorbed material per unit weight of adsorbent increases with increasing concentration, but not in direct proportion (Figure 26).

Several types of isothermal adsorption relations may occur. The most common relationship between "q_e" and "c" is obtained for systems in which adsorption from the gas leads to the deposition of an apparent single layer of sorbate molecules on the surface of the solid. Occasionally, multimolecular layers of sorbate may be adsorbed. The single layer adsorption can be described by the Langmuir adsorption model and the multilayer adsorption by the Brunauer, Emmett, Teller (BET) model.

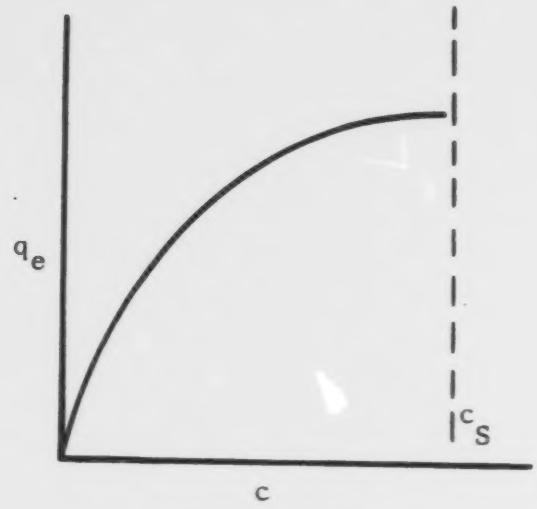

a. Langmuir

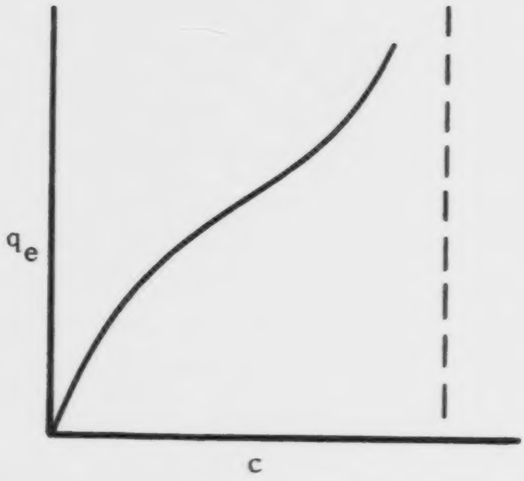

b. BET

Figure 26. Typical isotherms for Langmuir and BET adsorption patterns.

The Langmuir treatment is based on the assumption that maximum adsorption corresponds to a saturated monolayer of sorbate molecules on the adsorbent surface, that the energy of adsorption is constant, and that there is no transmigration of adsorbate in the plane of the surface. Figure 26 is a typical isotherm for the Langmuir pattern. The Langmuir isotherm is:

$$q_e = \frac{Q^\circ Kc}{1 + Kc} \tag{36}$$

where q_e = the amount of sorbate adsorbed per unit weight of adsorbent in equilibrium with concentration "c", mol/g

Q° = number of moles of adsorbate adsorbed per unit weight of adsorbent in forming a complete monolayer on the surface, mol/g

K = equilibrium constant, ℓ/mol

c = concentration or partial pressure of adsorbate in gas phase, mol/ℓ or mm Hg

The BET model assumes that a number of layers of adsorbate molecules form at the surface and that the Langmuir equation applies to each layer. A further assumption of the BET model is that a given layer need not complete formation prior to the initiation of subsequent layers. For adsorption from the gas phase with the additional assumption that layers beyond the first have equal energies of adsorption, the BET equation takes the simplified form:

$$q_e = \frac{B\ c\ Q^\circ}{(c_s - c)\ [1 + (B-1)(c/c_s)]} \tag{37}$$

where c_s = saturation concentration of the adsorbate, mol/g

c = measured concentration in gas at equilibrium, mol/ℓ

B = a constant expressive of the energy of interaction with the surface, ℓ/mol

Q° = number of moles of adsorbate adsorbed per unit weight of adsorbent in forming a complete monolayer on the surface, mol/g

q_e = number of moles of adsorbate adsorbed per unit weight at concentration "c", mol/g

One other question for isothermal adsorption, the Freundlich or van Bemmelen equation, has been widely used for many years. This equation is a special case for heterogeneous surface energies in which the energy term, "b", in the Langmuir equation varies as a function of surface coverage, "q_e", strictly due to variations in heat of adsorption. The Freundlich equation has the general form:

$$q_e = K_F\ c^{1/n} \qquad (38)$$

where "K_F" and "n" are constants and $n > 1$.

Rate Processes - There are essentially three consecutive steps in the adsorption of materials from gas by porous adsorbents, any one of which may be a rate determining step in a certain region of operating conditions.

The first step is the transport of the adsorbate through a surface film to the exterior of the adsorbent. The transport rate for adsorbate between the bulk of the gas phase and the outer surfaces of the sorbent granules is governed by the molecular diffusivity and, in turbulent flow, by the eddy diffusivity which controls the effective thickness of the boundary layer.

One may assume that the concentration of sorbate at the point in the hydrodynamic boundary layer immediately adjacent to the external surface of the particle is in equilibrium with the average solid-phase concentration on the internal surfaces. This condition may be stated algebraically as:

$$\frac{dq}{dt} = k_G \, a \, \frac{\varepsilon}{\rho_s} (c - c_e) \qquad (39)$$

where k_G = mass-transfer coefficient, cm²/s
a = effective area for mass transfer across the fluid film per unit volume of bed, cm²/cm³
ε = void fraction, fraction
ρ_s = density of the solid in the bed, g/cm³
c = concentration of the sorbate in bulk gas phase, g/cm³
c_e = concentration of sorbate in bulk gas phase in equilibrium with the coexisting solid phase concentration, g/cm³
q = concentration of sorbate on solid surface, g/cm³

For packed bed, Wilke and Hougen (1945) gave the following equation for evaluating the mass-transfer coefficient:

$$k_G \, a = \frac{10.9 \, u_G \, (1-\varepsilon)}{d_c} \left(\frac{D_G}{d_c \, u_G}\right)^{0.51} \left(\frac{D_G \, \rho_G}{\mu_G}\right)^{0.16} \qquad (40)$$

where u_G = superficial gas velocity, cm/s
ε = void fraction , fraction
d_c = granule diameter, cm
D_G = gas phase diffusivity, cm²/s
ρ_G = gas phase density, g/cm³
μ_G = gas phase viscosity, g/cm-s

The second of the three consecutive steps in sorption by porous adsorbents, with the exception of a small amount of adsorption that occurs on the exterior surface of the adsorbate after transport across the exterior film, is the diffusion of the adsorbate within the pores of the adsorbent. The driving force approximation for pore diffusion is:

$$\frac{dq}{dt} = k_{pore}\, a\, \xi\, (q_e - q) \qquad (41)$$

where k_{pore} = pore diffusion coefficient, cm^2/s
a = outer surface area of particles per unit bed volume, cm^2/cm^3
ξ = intraparticle void ratio, dimensionless
q = concentration of sorbate on solid surface, g/cm^3
q_e = local concentration of sorbate in the solid phase that prevails at the outer surface and is assumed to be in equilibrium with the coexisting gas phase at concentration "c", g/cm^3

According to Vermenlen and Quilici (1970):

$$k_{pore}\, a = \frac{60\, D_{pore}}{d_c^{\,2}}\, (1-\varepsilon) \qquad (42)$$

where D_{pore} = pore diffusity, cm^2/s
d_c = solid diameter, cm
ε = bed void fraction, dimensionless

Pore diffusivity can be expressed as:

$$D_{pore} = \frac{\xi}{\lambda}\left[\frac{3}{4\,\bar{r}}\left(\frac{\pi\, M}{2\, R\, T}\right)^{0.5} + \frac{1}{D_G}\right]^{-1} \qquad (43)$$

where D_{pore} = pore diffusivity, cm^2/s
ξ = internal void fraction of the solid, fraction
$\bar{r}$ = average pore radius, cm
λ = tortuosity factor (usually between 2 and 6), dimensionless
R = universal gas constant, J/gmol-°K
T = absolute temperature, °K
M = molar weight, g
D_G = gas phase diffusivity, cm^2/s

The third and final step is the adsorption of the adsorbate on the interior surfaces of the adsorbent (e.g. porous granules). The following reaction schematic for the adsorption process is considered:

$$\text{(sorbate)} + \text{(sorbent)} \rightarrow \text{(sorbate} \cdot \text{sorbent)}$$

If a Langmuir-type adsorption equilibrium is assumed, a general expression for the rate of adsorption at the solid surfaces may be given as:

$$\frac{d\left[\text{(sorbate}\cdot\text{sorbent)}\right]}{dt} = k\left[\text{(sorbate) (sorbent)} - \frac{\text{(sorbate}\cdot\text{sorbent)}}{K}\right] \quad (44)$$

where K = Langmuir equilibrium constant, ℓ/mol
k = rate constant for second-order surface reaction controlled kinetics, ℓ/mol-s

If the ultimate monolayer capacity of the adsorbent for the adsorbate is designated by the term Q°, then (Q°-q) represents the unused capacity of the adsorbent. Substitution into equation (44) yields:

$$\frac{dq}{dt} = k\left[c\ (Q^\circ - q) - \frac{q}{K}\right]$$

The gas-solid heterogeneous reaction may be either a noncatalytic or a catalytic reaction. In this report, we will consider the heterogeneous, noncatalytic reaction. The treatment of this type of reaction requires the consideration of mass transfer between phases, the contacting patterns of the reacting phase, and the reaction kinetics. Levenspiel (1972) and the Chemical Engineers' Handbook present a detailed treatment of this subject. The following is a brief summary of those discussions.

A heterogeneous non-catalytic reaction may be represented by:

$$A\ (\text{gas}) + b\ B\ (\text{solid}) \rightarrow \text{Products}$$

The products may be gas, solid or both. There are several models available to describe the progress of the above reaction. The unreacted core model seems to work reasonably well in a wide variety of situations. This model considers that the reaction occurs first at the outer skin of the solid. It can leave behind both completely reacted material, and inert solid material residue. Thus, at any time there exists an unreacted core of material which shrinks in size during reaction. Two different cases may be considered for this model. The first assumes that the continuous formation of solid product (inert residue) without its flaking off would maintain the particle size unchanged. In the second case the particle size changes as the reaction progresses owing to the formation of gaseous products, flaking off of the solids, etc.

Unreacted Core Model for Spherical Particles of Unchanging Size

This model visualizes the reaction occurring in three successive steps. Either one of the three steps may be rate determining:

Step 1: Diffusion of gaseous reactant "A" through the film surrounding the solid to the exterior surface of the solid.

Step 2: Penetration and diffusion of the reactant "A" through the blanket of residue to the surface of the unreacted core.

Step 3: Reaction of gaseous reactant with solid at the reaction surface.

If the resistance of the gas film is the controlling factor, the reaction rate is equal to the diffusion rate of the gas reactant from the bulk phase to the interface. The chemical reaction can be assumed to be instantaneous. Thus, the concentration of the gas at the solid surface is zero and the concentration driving force for diffusion is constant at all times during the reaction of the particle. In terms of the shrinking radius of the unreacted core, the reaction rate is:

$$-\left(\frac{\rho_s\ r_c^2}{R^2}\right)\frac{dr_c}{dt} = b\ k_G\ c \tag{45}$$

where ρ_s = density of reactant "B", g/cm³
r_c = radius of unreacted core, cm
R = original radius of the reacting particle, cm
b = stoichiometry constant, dimensionless
k_G = mass transfer coefficient, cm²/s
c = concentration of gas reactant "A" in the bulk gas phase, g/cm³
t = time, s

Rearranging and integrating, we find how the unreacted core shrinks with time,

$$t = \frac{\rho_s\ R}{3b\ k_G\ c}\left[1 - \left(\frac{r_c}{R}\right)^2\right] \tag{46}$$

Let the time for complete reaction of a particle be "τ". Then by taking "$r_c=0$" in equation (46), we find,

$$\tau = \frac{\rho_s\ R}{3b\ k_G\ c} \tag{47}$$

The radius of the unreacted core expressed in terms of fractional time for complete conversion is obtained by combining equations:

$$\frac{t}{\tau} = 1 - \left(\frac{r_c}{R}\right)^3 = x_B \qquad (48)$$

where x_B = fraction of reactant "B" converted into product

By using the same approach, the integrated rate equations under other conditions are:

Diffusion through residue layer controls:

$$\frac{t}{\tau} = 1-3\ (1-x_B)^{2/3} + 2\ (1-x_B) \qquad (49)$$

$$\tau = \frac{\rho_s\ R^2}{6\ b\ D_e\ c} \qquad (50)$$

where D_e = effective diffusion coefficient of gaseous reactant in the residue layer, cm^2/s

Chemical reaction controls:

$$\frac{t}{\tau} = 1-\ (1-x_B)^{1/3} \qquad (51)$$

$$\tau = \frac{\rho_s\ R}{b\ k\ \ c} \qquad (52)$$

where k_s = first order rate constant for the surface reaction.

Unreacted Core Model for Shrinking Spherical Particles

When no adherent residue forms, the reacting solid particle shrinks during reaction, finally disappearing. For a reaction of this kind we visualize the following three steps occurring in succession.

Step 1: Diffusion of reactant "A" from the main body of gas through the gas film to the surface of the solid.

Step 2: Reaction on the surface between reactant "A" and solid.
Step 3: Diffusion of reaction products from the surface of the solid through the gas film back into the main body of gas.

As with constant size particles, the following rate expressions result when one or the other of the resistances control.

Diffusion through gas film controls:

Small particle (Stokes regime)

$$\frac{t}{\tau} = 1 - (1-x_B)^{2/3} \tag{53}$$

$$\tau = \frac{\rho_s \; y_A \; R^2}{2 \; b \; D_G \; c} \tag{54}$$

where y_A = mole fraction of reactant "A" in gas phase
D_G = gas diffusivity, cm^2/s

Large particle (u_G = constant)

$$\frac{t}{\tau} = 1 - (1-x_B)^{0.5} \tag{55}$$

$$\tau = (\text{constant}) \frac{R^{3/2}}{c} \tag{56}$$

Chemical reaction controls: When chemical reaction controls, the behavior is identical to that of particles of unchanging size; therefore, equations (51) and (52) will represent the time-conversion behavior of single particles, both shrinking and of constant size. With this information on reaction kinetics, we can determine the required granular bed size for various gas-solid contacting schemes (fixed bed batch process, continuous moving bed, etc.).

Cake Filtration

Granular bed filters usually have larger pore sizes and greater thickness than the fibrous filter. Whether internal cakes will form depends largely on the granule size. If the granules of the bed are large, dendrites will not bridge to create an internal cake. On the other hand, if the grains are sufficiently small, dendrites will bridge to form an internal cake.

Lee (1975) called the internal cake a rooting cake and it is the foundation to support the formation of a surface cake. Once a surface cake is formed, filtration efficiency no longer depends upon the depth of the granular bed but rather on the thickness and structure of the surface cake. The cake filtration results in a much higher efficiency than the original granular bed. This is because particle collection by sieving becomes a more important collection mechanism.

Leith, et al. (1976) and Leith and First (1977) studied high velocity cake filtration of fabric filters. Three mechanisms were described by them by which particles can pass through a fabric filter or a granular bed. The three mechanisms are:

1. Straight through penetration
2. Seepage or bleeding penetration
3. Pinhole plug penetration

In straight through penetration, particles pass through the filter without stopping; i.e., they are not collected by the filter. Once a particle lands on or in the filter, it needs not necessarily remain at its point of initial impact. As the dust deposit builds up, the dust may work its way through from the dirty to the clean side of the filter. This may result from the drag force exerted on the particle deposits by the gas moving past. Penetration of this sort is called seepage or bleeding. The pinhole plug mechanism postulates a plug of deposited particles dislodged from the dust deposit and moves out of it, leaving behind a pinhole. Figure 27 is a schematic representation of penetration mechanisms.

The size distribution of particles passing through the filter by the straight through mechanism should reflect a dependence

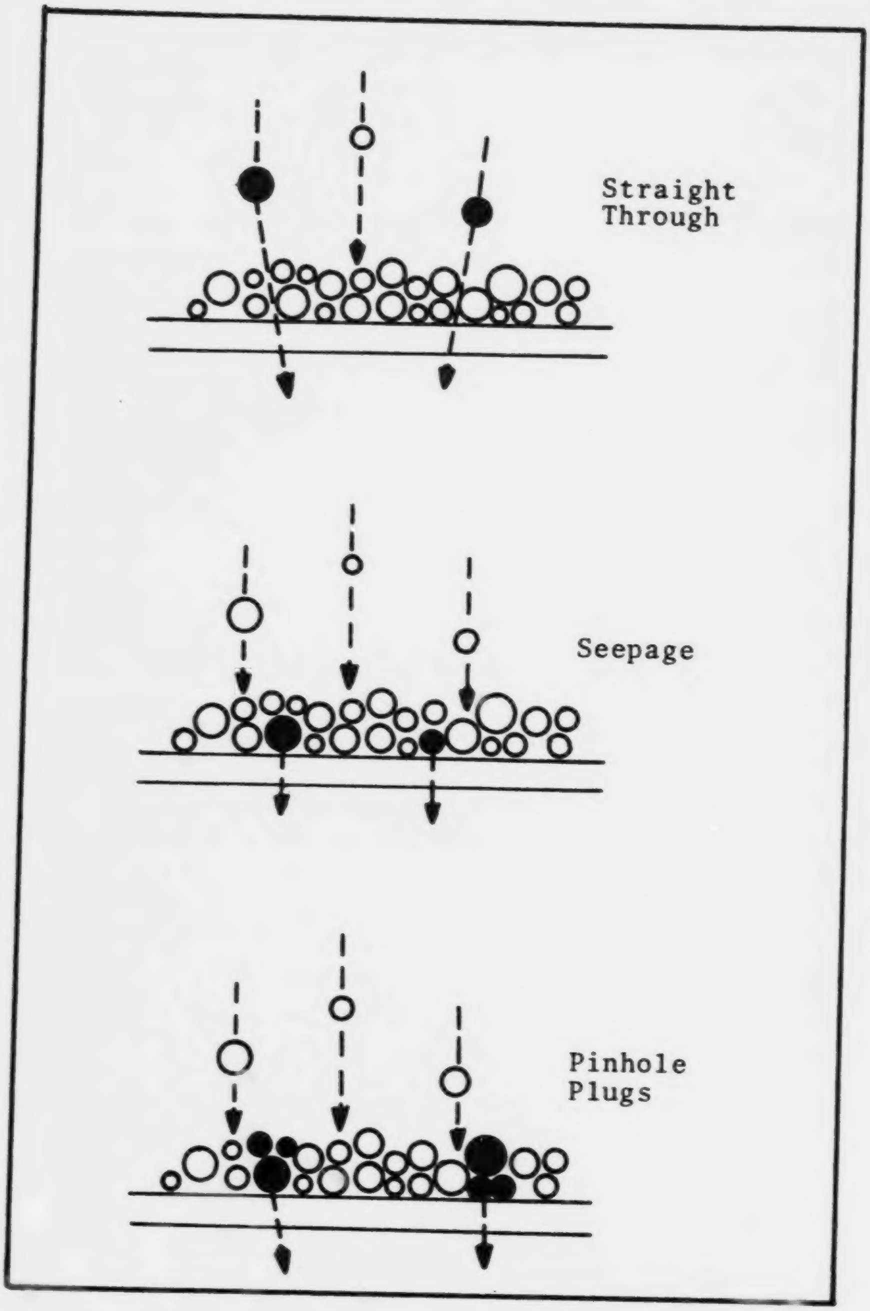
Straight
Through
Seepage
Pinhole
Plugs

Figure 27. Schematic representation of fly ash emission mechanisms.

on the forces causing particles to be collected there: inertia, interception, diffusion, gravity, etc. However, the size distribution of the particles which pass through by seepage or pinhole plugs should be the same as the size distribution of the deposited dust; that is, very close to the size distribution of dust fed to the filter.

Using a series of tagged dusts, the proportion of total dust emitted which is accountable to each emission mechanism was measured by Leith et al. (1976) in relation to face velocity and deposit thickness. Deposit thickness is defined as:

$$X = \frac{W}{\rho_p\ (1-\varepsilon)} = \frac{C_{pi} t\ u_G}{\rho_p\ (1-\varepsilon)} \tag{57}$$

where X = dust deposit thickness, μm or cm
ρ_p = particle density, g/cm³
W = particulate load, g/cm²
C_{pi} = inlet particle concentration, g/cm³
u_G = superficial gas velocity, cm/s
t = time since last cleaning, s

They found significant trends in the dust penetration mechanism data. The time-mechanism interaction was highly significant. As time increases and the dust deposit thickens, the mechanisms by which dust penetrates the filter change. Straight through penetration rapidly diminishes in importance although it is important immediately after a filter cleaning cycle. The emitted dust accountable to the seepage mechanisms is relatively constant during the entire filtration cycle. The pinhole plug mechanism rapidly rises in importance after cleaning, passes through a maximum, and then declines as the dust deposit becomes thicker and pressure drop through the deposit increases. Figure 28 is an illustration of the trends.

The velocity mechanism interaction was not significant. At any fixed time, the fraction of dust emitted by each penetration mechanism is fairly constant at all velocities tested.

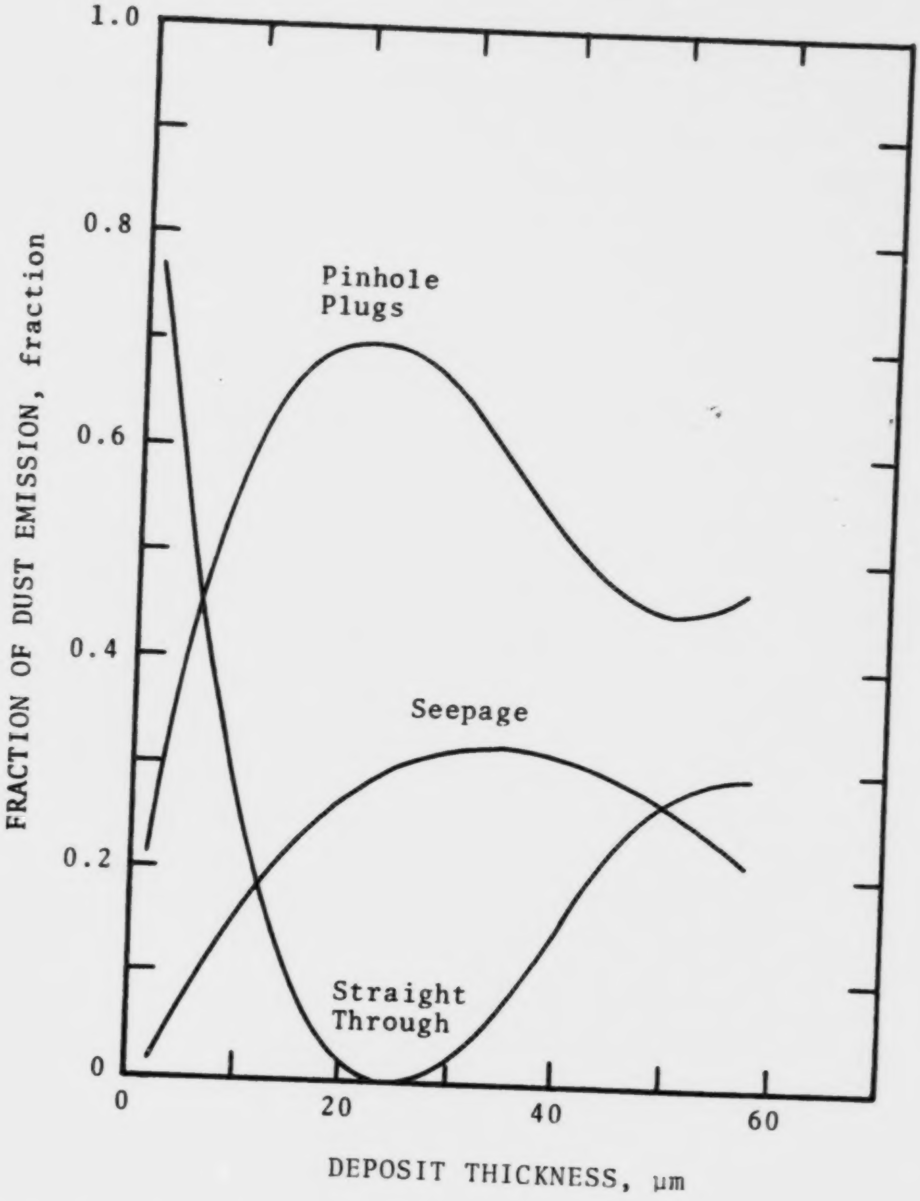

Figure 28. Fraction of total fly ash emitted by various mechanisms as a function of deposit thickness.

Miyamoto and Bohn (1975) studied the effect of particle loading on granular bed filter collection efficiency. Their results were presented in Figures 13, 14 and 15 in an earlier section of this report.

Under contract with EPRI, Squires and his co-workers at City College of New York have experimentally determined the collection efficiency of a granular bed with filter cake. A final report has recently been published (Lee et al., 1977).

Pressure Drop

Clean Bed -

Several investigators have shown that the flow through packed beds can be described by:

$$-\Delta P = \frac{f\ Z\ u_G\ (1-\varepsilon)\rho_G}{d_c\ \ \varepsilon^3} \qquad (58)$$

where ΔP = pressure drop across packed bed, g/cm-s^2
f = friction factor, dimensionless
u_G = superficial gas velocity, cm/s
ρ_G = gas density, g/cm^3
ε = bed porosity, fraction
d_c = bed particle diameter, cm

Figure 29 is a plot of friction factor versus Reynolds number for a fixed bed. Ergun (1952) has defined a Reynolds number as:

$$N_{Re} = \frac{d_c\ u_G\ \rho_G}{\mu_G\ (1-\varepsilon)} \qquad (59)$$

For laminar flow with $N_R < 1.0$; and by analogy to flow in many other systems, we can approximate "f" by a constant divided by "N_{Re}." An analysis of experimental data indicates that the constant is 150. Therefore, for laminar flow we have:

$$f = \frac{150}{N_{Re}} \qquad (60)$$

This is referred to as the Kozeny-Carman equation. For a given bed and fluid, it predicts that the flow rate is proportional to the pressure drop, which is D'Arcys law.

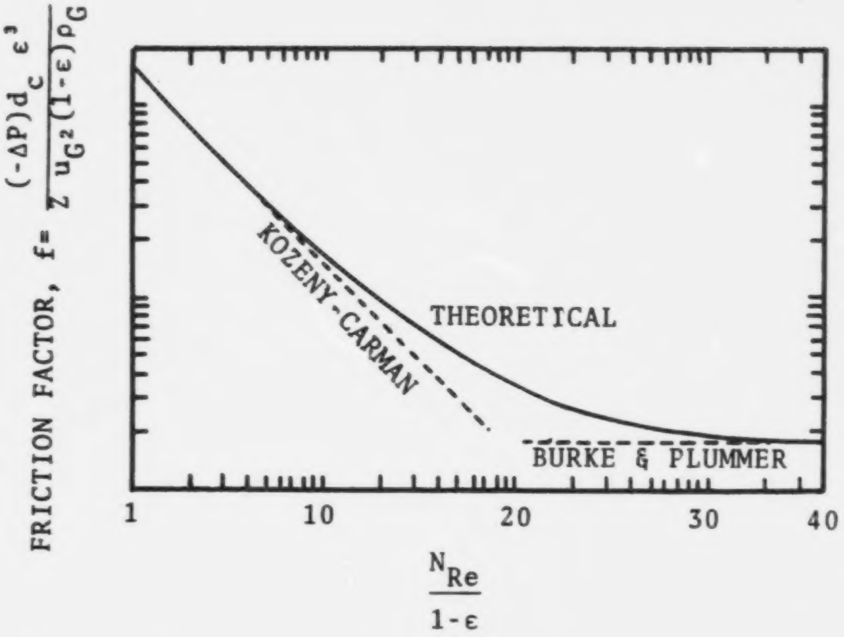

Figure 29. A comprehensive plot of pressure drop in fixed beds.

For completely turbulent flow, it is reasoned that "f" should approach a constant value and that all packed beds have the same relative roughness. The constant is found by experiment to be 1.75, so we have:

$$f = 1.75 = \frac{(-\Delta P)\, d_c\, \varepsilon}{Z\, u_G^2\, \rho_G\, (1-\varepsilon)} \qquad (61)$$

This is called the Burke-Plummer equation.

A consideration of flow at intermediate Reynolds numbers led Ergun (1952) to propose as a general equation:

$$f = \frac{150}{N_{Re}} + 1.75 \qquad (62)$$

Filter Cake Resistance to Gas Flow -

Miyamoto and Bohn (1975) studied the effect of particulate load on pressure drop. Figures (30) through (32) show their results. The pressure drop remained constant until the particulate load of the filters reached a threshold load, then increased rapidly as shown in the figures.

In granular bed filters, the flow resistance should change little so long as the large pores are open, but will increase when the large pores are closed by surface cake. Depending on whether the compaction effect of the filter cake is present, the increase of pressure drop is at a different rate.

No compaction effect - The pressure drop across the surface cake is given by D'Arcy's law, i.e.,

$$-\Delta P = \frac{\mu_G\, u_G\, Z}{K_d} \qquad (63)$$

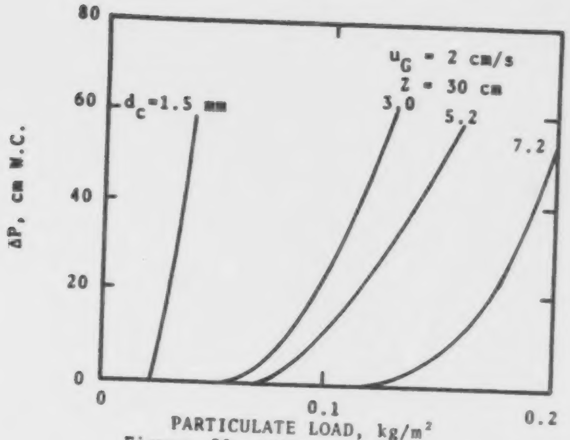

Figure 30. Effect of mean granule diameter on pressure drop (Miyamoto and Bohn's data).

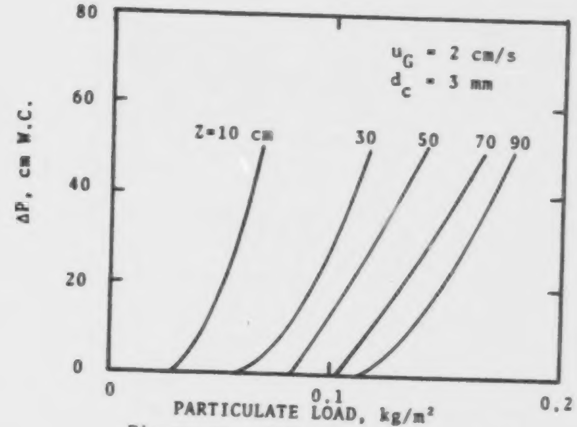

Figure 31. Effect of bed depth on pressure drop (Miyamoto and Bohn's data).

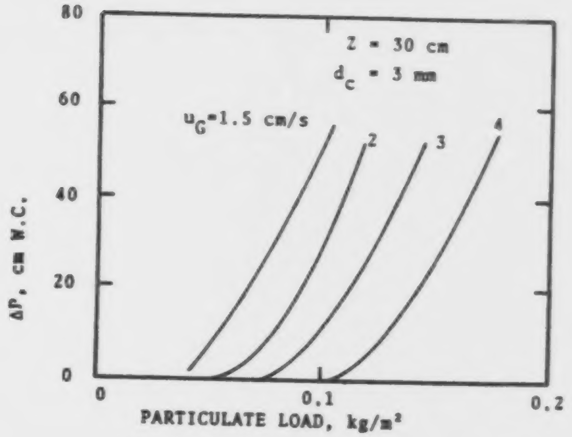

Figure 32. Effect of superficial gas velocity on pressure drop (Miyamoto and Bohn's data).

where Δp = pressure drop across packed bed, g/cm-s²
μ_G = gas viscosity, g/cm-s
u_G = superficial gas velocity, cm/s
Z = bed depth, cm
K_d = D'Arcy permeability, cm²

For laminar flow, it becomes

$$-\Delta p = \frac{150\ Z\ u_G^2\ (1-\varepsilon)\ \rho_G}{N_{Re}\ d_c\ \varepsilon^3} \tag{64}$$

where ε = bed porosity, fraction
ρ_G = gas density, g/cm³
d_c = granule diameter, cm
N_{Re} = Reynolds number, dimensionless

This is referred to as the Kozeny-Carman equation.

By combining equations (63) and (64) we obtain:

$$-\Delta p = \frac{150\ \mu_G\ Z\ u_G\ (1-\varepsilon)^2}{d_c^{\,2}\varepsilon^3} \tag{65}$$

Substituting equation (57)(X = Z) into equation (65) gives:

$$-\Delta p = \frac{150\ \mu_G\ C_{pi} t\ u_G^2\ (1-\varepsilon)}{d_c^{\,2}\varepsilon^3\rho_p} \tag{66}$$

where Δp = pressure drop across filter cake, g/cm-s²
μ_G = gas viscosity, g/cm-s
t = time since last cleaning, s
u_G = superficial gas velocity, cm/s
ε = filter cake porosity, fraction
d_c = granule diameter, cm
ρ_p = particle density, g/cm³
C_{pi} = inlet particulate concentration, g/cm³

Equation (66) predicts that at constant inlet conditions, the pressure drop across the surface cake varies linearly with time as long as the porosity of the filter cake remains constant (no compaction effect present). It also predicts a linear relationship between pressure drop and the square of the superficial gas velocity, after the same time period, for equal loadings and bulk density of the filter cake.

Compaction Effects - Leith et al (1976) also have studied the compaction of filter cake and its implications. They found that Kozeny-Carman's equation yields excellent results for powders which are compressed to a specified porosity provided the particles are isometric.

Compaction of the cake is a complicated phenomenon which is related to the increased drag exerted by the gas on the cake. Although the dust on the surface of the cake is under negligible mechanical stress due to this drag, the dust below the surface must support the drag experienced by the dust layer above it. At the bottom of the cake, the compressive stress is the greatest and equals the total pressure drop across the cake, plus the stress due to the impact of new particles.

Limited studies have been done to determine the effects of increased velocities on permeability. Stephan et al. (1960) observed a 60% change in this factor when velocity was increased from 1.8 to 3.0 m/min with clean air, and the change was noted to take place in 5 discrete collapses. The cake was initially deposited at 1 m/min (3.4 ft/min). Borguardi et al (1968) reported a similar change with the same dust (fly ash). These studies provide some insight into cake collapse. However, if the cake is formed at high velocity, and the velocity remains constant, the compaction of the cake may proceed more gradually due to tighter initial packing.

Orr (1966) indicated that compaction of cake can take place by three mechanisms:

1. sliding,
2. elastic and plastic deformation,

and 3. fragmentation.

The latter is unlikely except for extremely fragile particles due to the relatively small compressive stresses. The most likely mechanism is sliding which is opposed by frictional and cohesive forces between particles. Compaction effects are often described by the following exponential expression:

$$\varepsilon = \varepsilon_i \exp(-a F) \tag{67}$$

where ε = final void fraction, fraction
ε_i = initial void fraction, fraction
a = constant, $cm\text{-}s^2/g$
F = compression stress, $g/cm\text{-}s^2$

Differentiating equation (67) gives:

$$\frac{d\varepsilon}{dF} = - a \varepsilon \tag{68}$$

Differentiating equation (57) yields:

$$dX = \frac{dW}{(1-\varepsilon)\rho_p} + \frac{W}{\rho_p} + \frac{d\varepsilon}{(1-\varepsilon)^2} \tag{69}$$

D'Arcy's equation is

$$\frac{dp}{dX} = - \frac{\mu_G u_G}{K_d} \tag{70}$$

Combining equations (69) and (70) we obtain:

$$- \frac{K_d}{\mu_G u_G} dp = \frac{dW}{(1-\varepsilon)\rho_p} + \frac{W}{\rho_p} \quad \frac{d\varepsilon}{(1-\varepsilon)^2} \tag{71}$$

From the Kozeny-Carman equation

$$K_d = \frac{d_c{}^2 \varepsilon^3}{150 (1-\varepsilon)^2} \tag{72}$$

Combining equations (71) and (72) yields

$$dp = - \frac{150\ \mu_G\ u_G}{d_c{}^2\ \rho_p} \left| \frac{1-\varepsilon}{\varepsilon^3}\ dW + \frac{W}{\varepsilon^3}\ d\varepsilon \right| \qquad (73)$$

For a small increment of cake

$$dF = -\ dP \qquad (74)$$

Combining equations

$$\frac{dW}{d\varepsilon} = \frac{k\ \varepsilon^2 + W}{(\varepsilon-1)} \qquad (75)$$

where k = constant, g/cm²

$$= \frac{d_c{}^2\ \rho_p}{150\ a\ \mu_G\ u_G}$$

Solving equation (75) with boundary condition,

$\varepsilon = \varepsilon_i$ at $W = 0$, yields

$$\frac{W}{k} = \varepsilon^2 - 2\varepsilon - 2(1-\varepsilon)\ln(1-\varepsilon) - (1-\varepsilon)\left[\frac{2\varepsilon_i - \varepsilon_i{}^2 + 2(1-\varepsilon_i)\ \ln\ (1-\varepsilon_i)}{(1-\varepsilon_i)}\right] \qquad (76)$$

Since the total compressive stress on the cake is equal to "p", equation (67) can be rewritten as,

$$\varepsilon = \varepsilon_i\ \exp\ [\ -a\ (\Delta p)] \qquad (77)$$

Substituting equation (76) into equation (77) yields,

$$\frac{W}{k} = \varepsilon_i{}^2 \left[e^{-a(\Delta p)}\right]^2 - 2\ \varepsilon_i\ e^{-a(\Delta p)} - 2\left[1-\varepsilon_i e^{-a(\Delta p)}\right] \ln \left[1-\varepsilon_i e^{-a(\Delta p)}\right]$$
$$- \left[1-\varepsilon_i\ e^{-a(\Delta p)}\right] \frac{\left[2\ \varepsilon_i - \varepsilon_i{}^2 + 2(1-\varepsilon_i)\ \ln\ (1-\varepsilon_i)\right]}{1-\varepsilon_i} \qquad (78)$$

Since $$W = C_{pi} u_G \, t \tag{79}$$

We have

$$t \left(\frac{C_{pi} u_G}{k}\right) = \varepsilon_i{}^2 \left[e^{-a(\Delta p)}\right]^2 - 2\varepsilon_i \, e^{-a(\Delta p)} - 2\left[1-\varepsilon_i \, e^{-a(\Delta p)}\right] \ln\left[1-\varepsilon_i \, e^{-a(\Delta p)}\right] - \left[1-\varepsilon_i \, e^{-a(\Delta p)}\right] \frac{\left[2\varepsilon_i - \varepsilon_i{}^2 + 2(1-\varepsilon_i) \ln(1-\varepsilon_i)\right]}{1-\varepsilon_i} \tag{80}$$

A plot of pressure drop versus time for cake buildup can be a curve fitted to equation (80) and the constants a, ε_i, and k evaluated by regression analysis.

SECTION 4

COMPARISON BETWEEN MODEL PREDICTION AND DATA

Table 14 is a summary of available design equations. These equations have been discussed in detail in an earlier section. In this section, predictions by these equations will be compared with data reported in the literature. Only those data which have been obtained under controlled conditions and for a well-defined GBF system will be utilized to test the models.

DATA REPORTED BY McCAIN

McCain (1976) conducted a performance test on a Rexnord gravel bed filter. The gravel bed filter was installed to clean emissions from a clinker cooler in a Portland cement plant.

Samples were taken simultaneously at the filter inlet and outlet with cascade impactors. Grade efficiencies were then calculated from impactor data. The operating conditions of the gravel bed and McCain's data are discussed in detail in a later section. Comparison between McCain's data and model predictions are shown in Figure 33.

According to Jackson and Calvert, the empirical constant, "C_1", in their equation was 21.4 for a bed of 1.27 cm (0.5 in.) diameter packing elements. As can be seen from Figure 33, with a constant of this value the model over predicts the performance of the granular bed. A value of 10 for the constant will give a much better fit with the data.

The single granule collection efficiency, "η", in Paretsky et al.'s equation includes the collection by: (1) Brownian diffusion, (2) direct interception, (3) inertial impaction, and (4) gravity settling. If every interaction term between the four collection mechanisms is neglected, then:

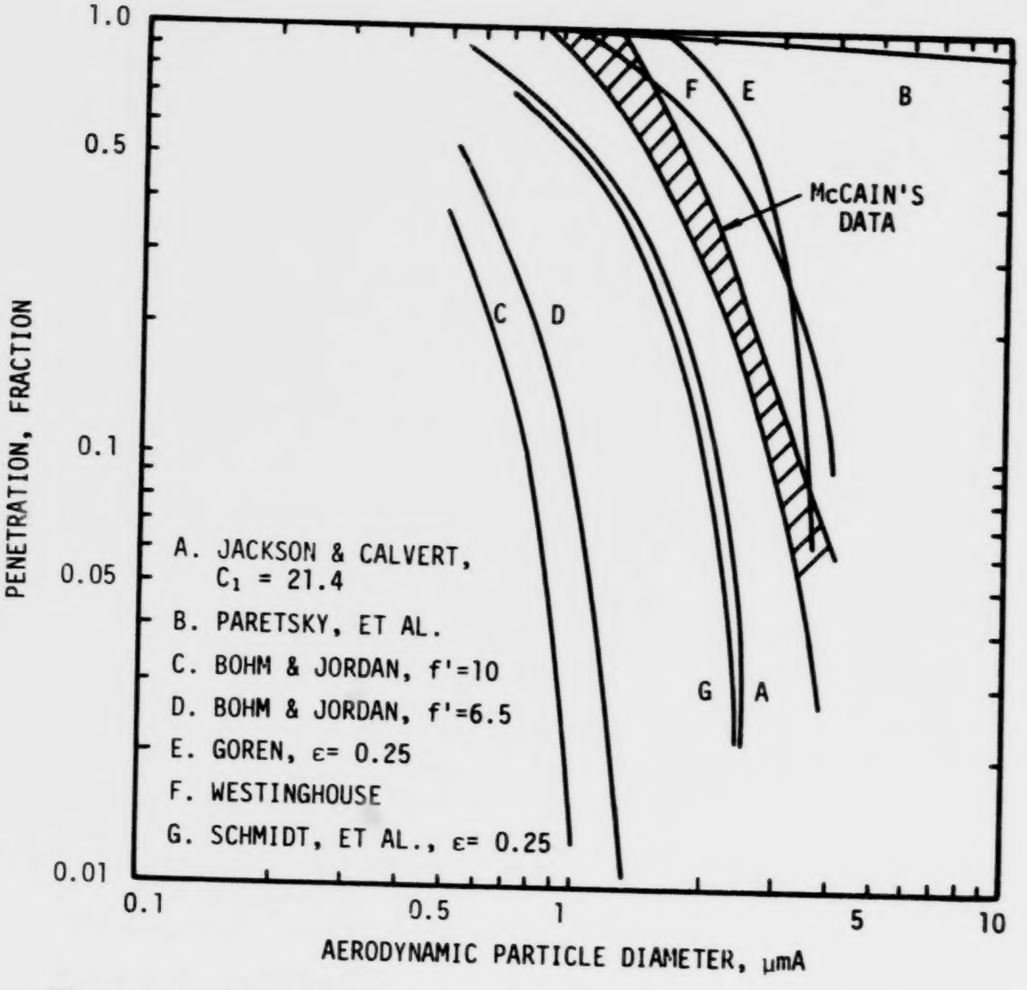

Figure 33. Comparison of McCain's gravel bed particle collection data with design equation predictions.

TABLE 14. AVAILABLE EQUATIONS FOR THE PREDICTION OF PARTICLE COLLECTION IN A GRANULAR BED

Investigator	Equation	Notes
Jackson and Calvert (1968)	$Pt_d = \exp\left[-C_1 \frac{Z}{d_c} K_p\right]$	Impaction only.
Paretsky et al. (1971)	$Pt_d = \exp\left[-\frac{3}{2}\frac{1-\varepsilon}{\varepsilon}\frac{Z}{d_c}\eta\right]$	
Miyamoto and Bohn (1974)	$Pt_d = \exp\left[-\frac{6(1-\varepsilon)Z}{d_c}\frac{N_{Nu}}{N_{Pe}}\right]$	Collection by diffusion only.
Gebhart et al. (1973)	$Pt_d = \exp\left[-6.39\frac{D_p{}^{2/3} Z}{u_{Gi}{}^{2/3} R_c{}^{5/3}}\right]$	Collection by diffusion only
Böhm and Jordan (1976)	$Pt_d = \exp\left[-\left(\frac{2 k T \varepsilon f}{3\pi d_p u_G} + \frac{d_p^2 g \rho_p \varepsilon d_c}{36 u_G} + \frac{\pi d_p^2 \rho_p u_G}{18\varepsilon}\right)\frac{4 f' Z}{\mu_G d_c{}^2}\right]$	Collection by diffusion. Gravity settling and impaction.

Continued

TABLE 14. (continued)

Investigator	Equation	Notes
Goren (1977)	$Pt_d = \exp\left[-\frac{3}{2}(1-\varepsilon)\frac{Z}{d_c}\left(1250\, K_p^{2.25} + \left(\frac{u_t}{u_G}\right)^{0.75} + 200\, N_{Pe}^{-2/3}\right)\right]$	Collection by impaction, gravity settling, and diffusion
Westinghouse (Ciliberti, 1977)	$Pt_d = \exp\left[-5.8\frac{K_p Z}{d_c} - 3.75\left(\frac{d_p}{d_c}\right)^2\frac{Z}{d_c}\right.$ $\left. 3.572\frac{D_p^{2/3}\, Z}{u_G^{2/3}\, d_c^{5/3}}\right]$	Collection by impaction, interception, and diffusion
Schmidt, et al. (1978)	$Pt_d = \exp\left[-\frac{7.5\, Z\, (1-\varepsilon)}{d_c}\left(\frac{8}{N_{Pe}} + 2.038\, N_{Re}^{1/8}\, N_{Pe}^{-5/8} + 1.45\left(\frac{d_p}{d_c}\right)^2 + 3.97\, K_p + \frac{u_t}{u_G}\right)\right]$	Collection by diffusion, interception, impaction, and gravity settling

$$\eta = \eta_D + \eta_{DI} + \eta_I + \eta_{GS}$$

and, $$Pt_d = (Pt_d)_D \, (Pt_d)_{DI} \, (Pt_d)_I \, (Pt_d)_{GS}$$

where η = single granule collection efficiency, fraction
Pt_d = particle penetration, fraction
and subscripts D, DI, I and GS refer to diffusion, direct interception, and gravity settling, respectively

As can be seen from Figure 33 for this particular granular bed filter, their equation predicts that the collection efficiency will be very low. This is not in agreement with McCain's data. This discrepancy may result from Paretsky et al. basing their equation on collection by an isolated sphere. At a gas velocity of 80 cm/s (superficial gas velocity in the granular bed during McCain's tests), the dominant collection mechanism is inertial impaction. For particle collection by inertial impaction onto a single spherical collector, it may be generally assumed that there will be no collection if the inertial impaction parameter is below a critical value. The critical value of impaction parameter is about 0.083 for an isolated spherical collector. For the test conditions in McCain's tests, this is equivalent to the impaction parameter of a 10 μmA diameter particle. Therefore, for particles with diameters smaller than 10 μmA, there should be no collection by impaction.

Böhm and Jordan (1976) derived their equation by visualizing the granular bed as a system of parallel capillaries. The ratio of granule diameter to initial capillary diameter, "f", changes during the filtration period due to accumulation of collected particles. According to Böhm and Jordan,

$$6.5 \leq f' < 10$$

The predicted particle penetration for f' = 6.5 and f' = 10 is plotted in Figure 33. By assuming there was no surface cake and the pressure drop across the bed was 80% of the overall pressure drop, the bed porosity was estimated to be 0.25 (by Ergun's equation). With this value for bed porosity, Böhm and Jordan's equation predicted too low a particle penetration. If we assume f' = 0.75 the prediction will match the data. However, this assumption is unrealistic because for f' < 1, the capillary diameter will be greater than the granule diameter.

The predicted penetration based on Goren's model for $\varepsilon = 0.25$ is higher than measured.

As mentioned earlier, the dominant collection mechanism was inertial impaction for the operating conditions of the filter during McCain's tests. Both Miyamoto and Böhm's equation and Gebhart et al.'s equation are for particle collection by diffusion only. Therefore, these two equations are not suitable for comparing with McCain's data.

For collection by impaction, Westinghouse's model and Schmidt et al.'s model reduce to:

Westinghouse: $Pt_d = \exp\left(-5.8 \frac{Z}{d_c} K_p\right)$

Schmidt et al.: $Pt_d = \exp\left[-29.85 (1-\varepsilon) \frac{Z}{d_c} K_p\right]$

Except for the constant, these equations are identical to that of Jackson and Calvert (1968). Predictions by these equations are compared with McCain's data in Figure 33. Bed porosity is assumed to be 0.25. As can be seen, Westinghouse's model slightly overestimated the penetration and Schmidt et al.'s model underestimated particle penetration.

DATA REPORTED BY HOOD

Hood (1976) reported the evaluation of the Combustion Power Company's moving gravel bed filter on the control of particulate emissions from a hog-fuel fired boiler. The gravel bed filter was a prototype unit with suggested capacity of 1,133 Am³/min (40,000 ACFM). The bed was packed with an intermediate size gravel which was retained on a 3.2 mm (1/8 in.) wire mesh and passed a 6.4 mm (1/4 in.) mesh screen. The bed was a single down-flowing annulus 2.6 m (8.5 ft) O.D. and 1.8m(6 ft) I.D.

During sampling the unit was operated at a flow rate of 1,558 m³/min (55,000 ACFM). The gas temperature was 177°C (350°F).

Particle size distribution and concentration were sampled with cascade impactors. Particle penetration was calculated from the cascade impactor data.

Figure 34 shows the comparison between Hood's results and predictions by available design equations. The bed porosity was calculated to be 0.25 (from Ergun's equation). As can be seen from Figure 34, none of the available design equations agrees with the measured performance.

Under the sponsorship of ERDA, Combustion Power Company conducted experimental studies on their GBF system to correlate the collection efficiency of the GBF with mechanical and process parameters. Parameters studied included superficial gas velocity, dust loading, particle size and distribution, granule diameter, granule circulation rate, and bed thickness.

The GBF was a pilot unit and was operated at ambient temperature. Redispersed hydrated alumina was used as test dust.

A.P.T. has acquired some data with cascade impactors on this GBF system. Figures 35 through 37 show part of the data along with predictions by available design equations. The model predictions do not agree with the data.

DATA BY KNETTIG AND BEECKMANS

As mentioned earlier, all of the available equations are for the prediction of particle collection by clean beds. The granular bed filter data reported by McCain and by Hood are data obtained on industrial installations. The beds will not be clean. In the following sections, data obtained on laboratory scale clean granular bed filters will be used to test the design equations.

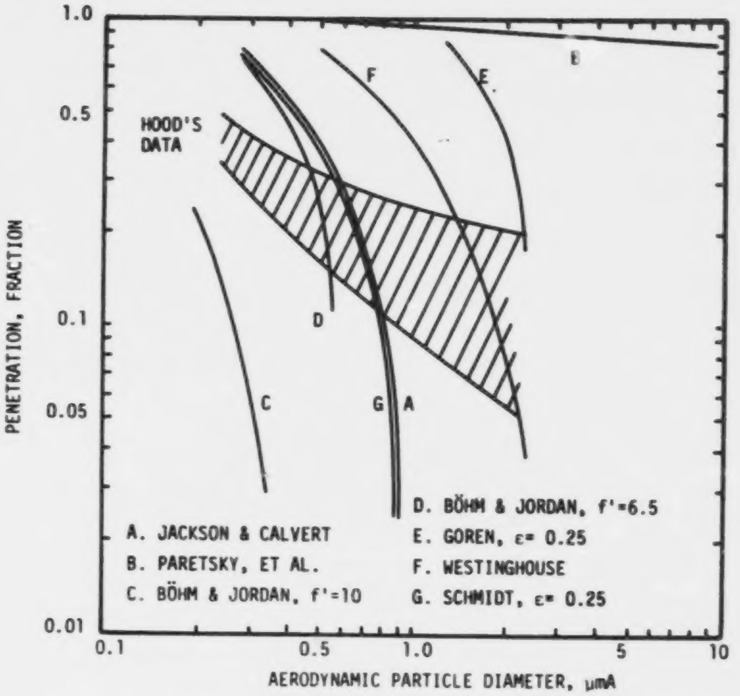

Figure 34. Comparison of Hood's data with predictions by available design equations.

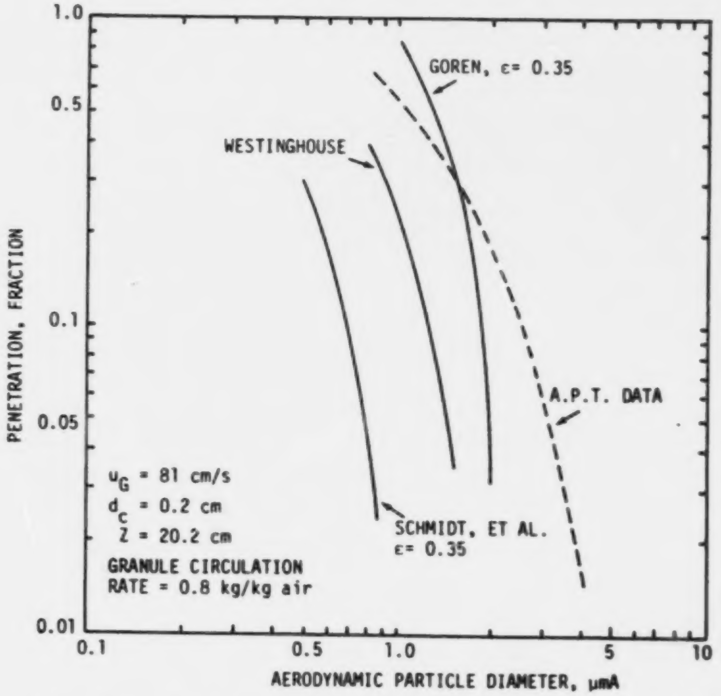

Figure 35. Experimental and predicted performance of CPC GBF (A.P.T. data).

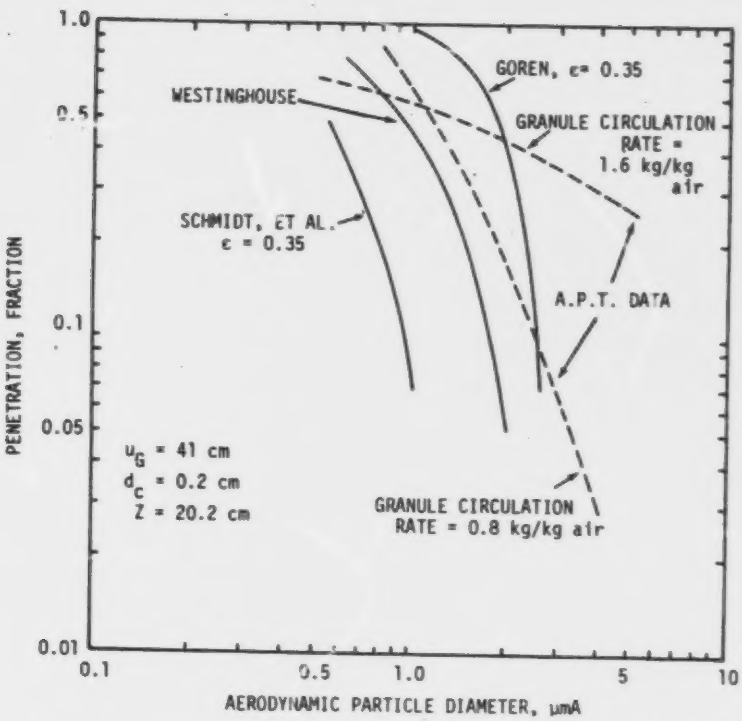

Figure 36. Experimental and predicted performance of CPC GBF (A.P.T. data).

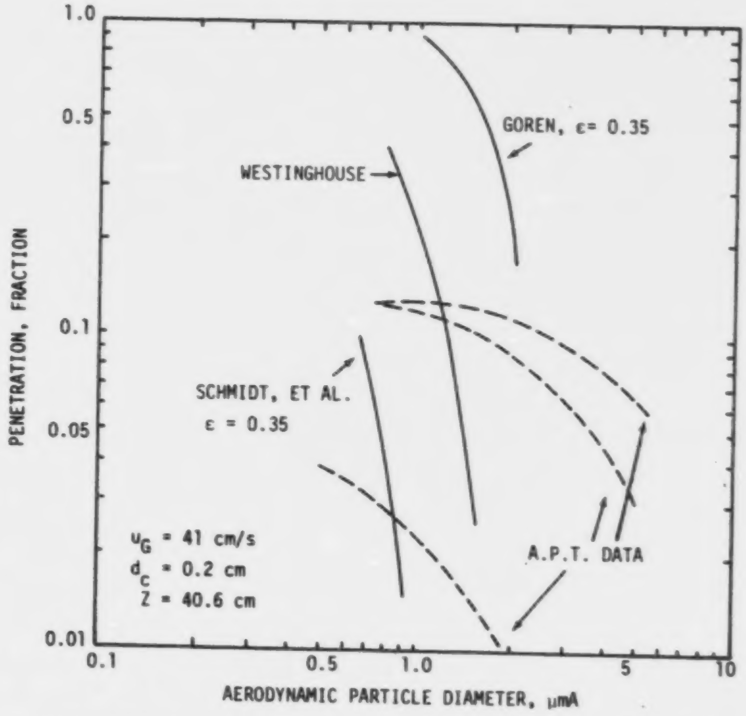

Figure 37. Experimental and predicted performance of CPC GBF (A.P.T. data).

Knettig and Beeckmans (1974) studied the capture of monodisperse aerosol particles in the size range of 0.8-2.9 μm in a screen supported and in a grid supported fixed bed of 425 μm glass beads. Test results showed a linear relationship between collection efficiency, expressed in transfer units, and bed height. Impaction appears to have been the primary collection mechanism because collection efficiency increased with both superficial gas velocity and aerosol particle size. Transfer units are related to penetration by:

$$NTU = -\ln Pt_d \qquad (81)$$

In terms of number of transfer units, various design equations become:

Jackson and Calvert: $$\frac{NTU}{Z} = \frac{C_1 K_p}{d_c} \qquad (82)$$

Paretsky et al.: $$\frac{NTU}{Z} = \frac{3}{2}(1-\varepsilon)\frac{\eta}{d_c} \qquad (83)$$

Goren: $$\frac{NTU}{Z} = \frac{3}{2}(1-\varepsilon)\frac{\eta}{d_c} \qquad (84)$$

Böhm and Jordan: $$\frac{NTU}{Z} = \frac{2\pi f'}{9\varepsilon}\frac{K_p}{d_c} \qquad (85)$$

Westinghouse: $$\frac{NTU}{Z} = 2.9\frac{K_p}{d_c} \qquad (86)$$

Schmidt, et al.: $$\frac{NTU}{Z} = 29.85(1-\varepsilon)\frac{K_p}{d_c} \qquad (87)$$

Table 15 compares data with predictions. None of the predictions agree with the data. Jackson and Calvert's equation (1965) and Bohm and Jordan's (1976) equations overpredict efficiency. Paretsky et al.'s equation predicts no particle

TABLE 15. COMPARISON OF KNETTIG AND BEECKMAN'S DATA AND PREDICTIONS

Support	Superficial Gas Velocity cm/s	Particle Diameter μm	$\left(\frac{NTU}{Z}\right)$ experiment	(NTU/Z) Predicted					
				Jackson & Calvert $C_1 = 10$	Paretsky	Bohm & Jordan $f'=6.5$	Goren	Westinghouse	Schmidt
Screen Support	8.2	0.8	0.05	0.28	0	2.5	0.004	0.078	0.48
		1.6	0.076	1.03	0	10.0	0.07	0.14	0.88
		2.9	0.27	3.23	0	32.9	0.98	0.25	1.54
	11.2	0.8	0.054	0.38	0	3.4	0.008	0.106	0.66
		1.6	0.08	1.4	0	13.7	0.15	0.19	1.20
		2.9	0.306	4.4	0	45.0	1.98	0.34	2.10
Grid Support	8.2	0.8	0.042	0.28	0	2.5	0.004	0.78	0.48
		1.6	0.058	1.03	0	10.0	0.07	0.14	0.88
		1.9	0.336	3.23	0	32.9	0.98	0.25	1.54
	11.2	0.8	0.044	0.38	0	3.4	0.008	0.106	0.66
		1.6	0.074	1.4	0	13.7	0.15	0.19	1.20
		2.9	0.362	4.4	0	45.0	1.98	0.34	2.10

collection. This does not agree with the experimental data. Goren's equation underestimates penetration for particles smaller than 1.6 μm and predicts too low a penetration for particles larger than 1.6 μm in diameter.

DATA BY PARETSKY, ET AL.

Paretsky et al. (1971) studied the filtration of dilute aerosols by beds of sand. Test conditions and data were reported in an earlier section. Their data obtained with a bed of 1,200 to 1,700 μm (-10+14 mesh) angular sand are compared with various models in Figure 38.

The agreement between Paretsky et al.'s data and theory is good for gas velocities less than 10 cm/s. For higher gas flow rates; i.e., in the region where particle collection by impaction is dominant, the theory underestimates the collection efficiency.

Agreement between Böhm and Jordan's equation and Paretsky et al's data is poor in the high gas flow region. In the diffusional collection region the agreement is fair.

Predictions by other models do not agree with Paretsky's data.

DATA BY GEBHART, ET AL.

Gebhart et al. (1973) published an extensive experimental study on the collection of aerosol particles by diffusion in packed beds consisting of uniform glass spheres. They derived an experimental correlation to predict the diffusional collection in a granular bed.

Figure 39 shows the predicted diffusional collection in a granular bed filter by the equation proposed by Paretsky et al. along with the Gebhart et al. data. The agreement between theory and data is fair.

Both Goren's equation and Böhm and Jordan's equation predict much too low a penetration when compared with the Gebhart et al. data.

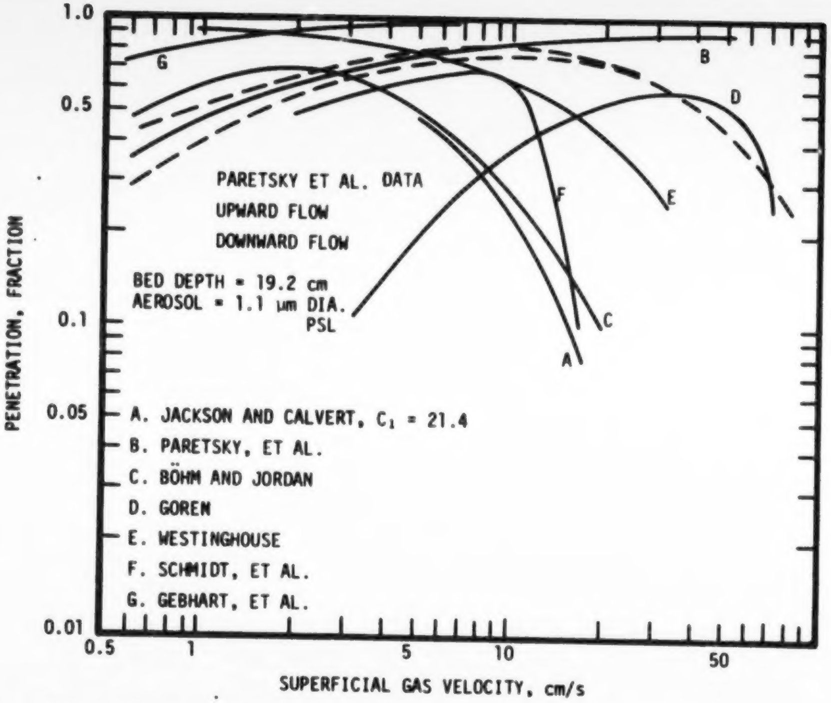

Figure 38. Comparison of Paretsky, et al. data with predictions by available design equation.

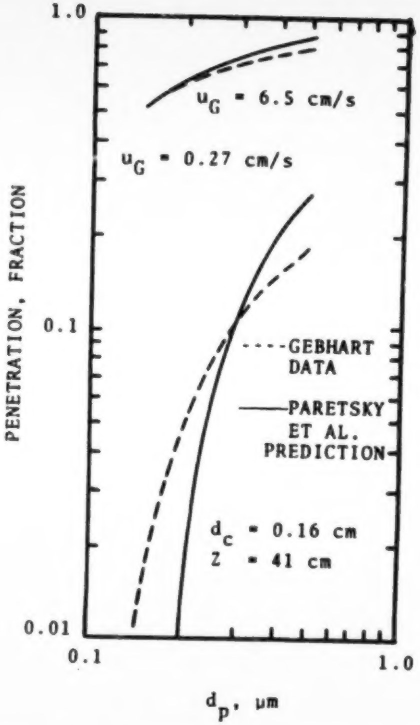

Figure 39. Comparison of Gebhart et al. data and predictions by Paretsky et al. equation. Collection is in the diffusion regime.

CONCLUSIONS

Based on the comparisons between theory and data presented above the following conclusions may be drawn:

1. For superficial gas velocities less than 10 cm/s, Paretsky's equation can be used to predict granular bed filter performance.
2. For superficial gas velocities greater than 10 cm/s, the primary collection mechanism is impaction. The available models have not been shown to be satisfactory for the prediction of granular bed collection efficiencies.

SECTION 5

EXPERIMENT

APPARATUS

The need for some experimental work became apparent in the course of the present research. A practical granular bed filter should be operated at a high gas flow rate where inertial impaction is the principal particle collection mechanism. Available design equations were not adequate for predicting granular bed collection efficiencies in the inertial impaction regime.

To obtain further information on the mechanism of particle collection by impaction and to generate additional clean bed performance data, the experimental apparatus shown in Figure 40 was constructed. Filtered room air was used for the study and all flow rates were monitored with rotameters. Monodisperse polystyrene latex aerosol was generated using a Collison atomizer. The aerosol mist from the generator mixed with a stream of dilution air and passed through a dryer to vaporize the water. Static charges were removed by passing the aerosol through a charge neutralizing section. The charge neutralizing section consisted of a Krypton-85 charge neutralizer.

Following the neutralizing section the aerosol was further diluted with filtered room air and then passed into the granular bed test section. Gas flow through the granular bed was controlled by using a bypass vent.

The granular bed test section was made of 10.2 cm (4 in.) I.D. glass pipe and the filter was a bed packed with either iron shot or sand. The aerosol concentrations before and after the bed were measured with an optical counter. Pressure drop was monitored with calibrated gauges.

Five grades of iron shot and one grade of sand were used as bed materials. The iron shots were SAE S-110, S-170, S-230, S-280, and S-330. Figure 41 shows the size distributions of

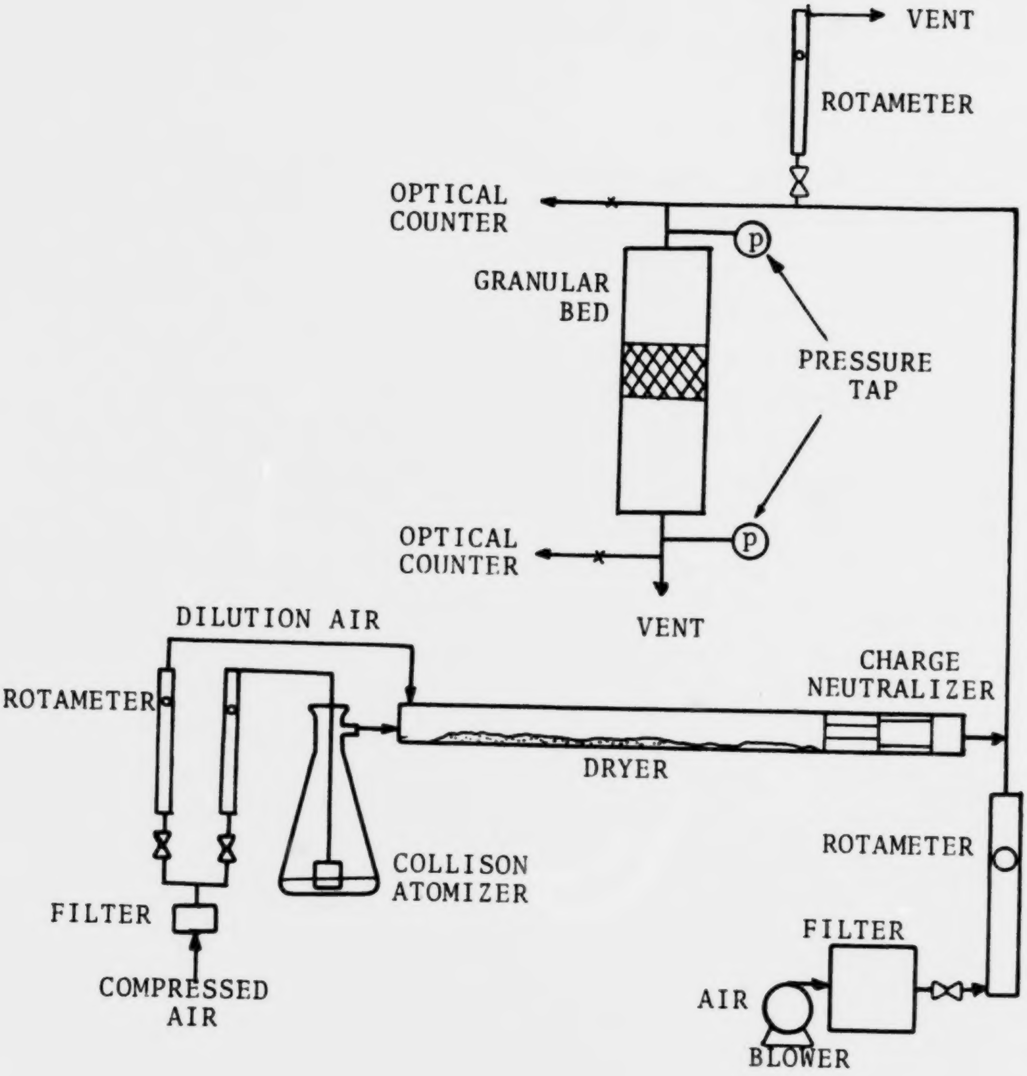
VENT
ROTAMETER
OPTICAL COUNTER
GRANULAR BED
PRESSURE TAP
OPTICAL COUNTER
VENT
DILUTION AIR
ROTAMETER
CHARGE NEUTRALIZER
DRYER
COLLISON ATOMIZER
ROTAMETER
FILTER
COMPRESSED AIR
FILTER
AIR
BLOWER

Figure 40. Schematic diagram of the experimental apparatus.

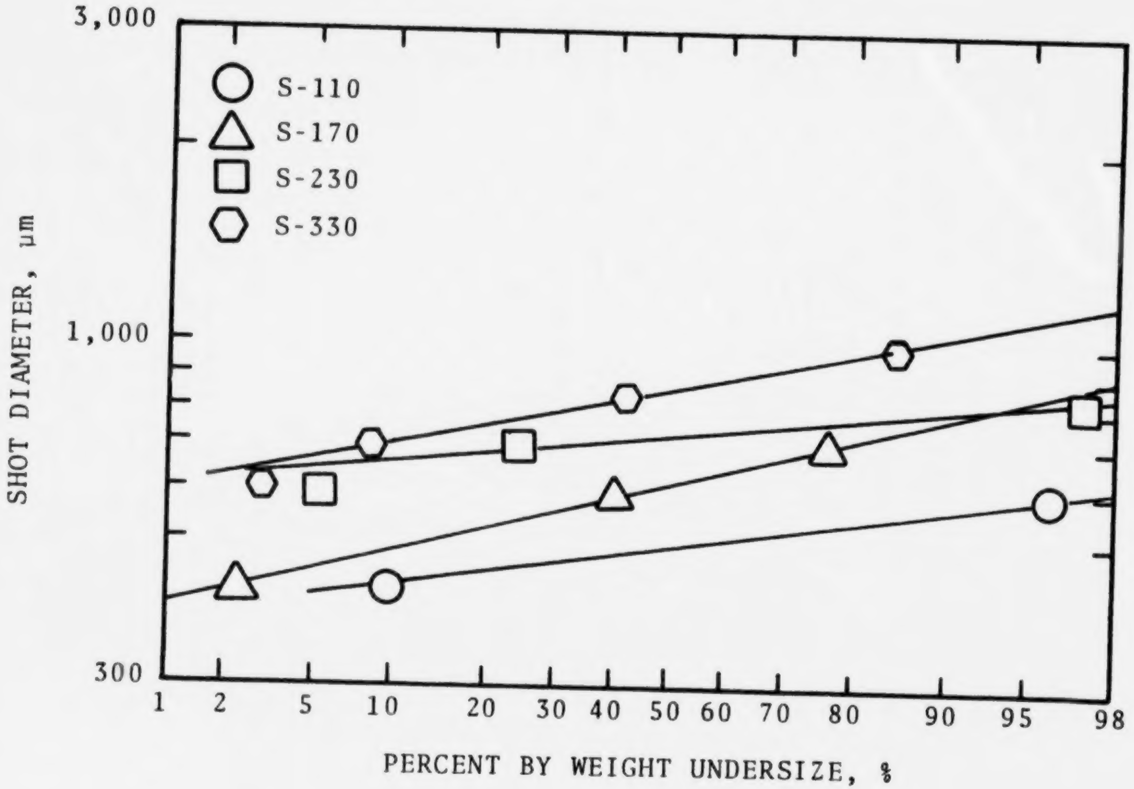

Figure 41 . Particle size distribution for iron shot.

these shots as measured with sieves. The mass median diameters are 490 µm, 620 µm, 730 µm, 790 µm, and 860 µm for S-110, S-170, S-230, S-280, and S-330 shots, respectively. The sand was Agsco #2 quartz which was obtained from Exxon Research and Engineering Company. This sand is the same as Exxon used in their Ducon granular bed filter. The granule size of the sand is -30 +50 mesh. The median diameter is 400 µm.

The experiments were conducted with 0.5 µm, 0.76 µm, and 1.1 µm diameter polystyrene latex monodisperse particles. Figures 42 through 53 show the data. In general, collection efficiency increases with decreasing granule size, increasing bed depth, and increasing superficial gas velocity.

DATA ANALYSIS

Table 16 is a list of pressure drops and collection efficiencies of 1.1 µm diameter PSL at a superficial gas velocity of 50 cm/s. It reveals that less pressure drop is required for particle collection with small granules as bed material and shallow beds instead of deep beds.

For a granular bed with a bed depth of 3.2 cm and operated at a superficial gas velocity of 50 cm/s, the collection efficiencies for 1.1 µm diameter particles are 22% and 53%, respectively, for 620 µm and 490 µm diameter iron shot. The pressure drop increases from 10 cm W.C. for 620 µm diameter granules to 21 cm W.C. for 490 µm granules. The increase in pressure drop is 110%. However, by using the finer grade of granules, the increase in efficiency is 140%.

Table 17 is a list of pressure drops for various beds whose collection efficiencies are 50% for 1.1 µm diameter particles. As can be seen the pressure drops for shallow beds are less than for deep beds.

For a shallow bed to have the same collection efficiency as a deep bed, it has to run at a high superficial gas velocity. Therefore, the gas flow capacity of a shallow bed is higher than that of a deep bed. However, there is a limit on how high a gas

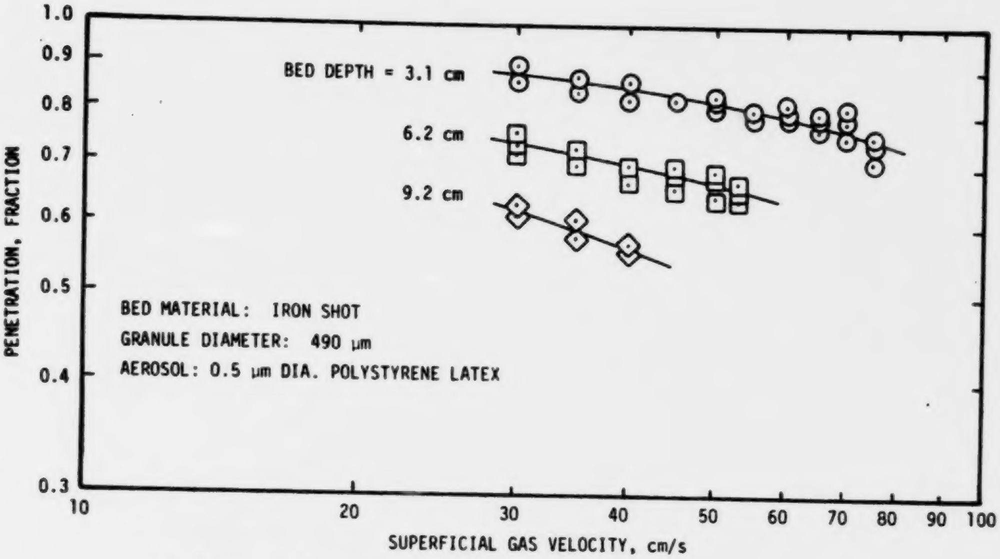

Figure 42. Experimental particle penetration of a clean granular bed filter.

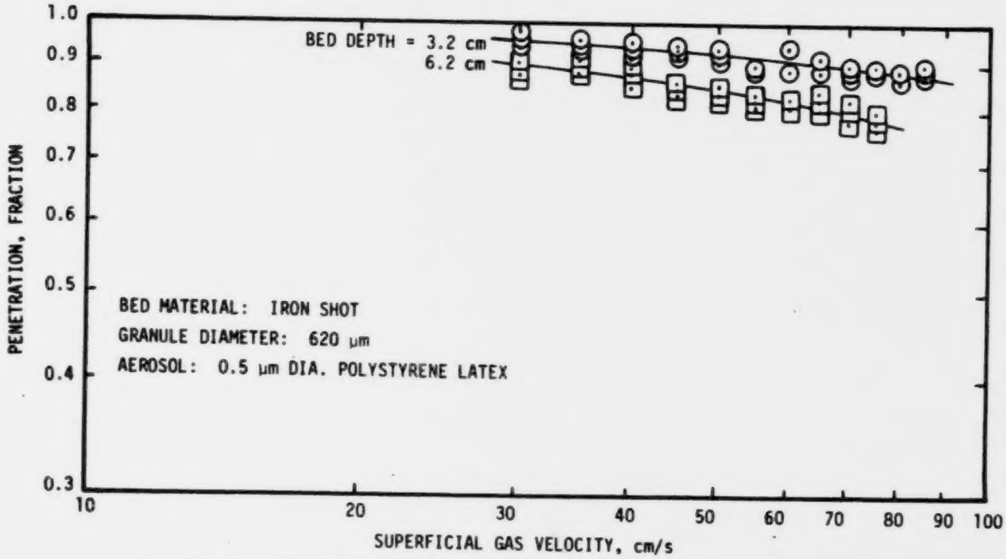

Figure 43. Experimental particle penetration of a clean granular bed filter.

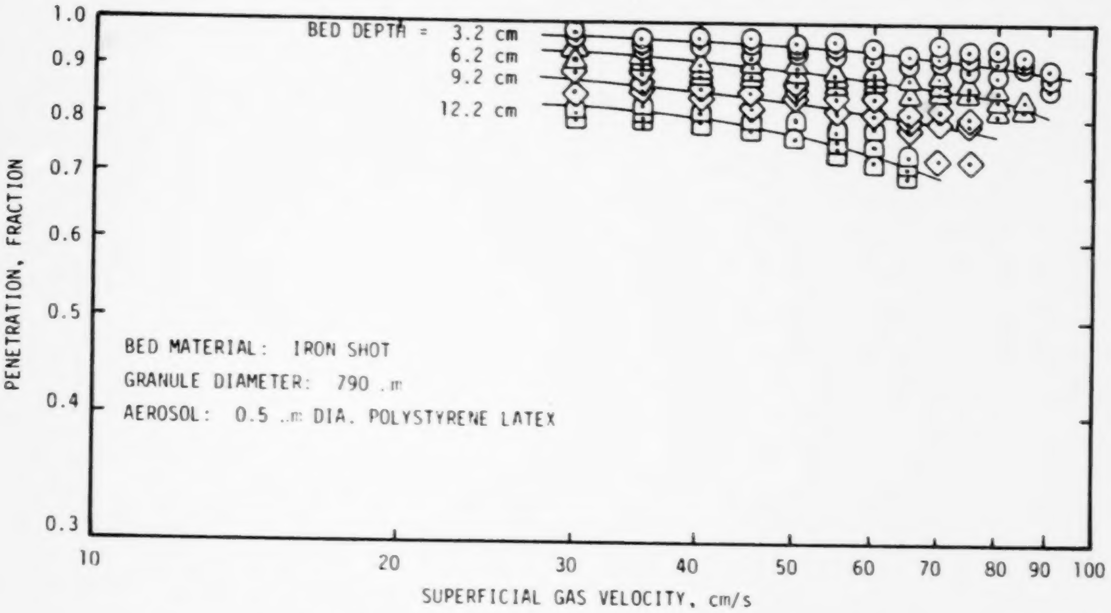

Figure 44. Experimental particle penetration of a clean granular bed filter.

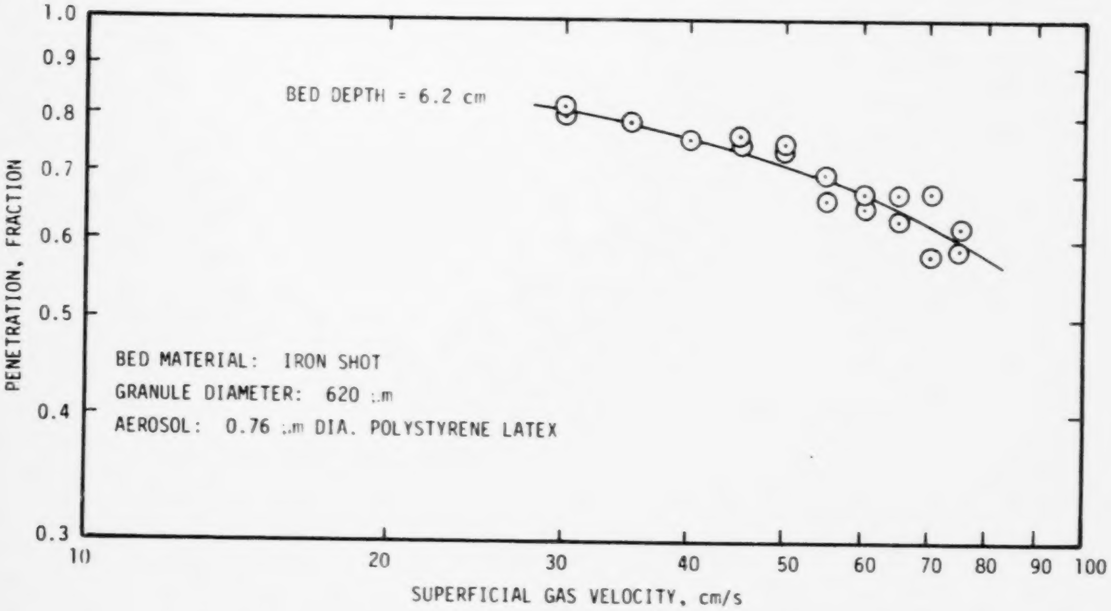

Figure 45. Experimental particle penetration of a clean granular bed filter.

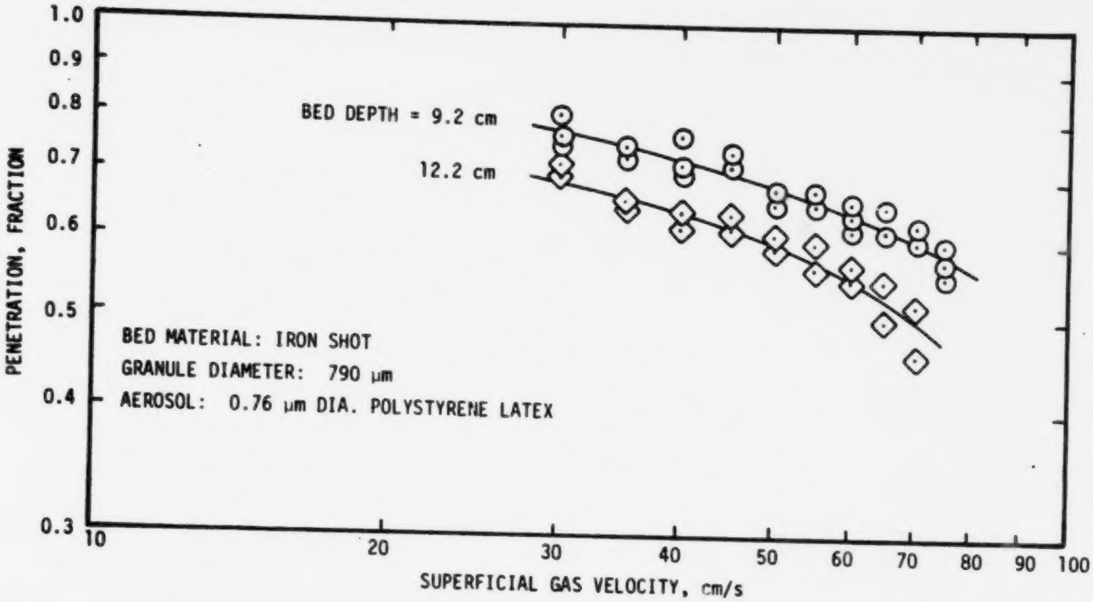

Figure 46. Experimental particle penetration of a clean granular bed filter.

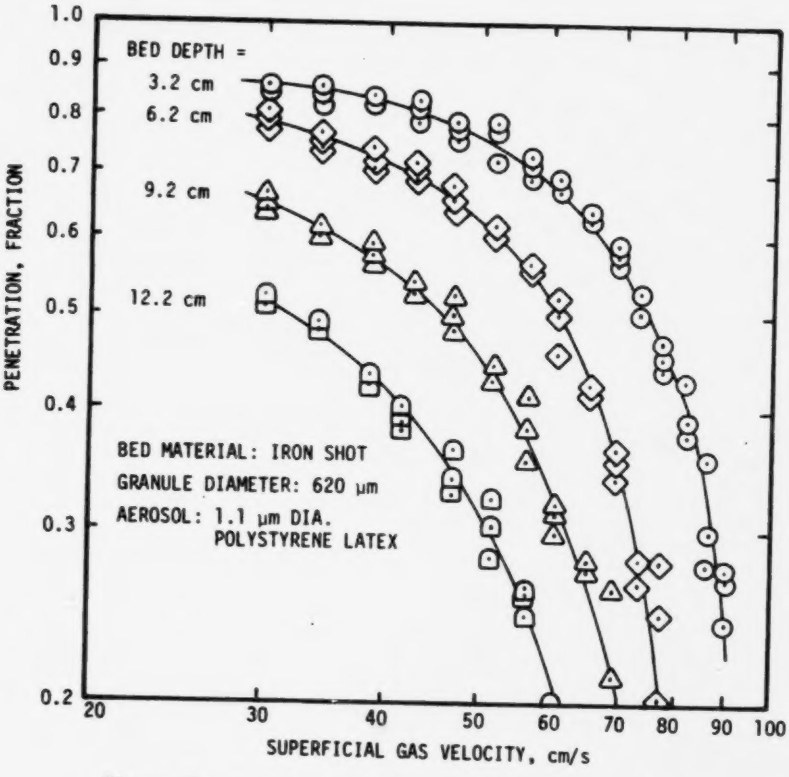

Figure 47. Experimental particle penetration of a clean granular bed filter.

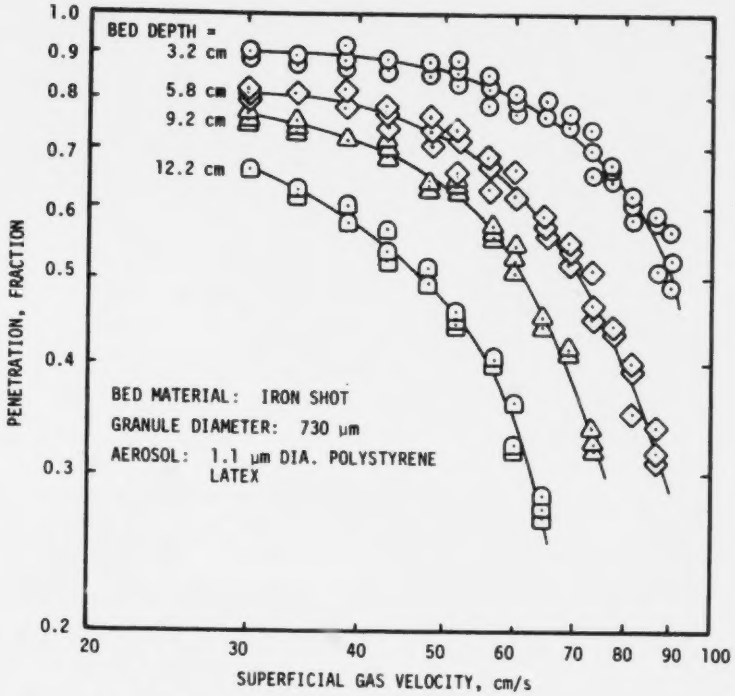

Figure 48. Experimental particle penetration of a clean granular bed filter.

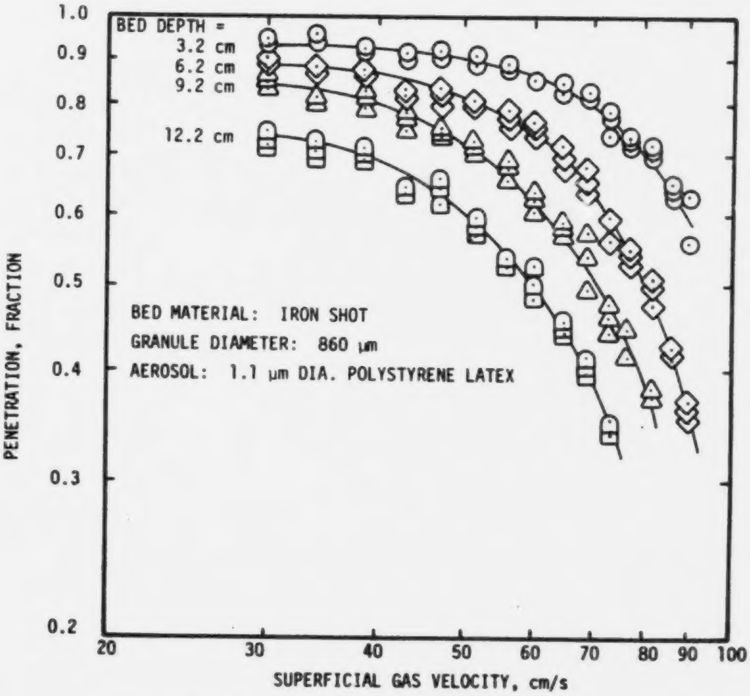

Figure 49. Experimental particle penetration of a clean granular bed filter.

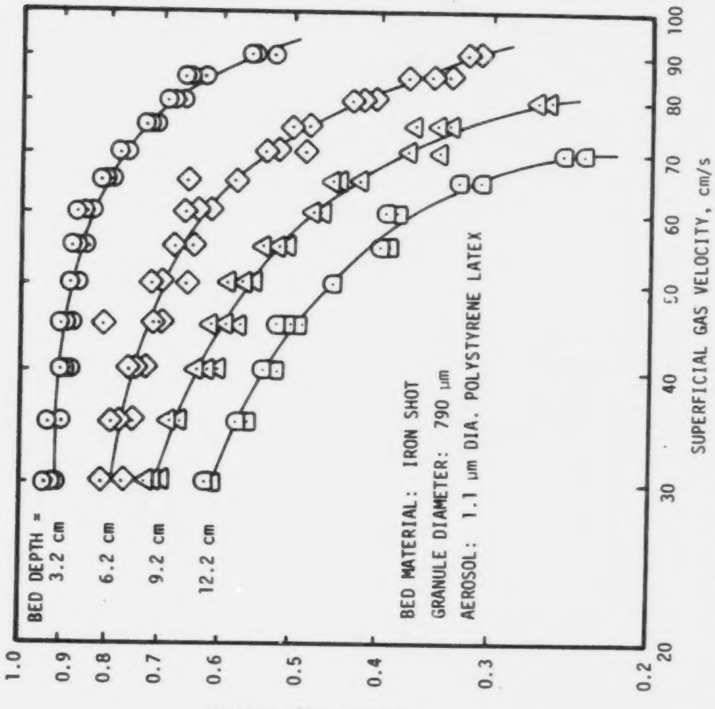

Figure 50. Experimental particle penetration of a clean granular bed filter.

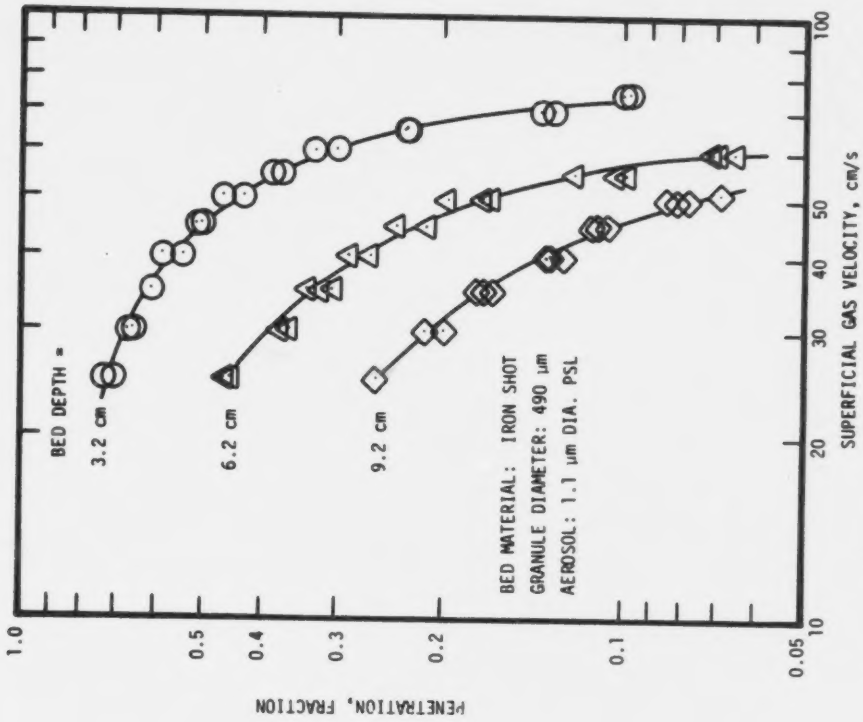

Figure 51. Experimental particle penetration of a clean granular bed filter.

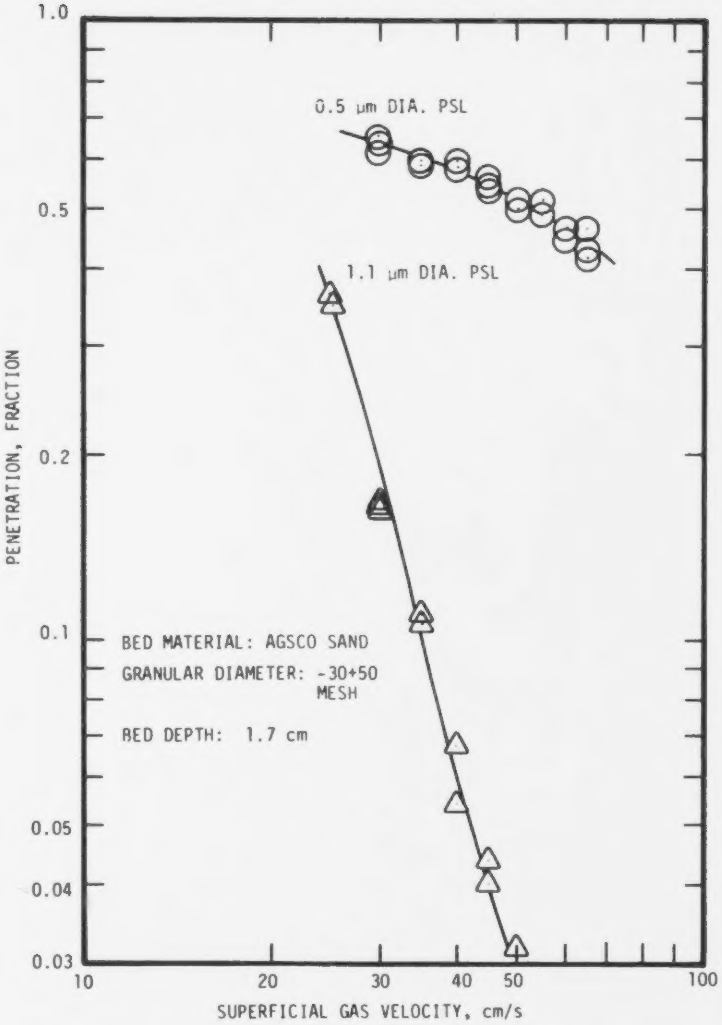

Figure 52. Experimental particle penetration of a clean granular bed filter.

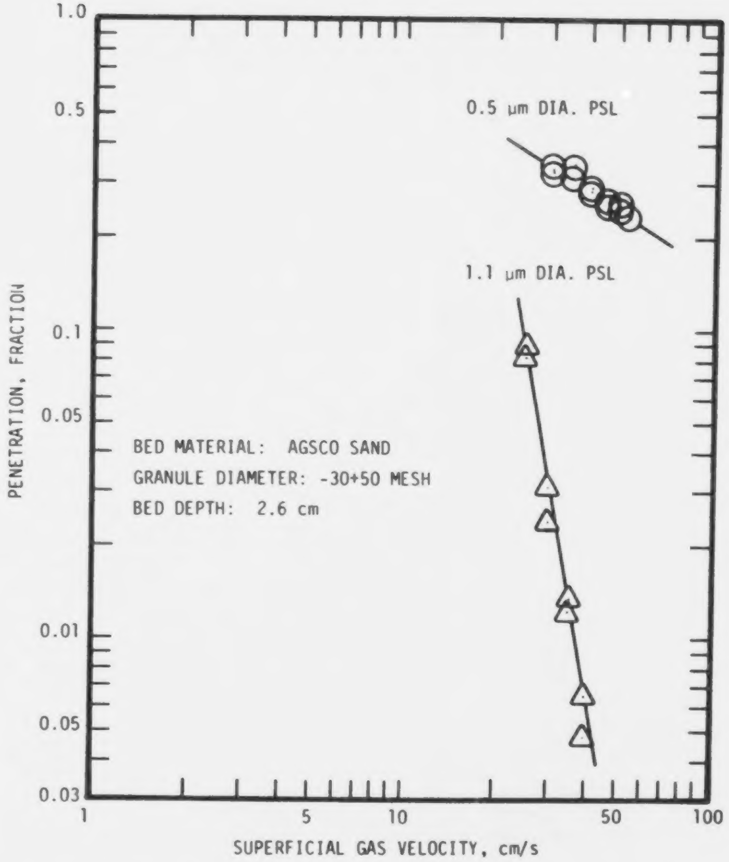

Figure 53. Experimental penetration of a clean granular bed filter.

TABLE 16. PRESSURE DROP AND COLLECTION EFFICIENCY FOR 1.09 μm DIAMETER PARTICLES AT A SUPERFICIAL GAS VELOCITY OF 50 cm/s

Granule Diameter (μm)	Bed Depth = 3.2 cm		Bed Depth = 6.2 cm		Bed Depth = 9.2 cm		Bed Depth = 12.2 cm	
	% Coll.	ΔP (cm W.C.)	% Coll.	ΔP (cm W.C.)	% Coll.	ΔP (cm W.C.)	% Coll.	ΔP (cm W.C.)
490	53	21	83	38	93	--	--	--
620	22	10	38	20	55	28	68	37
730	14	7	27	14	35	21	53	27
790	12	65	30	12	44	18	55	23
860	10	6	19	12	27	28	38	23

TABLE 17. PRESSURE DROP FOR 50% COLLECTION OF 1.1 μm DIAMETER PARTICLES

Granule Diameter (μm)	Pressure Drop (cm W.C.)			
	Bed Depth 3.2 cm	Bed Depth 6.2 cm	Bed Depth 9.2 cm	Bed Depth 12.2 cm
490	19	--	--	--
620	17	24	26	22
730	16	23	27	25
790	15	20.5	22	21
860	15	23	28	30

velocity the bed can be safely operated without the danger of causing particle reentrainment.

PRESSURE DROP DATA

The pressure drop data obtained with the iron shot bed material were analyzed. Figures 54 through 58 show the experimental and predicted pressure drops. The prediction was based on Ergun's equation. As can be seen, the predicted pressure drop is lower than that measured.

The pressure drop prediction based on Ergun's equation is very sensitive to the bed porosity. The difference in the predicted and measured pressure drops might be caused by an error in bed porosity determination. The bed porosity was calculated from the measured weight of a bed of known volume. It is very difficult to accurately determine bed porosity by this method.

By fitting Ergun's equation to the pressure drop data, the void fraction of the bed was obtained. Table 18 shows the result along with the measured void fractions. The measured void fraction is very close to calculated void fraction.

TABLE 18. MEASURED AND CALCULATED VOID FRACTION OF THE GRANULAR BED

Shot No.	Average Diameter μm	Measured Void Fraction	Void Fraction From Pressure Drop Data
S-110	490	0.39	0.37
S-170	620	0.39	0.39
S-230	730	0.41	0.40
S-280	790	0.41	0.40
S-330	860	0.40	0.39

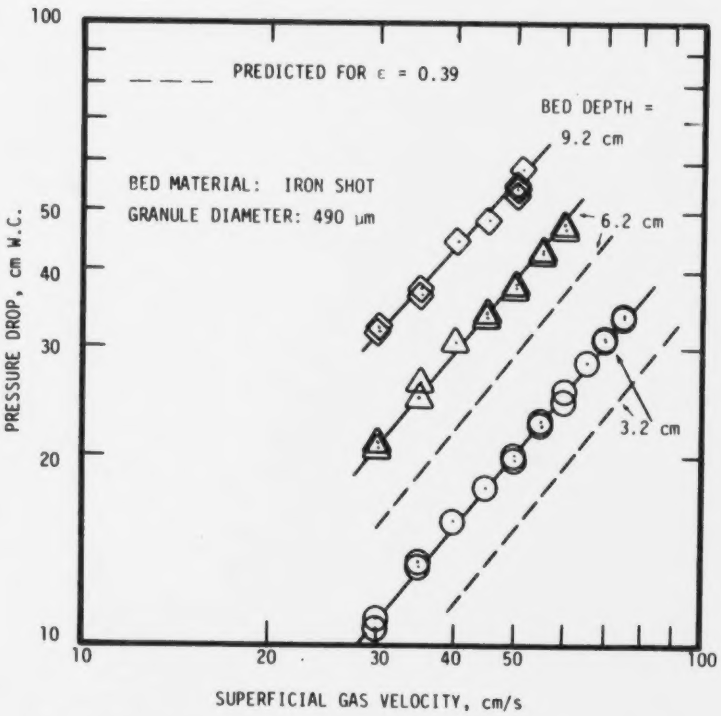

Figure 54. Experimental and predicted pressure drops across a clean granular bed filter.

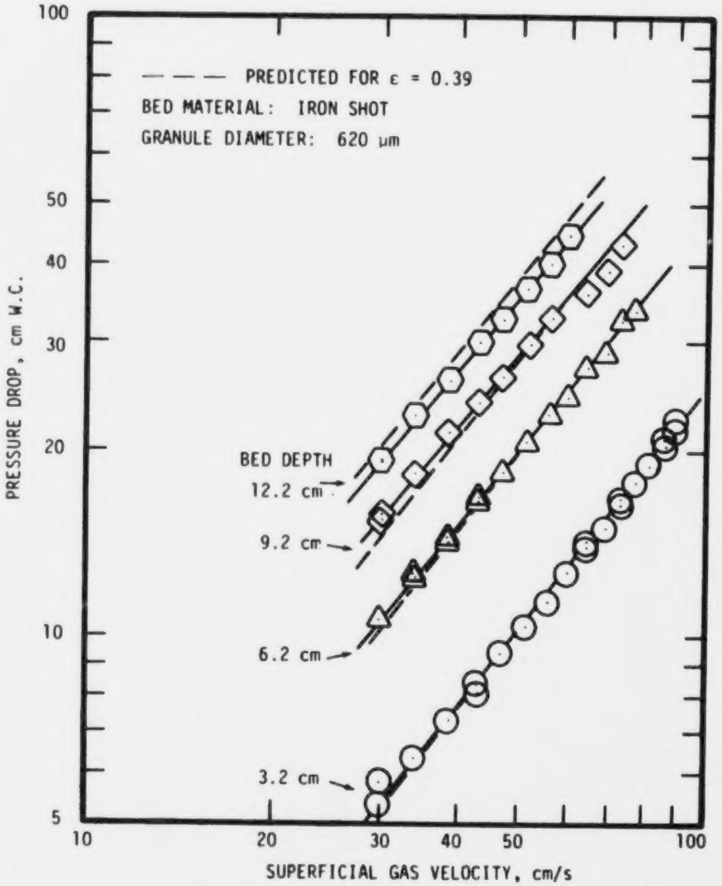

Figure 55. Experimental and predicted pressure drops across a clean granular bed filter.

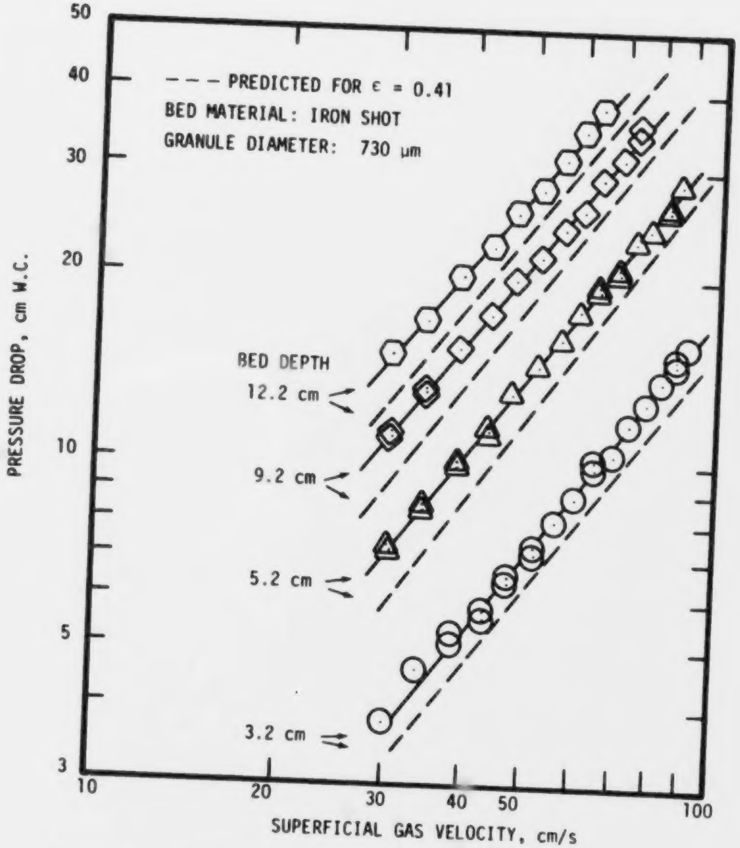

Figure 56. Experimental and predicted pressure drops of a clean granular bed filter.

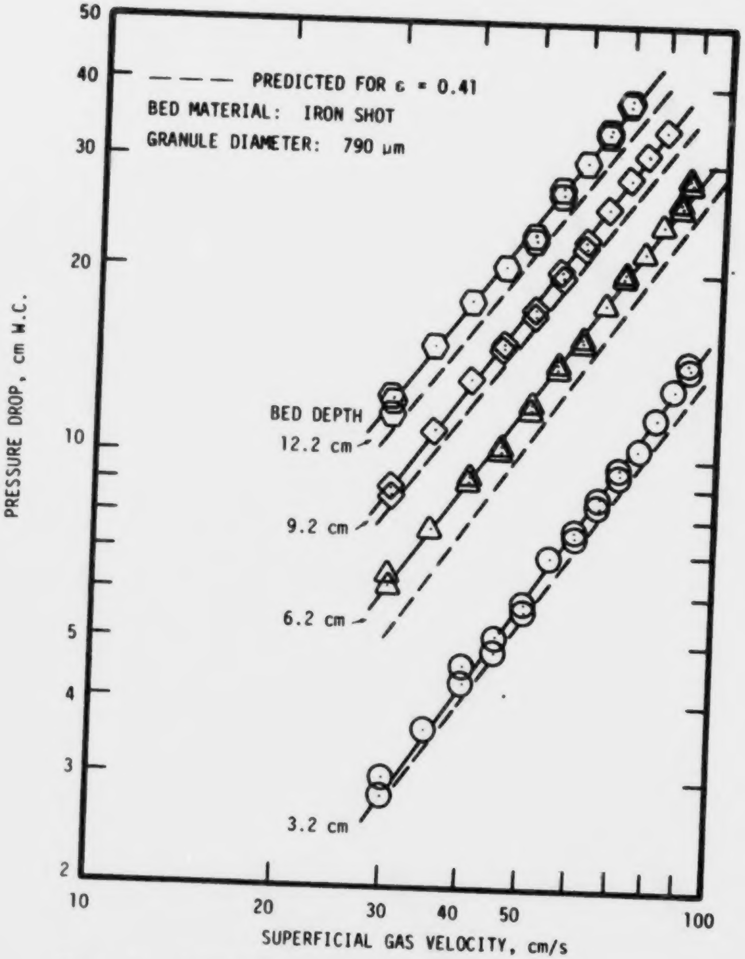

Figure 57. Experimental and predicted pressure drops across a clean granular bed filter.

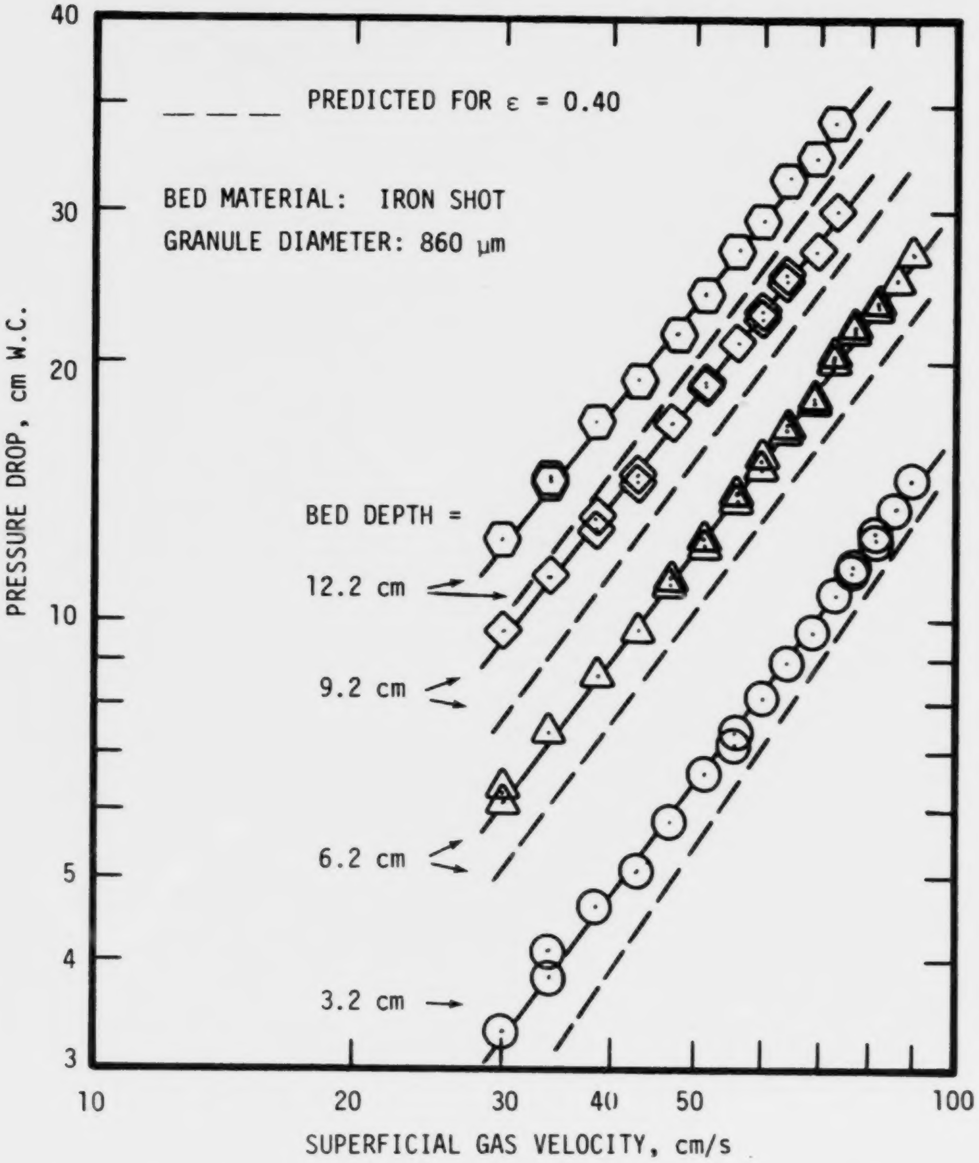

Figure 58. Experimental and predicted pressure drops across a clean granular bed filter.

SECTION 6

DESIGN MODEL

MATHEMATICAL MODELING

The granular bed can be envisioned as a great number of impaction stages connected in series (Figure 59). Particle collection is by impaction as in a cascade impactor. The jet openings are the pores in each layer of granules. It is assumed that the jet diameters in the granular bed are of uniform size with a diameter equal to the hydraulic diameter of the void space. The gas velocity in the jet is the average interstitial gas velocity.

If 'η' is the collection efficiency of one impaction stage, the particle penetration for the granular bed will be

$$Pt_d = (1-\eta)^N \tag{88}$$

where Pt_d = penetration for particles with diameter d_p, fraction
η = single stage collection efficiency, fraction
N = number of impaction stages, number

As in some cascade impactors, each layer of granules served both as the jet plate and as the collection plate. Therefore, each layer of granules is an impaction stage and "N" is equal to the number of granular layers in a bed. For a randomly packed bed

$$N = \frac{3}{2}\frac{Z}{d_c} \tag{89}$$

where Z= bed depth, cm
d_c = granule diameter, cm

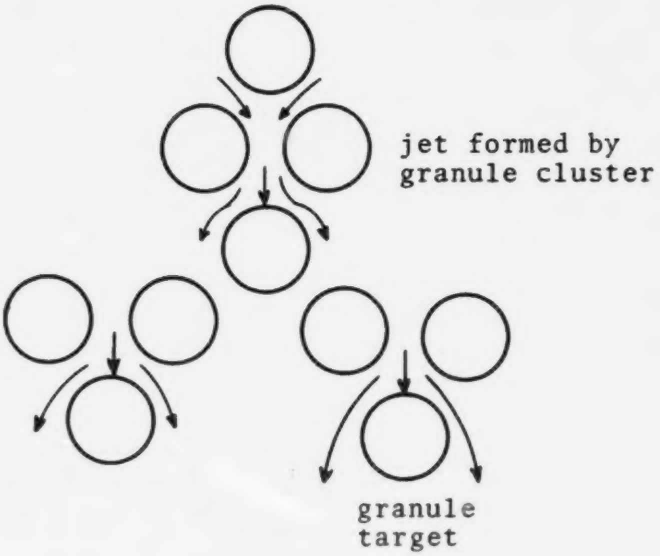
jet formed by
granule cluster
granule
target

Figure 59. Diagram of granular bed showing impaction concept.

and

$$Pt_d = (1-\eta)^{1.5 \frac{Z}{d_c}} \tag{90}$$

The impaction collection efficiency, "η" is a function of "K_p", the inertial impaction parameter. The impaction parameter is defined as

$$K_p = \frac{C' \rho_p d_p^2 u_j}{9 \mu_G d_j} \tag{91}$$

where
C' = Cunningham slip factor, dimensionless
ρ_p = particle density, g/cm^3
d_p = particle diameter, cm
u_j = jet velocity, cm/s
μ_G = gas viscosity, g/cm-s
d_j = jet diameter, cm

Since

$$u_j = u_{Gi} = \frac{u_G}{\varepsilon} \tag{92}$$

and

$$d_j = 4r_H = \frac{2}{3} \frac{\varepsilon}{1-\varepsilon} d_c \tag{93}$$

where
u_{Gi} = average interstitial gas velocity, cm/s
ε = bed porosity, fraction
r_H = hydraulic radius, cm
d_c = granule diameter, cm

we have

$$K_p = \frac{3}{2} \frac{1-\varepsilon}{\varepsilon^2} \frac{C' \rho_p d_p^2 u_G}{9 \mu_G d_c} \tag{94}$$

The relation between "η" and "K_p" can be evaluated once the flow field is defined. Flow fields reported in the literature for inertial impaction, e.g., Ranz and Wong (1952) and Marple (1970), are adequate for $K_p > 0.15$. For $K_p < 0.15$, there is no suitable flow field reported in the literature. Therefore, the relationship between "η" and "K_p" could not be calculated analytically.

The relationship was back-calculated from equation (90) and experimental data. Figure 60 shows the results. The curve can be approximated by the following equation:

$$\eta = 10.0\ K_p^{3.23} \exp\left[0.27\ (\ln K_p)^2\right] \qquad (95)$$

for $3 \times 10^{-3} \leq K_p \leq 0.15$

There is scatter in the lower end of the curve. For $K_p < 10^{-2}$, "η" is very sensitive to experimental data. A few percent scatter in the data will cause "η" to fluctuate greatly. Figure 61 compares the experimentally determined "η" versus "K_p" curve with those reported by Ranz and Wong (1952), Stern, et al. (1962), and Mercer and Stafford (1969). All reported curves are for $K_p > 0.15$. As can be seen, the curve calculated in the present study matches other researchers' results. The curve determined in this study is a continuation of other researchers' curves.

Paretsky et al. (1971) and Knettig and Beeckmans (1974) studied the collection of monodispersed aerosol particles in granular bed filters. Their data were transformed into "K_p" versus "η" plots as shown in Figure 62.

Knettig and Beeckmans used 425 μm glass beads as granular material. Bed porosity was 0.38. Aerosol particles were 0.8, 1.6, and 2.9 μm in diameter. As can be seen from Figure 62, their data are close to the results of present study.

Paretsky et al. (1971) studied the filtration of 1.1 μm diameter polystyrene latex aerosols by beds of sand. They studied a bed of -10+14 mesh (1,200 to 1,700 μm) angular sand and a bed of -20+30 mesh (500 to 850 μm) sand at superficial gas velocities between 0.3 and 80 cm/s. Bed porosities were 0.41 and 0.43, respectively. Single stage collection efficiencies were calculated from their data. In the calculation, the granule diameters were assumed to be the arithmetical mean of the smallest and the largest granule size in the bed. The results are plotted in Figure 62. For a given inertial parameter, Paretksy et al.

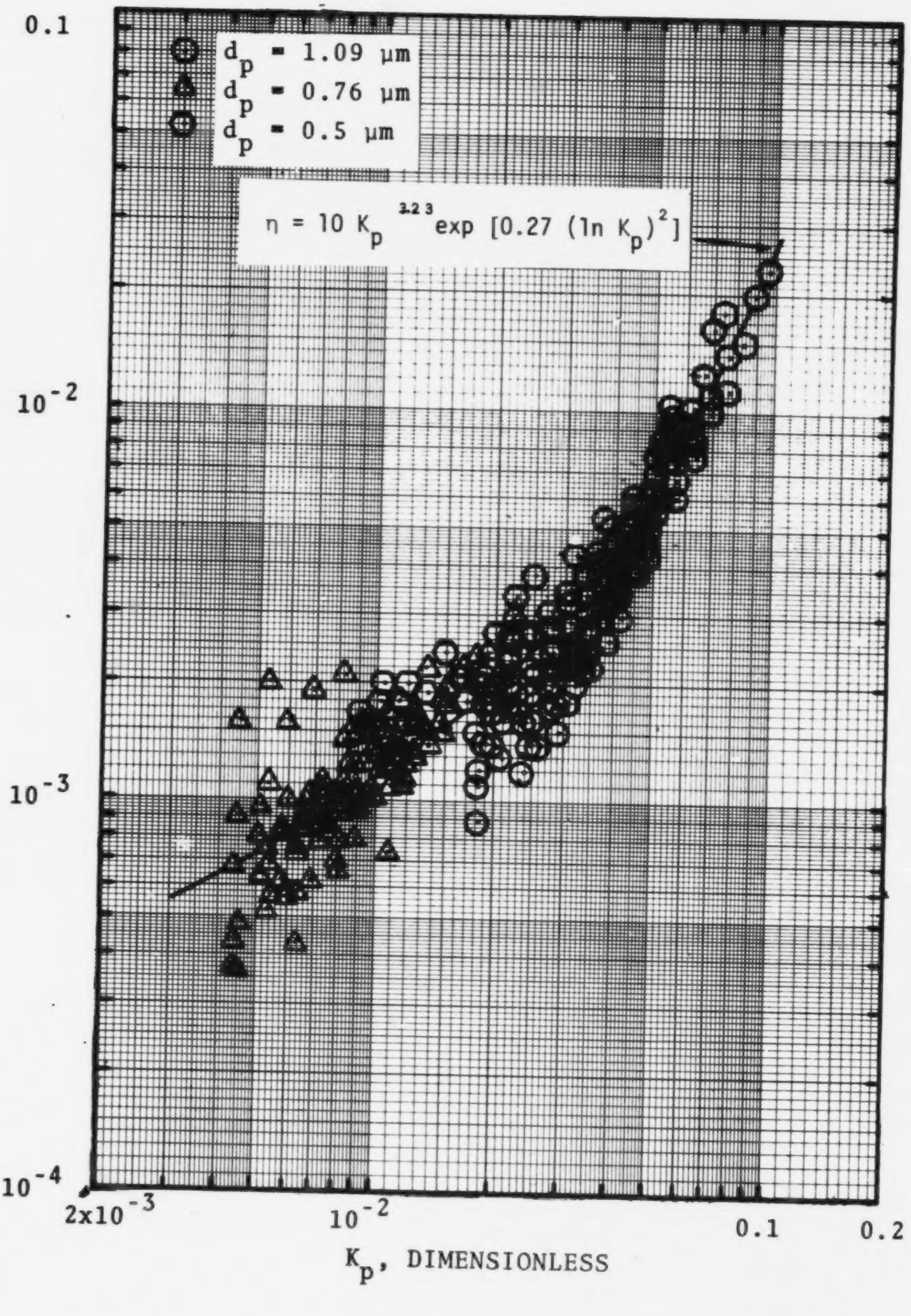

Figure 60. K_p versus η for round jet model for particle collection in a GBF.

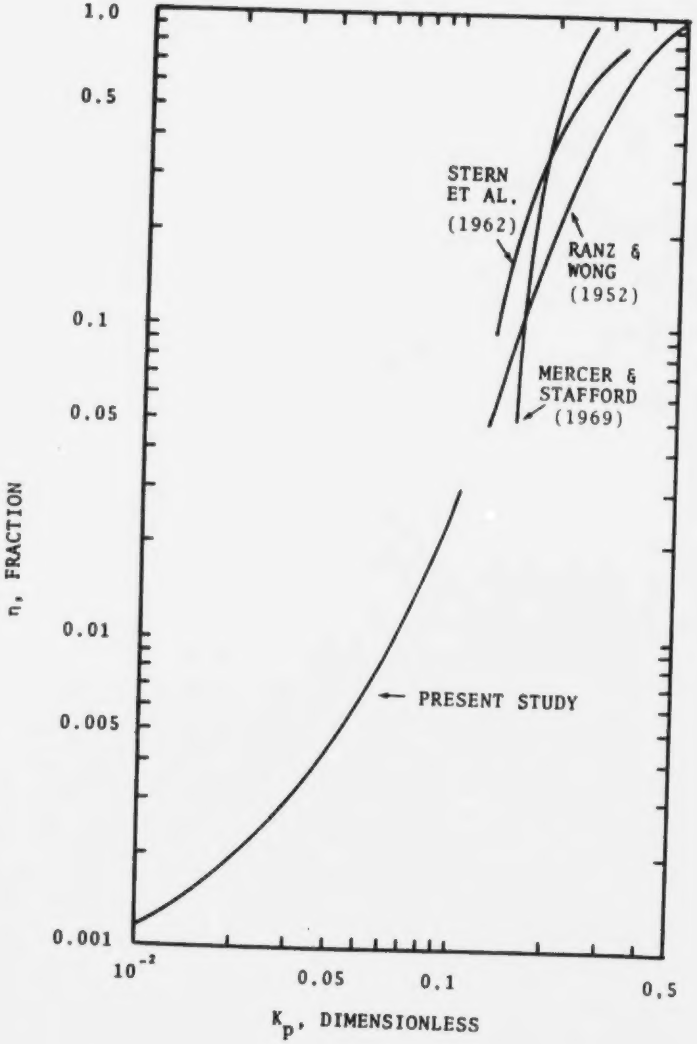

Figure 61. 'K_p' versus 'η' for round jet.

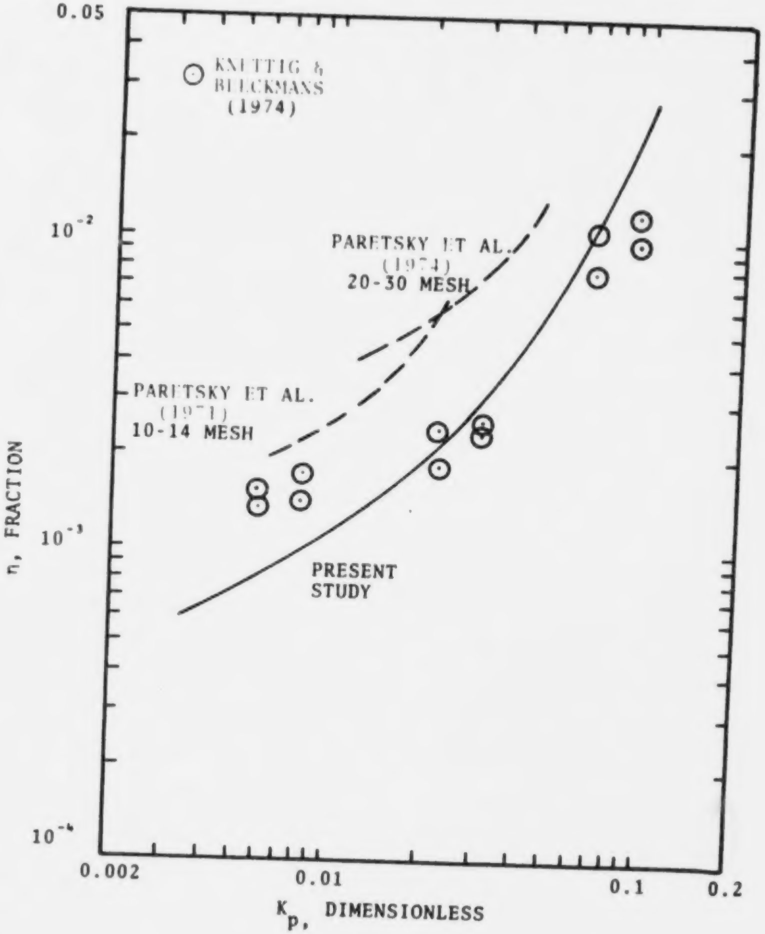

Figure 62. Efficiency vs. inertial impaction parameter for comparison.

data give a higher collection efficiency than reported in this study. Their data would be close to that of present study if the mean diameter were equal to the smallest granule diameter.

COMPARING MODEL PREDICTIONS WITH PERFORMANCE DATA

The design equation is for the prediction of particle collection by a clean bed. If no filter cake is formed and the collected particles are uniformly distributed in the bed, then the equation is still applicable. The design equation has been used to predict the performance of Rexnord gravel bed filters and the Combustion Power Company "dry scrubber."

Figure 63 shows the comparison between the data reported by McCain (1976) for a Rexnord gravel bed filter and the prediction by the present model. The prediction by the present model is close to the data.

Figure 64 shows the comparison of Hood's data with predictions. The predicted penetration is higher than that measured.

Figures 65 through 67 show the comparison of A.P.T.'s data for CPC GBF with predictions. The present model predictions agree with data for some runs but not for all runs. The present model is very sensitive to bed porosity. In the calculations, a bed porosity of 0.35 was used. If a bed porosity of 0.3 is used, the model would give a better fit with the data.

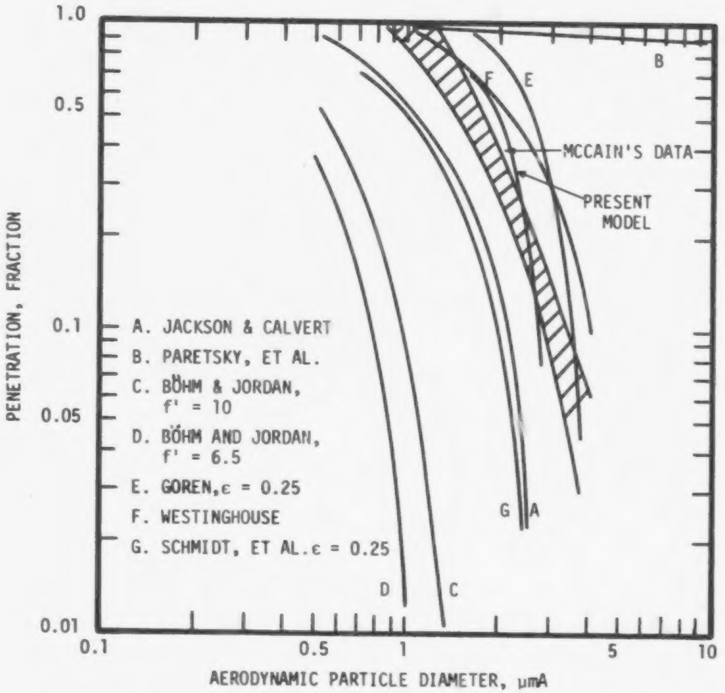

Figure 63. Comparison of McCain's gravel bed particle collection data with design equation predictions.

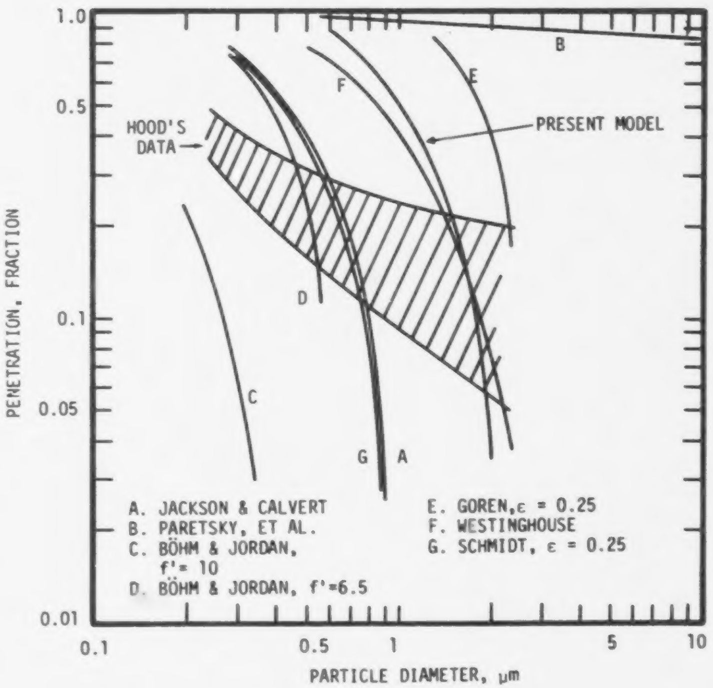

Figure 64. Comparison of Hood's data with predictions by available design equations.

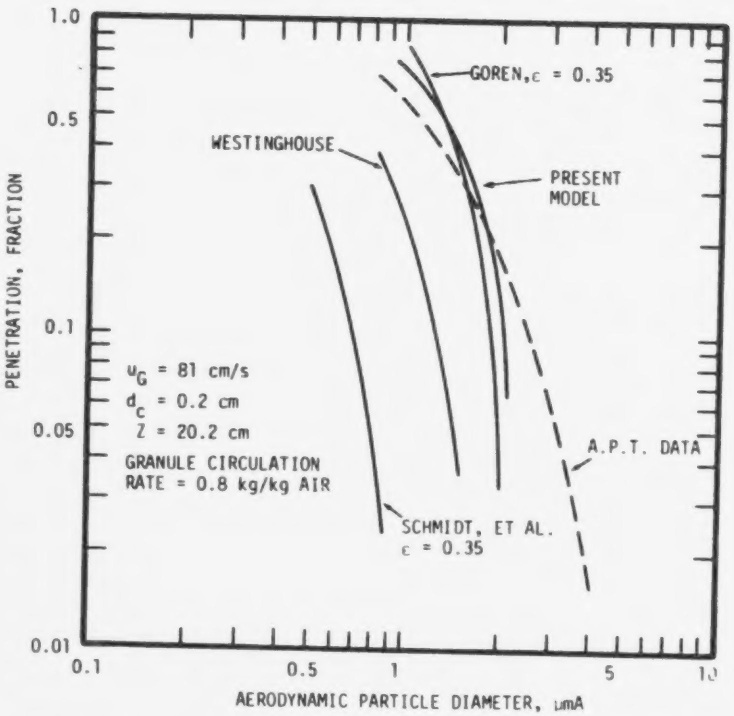

Figure 65. Experimental and predicted performance of CPC GBF (A.P.T. data).

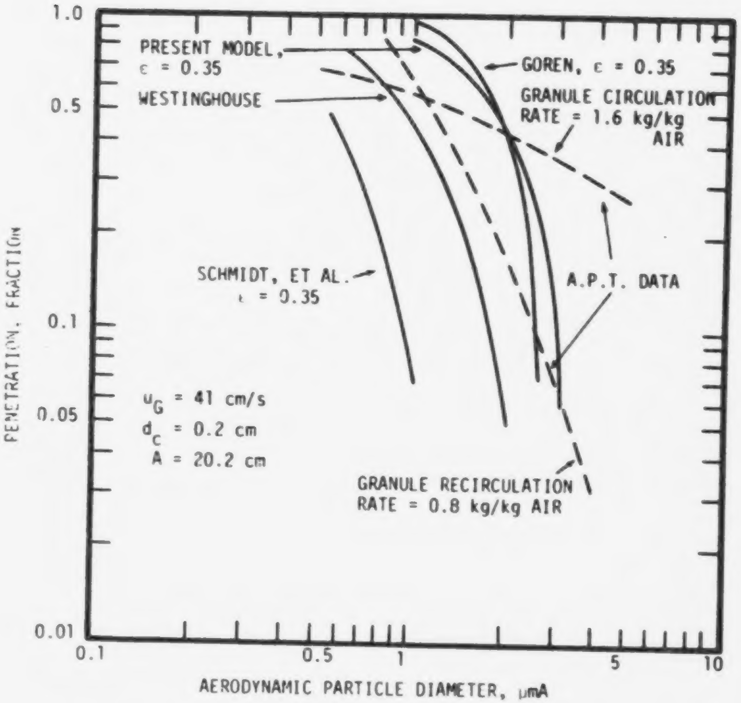

Figure 66. Experimental and predicted performance of CPC GPF (A.P.T. data).

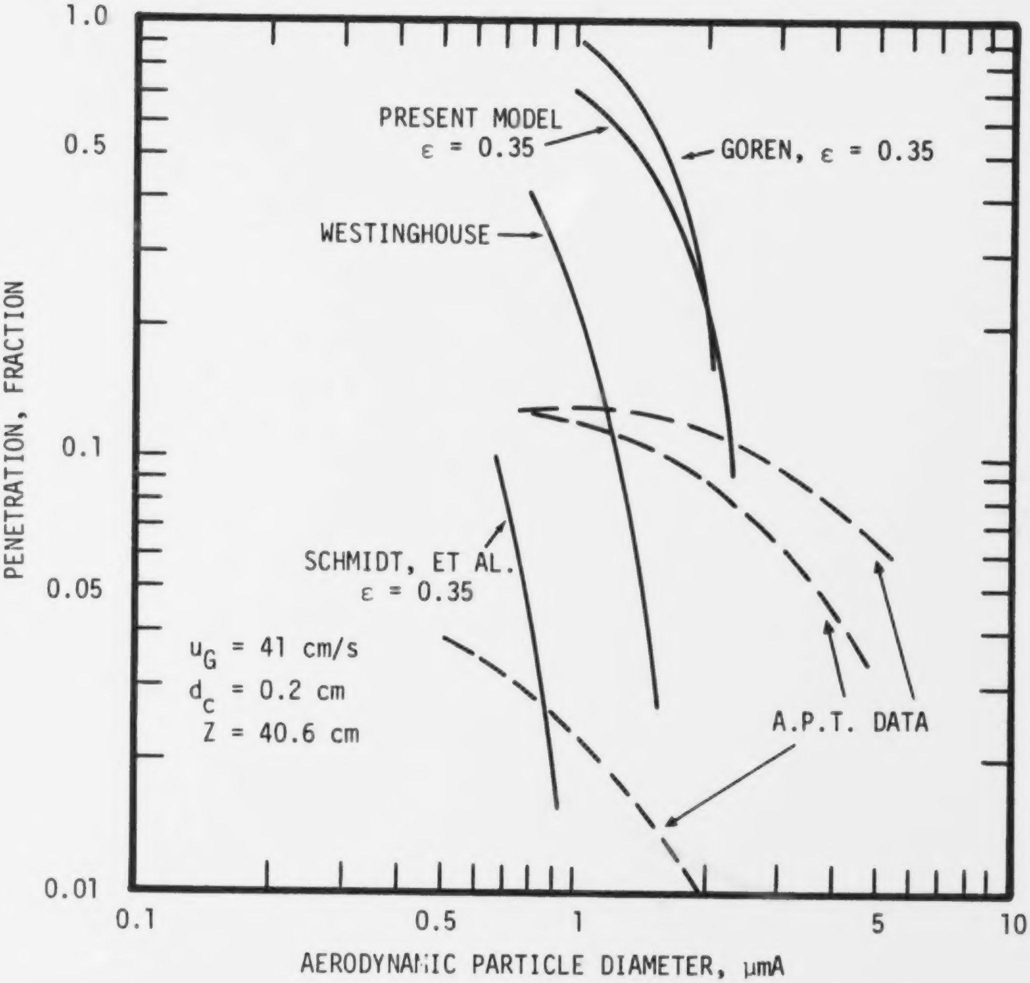

Figure 67. Experimental and predicted performance of CPC GBF (A.P.T. data).

SECTION 7

PRESENT TECHNOLOGY EVALUATION

GRANULAR BED FILTER SYSTEMS

GBFs have been used commercially for over 30 years, with several designs commercially available. Granular bed filters may be classified either according to bed structure or according to bed cleaning method. The first classification method is used in this report.

With respect to the bed structure, granular bed filters may be classified as continuously moving, intermittently moving, and fixed bed filters.

Continuously Moving Bed Filters

The continuously moving bed filter is usually arranged in a cross-flow configuration. The bed is a vertical layer of granular material held in place by louvered walls. The gas passes horizontally through the granular layer while the granules and collected dust continuously move downward and are removed from the bottom. The dust and granules are separated by vibration. The cleaned granules are then returned to the overhead hopper by a granule circulation system.

Several commercial designs fall into this category. They include the Dorfan Impingo filter, the Consolidation Coal Company filter, and the "dry scrubber" of the Combustion Power Company. The "dry scrubber" is the only one that is presently marketed.

Dorfan Impingo Filter -

The Dorfan Impingo filter was invented by Morton Dorfan and was offered commercially by Mechanical Industries, Inc. in the early 1950's. The device is a vertical panel filter in which the granular materials continuously fall through the panel. The granule flow rate is controlled by the setting of a rotary valve located near the bottom of the panel. The dust-laden gas is filtered by blowing the gas through the panel horizontally. Filtered dust is carried downward with the granules (Figure 68).

The opposite walls of the panel are not parallel but are slightly offset from the vertical so that the panel is tapered with its narrowest point at the top and widest at the bottom. The granules thus travel downward in a panel of constantly increasing cross-sectional area. The rationale is that the tapered construction acts to prevent hangups caused by size increases of the granules as the dust loading builds upon their surfaces.

Four units, each of 8 m^3/s (17,000 CFM) gas capacity and consisting of two cells, were installed in a plant to collect asbestos rock dust from a stream of flue gas coming from a direct fired dryer in which the rock was dried prior to milling. The granular bed was a 30 cm (1 ft) thick panel with 2.74 m x 4.27 m (9 ft x 14 ft) filtering area. The granules were raw asbestos rock ranging from 1.3 cm to 3.8 cm (0.5 to 1.5 in.) in diameter.

The dust was 100% finer than 100 mesh and 60% finer than 10 microns. The concentration entering the collector was approximately 14.8 g/m^3 (6 g/ft^3) and that leaving about 0.49 g/m^3 (0.2 g/ft^3).

The Dorfan Impingo filter installations are no longer in use and the equipment is not presently marketed.

Consolidation Coal Company Filter -

A granular bed filter was studied first on a pilot scale and then with a full-size installation by the Consolidation Coal Company in the period 1950-1952. This equipment was used for collecting dust from hot gases leaving coal drying operations. Lump coal [0.95 cm to 3.2 cm (3/8 in. to 1.25 in.)in size] was used as the bed granules. The design concept for the full size installation is shown in Figure 69.

The granules were fed from an overhead bin to two separate panels. The panel at each side consists of six separate cells facing the inlet gas which flowed through the beds from a central dust and exited via ducts at either side of the installation. Typical operating characteristics are given in Table 19.

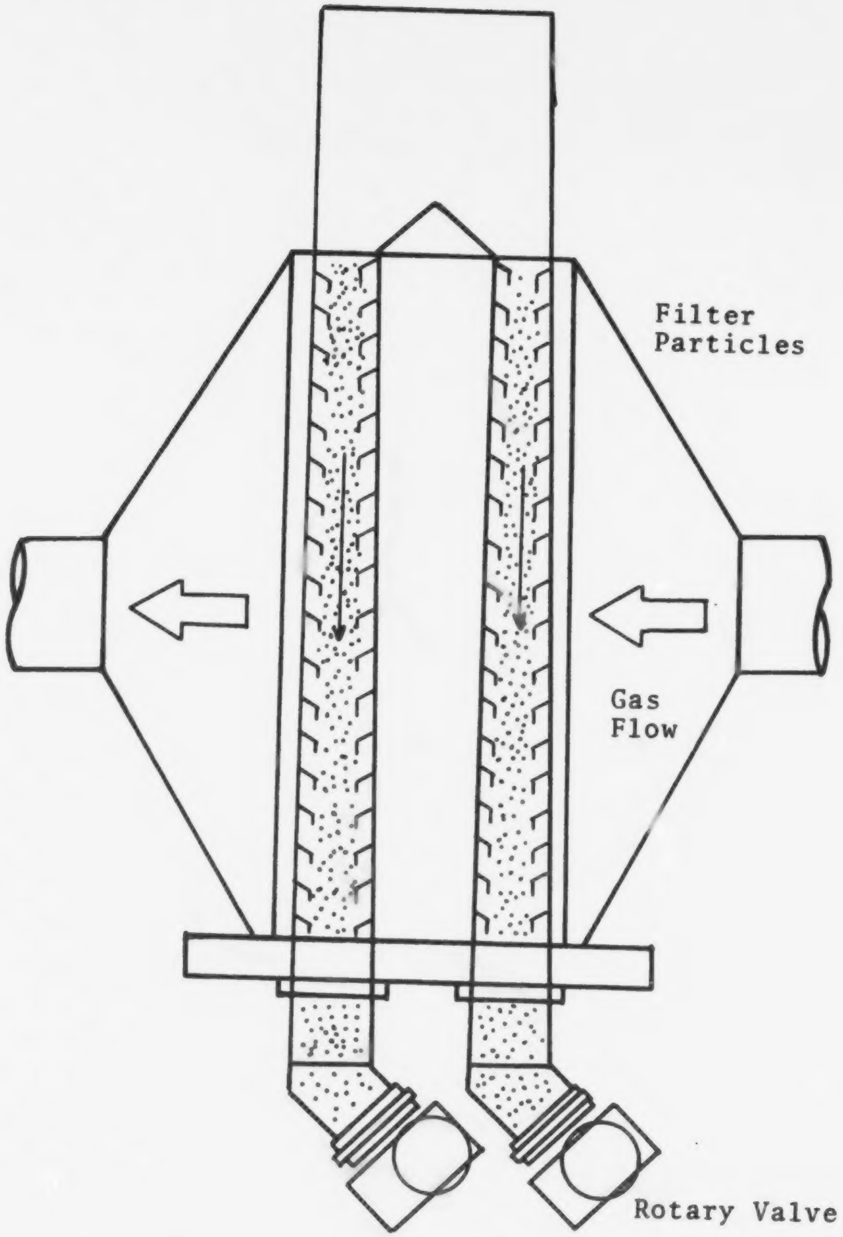
Filter Particles
Gas Flow
Rotary Valve

Figure 68. Dorfan Impingo Filter.

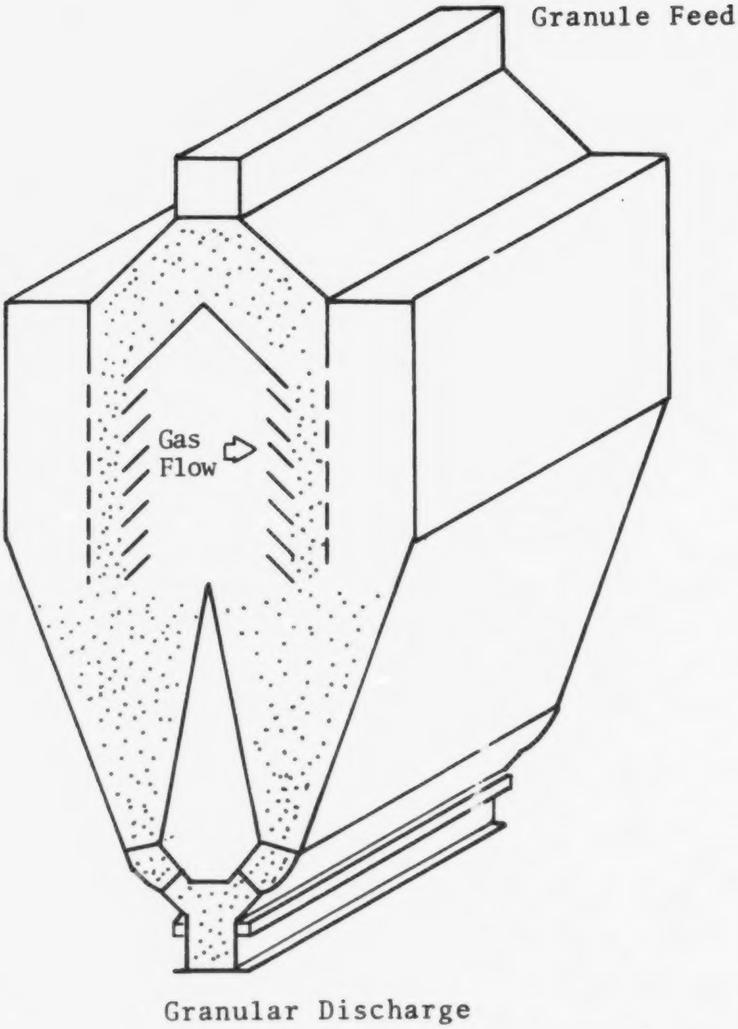
Granule Feed
Gas
Flow
Granular Discharge

Figure 69. Consolidation Coal Company filter.

TABLE 19. TYPICAL OPERATING CHARACTERISTICS OF CONSOLIDATION COAL COMPANY GRANULAR BED FILTERS

Type of service - recovery of dust from coal drying operation.

Size - Individual cell was 127 cm wide x 122 cm high x 51 cm thick (4'2" wide x 4' high x 20" thick). In the unit the filtering surfaces were divided into two banks of six cells each in parallel.

Capacity - 0.5 - 1.5 m^3/s per square meter of filter area (100 - 300 CFM/ft^2)

Total filter area - 18.6 m^2 (200 ft^2)

Inlet dust loading - 7.4 - 17.2 g/m^3 (3 - 7 gr/SCF)

Size of dust - 86% < 30 μm and 22% < 10 μm

Granular material - Coal, 0.95 cm to 3.2 cm (3/8" to 1-1/4")

Granule flow rate - 22 metric tons/hr

Operating temperature - 130°F

Pressure drop - 5.8 cm W.C.

Collection efficiency - 89 - 99%

Combustion Power Company "Dry Scrubber" -

The "Dry Scrubber" is currently offered commercially by Combustion Power Company. It is similar to the Dorfan Impingo Filter. It consists of a vertical bed of granules held in place by louvers. It is operated in cross-flow configuration. Gas flows horizontally through the bed and the bed continuously moves downward. Clean granules are introduced at the top and a mixture of dust and granules is removed from the bottom. Dusts and granules are separated in a shaking device.

Two models are produced by Combustion Power Company. Figure 70 shows the regular "Dry Scrubber." It is used when the particulate loading is low. For very high inlet particle loadings, the "Integral Cyclone Model" is recommended. It has a low energy cyclone wrapped around the outer shell of the standard "Dry Scrubber" (Figure 71).

Intermittently Moving Bed Filters

In the late 1950s, Squires modified the continuously moving bed design of the Dorfan filter to obtain a fixed bed device with intermittent movement of granular solids. The design is called the LS (Loose Surface) filter. It uses a finer grade granule than the Dorfan filter and the bed is stationary during filtration. The accumulated filter cake is removed by moving just the surface layer of granules.

Figure 72 shows one possible arrangement. The granular bed is a narrow vertical bed of granules (-50+60 mesh) held between a panel of louvers and a fine mesh screen. In some applications, a relatively coarse grade granule is used on the gas exit side to prevent blow-through of the smaller collecting granules. During operation the dusty gas flows horizontally through the panel bed. The particles collected by the bed build up a cake on the exposed bed surfaces and to some extent penetrate to the interstices. When the resistance of the cake has reached an undesirable level, the clean gas outlet valve is closed and a short pulse of compressed air is blasted in reverse flow through the granular bed. In continuous use, the valves operate on a timed cycle.

The blow-back pulse is sufficient to physically lift the

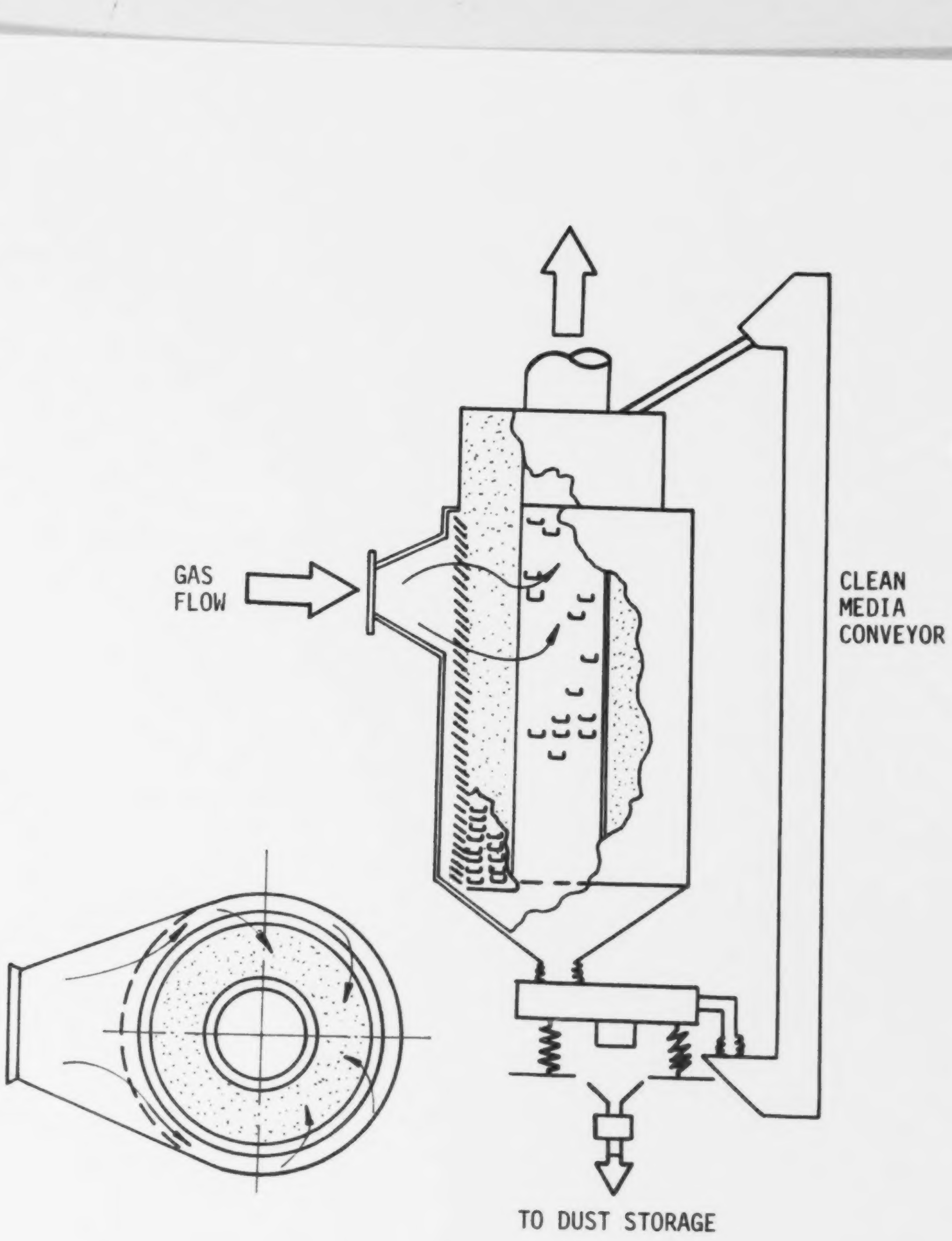
GAS
FLOW
CLEAN
MEDIA
CONVEYOR
TO DUST STORAGE

Figure 70. Combustion Power Company "Dry Scrubber."

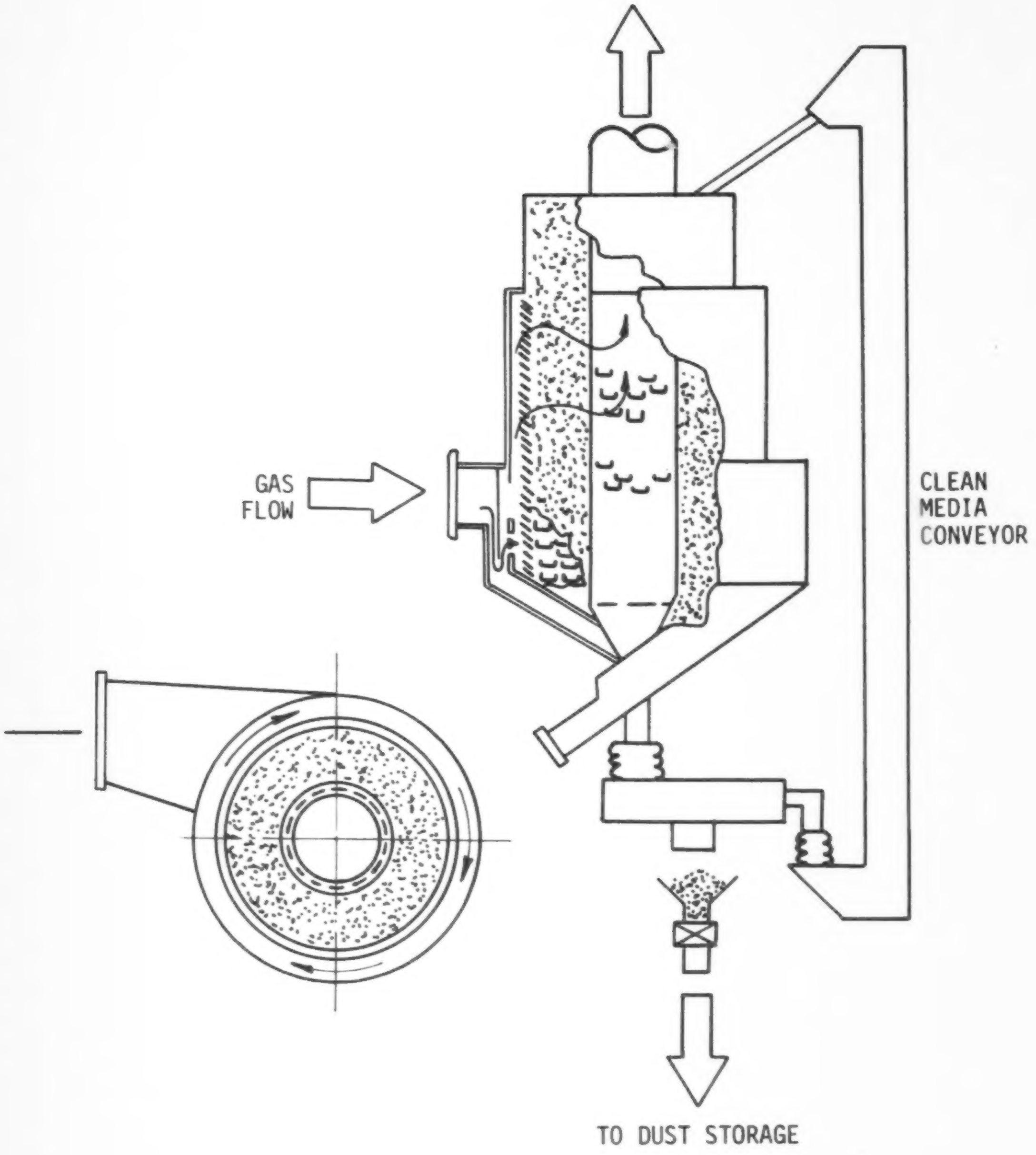
GAS
FLOW
CLEAN
MEDIA
CONVEYOR
TO DUST STORAGE

Figure 71. The intergral cyclone model of the "Dry Scrubber."

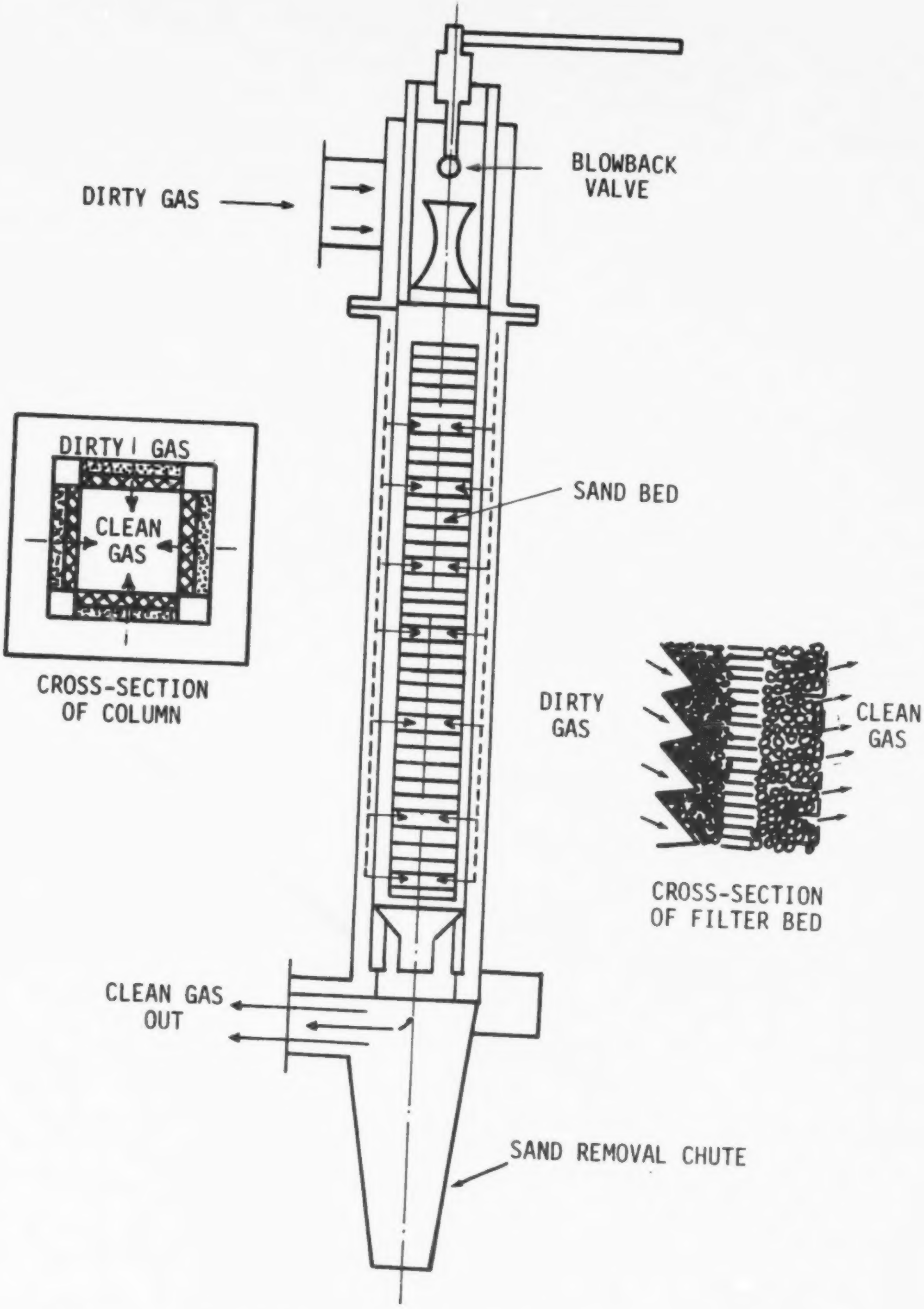
BLOWBACK VALVE
DIRTY GAS
DIRTY GAS
CLEAN GAS
SAND BED
CROSS-SECTION OF COLUMN
DIRTY GAS
CLEAN GAS
CROSS-SECTION OF FILTER BED
CLEAN GAS OUT
SAND REMOVAL CHUTE

Figure 72. Possible design for Squires Panel Bed Filter.

sand beds as a mass, with minimum inter-particle movement, so that a surface layer of granules between each pair of louvers is physically ejected from the panel and falls to the bottom of the filter vessel along with the collected filter cake. The expelled granule is immediately replaced by the downward movement of a fresh granule from the overhead hoppers.

The development of the LS filter has continued for the past ten years at the City College of the City University of New York with financial support from EPA and EPRI. This development work resulted in minor modifications of louver configurations (wishbone type louvers) and of the puff-back cleaning technique.

Fixed Bed Granular Filters

As opposed to the continuous and intermittent moving beds, fixed bed granular filters require no granule circulation. Collected particles in the bed are removed either mechanically or penumatically. There are three fixed bed devices. The "Lurgi-MB Filter" and the "Rex-Gravel Bed Filter" clean the bed mechanically. The "Ducon Granular Bed Filter" uses a reversed gas flow to clean the bed.

The Lurgi MB Filter -

Max and Wolfgang Berz designed a granular bed that requires no granule circulation. The cleaning is carried out by flowing a reverse flow of gas through the bed while subjecting it to mechanical vibration of sufficient magnitude to cause the inter-granule movement necessary for removal of entrapped particles.

The granular bed is a layer of loosely packed material such as gravel held on a horizontal sieve plate. Gravel sizes range from 1 to 6 mm in diameter. Figure 73 is a sketch of the system.

In operation, the dusty gas flows upward through the gravel bed and vents through the clean gas duct on top. The dust will be retained and gradually will buildup in the bed. This increases the pressure drop. As soon as the pressure drop of the filter exceeds a pre-determined level, the gas flow is stopped and the bed is cleaned. For some applications it is possible to stack two or more filter beds, one over the other, in a given device, with the bottom-most layer consisting of relatively coarse material to act as a pre-filter.

This granular bed filter was marketed commercially by Lurgi Appareteban Gesellschaft M.B.H. of Frankfurt, Germany. It was mostly used in cement plants. It was redesigned in 1968 and was withdrawn from the market at about the end of 1969. Its shortcoming lies in the strain imposed on the necessary flexing membranes associated with the vibrating technique. It is conceivable that at low temperatures where rubber membranes and spring-supported bed mounts are feasible, such a filter could operate with a reasonable life. However, at low temperatures it could not compete economically with baghouses. At high temperatures, metal bellows would be needed for the flexing membrane, and their life expectancy in the hot and dusty environment is too short for practical application.

Rex Gravel Bed Filter -

Berz designed an alternate arrangement of the "Lurgi-MB Filter" and marketed it through Gesellschaft fur Enstaubungsaulagen (GfE) of Munich, Germany. In the U.S. it is built and marketed by Rexnord in accordance with an exclusive license agreement with GfE. It is built in modules for the treatment of large gas volumes, with several modules arranged in parallel through a common raw gas duct and a common clean gas duct.

Each gravel bed filter module consists of a filter top section containing two horizontal beds connected in parallel, and a cyclone pre-cleaner located underneath. The operation of the system is illustrated in Figure 74. The raw gas enters the filter through an inlet chamber where immediate separation (settling) of very coarse materials takes place. From there, the gas enters the cyclone separator where more coarse dust is separated and removed through the discharge airlock at the outlet.

The gas then rises from the cyclone through the vortex tube and enters the filter chambers. It passes from the top of the horizontal filter beds to the bottom, so that the remaining fine

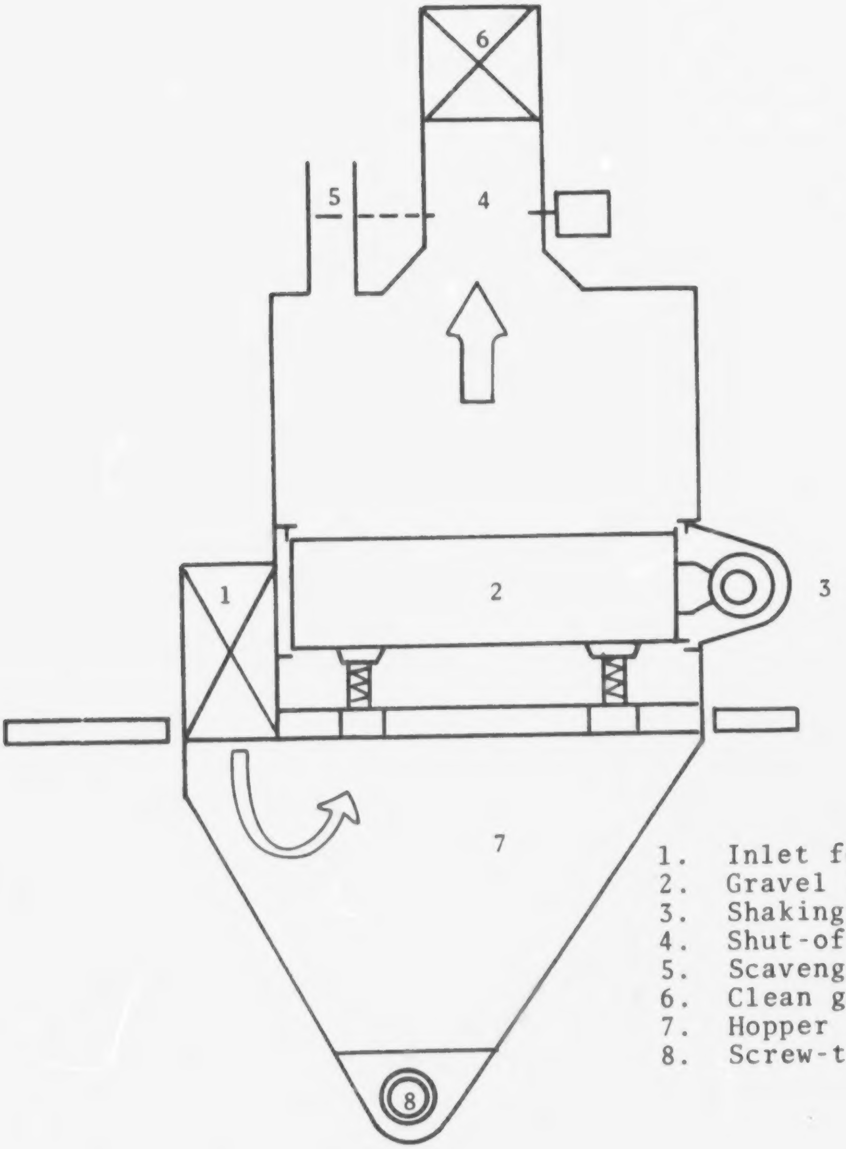

1. Inlet for dirty gas
2. Gravel layer
3. Shaking motor
4. Shut-off flap
5. Scavenging air flap
6. Clean gas outlet
7. Hopper
8. Screw-type discharger

Figure 73. Lurgi MB filter.

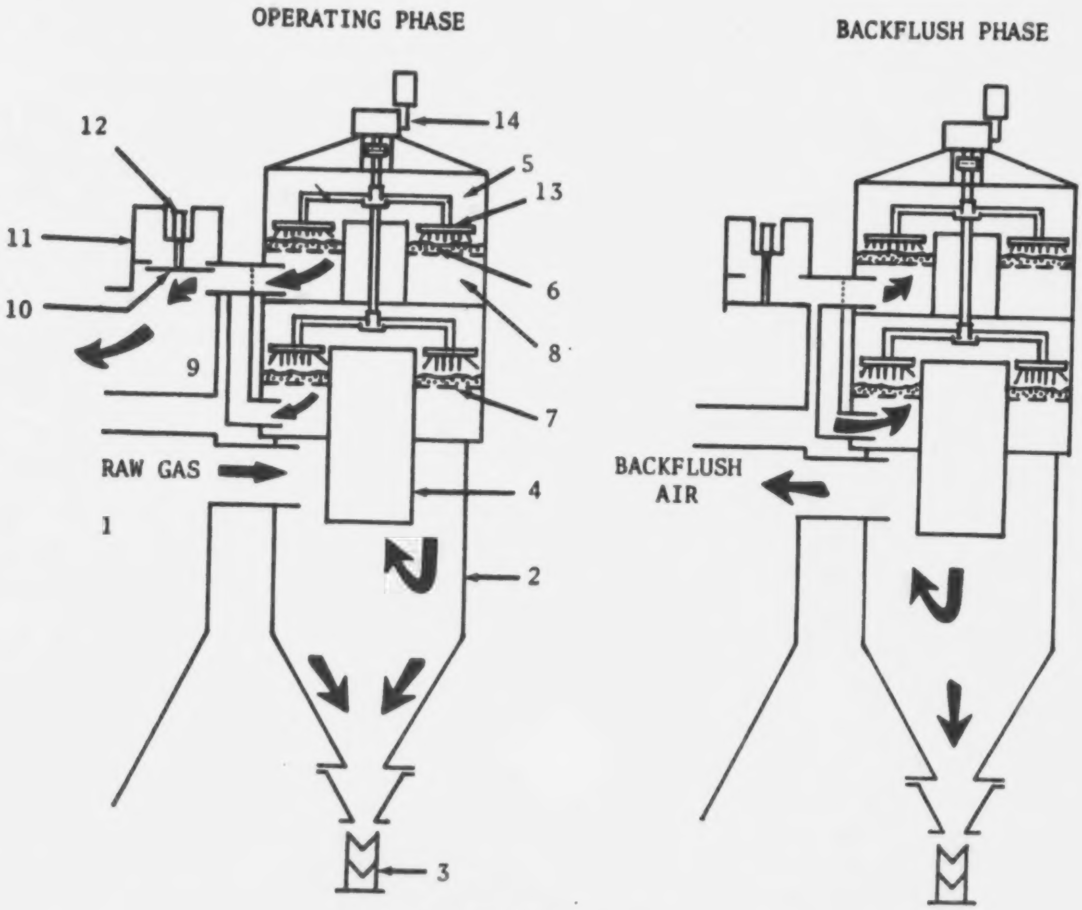
OPERATING PHASE
BACKFLUSH PHASE
12
14
5
13
11
6
10
8
9
7
RAW GAS
4
1
2
3
BACKFLUSH AIR

1. INLET CHAMBER
2. PRIMARY COLLECTOR (CYCLONE)
3. DOUBLE TIPPING GATE (DUST DISCHARGE)
4. VORTEX TUBE
5. FILTER CHAMBER
6. GRAVEL BED
7. SCREEN SUPPORT FOR BED
8. CLEAN GAS COLLECTION CHAMBER
9. EXHAUST PORT
10. BACKWASH CONTROL VALVE
11. BACKWASH AIR INLET
12. VALVE CYLINDER
13. STIRRING RAKE
14. STIRRING RAKE MOTOR/REDUCERS

Figure 74. Rexnord gravel bed filter.

dust is deposited on the quartz grains and in the interstices of the bed. The cleaned gas flows through the clean gas collection chamber and passes through the 3-way valve into the clean gas duct.

Cleaning of the filter unit can be initiated by means of a pre-set sequencer or by automatically monitoring the pressure differential across the filter bed. During the cleaning cycle, the unit is isolated from the gas stream by the 3-way valve. Then backwash air is admitted to the filter chamber in a reverse flow direction. It is either forced in by using a backwash air blower or sucked in by negative pressure. The backwash air loosens the filter bed.

During the cleaning process the rake-shaped double arm stirring device is rotated by the geared motor. This helps the dust to be removed from the gravel and entrained by the backwash cleaning operation. The large agglomerated dust particles are carried by the backwash air via the vortex tube into the precipitator, where the velocity is reduced and the gas stream deflected so that a large percentage of the dust is settled out. The backwash air, containing the remaining dust, mixes with the dust-laden air in the raw gas duct and is then subjected to cleaning in the remaining units of the filter.

Ducon Granular Bed Filter -

The Ducon granular bed filter (Figure 75) consists of multiple beds of sand stacked vertically within two perforated concentric metal tubes. The beds of sand grains rest on slotted inner screen supports having opening dimensions slightly smaller than the diameter of sand grains. Above each bed there is an annular space with an outer screen similar to the inner screen. Thus, each sand bed contained within the two concentric cylinders is supported and caged by slotted metal retaining screens. Figure 76 shows a typical filter element. The elements are supported from a clean gas plenum within a housing. The basic arrangement is exemplified in the cutaway sketch of a typical 4-element unit shown in Figure 75.

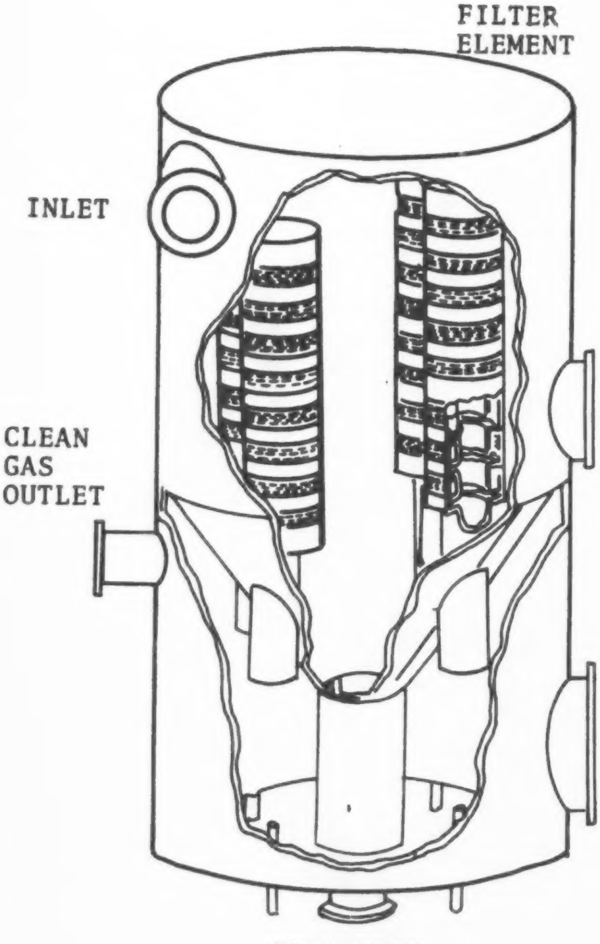
FILTER ELEMENT
INLET
CLEAN GAS OUTLET
COLLECTED DUST OUTLET

Figure 75. Ducon granular bed filter.

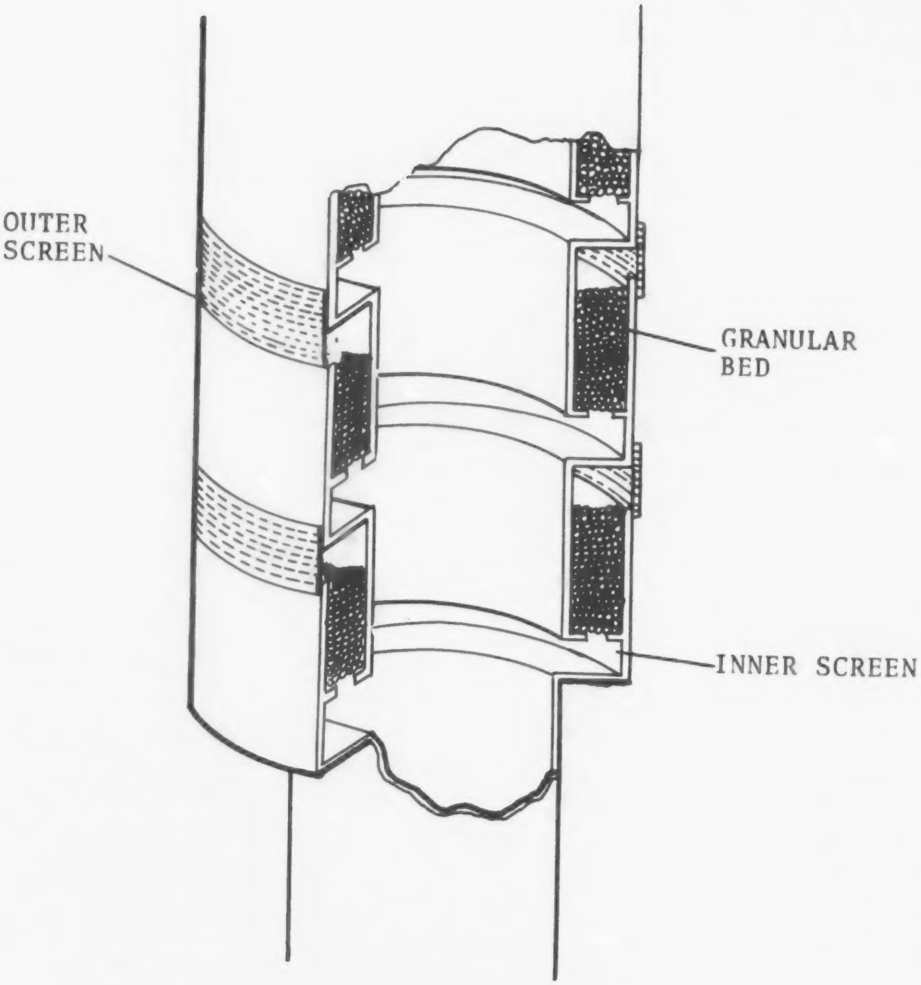
OUTER SCREEN
GRANULAR BED
INNER SCREEN

Figure 76. Filter element.

In operation, particle laden gas entering the dusty side of the filter housing passes through the element's outer retaining screens, flows downward through the inner cylinder into the clean gas plenum to the vessel outlet nozzle. The particles are deposited on the surface and within the interstices of the sand beds. To clean the element, a small volume of compressed air is introduced in a reverse pulse which induces blowback gas flow from the clean gas plenum, sufficient to momentarily fluidize all the sand beds within the element simultaneously. This blow-back gas flexes the bed in fluidized expansion, expelling interstitially deposited dusts, as well as any dusts on the bed surfaces, through the outer screen. The dust then falls into the collector hopper for eventual removal. Figures 77 and 78 illustrate the collection and cleaning cycles.

INDUSTRIAL USERS AND PERFORMANCES

Granular bed filters have been used in recent years on selected sources. While the use of granular beds has not been directed at the control of fine particulates, granular beds have been used successfully on cement and lime kilns, asphalt dryers, and clinker coolers. Of the three commercially available granular bed filter systems, only the Rexnord granular bed filter and the Combustion Power Company's moving bed granular bed filter have industrial installations. Ducon granular bed filters have been used in some pilot studies.

We surveyed industrial granular bed filter users to obtain performance data and to identify operating problems. The following is a summary of the results of this survey.

Rexnord Granular Bed Filter

There are over thirty industrial users of the Rexnord granular bed filters. Most of the installations are in Portland cement plants to control particulate emissions from clinker coolers. The average size of the dust particles from clinker coolers is relatively large, and the granular bed adequately meets the emission standards. However plugging of the granule retaining screens has occasionally caused problems.

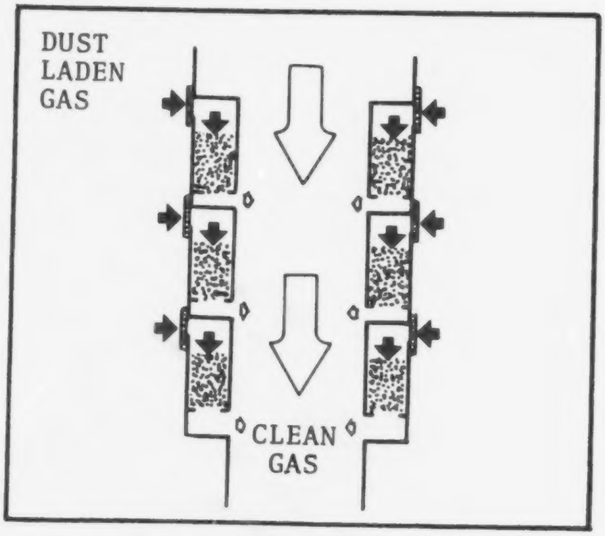
DUST
LADEN
GAS
CLEAN
GAS

Figure 77. Collection cycle.

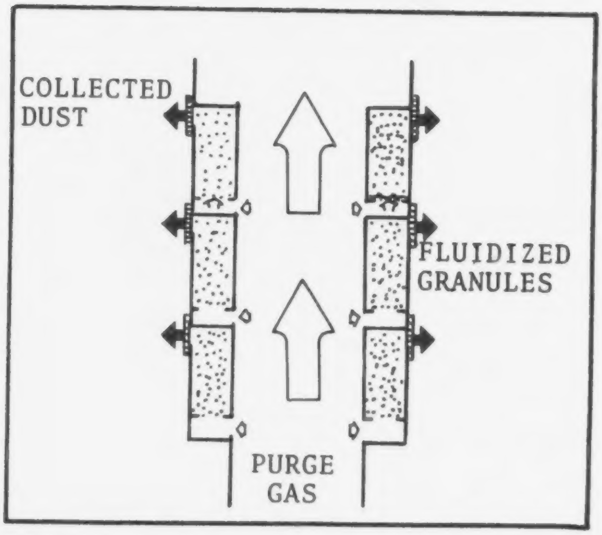
COLLECTED
DUST
FLUIDIZED
GRANULES
PURGE
GAS

Figure 78. Cleaning Cycle

There is one unit which is installed in a steel sinter plant to control the emissions from a windbox exhaust. The installation consists of 24 modules with a total capacity of 4,400 Nm³/min (240,000 ACFM @ 300°F). The bed is packed with 0.1 cm diameter gravel to a depth of 9 cm. The unit was started up in February 1976 and encountered several operational difficulties. Design modifications were required. Among the operational difficulties encountered were:

1. The gravel medium developed growth problems; i.e., collected dust adhered to granules and could not be removed.
2. Downcomer valves for dirty gas had to be modified.
3. Backflush fans were replaced by larger fans.
4. Heavier gauge bed support screens had to be substituted for the originals.
5. Backflush air preheater burners have malfunctioned repeatedly.

Some users supplied cost data. Table 20 summarizes the cost data available.

McCain (1976) conducted a performance test on a Rexnord granular bed installed in a Portland cement plant. Samples were taken simultaneously at the filter inlet and outlet with cascade impactors. Particle size distributions and grade efficiencies were calculated from the impactor data.

The particles were found to have a mass median diameter of about 200 μmA. The overall collection efficiency was found to be from 99.3 to 99.7%. The system pressure drop ranged from 9.6 to 14 cm W.C. (3.8 to 5.5 in. W.C.). The system energy usage during the tests was approximately 1,780 joules/Nm³ (47.7 in W.C.). Figure 79 shows the grade efficiency curves for three sampling runs reported by McCain for three cascade impactor runs. Table 21 lists the operational conditions for the granular bed filter during the test period.

Combustion Power Company's Moving Bed Granular Bed Filter

Four units have been on line. All installations are on hog-mill waste combustors. A prototype unit was installed at

TABLE 20. SUMMARY OF REXNORD GRAVEL BED USERS

Plant/ Date Install.	Gas Capacity Am /min	Gas Temperature °C	Pressure Drop cm W.C.	Capital Cost $	Annual Power Cost $	Annual Maintenance Cost $
A 6/73	5,100 (180 M ACFM)	126 (258°F)	36 (14"W.C.)	750,000	78,000	---
B 4/75	3,820 (135 M ACFM)	163 (325°F)	19 (7.5"W.C.)	2,500,000	---	6,000
C 1974	4,020 (142 M ACFM)	182 (360°F)	13 (5"W.C.)	1,400,000	8,000	4,000

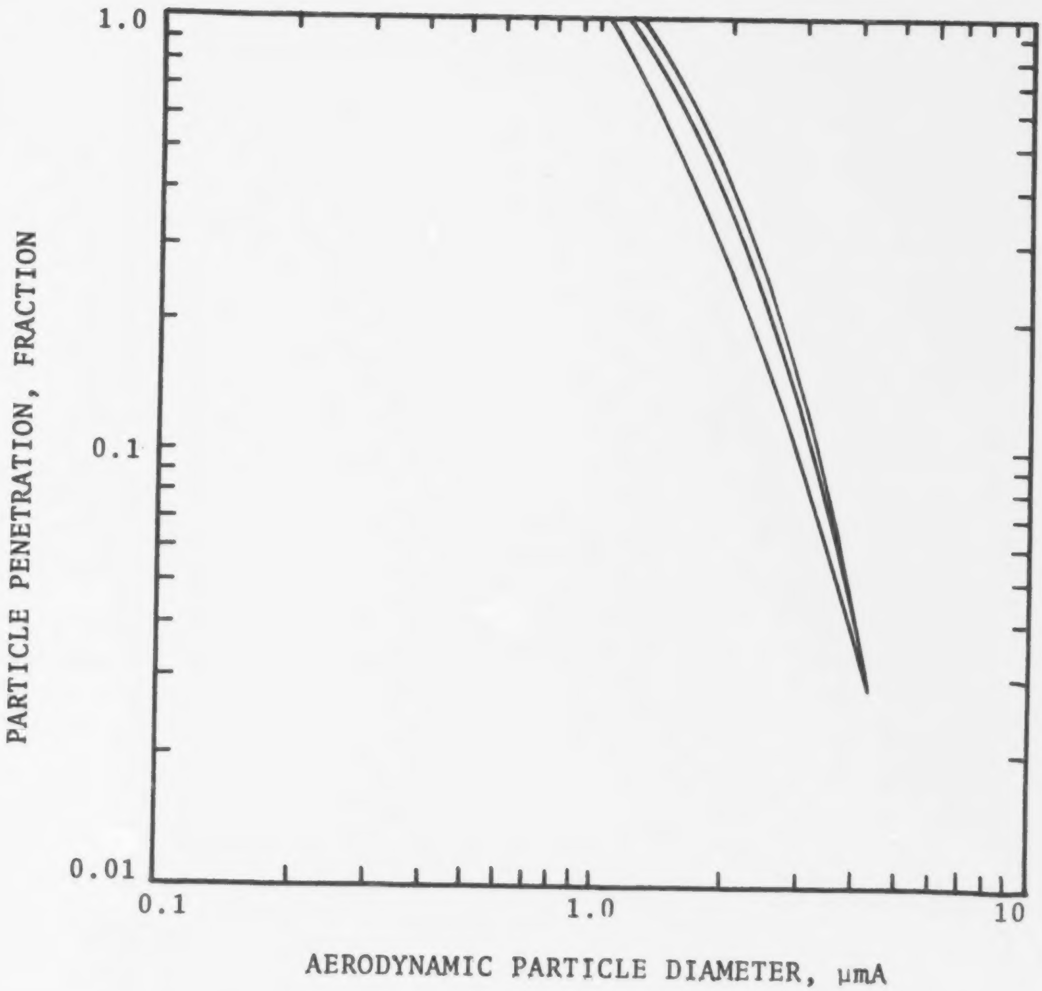

Figure 79. Experimental grade efficiency curve of a Rexnord gravel bed filter (McCain, 1976).

TABLE 21. DESIGN SPECIFICATIONS OF THE SYSTEM AS TESTED

Inlet Volume Flow: 2,266 ACM/min at 204°C
(80,000 ACFM at 400°F)

Backflush Volume Flow: 317 ACM/min at 66°C
(11,200 ACFM at 150°F)

Pressure Drop: 25.3 cm W.C. (10 in. W.C.)

Gravel Size: 4 mm (5/32 in.) x no. 6 mesh

Bed Depth: 11.4 cm (4 1/2 in.)

Bed Area: 3.72 m^2/bed (40 ft^2/bed)

(For a total of 59.5 m^2 of bed area with
52 m^2 actively filtering in normal operation)

the Weyerhaeuser Company, Snoqualmie Falls, Washington Plant. This unit was single down-flowing sand annulus 2.6 m (8.5 ft) O.D. and about 1.8 m (6 ft) I.D. with an effective filtering height of 4.9 cm (16 ft). The surface area was calculated at 34 m^2 (365 ft^2). The granules were angular in shape and ranged from 3.2 mm to 6.4 mm (1/8 in. to 1/4 in.) in average diameter. The granules moved downward through the annulus in gravity flow at a bulk velocity of 61 to 122 cm/hr (2 to 4 ft/hr). The granule inventory was of the order of 36 metric tons though only about 18 metric tons were in the region exposed to gas flow. The manufacturer suggested capacity was 1,133 Am^3/min (40,000 ACFM).

Hood (1976) reported the performance test data on this unit. The experimental penetration curves are shown in Figure 80 for three cascade impactor sampling runs. As can be seen, the unit performed at an efficiency of from 75 to 95% in the removal of particulates of 2 μm in diameter, at an efficiency of 70 to 90% for particulate removal of 1 μm in diameter, and at an efficiency of 65 to 80% for particles 0.5 μm in diameter. The efficiency of the unit was low for the removal of particles of 0.25 μm in diameter. The data indicated that in the removal of particles in the lower size ranges the unit performed at an efficiency of between 45 and 65%.

Under the sponsorship of the Department of Energy, Combustion Power Company conducted parametric studies on their GBF system to correlate the collection efficiency of the GBF with mechanical and process parameters. Parameters studied included superficial gas velocity, dust loading, particle size distribution, granule diameter, granule circulation rate, bed thickness and length of bed.

The GBF was a pilot unit and was operated at ambient temperature. Figure 81 shows the system. The granular bed material (alumina) flows downward between two concentric cylinders. The gas passes through the bed and is filtered by the granules. The granules are recycled pneumatically and the collected dust particles are disengaged from the granules and sent to a conventional baghouse.

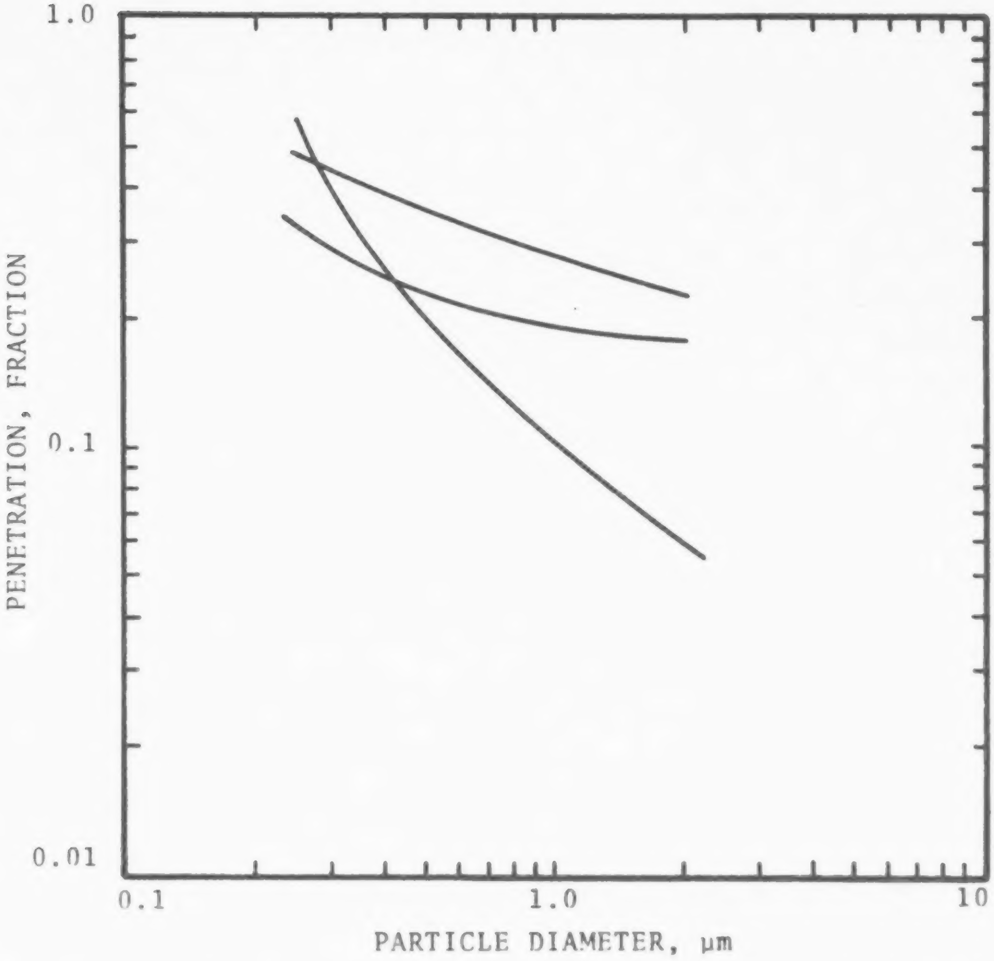

Figure 80. Experimental penetration curves for CPC dry scrubber (Hood, 1976).

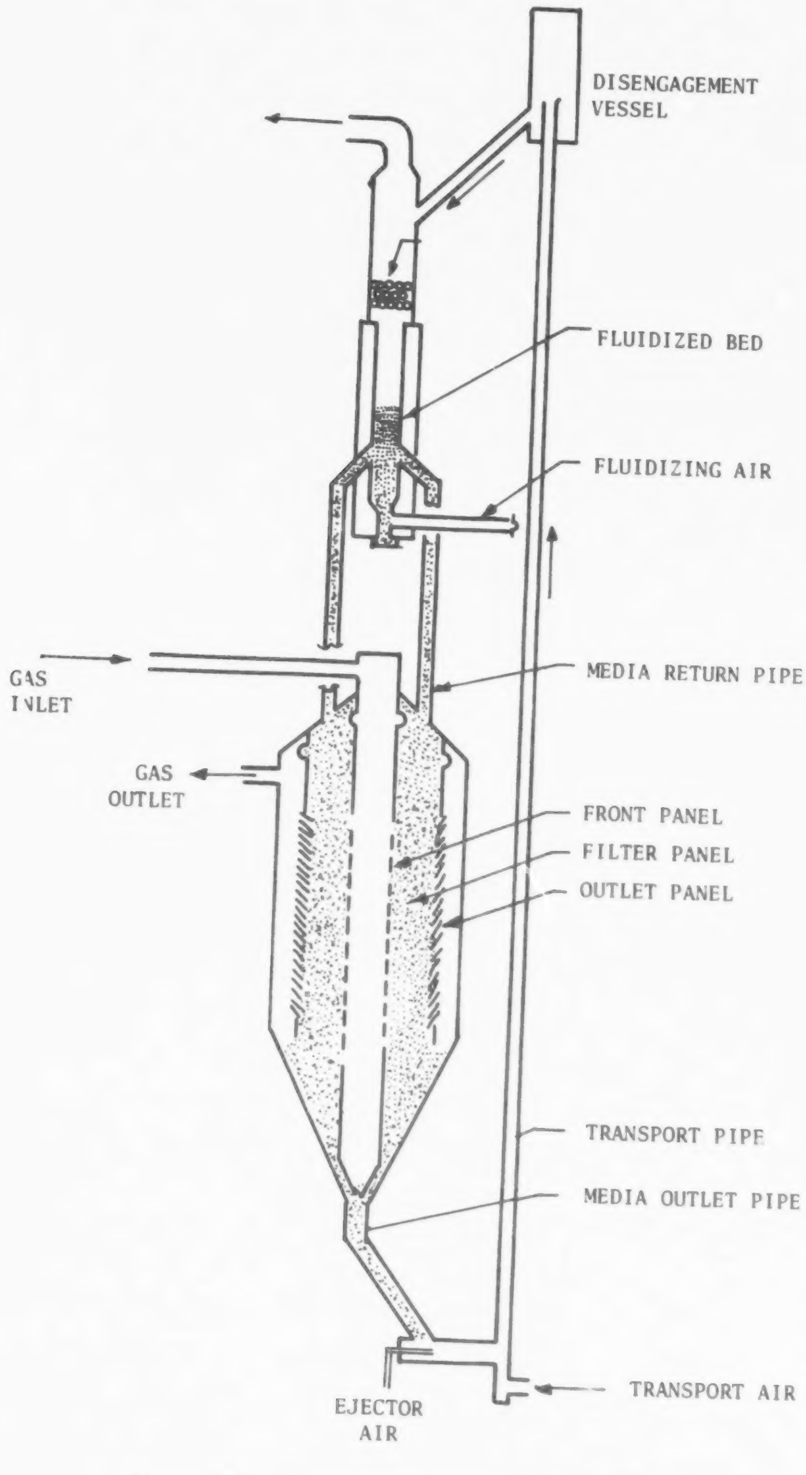
DISENGAGEMENT VESSEL
FLUIDIZED BED
FLUIDIZING AIR
GAS INLET
MEDIA RETURN PIPE
GAS OUTLET
FRONT PANEL
FILTER PANEL
OUTLET PANEL
TRANSPORT PIPE
MEDIA OUTLET PIPE
TRANSPORT AIR
EJECTOR AIR

Figure 81. Continuous moving bed GBF.

The performance of this device has been reported by Guillory (1978), Wade, et al. (1978) and Wigton and Wade (1978). Test parameters for the nominal, thick bed, thin bed, short bed, and small collector granule configurations are listed in Table 22. Particle concentrations ranged from 0.46 to 4.6 g/Nm³ (0.2 to 2.0 gr/SCF). Different test dusts were used in order to vary the mass median particle diameter from 3 to 10 μmA. The superficial gas velocity was varied from 20 to 80 cm/s (40 to 160 ft/min). The granule flow rate was varied to 0.4 to 1.6 kg of granule/kg of air. Pressure drop ranged from 1.2 to 5.7 kPa (5 to 23 in W.C.).

Fractional efficiency curves are shown in Figures 82 through 86. The overall penetrations are correlated with the pressure drop function and are tabulated in Table 23. The pressure drop function was defined as:

$$\Theta = \frac{\Delta P \; C_p}{u_G \; M_m} \qquad (96)$$

where Θ = pressure drop function

ΔP = pressure drop, cm W.C.

u_G = superficial gas velocity, cm/s

M_m = media rate, kg granules/kg air

In general the CPC moving bed filter was found to be capable of particle removal efficiencies in excess of 98% for particles in the 1 to 10 μmA diameter range. Submicron particles were collected at an efficiency in excess of 90% in cases with high velocities, high loadings, and low media rates. Beds with larger thickness to granule diameter ratios were most effective in the capture and retention of particles in the 2 to 5 μmA diameter range. Also, intermittent media movement was shown to improve efficiency by a few percent. No cost data were available.

Ducon Granular Bed Filter

There is no current industrial user of the Ducon granular bed filter. However, one test unit was installed in a refinery

TABLE 22. TEST PARAMETERS FOR CPC MOVING BED FILTER (from Wade, et al., 1978)

Configuration	Granule Diameter, mm	Active Bed Length, cm	Bed Thickness, cm
Nominal	2	134.6	20.3
Thick Bed	2	134.6	40.6
Thin Bed	2	134.6	10.2
Short Bed	2	67.3	20.3
Small Medium	0.8	134.6	20.3

TABLE 23. CPC MOVING BED FILTER OVERALL PENETRATION CORRELATION

Configuration	Correlation
Nominal	$\overline{Pt} = 0.06\ \Theta^{-0.5}$
Thick Bed	$\overline{Pt} = 0.0175\ \Theta^{-0.7}$
Thin Bed	$\overline{Pt} = 0.091\ \Theta^{-0.47}$
Short Bed	$\overline{Pt} = 0.0425\ \Theta^{-0.46}$
Small Medium	$\overline{Pt} = 0.0259\ \Theta^{-0.59}$

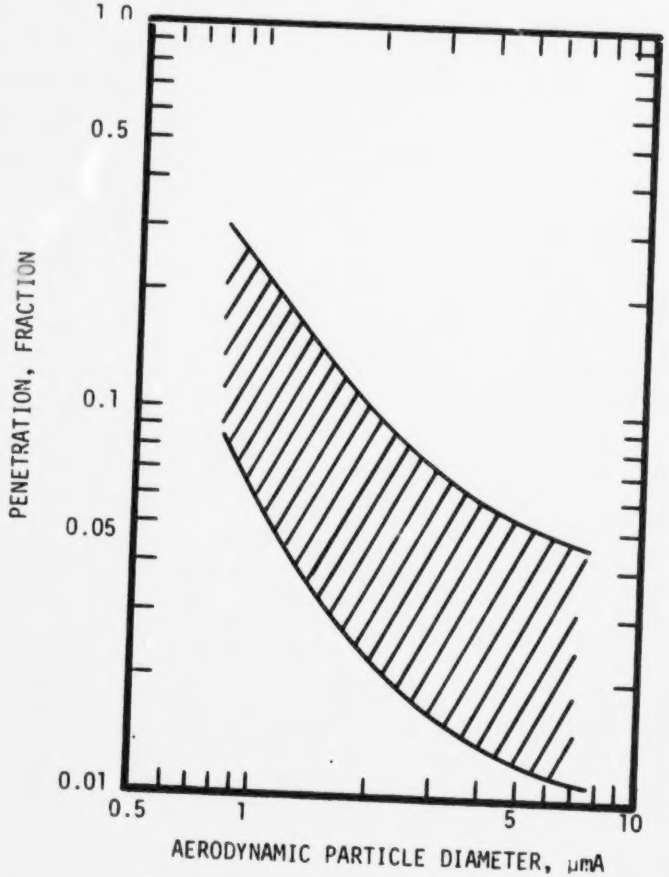

Figure 82. Experimental grade penetration (CPC data for nominal configuration).

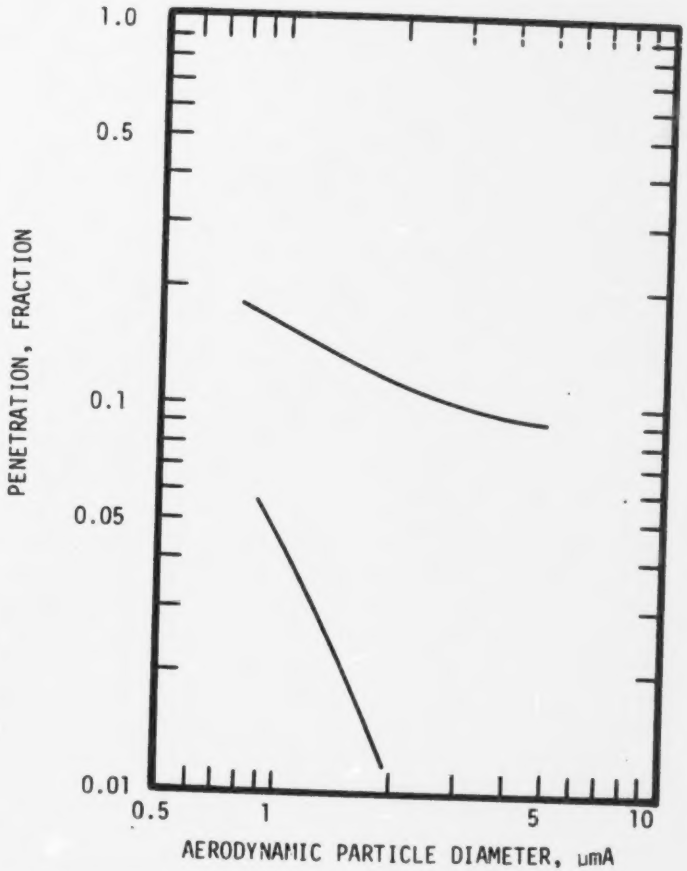

Figure 83. Experimental grade penetration (CPC data for thick bed configurations).

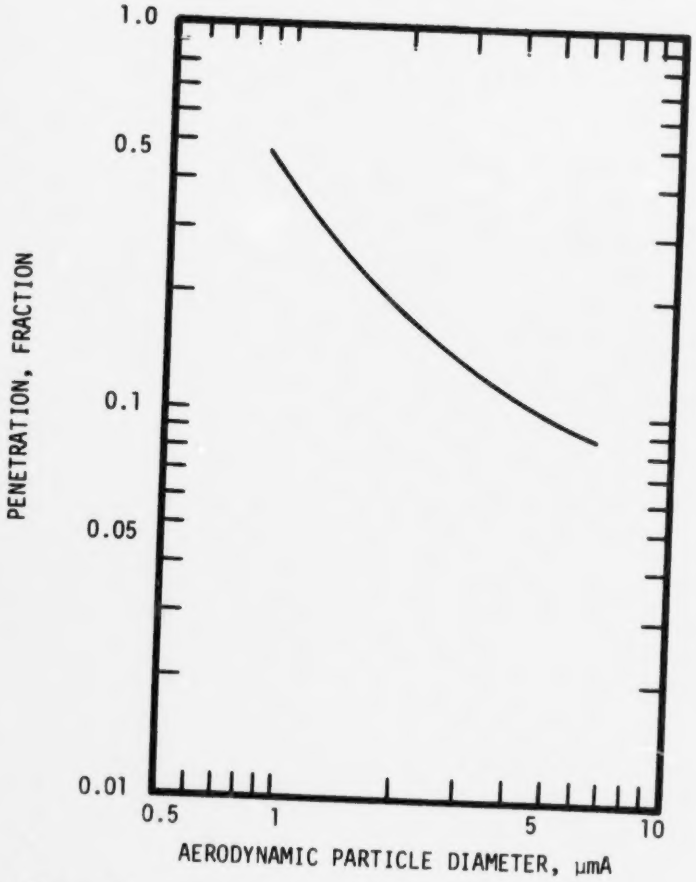

Figure 84. Experimental grade penetration (CPC data for thick bed configuration).

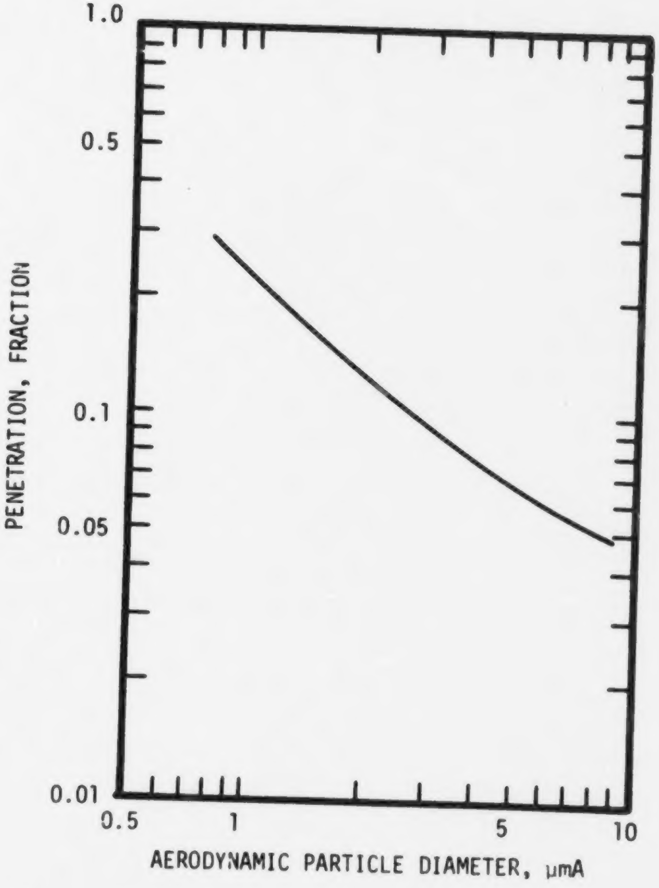

Figure 85. Experimental grade penetration (CPC data for short bed configuration).

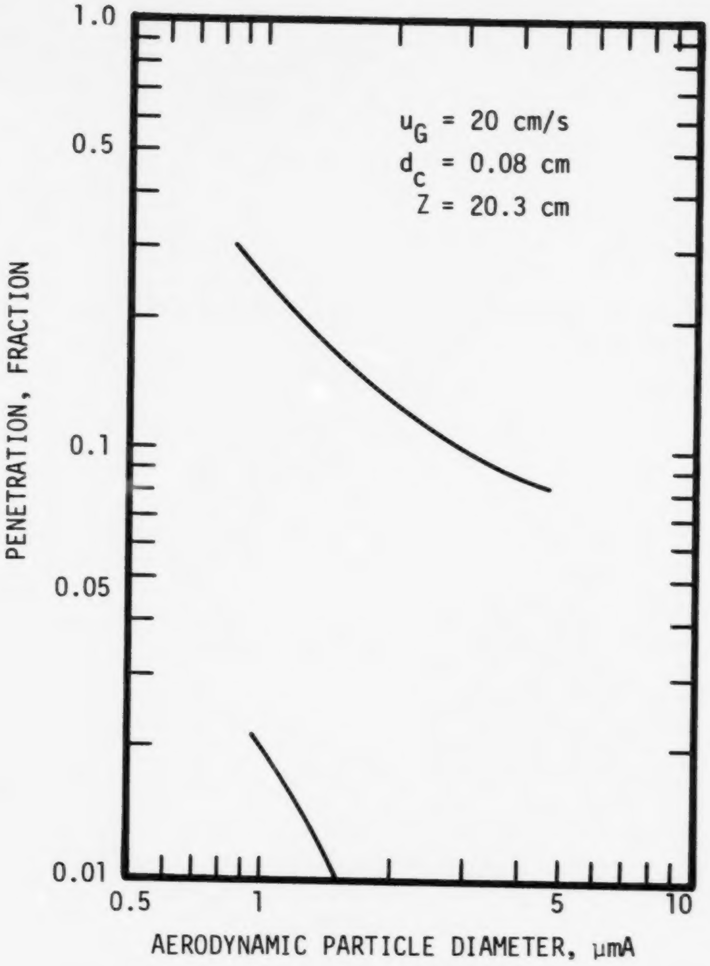

Figure 86. Experimental grade penetration (CPC data for small granule configuration).

to control the particulate emission from the regenerator of a fluid catalytic cracking (FCC) unit. The unit had four filter elements; each had 14 beds. The bed was a 6.3 cm (2.5 in.) deep bed of 760 µm sand. The face velocity was between 15 and 45 cm/s (0.5 and 1.5 ft/s). Gas temperature at the inlet was 371 to 482°C (700 to 900°F).

The overall collection efficiency reported by Kalen and Zenz (1973) was 85 to 98% for particles with a mass median diameter of 35 µm and a geometric standard deviation of about 4. No grade penetration or efficiency curves were given by them.

The grade penetration curve was calculated for the Ducon granular bed filter based on the information provided by Kalen and Zenz (1973). Figure 87 shows the results. The shaded area is the range of calculated points.

A high temperature and pressure design of the Ducon filter was tested at the Exxon miniplant (Hoke, et al. (1978). The performance data for all runs through November, 1977 are listed in Table 24. The efficiencies are based on air inlet concentration of 2.3 g/Nm^3 (1.0 gr/SCF) which is the average for the emissions from the secondary cyclone. The lowest demonstrated particulate outlet concentration was 68.6 mg/Nm^3 (0.03 gr/SCF) however, they were unable to maintain this level of performance for more than a few hours of operation. At times the filtration efficiency was very poor and the outlet particulate concentration was as high as 700 to 1,200 mg/Nm^3 (0.3 to 0.5 gr/SCF). Fractional efficiency data are presented in Figure 88.

EVALUATION

Granular bed filters perform in many respects in a manner analogous to fiber filtration systems. The major difference appears to be the size differences between the fiber used in fabric filters and the granules in granular bed filters.

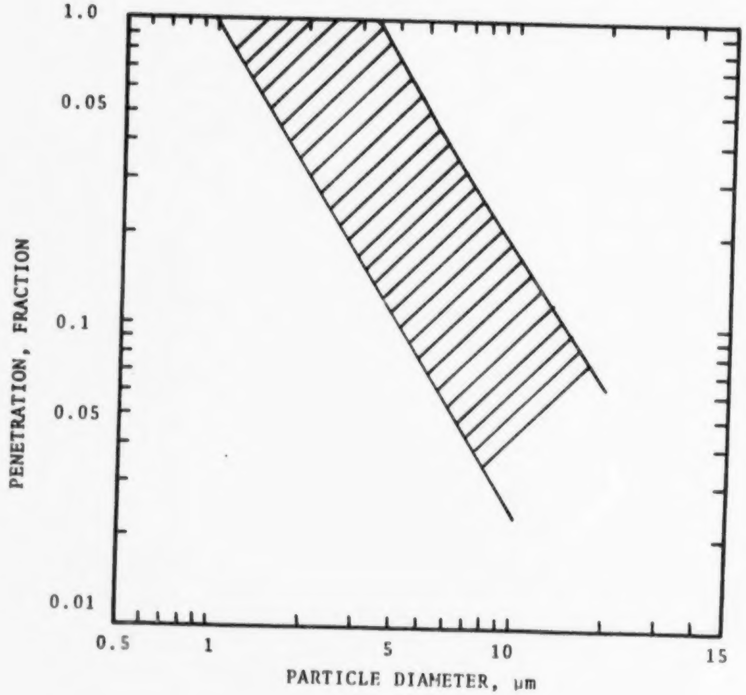

Figure 87 . Fractional penetration curve for Ducon granular bed.

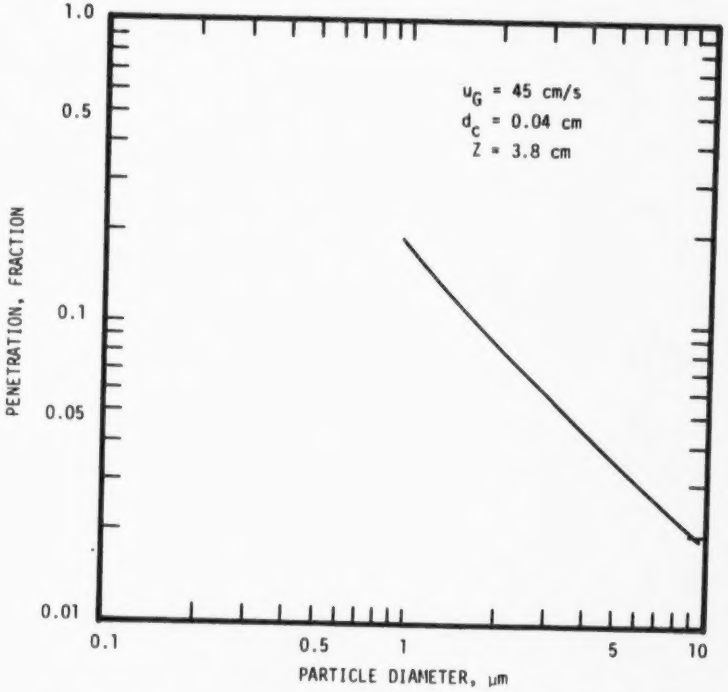

Figure 88. Fractional penetration for Ducon GBF (from Bertrand, et al., 1977).

TABLE 24. GRANULAR BED FILTER PERFORMANCE (FROM BERTRAND, ET AL., 1977)

Run Number	Outlet Concentration gr/SCF	Outlet Concentration g/m³	Collection Efficiency* (%)
54	0.69	1.57	31.0
57	0.04-0.08	0.09-0.18	92.0-96.0
59 (Sample 1)	0.08	0.18	92.0
59 (Sample 2)	0.28	0.64	72.0
59 (Sample 3)	0.54	1.23	46.0
61	0.46	1.05	54.0
62.1	0.03	0.07	97.0
62.3	0.21	0.48	79.0
63 (Sample 1)	0.05	0.11	95.0
63 (Sample 2)	0.07	0.16	93.0
63 (Sample 3)	0.12	0.27	88.0
64 (Sample 1)	0.28	0.64	72.0
64 (Sample 2)	0.29	0.66	71.0
64 (Sample 3)	0.27	0.61	73.0
65 (Sample 1)	0.05	0.11	95.0
65 (Sample 2)	0.06	0.14	94.0
66	0.06	0.14	94.0

---

* Based on a 2.3 g/Nm^3(1.0 gr/SCF) inlet concentration

Generally, for low to medium temperature applications, granular bed filters are not economically competitive with fabric filters even though the gas flow capacity of granular bed filters is much higher than that of fabric filters. Because granular bed filters are not mass produced and the weight of the bed requires special support, the cost of granular bed filters is much higher than that of fabric filters. Also, granular bed filters generally have lower efficiencies than fabric filters.

The best potential applications of granular beds as devices to control particle emissions are in situations which require the control of effluents under both corrosive and high temperature conditions. GBFs are most successful in controlling emissions of particulates that agglomerate easily as in the case of cement dust.

Cleaning Methods

During the operation of a granular bed filter, dust deposits in the interstices of the bed and on the surface. It is necessary to clean the dust from the bed to prevent it from saturating the bed and causing high pressure drop.

Depending on bed structure, different cleaning methods are used. Fixed bed GBFs, such as Ducon GBF and Rexnord GBF, apply a reverse gas flow to blow the dust out. In the continuously moving bed and intermittently moving bed GBFs, the bed is cleaned by removing both the granules and the dust from the filter and repacking the filter with clean granules.

The advantages and disadvantages of present GBF systems are discussed in the following paragraphs.

Fixed Bed GBFs

The fixed bed GBFs are usually horizontal beds. Beds are cleaned by reverse gas flow. The reverse flushing gas may be used to fluidize the bed and elutriate the dust deposits as in the case of the Ducon granular bed system.

The advantage of fixed bed GBFs is that they require no granule recirculation system and therefore have a lower operating cost.

The disadvantages are:

1. Leakage or bypassing;
2. Plugging of retaining grids, and loss of granules when retaining grids are not used;
3. Efficiency decreases with time (particle seepage); and
4. Ineffective bed cleaning.

Leakage or Bypassing -

Dust loosened in the cleaning cycle may be carried directly to the stack when the bed is put back on line. This problem has been described by Kalen and Zenz (1973) with the Ducon GBF and by McCain (1976) with the Rexnord GBF.

Plugging of Retaining Grids -

The collection efficiency of the granular bed can be increased by using finer grades of granules. However, grids with openings smaller than the granules need to be used. This increases the tendency to accumulate dust deposits on the grid and eventually causes plugging. This problem was experienced by Rexnord GBF users and by Exxon Research and Engineering Company with the Ducon granular bed installed at their pressurized fluidized bed combustor miniplant. At Exxon, the inlet retaining grid of the Ducon granular bed filter plugged quickly even when the inlet grid was a 10 mesh screen. The deposited dust on the screen could not be blown out by reverse gas flow. Shutdown of the plant was required to remove the dust manually.

In solving this plugging problem, Exxon has eliminated the inlet retaining grid by increasing the free board above the bed (Bertrand, et al., 1977). However, this arrangement causes granules to be blown out and lost from the filter beds. In subsequent tests Exxon lowered the blow back gas velocity. Some indications of particle buildup in the filter beds at the low blow back velocities were noted. In one run about 35% of the bed was fly ash which was not blown out of the bed. It was also found that if the filter beds were overloaded with fine particles, the particles tended to move to the top of the filter bed during blow back where they prilled, forming larger spheres which could not be removed except at much higher blow back velocities. Exxon has tried using heavier granules, however, some of the material was still lost during blow back.

Efficiency Decreases with Time -

For non-agglomerating dust, the blow back cleaning technique will decrease the collection efficiency of the bed with each cleaning cycle. During blow back, collected dust redisperses into the gas stream. However, the fine particles will remain in suspension. This will increase the particle loading of fine particles in the gas stream. Since the blow back gas is cleaned by other beds and the collection efficiency of the bed is less than 100%, the fine particle penetration will progressively increase with each cleaning cycle, (i.e., the efficiency of the bed goes down). Exxon (Bertrand, et al. 1977) has noticed this decrease in efficiency with time. In one test by Exxon, the filtration efficiency was fairly high at the start of the run. The outlet particulate loading was about 0.12 g/m^3 (0.05 g/SCF). The outlet loading increased somewhat during the run to 0.17 g/m^3 (0.07 g/SCF) and finally to 0.25 g/m^3 (0.1 g/SCF) at the end of the 12 hour test.

Ineffective Bed Cleaning -

Cleaning by reverse gas flow is not an effective cleaning method especially when the cleaning duration is short. The cleaning efficiency is even lower when particles are charged.

Generally, an adhesive force exists between the collected dust and the granules. To separate the collected dust from granules by reverse gas flow, the aerodynamic drag force must be higher than the adhesive force between the dust and granules. For those particles which have a strong adhesive force, as in the case of charged particles, dust will not be removed completely from the granules by the reverse gas flow alone. Thus, dust will gradually accumulate in the bed. In testing the Ducon GBF, Exxon (Bertrand et al., 1977) discovered a large accumulation of fly ash in the bed, uniformly distributed through the filter medium.

The accumulation of dust in the filter bed has some significant consequences. The dust can approach the outlet section of the filter and plug the retaining screens. Once the dust reaches the retaining screen, it could be entrained and blown out of the filter bed during the filtration step.

Continuously Moving Bed GBFs

This method is normally limited to vertical panel filters. Dust and granules are continuously removed at the bottom of the GBF. The advantage of this type of bed structure is that the collected dust and granules are separated outside the GBF. This method does not increase the particle loading in the gas stream and the cleaning is more effective compared to reverse gas flow.

The disadvantages are:

1. Costly solid handling system
2. Solids distribution
3. Solid flow
4. Particle reentrainment
5. Erosion
6. Heat loss

Solid Handling -

A costly granule circulation system and dust/granule separation system is required. Under low to medium gas temperature environments, collected dust and granules may be separated by shaking. Cleaned granules are transported to the top of the panel by mechanical means. In high temperature and pressure (HTP) applications, these methods are not feasible. Other methods of transport and separation are required.

Under HTP conditions, granules could be transported by pneumatic means or some improved mechanical means. Depending on the mass flow rate ratio, pneumatic transport may require a large quantity of compressed gas. This will increase the capital cost and operating cost.

Dust and granules under HTP conditions are difficult to separate by mechanical shaking because of the requirement for a suitable metal bellows or seal for the moving mechanism. It may be possible to separate dust and granules by sending them through a baffled "rattler." Dust would be shaken off the granules when the granules hit the baffle. The dust would then be elutriated out of the rattler with air and later cleaned by means of a conventional separator such as a baghouse and cyclone at lower temperature. This setup requires the investment of low temperature secondary cleanup systems.

Solid Flow -

The downward movement of the solids can create a dead zone near the filter surfaces because some granules are retained by the louvers. These zones could eventually be saturated with dust and lead to plugging of the louvers.

Recently, Combustion Power Company made a design change to alleviate this problem. In the new design, gas flows from the inside core radially outward through the bed. The inlet louvers are replaced with slotted panels. During operation, solids flow downward as well as spill through the slots. This design eliminates the dead zone.

Particle Reentrainment -

The grinding of the granules due to the relative motion of the filter granules can dislodge the collected particles and allow them to be reentrained into the gas stream. The reentrainment rate depends on the granule recirculation rate and filtration gas velocity. At high recirculation rate, collected particles are easier to dislodge. At too low a recirculation rate, the bed may be saturated with collected dust. Depending on the inlet particle loading, there exists an optimal granule recirculation rate. Under the sponsorship of the Department of Energy, CPC conducted a parametric test (Wade, 1977, Guillory, 1977) on their GBF. The granule recirculation rate was one of the parameters CPC studied. They showed that low recirculation rate and intermittent media movement improved collection efficiency by a few percent. This improvement could be attributed to a lower particle reentrainment.

Solids Distribution -

Solids distribution to the filter panels may present some difficulties. It is not easy to distribute the solids evenly to the panels.

Erosion -

Solids retaining elements will be subjected to erosion by the moving granular bed. Selection of materials that can resist erosion in HTP conditions becomes a problem. Under the sponsorship of ERDA, Combustion Power Company designed and constructed a full scale filter to treat the total gas flow from the CPU-400 fluidized bed combustor at 1,000 kg/min (2,200 lb/min). The gas temperature was at 704°C (1,300°F). The retaining louvers were made of RS 330 steel. During a shakedown test in December 1975, the louvers had a structural failure in about twenty hours of operation.

Heat Loss-

Granules are withdrawn from the bed for cleaning. To keep the granules hot, substantial energy may be required for HTP conditions. If the granules are recirculated by pneumatic means it is necessary to pre-heat the transport air to minimize heat loss from granules.

Intermittently Moving Bed

Intermittent movement is normally limited to vertical panel filters. The granules are intermittently removed in a cross-flow arrangement, as in CCNY's panel bed. The advantages of this type of bed structure are external granule/dust separation and minimum disturbance to the rooting cake. A rooting cake is the foundation on which the surface cake is formed. The surface cake is formed readily without disturbing the rooting cake and filtration efficiency is higher.

The disadvantages are the same as discussed earlier for the continuously moving bed. In addition, the intermittently moving bed suffers the following disadvantages.

1. Low gas capacity
2. High operating cost and heat loss

Low Gas Capacity -

During cleaning, about two to three layers of granules are removed from the bed. To prevent the dust from being carried deep into the bed by the gas, the filtration velocity should be kept as low as possible to reduce the aerodynamic drag force. CCNY usually operates the panel bed filter at about 15 cm/s (30 ft/min). This velocity is about one third the velocity used in the fixed bed and continuously moving bed GBFs. Thus, more filtration area is required.

High Operating Cost and Heat Loss -

To prevent the dust from penetrating deep into the bed, surface layers are ejected frequently. Depending on dust loading, the surface layer has been removed as frequently as every 30 seconds in the operation of the CCNY panel bed GBF. At 30 second "puff-back" frequency, the volume of the reverse gas flow is about 1% of the total volume of gas treated. The reverse gas flow has a pressure of about 140 kPa (20 psi) higher than the pressure of the gas to be treated. The costs to operate the compressor which supplies the reverse gas flow may be substantial if the gas is to be treated at high pressure.

This cleaning method has another drawback. The "puff-back" gas will have to be pre-heated in order to prevent significant heat loss. To maintain the gas temperature by pre-heating the puff-back gas, the energy requirement is high.

SECTION 8

POTENTIAL FOR HTP APPLICATIONS

Fluidized bed coal combustion and low-BTU coal gasification are among the advanced energy processes which require high temperature and high pressure (HTP) particulate cleanup. In addition, HTP cleanup might be required for other high temperature and/or high pressure processes as reported by Parker and Calvert (1977).

The suitability of granular bed filters (GBF) for controlling particulate emissions from advanced energy processes is not limited by the gas temperature and pressure. By properly selecting the adequate granules and structural materials, the granular bed filters should be capable of operating at any temperatures and pressures encountered in advanced energy processes.

CLEANUP REQUIREMENTS

In order to evaluate the potential of GBFs for HTP cleanup, it is necessary to consider the following:

1. The cleanup requirements.
2. The performance characteristics of GBFs.
3. The particulate size distribution and concentration in the inlet gas.
4. Capital and operating cost estimates for GBFs.
5. Permissible costs for HTP gas cleanup.

The points listed above are discussed in this section. A summary and conclusions section is given at the end of this section.

Parker and Calvert (1977) have reviewed and evaluated the cleanup requirements for various processes. The conditions for HTP particle collection are summarized in Table 25. As can be seen from Table 25 gas temperatures range up to 1,100°C (2,000 F) and pressures range up to 70 atm. Granules, such as quartz sand and ceramics, can handle these extreme conditions.

The Ducon GBF, Combustion Power Company moving bed filter, and the CCNY panel bed filter, all can be designed to be operated

TABLE 25. CONDITIONS FOR HIGH TEMPERATURE AND PRESSURE PARTICULATE COLLECTION

PROCESS	TEMPERATURE °C	PRESSURE atm	TYPICAL GAS COMPOSITION mol %	EXPECTED PARTICULATE COMPOSITION
Open cycle coal-fired gas turbine	650-1,000	4-10	83% N_2, 15% CO_2, 2% O_2, H_2O, SO_x, NO_x, CO, and gaseous hydrocarbons	coal ash, unburnt carbon
Fluidized bed coal combustion	800-900	~1-20	80% N_2, 10% CO_2, 6% O_2, 4% H_2O, + SO_2, NO, CO	60 wt % ash, 30% unburnt carbon, 10% sorbent
Coal gasification	150-1,100	~1-70		ash, unburnt carbon, sorbent, possibly tar
O_2 blown			30% H_2, 25% CO, 15% CO_2, 20% H_2O, 3% CH_4, H_2S, N_2	
Air blown			50% N_2, 12% H_2, 20% CO, 10% H_2O, 6% CO_2, + CH_4, H_2S	
FCC regenerator	300-800	~1-3	68% N_2, 5% CO, 3% O_2, 8% CO_2, 16% H_2O, + NO_x, SO_x, NH_3, HCN, aldehydes, hydrocarbons	catalyst dust depends on catalyst type, commonly silica and alumina
Metallurgical furnaces	250-1,000	~1	N_2, CO_2, O_2	very fine metal fume
MHD power generation	300-800	~1	---	K_2CO_3 seed particles

at HTP. The Rexnord GBF can be operated at high temperature but not at high pressure. Rexnord does not recommend that their GBF be used at HTP. They have designed a new type of filter for these conditions. The new design is similar to the CPC moving bed GBF.

The use of granular bed filters for HTP applications is limited by the particulate and gaseous pollutant removal efficiencies. Particulate cleanup requirements for HTP processes vary depending on the intended use of the gas. If it is to be vented, the gas must be cleaned sufficiently to meet the emission standards. Current new source performance standards are 43 mg/MJ (0.1 lb/10^6 BTU), however, a stricter standard of 13 mg/MJ (0.03 lb/10^6 BTU) has been proposed.

If the hot gas is to be expanded through a gas turbine, then the gas must meet the turbine requirement for cleanliness. A gas containing dust particles can severely erode and corrode turbine blades and other internal components. Also, deposition of dust particles on the turbine blades can impair the aerodynamic performance of the turbine.

A large number of research investigations have been reported which deal with turbine blade erosion and deposition problems. Much of this work was done in connection with military gas turbines for helicopter and tracked-ground vehicle engines. Similar research has also been conducted with industrial gas turbines. Generally, it is believed that large particles (over 2-5 μm diameter) cause severe erosion damage and must be removed. Particles smaller than 1-2 μm diameter cause much less erosion damage. However, there is a scarcity of data concerning the tolerance of turbines for fine particles.

From the available data on turbine tolerances for particulate matter, it appears that effectively all particles larger than about 2 μm must be removed from the gas. It has been suggested (Westinghouse, 1974) that a mass loading of 370 mg/Nm^3 (0.15 gr/SCF) for particles smaller than 2 μm would allow a satisfactory turbine life. The particulate removal requirements imposed by the gas turbine limitations may not be as stringent as the emission standard. If there were a sufficient loading of particulate smaller than 2 μm, it would be possible for the gas to be cleaned sufficiently to protect the turbine while still exceeding the emissions regulation of 0.1 lb/10^6 BTU (approximately 0.05 gr/SCF).

Recently Sverdrup and Archer (1977) proposed that to protect the turbine, the particulate concentration should be no more than 5 mg/Nm^3 (0.002 gr/SCF) and there should be no particles larger than 6 μm in diameter.

PREDICTED GBF PERFORMANCE

Figure 89 gives the predicted granular bed performance for several conditions. It shows the effects of temperature and pressure on particle penetration through a granular bed filter. The predictions were made for a bed packed with 400 μm diameter granules to a depth of 3.8 cm (1.5 in.). Other assumptions were: an approaching gas velocity of 45 cm/s, no surface cake formed, the collected dust was uniformly distributed in the bed, the average void fraction of the bed between cleaning cycles was 0.25, and the particle density was 1.5 g/cm^3.

As concluded in a report by Calvert and Parker (1977), high temperature and pressure particle collection is more difficult than at low temperatures. The predicted penetration for the granular bed filter at 875°C and 10 atm is much higher than that for ambient conditions.

If the particle size distribution of a source were known, it would be possible to predict whether a granular bed filter would be able to meet various cleanup requirements. The equation relating the fractional penetration (for a specific particle diameter) to the overall penetration is:

$$\overline{Pt} = \int_0^\infty Pt_d \, f(d_p) d(d_p) \qquad (97)$$

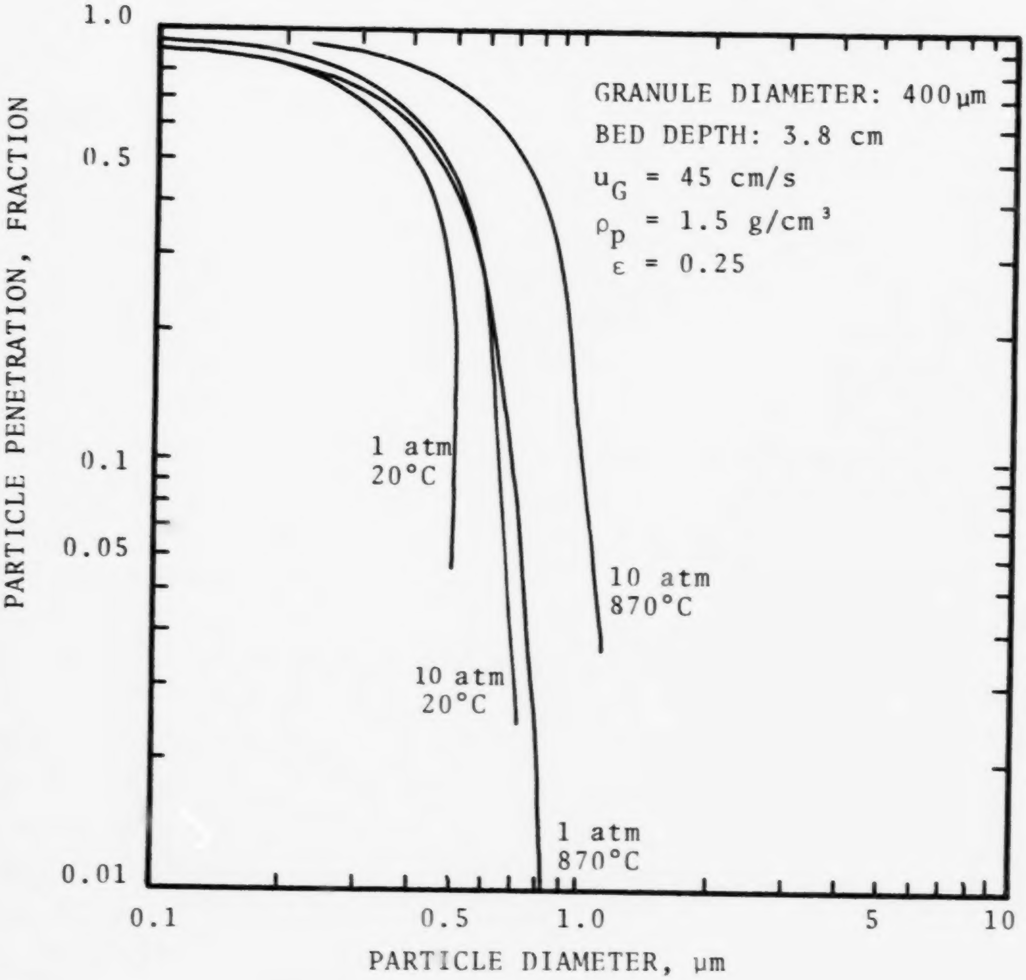

Figure 89. Predicted GBF performance.

where $\overline{Pt}$ = overall penetration, percent or fraction

Pt_d = penetration for particles with diameter, d_p, fraction

$f(d_p)$ = particle size frequency distribution

d_p = particle diameter, μm or cm

Particle Size and Concentration

Information on particle size distribution and mass loading of particles leaving HTP sources is scarce. The best available data are those reported by Exxon Research and Engineering Company (Hoke, 1976, 1977). Exxon has a pressurized fluidized bed coal combustor miniplant. The gas leaves the combustor at a temperature of about 870°C (1,600°F) and a pressure of about 10 atm. First it passes through a primary cyclone which removes larger particles (including unburnt carbon) and recycles these particles to the combustor. The gas leaves the primary cyclone and passes through a secondary cyclone. This removes more large particles and reduces the mass loading to the order of 2.5 g/Nm³ (1 gr/SCF). A Ducon GBF is connected to the outlet of the secondary cyclone to further clean the gas stream.

Hoke (1976) reported the particle size distribution at the secondary cyclone exit. It was obtained by sieve and Coulter counter analysis. The particles have a mass mean diameter of 8 μm and geometric standard deviation of 2.7 (Figure 90).

Overall collection efficiency was calculated graphically from equation (97) for this size distribution and for a granular bed packed to a depth of 3.8 cm with 400 μm diameter granules. The approach velocity of the gas was assumed to be 45 cm/s. The overall penetration was calculated to be 2.8% (collection efficiency 97.2%). Therefore, the predicted emissions will be 0.07 g/Nm³ (0.028 gr/SCF) and it is in compliance with the current standard for particulate emissions (0.1 lb/10^6 BTU or about 1.14 g/Nm³). However, it will not meet the proposed new standard (0.03 lb/10^6 BTU or about 0.04 g/Nm³).

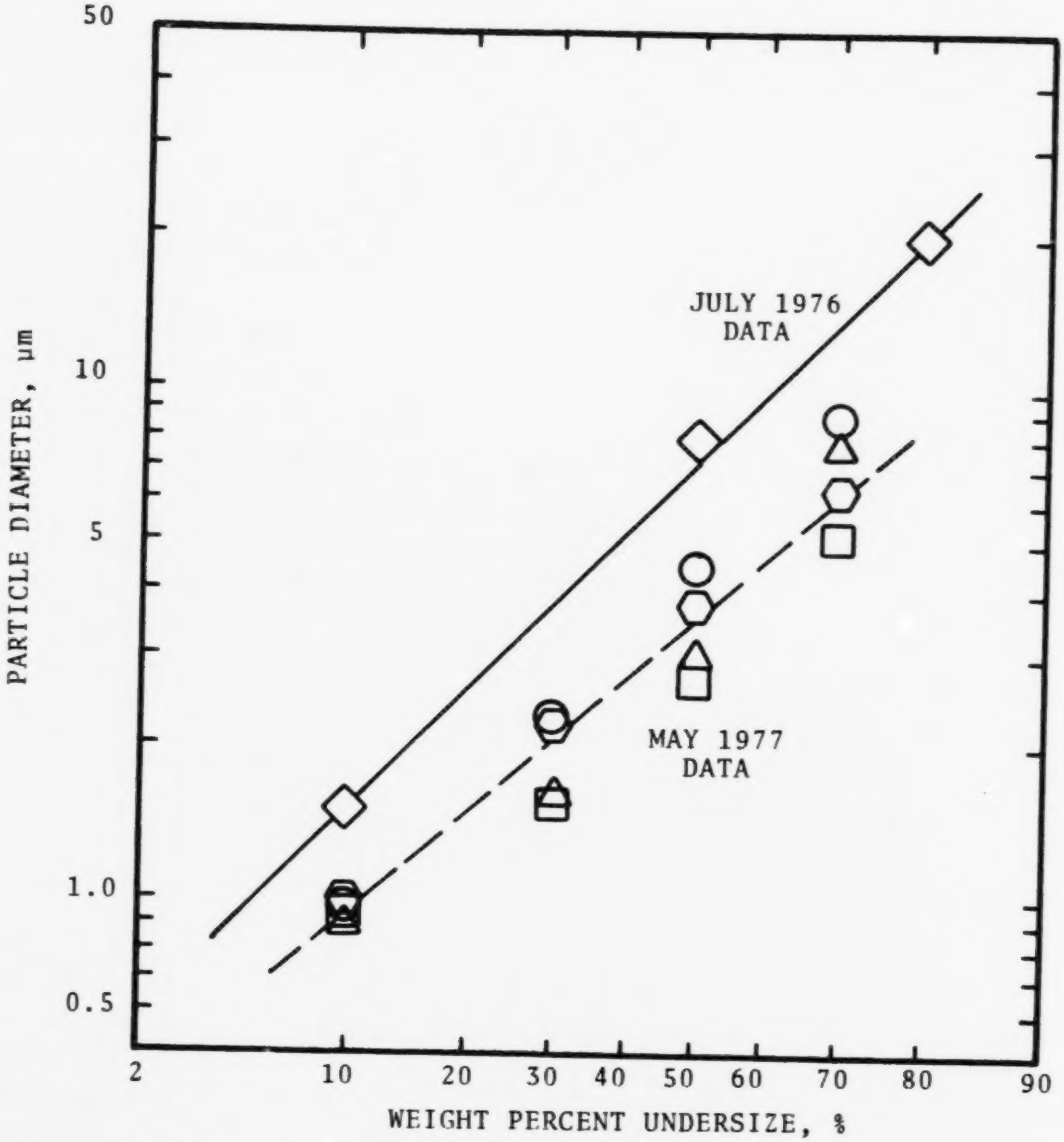

Figure 90. Particle size distributions from Exxon miniplant fluidized bed coal combustors. From monthly report #77, July 1976 and report #86, May 1977.

As revealed in Figure 89 , the predicted penetration decreases rapidly around 1 μm. The predicted penetration for 2 μm particles is effectively zero. Therefore, there should be no particles bigger than 2 μm in the GBF exhaust. The predicted loading of 0.07 g/Nm³ (0.028 gr/SCF) meets the turbine requirement suggested by Westinghouse (1974); but, it does not meet the requirement proposed by Sverdrup and Archer (1977).

Hoke (1977) reported some new data on particle size distribution at the secondary cyclone exit. The mass median diameter is 3.5 μm and the geometric standard deviation is 2.9.

The overall penetration for this size distribution will be 4.99 (95.1% overall collection efficiency). The emission will be 0.12 g/Nm³ (0.049 gr/SCF). This still satisfies the current emission standard (approximately 0.06 gr/SCF) and also meets the turbine requirement suggested by Westinghouse).

From the above discussion, it appears that improvements in GBF designs are required in order to improve collection efficiency and resolve operation problems. However, theoretical collection efficiencies appear to be sufficient to meet the current emissions regulations for particulates. Performance may be satifactory for protecting gas turbines, however, this will depend strongly on the amount of submicron particles a turbine can tolerate.

GASEOUS POLLUTANTS

In pressurized fluidized bed combustion, besides the emission of particulates, gaseous pollutants such as SO_2 and alkali metal compounds may also be present in the flue gas from the combustor. The presence of SO_2 might not have any ill effect on the operation of the gas turbine. The SO_2 may be removed from the gas stream at HTP with a GBF with dolomite or alumina as granular material or be removed by conventional means after the gas has been expanded through the turbine.

The presence of alkali metal compounds, such as sodium and potassium chlorides will contribute to hot corrosion of the gas turbine. Therefore, to protect the turbine, the concentrations of alkali metal compounds in the flue gas have to be reduced to a tolerable level. A direct method for accomplishing this is by controlling the combustion to minimize the evolution of alkali metal compounds. An alternative method is to use GBFs with some sort of sorbents as granular material to remove particulates and alakli metal compounds simultaneously.

Limited work has been done in this area. Swift et al. (1977) have shown that activated bauxite, which is a thermally treated high alumina content natural bauxite ore, was efficient at removing NaCl vapor at 900°C and atmospheric pressure.

As with the case of particulate matter, the acceptable level of alkali metal vapor in flue gas stream is not well established. Therefore, it is impossible at this time to speculate whether the GBFs are able to remove harmful vapors to acceptable levels.

PRELIMINARY COST ESTIMATE

Granular bed filter technology is still in the developmental stage and there are no proven designs to be used in HTP cleanup. Many of the cost factors have not been established. Therefore, it is extremely difficult to do a detailed cost analysis.

In the following section, the relative capital and operating costs between a HTP fixed bed GBF, a HTP intermittently moving bed, and a HTP moving bed system are presented. The cost estimates were performed for the GBF layouts presented in Figures 72, 81 and 91. It should be noted that these designs might not be the optimum.

Basis

In this report, the estimate was based on the cleanup requirement for one gas turbine. The seventeen-stage axial flow compressor is designed to develop a pressure ratio of approximately 10 to 1 while using 345 kg/s (761 lb/s) air at IOS (International Organization for Standardization) ambient conditions (298.33°K dry bulb temperature with 60% relative humidity). The four-stage expander is designed to operate with a turbine inlet temperature of 1,233°K (1,760°F), and under these conditions the net output has been calculated to be approximately 71 MW (Beecher, et al. 1976). If the turbine inlet temperature were 1,143°K instead of 1,233°K and the turbine efficiency remained the same, the turbine power output would be about 66 MW. The flow rate of 760 lb/s at ambient conditions is approximately 6,700 m^3/min at 870°C and 10 atm (237,000 ACFM at 1,600°F and 10 atm) and 7,220 m^3/min at 960°C and 10 atm (255,000 ACFM at 1,760°F and 10 atm).

The following were used as the basis for the cost estimate:

1. Inlet gas temperature: 870°C (1,600°F)
2. Inlet gas pressure: 10 atm
3. Outlet gas pressure: 1 atm
4. Net turbine power output: 66 MW
5. Gas volume flow rate: 6,700 Am^3/min at 870°C
6. Total power output for combined cycle plant: 355 MW

Capital Costs

Since the GBF's are non-standard fabricated units, the estimated fabricated cost was based on the costs of raw materials and labor requirements. Costs for design, administration, contingency, engineering, etc. were not included. Auxiliary equipment was priced based on vendor's quotations. Equipment cost was bare module cost, not installed cost. The cost for this study was developed in terms of fourth quarter 1978 U.S. dollars.

Fixed Bed GBF -

The fixed bed GBF is designed for a superficial gas velocity of 40 cm/s (80 ft/min). Total bed area required is 275 m^2 (2,960 ft^2). Eight GBFs are required. Each GBF has 48 filter elements and each filter element has 16 beds. Total bed area per GBF is 34.3m^2(370 ft^2).

The GBF shell is a pressure vessel. The dimensions are shown in Figure 91 . It is made of 3.8 cm (1.5 in.) thick carbon steel lined with 15 cm (6 in.) thick refractory. There is also an inner of 0.32 cm (1/8 in.) thick type-316 S.S.

The filter element consists of two perforated concentric tubes made from type-316 S.S. Beds of granules are stacked vertically

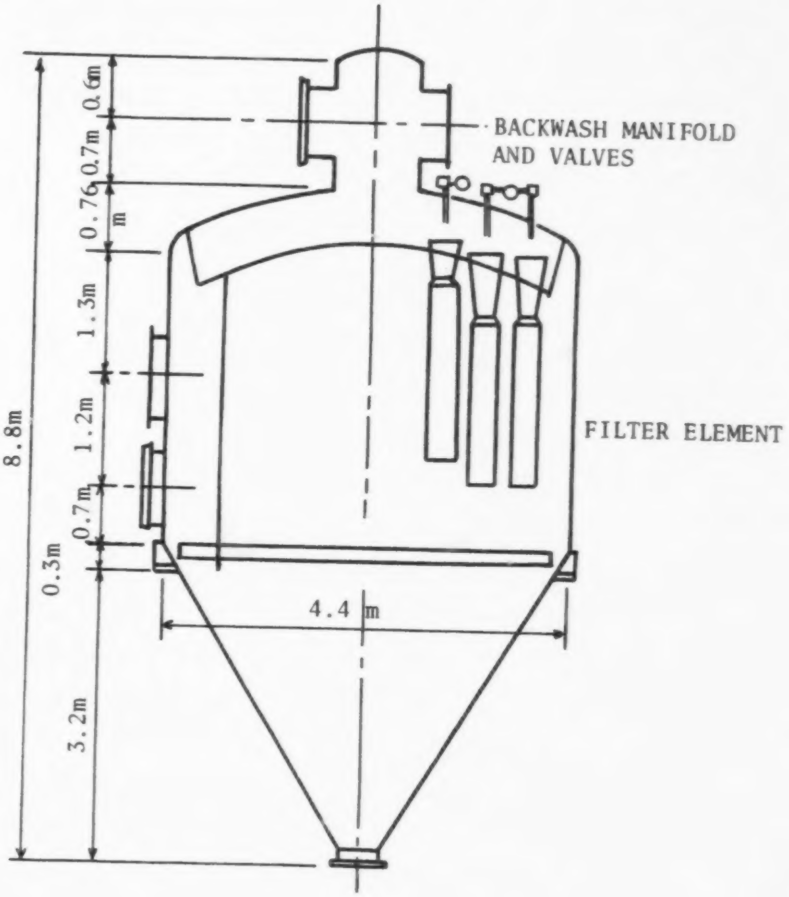
0.6m
0.7m
0.76 m
1.3m
1.2m
0.7m
0.3m
8.8m
3.2m
4.4 m
BACKWASH MANIFOLD AND VALVES
FILTER ELEMENT

Figure 91. Fixed bed GBF.

within the annulus. The O.D. of the outer tube is 30 cm (1 ft) and the I.D. of the inner tube if 19 cm (7.5 in.).

Material costs used in the estimates are: carbon steel \$1.00/kg (\$0.45/lb); 316 S.S. \$9.90/kg (\$4.48/lb); castable refractory \$0.74/kg (\$0.34/lb). Fabrication labor costs are: carbon steel, \$1.00/kg (\$0.45/lb); 316 S.S., \$3.96/kg (\$1.80/lb); castable refractory, \$0.74/kg (\$0.34/lb).

The fabricated costs of the GBF system are as follows:

Pressure Vessel	\$960,000
Filter Elements	693,000
Blowback Valves, Piping & Lock Hopper	925,000
Ductwork (refractory lined)	247,000
Compressor	179,000
Total	\$3,004,000

The estimated GBF bare module cost is \$448.36/Am^3 (\$12.68/ACFM).

The compressor indicated is for the supply of reverse gas flow during cleaning. It has a capacity of about 102 m^3/min (3,600 SCFM) and the developed pressure is 1,388 kPa (200 psig).

Continuously Moving Bed GBF -

The arrangement of the moving bed is shown in Figure 81. The bed is a single downflowing annulus 2.6 m (8.5 ft) O.D. and 2.3 m (7.5 ft) I.D. The height of the filtering surface is 4.9 m (16 ft). The bed is placed in a 3.7 m (12 ft) diameter pressure vessel.

Each GBF can handle a gas capacity of 1,130 Am^3/min (40,000 ACFM) at a superficial gas velocity of 50 cm/s (100 ft/s). Therefore, six GBFs are required to treat the gas for one gas turbine.

The pressure vessel consists of three layers. The outside shell is 3.8 cm thick carbon steel. The inner layer is 16 gauge (1/8") 316 S.S. In between there is a 15 cm (6 in.) thick layer of refractory. The material and labor costs to fabricate the pressure vessel are the same as presented in the last section.

The outer panel of the granular bed is a perforated wall and the inner retainer is a slotted panel. Since granules are continuously moving downward, the bed retaining walls should be made of erosion resisting materials; e.g., Hastelloy C, RA 330, and RA 333. The material cost used in this cost estimate is \$39.40/kg (\$17.90/lb). Fabrication labor cost is estimated to be \$7.92/kg (\$3.60/lb).

Under HTP conditions, it is impractical to separate dust and granules by shaking apparatus and to transport granules by mechanical means. Therefore, pneumatic transport and solid/dust separation techniques were designed into the GBF system. It is assumed that the weight of granules recirculated is equal to the weight of gas treated; i.e., granule recirculation rate is 345 kg/s (760 lb/s). Granules are withdrawn from the bed by means of an ejector and are transported to a granule holding tank above the GBF. The mass flow rate ratio of granules to transport air is assumed to be 20 g/g.

The granules flow from the granule holding tank by gravity into a baffled rattler section. In the rattler section, the dust is knocked off the granules and elutriated by an air stream which is also used as the fluidizing air to help the flow of granules. The mass flow rate ratio of granules to the fluidization air is assumed to be 80 g/g. All granule transport lines are carbon steel pipe lined with refractory and erosion resisting metal liners.

The fabricated cost of the GBF system is as follows:

Pressure Vessel	\$ 791,000
Filter Retaining Walls & Stiffeners	2,156,000
Hot Gas Piping	52,000
Granule Cleaning Ductwork	110,000
Ductwork	185,000
Compressor	784,000
Secondary Collector (incl. ductwork)	150,000
Total	\$4,228,000

The estimated fabricated cost is about \$631.04/Am^3 (\$17.84/ACFM), which is 141% higher than that for the fixed bed system.

The cost of continuously moving bed systems can be reduced if a better method for granule recirculation is found. In the estimate, low bulk density pneumatic transport is used for granule transport. Other transport methods such as dense-phase pneumatic transport may be more cost efficient.

Some testing is required to determine whether the dense-phase vertical pneumatic transport of 1-2 mm solids is feasible. If it is feasible, the capital cost (compressor cost) and operating cost will be lower than predicted in this estimate.

Intermittently Moving Bed GBF -

One possible arrangement for the intermittently moving bed GBF is shown in Figure 72. Each square filtration module is 0.56 m x 0.56 m x 4.6 m (22 in. x 22 in. x 15 ft). Active filtration area per module is 5.57 m (60 ft , each side is 1 ft x 15 ft).

Filtration velocity is about 15 cm/s (30 ft/min). Therefore, total filtration area required is 21,970 m^2 (236,500 ft^2) and the number of filtration module required is 132. The filter elements are made of Hastelloy "C". Since the panel is a louvered wall, material requirement is 8 times the unit length of the panel (Wu, 1977).

It is possible to place 17 modules in a pressure vessel 4.88 m (16 ft) in diameter. Thus, eight GBFs are required for each gas turbine.

As in the case of the continuously moving bed GBF, granule circulation and dust/granule separation are accomplished by pneumatic means.

The cost data used in the estimate were the same as used previously. The estimated costs are as follows:

Pressure Vessel	$1,050,000
Filter Elements	5,186,000
Ductwork	250,000
Blowback Cleaning System	132,000
Compressor	92,000
Lock Hopper & Granule Cleaning System	720,000
Total	$7,430,000

The estimated fabricated cost is about \$1,108.96/Am^3 (\$31.35/ACFM) which is 247% higher than that of the fixed bed system and about 176% higher than that of the continuously moving bed system.

The greatest cost item is that of the filter element. The cost can be reduced if the GBF is run at a higher filtration velocity. The filtration velocity used in this estimate is that recommended by Squires (Wu, 1977). Research work is required to determine whether it can be run at higher filtration velocities.

Operating Power Costs

The operating power costs for the GBF systems described above were estimated in this study and include those due to the following:

1. Pressure drop across the bed.
2. Power requirement to operate the compressor which is used either for cleaning or for pneumatic transport of solids.
3. Cost to heat the transport air and cleaning air to the bed temperature.
4. Heat loss to the surroundings.

Pressure drop and heat losses cause the gas temperature and pressure at the turbine inlet to be lower than it would be without cleanup. Lower gas temperatures and pressures reduce the turbine power output which in turn lowers the revenue.

The fixed bed operating power cost (not including depreciation) is the lowest among the three systems. The operating power costs of the continuously moving bed and the intermittently moving bed are about 7.4 times and 4 times higher than the fixed bed, respectively.

More than 60% of the moving bed operating cost is due to the compressor for pneumatic transport. The moving bed operating cost can be lowered if better solids transportation methods are found.

In the intermittently moving bed system, the high operating cost is also due to the compressor. However, the compressor is not for solids transport as in the continuously moving bed system. It is used for "puff-back" air. The "puff-back" air requirement per puff is 0.28 m³ (10 ft³) for each square filter unit. "Puff-back" frequency depends on dust loading. It is usually about one puff every half minute.

PERMISSIBLE COSTS

High temperature and pressure (HTP) particulate control is an important factor in determining the economic feasibility of many advanced energy processes. The energy process which relies most strongly on HTP gas cleanup is the pressurized fluidized bed (PFB) combustion process. The PFB process was described in detail as part of the Energy Conversion Alternatives Study (ECAS) - a cooperative effort of the Energy Research and Development Administration (now the Department of Energy), the National Science Foundation and the National Aeronautics and Space Administration.

For the PFB process to be economically competitive it is necessary to recover energy from the HTP effluent gas by expanding it through a gas turbine. To protect the turbine and not lose energy, it is essential that the gas be cleaned with a minimum loss of temperature and pressure.

The General Electric and Westinghouse Phase II ECAS reports (Brown et al. 1976 and Beecher et al. 1976) present detailed designs and cost estimates for PFB boiler power plants. The results are summarized in Table 26 (from Lewis Research Center, 1977). The overall cost of electricity for the General Electric design is presented in Figure 92 as a comparison with other advanced processes considered in ECAS Phase II. The reference steam cycle is a conventional coal-fired boiler power plant with wet lime stack gas scrubbers (Brown, 1976).

The advanced steam PFB designs assumed Ducon granular bed filters would be suitable for HTP particle collection. The ECAS reports were not explicit as to what percentage of the cost of electricity is attributable to the granular bed filters, although about 20% of the capital investment was for the cleanup system. Figure 92 shows that a cost difference of 5 to 6 mills/kWh exists between the PFB with cleanup and the reference steam cycle. We

TABLE 26. SUMMARY OF ECAS PHASE II PERFORMANCE AND COST RESULTS.

System and contractor	Net power, MW	Efficiency, percent			Capital cost, $/kWe		Cost of electricity, mills/kW-hr	
		Thermodynamic	Powerplant	Overall	ECAS ground rules	Constant mid-1975 dollars	ECAS ground rules	Constant mid-1975 dollars
1 - AFB/steam (General Electric)	814	43.9	35.8	35.8	632	447	31.7	25.8
2 - PFB/steam (General Electric)	904	41.3	39.2	39.2	723	411	34.1	27.4
3 - PFB/steam (Westinghouse)	679	42.3	39.0	39.0	549	401	28.1	23.5
4 - PFB/potassium/steam (General Electric)	996	47.8	44.4	44.4	934	660	39.9	31.2
5 - AFB/closed-cycle gas turbine/organic (General Electric)	476	50.1	39.9	39.9	1232	899	49.3	38.8
6 - Low-Btu gasifier/gas turbine/steam (General Electric)	585	44.2	39.6	39.6	771	562	35.1	28.6
7 - Low-Btu gasifier/gas turbine/steam (Westinghouse)	786	48.5	46.8	46.8	614	448	29.1	23.9
8 - Semiclean-fuel-fired gas turbine/steam (Westinghouse)	874	53.6	52.2	38.6	329	256	26.0	23.7
9 - Semiclean-fuel-fired gas turbine/steam (General Electric)	847	52.7	51.1	37.8	418	305	29.5	25.9
10 - Coal/MHD/steam (General Electric)	1932	54.0	49.8	48.3	720	478	31.8	24.1
11 - Low-Btu gasifier/molten-carbonate fuel cell/steam (United Technologies Corp.)	635	53.6	49.6	49.6	593	433	28.9	23.9

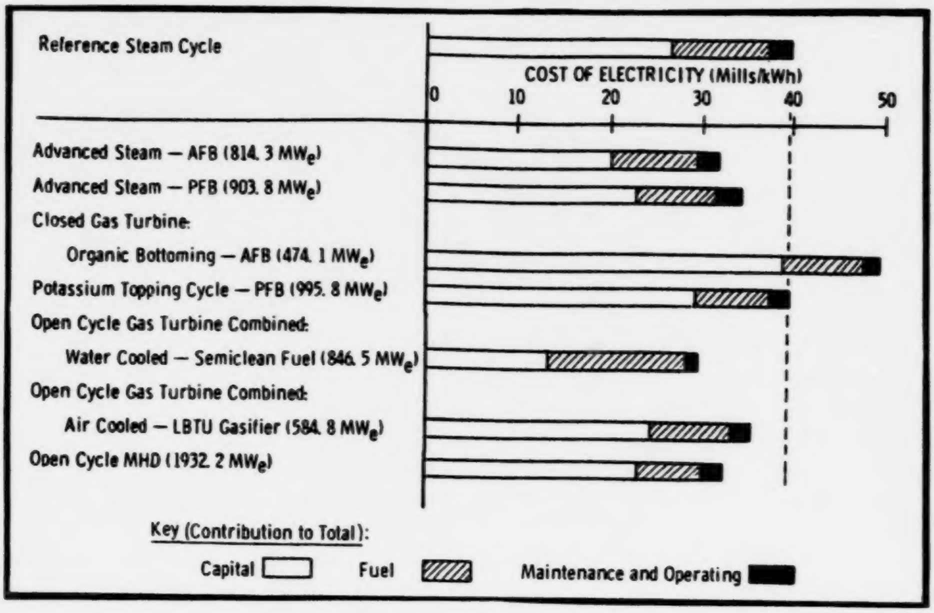

Figure 92. Summary G.E. Comparison of Cycles (Cost of Electricity at an assumed capacity factor of 65%).

estimate that the capital cost for cleanup would be about 8.5 mills/kWh so that cost difference between the PFB without cleanup and the reference steam plant with cleanup is about 14 mills/kWh. Therefore, one can conservatively state that a cost on the order of a few mills/kWh would make the PFB process economically competitive for further development. There is also the advantage of fuel conservation which is due to the higher overall efficiency of the PFB process as compared to a conventional power plant.

SUMMARY AND CONCLUSIONS

Particulate matter removal from gas at HTP is desirable for any process which involves the use of a turbine on the HTP gas stream. The degree of particulate cleanup required to protect the turbine is uncertain. Published estimates of turbine requirements range from a maximum 370 mg/Nm³ (0.15 gr/SCF) for particles smaller than 2 μm diameter (Westinghouse, 1974) to a maximum loading of 5 mg/Nm³ (0.002 gr/SCF) and no particles larger than 5 μm in diameter (Sverdrup and Archer, 1977).

Particle data obtained on the Exxon PFBC Miniplant range from 2.5 g/Nm³ of fly ash with d_{pg} = 9 μm and σ_g = 2.7 to the same loading with d_{pg} = 3.5 μm and σ_g = 2.9. The A.P.T. performance model when applied to the larger particle size distribution and the Ducon GBF in use on the Miniplant predicts outlet loadings around 70 mg/Nm³ and no particles larger than 2 μm diameter, which meets the Westinghouse turbine requirements and present New Source Performance Standard (NSPS) (about 140 mg/Nm³) but does not meet the Sverdrup and Archer turbine requirements or the proposed NSPS (abour 40 mg/Nm³).

For the smaller particle size distribution the A.P.T. model predicts that the Ducon GBF would give an outlet loading of about 120 mg/Nm³, which is close to the present NSPS.

A criterion for the permissible cost of HTP particulate removal can be estimated from the performance and cost estimate data available from the ECAS studies (Figure 92). The PFBC plant is a good example because its feasibility may depend on a satisfactory HTP cleanup system. The power generating difference between a PFBC and a conventional steam power plant is about 14 mills/kWh. A gas cleanup cost on the order of a few mills/kWh should be acceptable and even higher costs may be justifiable.

Cost estimates were made for three GBF systems for HTP cleanup of the combustion gas in a 355 MW combined cycle power plant. The gas turbine provides 66 MW of the plant capacity. Of the three GBF systems, the fixed bed system has the lowest estimated capital and operating costs. The capital costs of the continuously moving bed system and the intermittently moving bed system are predicted, respectively, 141% and 247% higher than the fixed bed system. With regard to the operating power cost, the continuously moving bed system and the intermittently moving bed system are about 7.4 times and 4 times higher than that of the fixed bed system.

By assuming a cost factor of 4 in the estimation of costs of engineering, installation, site preparation, contractor's fee, contingency, construction, and working capital cost, the capital investment of a continuously moving bed system would be $16,912,000; or $47.64/kWh of plant capacity. The operating power cost of the continuously moving bed system is about 0.48 mills/kWh of plant capacity. For a 10 year life, depreciation charge is about 0.55 mills/kWh of plant capacity. Thus, the estimated total operating cost would be about 1 mill/kWh for the continuously moving bed system. This cost figure is economically competitive when compared to the ECAS Phase II results.

However, it should be noted that no granular bed filter systems have been demonstrated to have high enough collection efficiency and reliable performance to satisfy HTP gas cleanup requirements. More development and redesign are necessary. Consequently, any estimates of cost and process economics should be considered highly speculative at this time. Adequate comparisons between GBF system economics must be based on proven pilot plant designs.

SECTION 9

RECOMMENDATIONS FOR FUTURE RESEARCH AND DEVELOPMENT

The primary objective of evaluating the feasibility of granular bed filters (GBF) for the collection of particulates at high temperature and pressure (HTP) has been achieved in this study. It has been shown that GBFs are capable of operating at HTP. Whether the GBF meets the cleanup requirements depends on the application. Present GBFs have the potential to meet the current emission standards. However, unless aided by other collection mechanisms, the present designs are not likely to meet the proposed NSPS for boilers or the turbine requirements proposed by Sverdrup and Archer (1977). More research and development work is required to improve the performance of GBFs. Future research and development work is needed in the following areas:

1. Efficiency improvements.
2. Bed cleaning methods
3. Other potential problems, such as sintering of the granules, granule transport method, etc.

EFFICIENCY IMPROVEMENT

The present investigation has shown that existing GBFs may not have a high enough collection efficiency for fine particles, especially when operating at high temperature. There are a few studies reported in the literature which show that the collection efficiency of the bed may be increased by:

1. Electrostatic augmentation
2. Cake filtration

Electrostatic Augmentation

The filtration efficiency can be enhanced by electrostatic augmentation. If the filtration medium is immersed in an electrostatic field, the dust particles will be driven in a direction that tends to increase the probability of impact between particles and the filter medium. Limited work has been done with electrostatically augmented granular beds. A.P.T. has carried out experimental work to study the effect of charging the bed and/or particles on the collection efficiency. This work will be presented in a separate report.

These small-scale experiments have demonstrated that the GBF collection efficiency can be improved greatly by charging the bed or by charging both the bed and particles. It is possible for the GBF to achieve a 99+% collection efficiency when an electrostatic field is imposed on the bed.

For industrial applications, the capital cost of electrostatically augmented GBFs will be higher than without augmentation. However, the increase in capital outlay is compensated by the reduction in operating cost. The electrostatically augmented GBF can be operated at much lower pressure drop by using a shallow bed and the energy cost to maintain the electrostatic field is small (5×10^{-6} mills/kWhe).

The next steps in evaluating the electrostatically augmented GBF should move toward a pilot-scale test on an actual source, such as, a fluidized bed coal combustor. More laboratory-scale studies are required to refine the technology and establish design criteria for the pilot plant. Areas which need further research include:

1. bed charging method.
2. electrode configurations.
3. bed structure.
4. HTP electrode insulation.
5. effects of polarity on efficiency.
6. cleaning methods

Most of these effects can be evaluated in the laboratory and the most promising combination can be tested on a pilot-scale plant.

Cake Filtration

There is good reason to believe that the GBF with a good surface cake would have a much higher filtration efficiency than the original clean bed. This would result from increased particle collection by sieving.

There is no published information on the efficiency of cake filtration. A small-scale laboratory research program could generate the needed information on cake filtration. One approach could be to build a cake on the surface of the GBF and then measure the collection efficiency using monodisperse particles. The effects of cake thickness, pressure drop, particle size distribution of the cake, and superficial gas velocity would be studied.

Further research is needed to determine the GBF operating conditions which result in cake formation. Whether or not there will be a surface cake depends largely on whether a rooting cake will be formed. During a filtration cycle, particles will deposit in the interstices of the bed and will coat the granules. If the granules of the bed are large, the coatings or dendrites will not bridge to create the rooting cake. On the other hand, if the granules are sufficiently small, dendrites will bridge to form an internal cake.

The formation of surface cake has been observed at CCNY (Wu, 1977) for ambient temperatures. However, at high temperatures, there was no indication that a surface cake was formed. Exxon Research and Engineering Company (Bertrand, et al., 1977) reported the same experience. No surface cake was observed in the Ducon GBF in their HTP fluidized bed coal combustor miniplant.

Westinghouse Research Laboratories reported some collection efficiency data for their laboratory scale GBF under ambient conditions (Ciliberti, 1977). The GBF utilized fluidized air to clean the bed. The reported overall collection efficiencies were high and the grade efficiency curves calculated from cascade impactor data were flat (i.e., almost independent of particle diameter). These phenomena indicated that a surface cake was present.

Surface cake formation at high temperature has been observed for filtration on a ceramic cloth medium (Shackleton and Kennedy, 1977). Therefore, the formation of surface cake appears to be dependent upon the substrate, although it is influenced somewhat by temperature. Research work is required to study the cake formation process at high temperatures. We recommend a pilot-scale study using actual combustion flyash. Variables to be studied should include bed granule diameter, bed structure, gas temperature and pressure, and bed operating conditions.

A small-scale laboratory study on cake filtration and the pilot plant study on the cake formation process could be studied concurrently.

BED CLEANING METHODS

To prevent the bed from becoming saturated with collected dust, it is necessary to clean the bed either periodically or continuously. The present bed cleaning methods were evaluated in this report. Major research and development work is needed to improve the efficiency of the present cleaning methods and to decrease the operating costs.

Present bed cleaning methods share a common problem - destruction of rooting cake. In the continuously moving bed system, the relative motion of bed granules prevents the formation of the internal cake. In the reverse gas flow cleaning method, the bed is either fluidized or stirred. Thus internal cakes are destroyed or deteriorated. The rooting cake needs to be rebuilt before a surface cake can be formed.

Since the rooting cake is the foundation of surface cake and the formation of a surface cake enhances the collection efficiency of the GBF, it is desirable to preserve the rooting cake during the cleaning cycle. Research work is required to develop cleaning methods that remove the surface cake and preserve the rooting cake.

OTHER RESEARCH RECOMMENDATIONS

There are many operational problems and uncertainties which need to be resolved before HTP granular bed filters can be considered sufficiently reliable and economical for commercial application. These problems include:

1. How to prevent particle seepage through the bed (during cleaning or filtration).
2. How to reduce temperature losses (especially during cleaning).
3. How to improve the efficiency and reduce the cost of granule regeneration and recirculation.
4. How to reduce pressure drop across bed.
5. How to prevent attrition of granules causing particle reentrainment.

Resolving these problems will not only help solve the HTP particle collection problem, but will improve granular bed filter technology for many other applications, especially where hot, corrosive gases are encountered.

RECOMMENDED RESEARCH PROGRAM

Of the above mentioned research and development recommendations, electrostatic augmentation is presently the most proven approach to improve the performance of the GBFs. It has been shown that the electrostatically augmented GBF has the potential to meet the most stringent cleanup requirements under ambient conditions. It is expected that the same statement will hold for HTP conditions where higher electric field can be imposed on the beds. Therefore, electrostatic augmentation is recommended as the approach having the best probability of success, based on present knowledge.

Another potential advantage of the electrostatic GBF is that it achieves high collection efficiency without the benefit of cake filtration. In actual applications, there might be filter cakes and further research may show the way to promoting surface cake. The presence of surface and rooting cakes will increase the collection efficiency of the GBF even more.

The capital cost of an electrostatic GBF will be slightly higher than that of regular GBFs. The additional cost is due to the requirement of a high voltage power supply and HTP insulation for the electrodes. However, the operating cost could be lower due to a lower drop in pressure. The estimated operating cost for the Ducon GBF is about 31.8 mills/m^3/min (0.9 mills/SCFM). For an electrostatically augmented Ducon, GBF, the operating cost would be 27.9 mills/m^3/min (0.79 mills/SCFM) to maintain the same efficiency.

A detailed program to demonstrate the feasibility of using electrostatic augmentation to improve GBFs for particulate control at high temperature is described below. We recommend a study of the electrostatically augmented GBF on a pilot plant scale of about 14.2 Am^3/min (500 ACFM). To duplicate actual industrial applications, fresh test dust should be produced instead of regenerated dust. Since GBFs will be used in advanced energy processes, it is desirable to test the electrostatically augmented GBF on these processes. A good approach would be to use an atmospheric fluidized bed combustor.

The GBF should be designed in such a way that it is easy to change from one configuration to another. Bed cleaning can be achieved either by fluidization or by continuously withdrawing granules and dust from the bed.

To aid in the design of the pilot plant, some small-scale experimental work should be conducted concurrently.

In outline, the objectives consist of the following tasks:

1. Conduct small-scale experiments to obtain design information.
2. Design the pilot plant.
3. Fabricate, install and start up the pilot plant.
4. Prepare a detailed test plan describing:
    a. The proposed test matrix.
    b. The measurement techniques to be used.
    c. The data handling methods.
5. Conduct test programs.
6. Analyze data, conduct engineering and cost analyses of various configurations.
7. Based on the above analyses, design and estimate the cost of a GBF system for HTP applications.
8. Recommend a test program to demonstrate a full-scale GBF system on an HTP source.

REFERENCES

Anderson, D.M. and L. Silverman, "Mechanisms in Electrostatic Filtration of Aerosols with Fixed and Fluidized Granules," report by the Air Cleaning Laboratory, Harvard University to the U.S. Atomic Energy Commission, No. NYU-4615, 1958. See also, "Development of a Triboelectrified Fluidized Bed for Aerosol Filtration," 5th Atomic Energy Commission Air Cleaning Conference, p. 140, USAEC, TID-7551, 1957.

Avco, Inc. "Evaluation of Granular Bed Devices," Avco Applied Technology Division, AVATD-0107-69-RR, June 1969.

Balasubramanian, M. and A. Meisen, "A Note on the Diffusional Deposition of Aerosol Particles in Packed Bed," J. of Aerosol Science, 6: 461-463 (1975).

Beecher, et al., "Energy Conversion Alternatives Study (ECAS) Westinghouse Phase II Final Report, Volume III - Summary and Advanced Steam Plant with Pressurized Fluidized Bed Boilers," NSF/RA-760590, NTIS PB 268-558, October 1976.

Berry, F.J. and J. Fournier, German Patent #676508 (1939).

Bertrand, et al., "A Regnerative Limestone Process for Fluidized Bed Coal Combustion and Desulfurization," Monthly Report no. 87, 1977.

Billings, C.E. and J. Wilder, "Handbook of Fabric Filter Technology, Volume I," NTIS PB 200-648 (1970).

Böhm, L. and S. Jordan, "On the Filtration of Sodium Oxide Aerosols by Multilayer Sand Bed Filters," J. of Aerosol Science, I: 311-318 (1976).

Borguardi, R.H., R.E. Harrington, and P.W. Sparte, "Filtration Characteristics of Fly Ash," J. of APCA, 18: 387 (1968).

Brown, et al., "Energy Conversion Alternatives Study (ECAS) General Electric Phase II Final Report, Volume II - Advanced Energy Conversion Systems, Conceptual Designs," NASA-CR 134949, NTIS PB 268-247, December 1976.

Brown, D.H., "Conceptual Design and Assessment of a Utility Steam Plant with Conventional Furnace and Wet Lime Stack Gas Scrubbers," NASA CR-134950, December 1976.

Calvert, S. and R. Parker, "Effects of Temperature and Pressure on Particle Collection Mechanisms: Theoretical Review," EPA 600/7-77-002, January 1977.

Calvert, S., Chapter 46 in "Air Pollution," A.C. Stern, editor, 3rd edition, Academic Press, New York, 1968.

Carney, S.D., U.S. Patent #2343401 (1944).

Ciliberti, D.F., Westinghouse Research Laboratories, personal communication.

Corman, J.C., and G.R. Fox, "ECAS-General Electric Phase II Final Report, Volume I: Executive Summary," NASA-CR 134949, NTIS #PB 268-455, December 1976.

Dennis, R., et al., "Special Incineration Studies - Institutional Design," 6th AEC Air Cleaning Conference, July 7-9, 1959, TID-7593, pg. 344-364 (1960).

Ergun, S., "Fluid Flow Through Packed Columns," Chemical Engineering Progress, 48: 89-94 (1952).

Fiechter, L.B., British Patent #135216 (1919).

Fiechter, L.B., British Patent #163039 (1922).

Figueroa, A.R., "Aerosol Filtration by Fixed and Fluidized Granular Beds," Ph.D. Dissertation, University of Cincinnati, (1975).

Figueroa, A.R., and W. Licht, "Filtration of Submicron Particles by Fixed and Fluidized Granular Beds," Paper #33b presented at the 81st AIChE National Meeting, Kansis City, Missouri, April 11-14, 1976.

Fournier, J., British Patent #450048 (1936).

Friedlander, S.K., "Mass and Heat Transfer to Single Spheres and Cylinders at Low Reynolds Numbers," AIChE Journal, 3: 43-48 (1957).

Fuchs, N. and A. Kirsch, "The Effect of Condensation of a Vapor on the Grains and of Evaporation from Their Surface on the Deposition of Aerosol in Granular Bed," Chem, Eng. Science, 20: 181-185 (1965).

Gebhart, J., C. Roth, and W. Stahlhofen, "Filtration Properties of Glass Bead Media for Aerosol Particles in the 0.1-2 μm Size Range," J. of Aerosol Science, 4: 355-371 (1973).

Goldman, L., "Experiences in the Use of Pebble-Bed Filters in Inorganic Chemical Plants," Staub, 24: 449 (1964).

Goren, S., in "Granular Bed Filter Development Program: Monthly Report for August 1977" by K.E. Phillips, prepared for the U.S. Energy Research and Development Administration under contract #EF-77-C-01-2579, October 1977.

Guillory, J.L, "Filtration Performance of a Moving Bed Granular Filter: Experimental Cold Flow Data," paper presented at the 5th International Conference on Fluidized Bed Combustion, Washington, D.C., December 12-14, 1977.

Guillory, J.L, "Granular Bed Filter Development Program," prepared for the U.S. Dept. of Energy, FE-2579-15, 1978.

Hoke, R.C., et al., "A Regenerative Limestone Process for Fluidized Bed Coal Combustion and Desulfurization," Monthly Report no. 77, July 1976.

Hood, K.T., "Evaluation of the Combustion Power Company Moving Gravel Bed Dry Scrubber on the Control of Particulate Emissions from a Hog Fired Boiler," NCASI special report, September 1976.

Jackson, S. and S. Calvert, "Entrained Particle Collection in Packed Beds," AIChE Journal, 12: 1075-1078 (1966).

Kalen, B. and F.A. Zenz, "Filtering Effluent from a Cat Cracker," Chem. Eng. Progress, 66: 67-71 (1973).

Klarding, N., British Patent #153263 (1921).

Knapsack-Griesham Aktiengesellschaft, Koln, Germany, British Patent #851776 (1960).

Knettig, P. and J.M. Beeckmans, "Capture of Monodispersed Aerosol Particles in a Fixed and in a Fluidized Bed," Canadian J. of Chemical Engineering, 52: 703-706 (1974).

Kovach, I.L., and D.G. Hanan, "Combined Dust, Aerosol and Vapor Removal Efficiency of Packed Activated Carbon Beds," Staub, 30: (12), 35-39 (1970).

Lapple, C.E., "Stack Contamination - 200 Areas, Interim Report," HDC-611, August 5-October 12, 1948.

Lee, K.C., "Filtration of Redispersed Power-Station Fly Ash by a Panel Bed Filter with Puffback," Ph.D. Dissertation, The City University of New York, (1975).

Lee, K.C., et al., "Panel Bed Filter," EPRI-AF-560, 1977.

Levenspiel, O., "Chemical Reaction Engineering," Wiley & Sons, New York, 1972.

Leith, D., S.N. Rudnick, and M.W. First, "High Velocity, High Efficiency Aerosol Filtration," NTIS PB 249-457, 1976.

Leith, D. and M. First, "Performance of a Pulse-Jet Filter at High Filtration Velocity, I - Particle Collection," J. of APCA 27: 534-539 (1977).

Levi, J.P. and J. Blume, French Patent #763077 (1934).

Lewis Research Center, "Evaluation of Phase II Conceptual Designs and Implementation Assessment Resulting from the Energy Conversion Alternatives Study (ECAS)," NASA TMX-73515, NTIS PB 270-017, April 1977.

Lynch, G.E., U.S. Patent #1766221 (1930).

Lynch, G.E., Fuel Economist, 12: 47 (October 1936).

Marple, V., "The Fundamental Study of Inertial Impactors," Ph.D. Thesis, University of Minnesota, 1970.

McCain, J.D., "Evaluation of Rexnord Gravel Bed Filter," EPA 600/2-76-164, NTIS PB 225-095, June 1976.

McFee, D.R., and J. Sedlet, "Plutonium-Uranium-Molybdenum Fume Characteristics and Sand Filtration," J. of Nuclear Energy, 22: 641-650 (1968).

Mercer, T.T. and R.G. Stafford, "Impaction from Round Jets," Ann. Occupational Hygiene, 12: 41-48 (1969).

Mercier, E. and M. Ehlinger, U.S. Patent #2493356 (1950).

Miyamoto, S. and H. Bohn, "Filtration of Airborne Particulates by Gravel Filters: I. Initial Collection Efficiency of a Gravel Layer, " J. of APCA, 20: 1051-1054 (1974).

Miyamoto, S. and H. Bohn, "Filtration of Airborne Particulates by Gravel Filters: II. Collection Efficiency and Pressure Drop in Filtering Fume," J. of APCA, 25: 40-43 (1975).

Nordstrom, O., Swedish Patent #56098 (1922).

Nordstrom, O., British Patent #217113 (1924).

Orr, C., Jr., "Particulate Technology, " p. 420, MacMillan Company, New York (1966).

Parker, R. and S. Calvert, "High Temperature and High Pressure Particulate Control Requirements," EPA 600/7-77-071, July 1977.

Payatakes, A.C., "Model of Aerosol Particle Deposition in Fibrous Media with Dendrite-Like Pattern: Application to Pure Interception During Period of Unhindered Growth," Filtration and Separation, 13: 602 (1976a).

Payatakes, A.C., "Model of the Dynamic Behavior of a Fibrous Filter; Application to Case of Pure Interception During Period of Unhindered Growth," Powder Technology, 14: 267 (1976b).

Payatakes, A.C., "Model of Transient Aerosol Particle Deposition in Fibrous Media with Dendrite Pattern," AIChE Journal, 23: 192-202 (1977).

Payatakes, A.C. and C. Tien, "Particle Deposition in Fibrous Media with Dendrite-Like Pattern: A Preliminary Model, " J. of Aerosol Science, 7: 85-100 (1976).

Paretsky, L., L. Theodore, R. Pfeffer, and A.M. Squires, "Panel Bed Filters for Simultaneous Removal of Fly Ash and Sulfur Dioxide: II. Filtration of Diluted Aerosol by Sand Beds," J. of APCA, 21: 204-209 (1971).

Paretsky, L.C., "Filtration of Aerosols by Granular Beds," Ph.D. Thesis, City University of New York (1972).

Perry, J.H. (editor),"Chemical Engineer's Handbook,"McGraw-Hill, New York, 1973.

Phillips, K.E. "Granular Bed Filter Development Program: Monthly Report for August 1977," prepared for the U.S. Energy Research and Development Administration under contract no. EF-77-C-01-2579, October 1977.

Ranz, W.E. and J.B. Wong, "Impaction of Dust and Smoke Particles," Ind. Eng. Chem. 44: 1371-1381 (1952).

Research Cottrell, U.S. Patent No. 2,990,912, July 4, 1961.

Schmidt, E.W., J. Gieseke, P. Gelfand, T.W. Lugar, and D.A. Furlong, "Filtration Theory for Granular Bed," J. of APCA, 28: 143-146, 1978.

Shackleton, M. and J. Kennedy, "Ceramic Fabric Filtration at High Temperatures and Pressure," paper presented at the EPA/ERDA Symposium on High Temperature/Pressure Particulate Control, Washington, D.C., September 20-21, 1977.

Sharapov, K.A., V.V. Leonov, I.L. Saklarnova, A.F. Skvartsov, and N.G. Braginets, "Study of a Multigradient Electromagnetic Filter for the Dry Cleaning of Gases," Stal' 963-964 (1975), Ref. Zh. Khim. GI775 (1976).

Solvay, E., British Patent #18573 (1889).

Squires, A.M. and R.A. Graff, "Panel Bed Filters for Simultaneous Removal of Fly Ash and Sulfur Dioxide: III. Reaction of Sulfur Dioxide with Half-Calcined Dolomite," J. of APCA, 21: 272-276 (1971).

Squires, A.M. and R. Pfeffer, "Panel Bed Filters for Simultaneous Removal of Fly Ash and SO_2: I. Introduction," J. of APCA, 20: 523 (1970).

Stephan, D.G., G.W. Walsh, and R.A. Herrick, "Concepts in Fabric Air Filtration," AIHA Journal, 21: L (1960).

Stern, A.C., H.W. Zeller, and A.I. Schekman, "Collection Efficiency of Jet Impactors at Reduced Pressures," Ind. and Eng. Fundamentals, 1: 273 (1962).

Strauss, W., and M.W. Thring, "Studies in High Temperature Gas Collecting," J. of the Iron and Steel Institute, 196: 62 (1960).

Sverdrup, E.F. and D.H. Archer, "The Tolerance of Large Gas Turbines to Rocks, Dusts, and Chemical Corrodants," presented at EPA/ERDA Symposium on High Temperature and Pressure Particulate Control, Washington, D.C. September 1977.

Swift, M.W.. et al. "Plans and Studies on Flue Gas Cleaning and Particulate Monitoring in PFBC," Proceedings of the EPA/DOE Symposium on High Temperature/ High Pressure Particulate Control, EPA 600/9-78-004, September 1977.

Taub, R., "Filtration Phenomena in a Packed Bed Filter," Ph.D. Dissertation, Carnegie-Mellon University, 1970.

Thomas, J.W. and R.E. Yoder, "Aerosol Size for Maximum Penetration Through Fiberglass and Sand Filters," Archives Ind. Health, 13: 545 (1956a).

Thomas, J.W. and R.E. Yoder, "Aerosol Penetration Through a Leak Shot Column, A Method of Particle Size Evaluation," AMA Archives Ind. Health, 13: 550 (1956b).

Thomson, T. and N. Nisbet, British Patent #216675 (1924).

Thring, M.W. and W. Strauss, "The Effect of High Temperatures on Particle Collection Mechanisms," Trans. Instru. Chem. Eng. 41: 248-253 (1963).

Tien, C., C.S. Wang and T.D. Barot, "Chain-Like Formation of Particle Deposition in Fluid Particle Separation," Science, 196: 983-985, 1977.

Veron, M., U.S. Patent No. 2,564,316 (1951).

Wade, G.L., "Performance and Modeling of Moving Granular Bed Filter," paper presented at EPA/ERDA Symposium on High Temperature/Pressure Particulate Control, Washington, D.C., September, 1977.

Wade, G., H. Wigton, J. Guillory, G. Goldbach, and K. Phillips, "Granular Bed Filter Development," Final report prepared for U.S. Dept. of Energy, No. FE-2579-19, 1978.

Wang, C.S., M. Beizail, and C. Tien, "New Concepts of Particle Deposition from Suspensions Flowing Past a Collector," paper #18b, presented at the AIChE 83rd national meeting Houston, Texas, March 1977.

Westinghouse Electric Corp., "Clean Power Generation from Coal," O.C.R., 84, NTIS: PB 234-188, April 1974.

Wigton, H. and G. Wade, "Granular Bed Filter Development Program," report prepared for the U.S. Dept. of Energy, No. FE-2579-18 (1978).

Wilson, E.J. and C.J. Geankoplis, Ind. Engineering Chemistry, 5: 9 (1966).

Wu, M.S., Air Pollution Technology, Inc., Personal Communication, 1977.

Zahradnik, R.L, J. Anyigbo, R.A. Steinberg, and H.L Toor, "Simultaneous Removal of Fly Ash and SO_2 from Gas Streams by a Shaft Filter Sorber," Env. Science and Tech., 4: 663-667 (1970).

U.S. ENVIRONMENTAL PROTECTION AGENCY
Office of Research and Development
Environmental Research Information Center
Cincinnati, Ohio 45268

OFFICIAL BUSINESS
PENALTY FOR PRIVATE USE, $300
AN EQUAL OPPORTUNITY EMPLOYER

POSTAGE AND FEES PAID
U.S. ENVIRONMENTAL PROTECTION AGENCY
EPA-335

If your address is incorrect, please change on the above label tear off; and return to the above address.
If you do not desire to continue receiving these technical reports, CHECK HERE ☐; tear off label, and return it to the above address.

Publication No. EPA-600/7-79-020

B835/9